THE ROLE OF THE CD8 CO-RECEPTOR IN CD8$^+$ T-CELL ACTIVATION

A thesis submitted in requirement of Cardiff University

For the degree of Doctor of Philosophy

****

Mathew Clement

School of Medicine

Institute of Infection & Immunity

****

2013

To Kello

ACKNOWLEDGEMENTS

I would like to take this opportunity to thank the Wellcome Trust for providing me with the funding to undertake this study. I would like to thank my supervisors, Professor Andy Sewell for his helpful suggestions along the journey, and especially Dr Linda Wooldridge. Her enthusiasm, guidance and excellent supervision spurred me on all the way from start to finish and her constant support gave me the confidence to complete this study. Thank you Linda! Big thanks has to go to all of the lab members both past and present who have helped provide a fun and yet professional environment in which to work, the special ones know who they are, including Jimmy "of the Man-Tooth clan"!

A massive thank you has to go to my parents who have always helped me with everything in life. It is with their unwavering support that has inspired me to always want to know more. I`ve finished writing it now Dad.

My biggest thanks have to go to my wife Kelly. She has had to put up with me during the whole process and has always stood by me and pretended to understand. Thank you Kello, without you, nothing is possible.

DECLARATION

This work has not previously been accepted in substance for any degree and is not concurrently submitted in candidature for any degree.

Signed …… (candidate) Date ……

STATEMENT 1

This thesis is being submitted in partial fulfillment of the requirements for the degree of PhD

Signed …… (candidate) Date ……

STATEMENT 2

This thesis is the result of my own independent work/investigation, except where otherwise stated. Other sources are acknowledged by explicit references.

Signed …… (candidate) Date ……

STATEMENT 3

I hereby give consent for my thesis, if accepted, to be available for photocopying and for inter-library loan, and for the title and summary to be made available to outside organisations.

Signed …… (candidate) Date ……

ABSTRACT

$CD8^+$ T-cells are essential for the immune control of pathogens and the natural eradication of cancer. $CD8^+$ T-cells also play a major role in the pathogenesis of autoimmunity and alloreactivity. $CD8^+$ T-cells recognize short peptide fragments (8-13 amino acids) presented at the target cell surface bound to Major Histocompatability Class I (MHCI) molecules. T-cell antigen recognition is unique in nature because it involves the binding of a single ligand (peptide–MHC [pMHC]) by two receptors (TCR and CD8). The CD8 glycoprotein, which serves as the coreceptor on MHCI-restricted T-cells, acts to enhance the antigen sensitivity of T-cells by binding to a largely invariant region of MHCI at a site distinct from the TCR docking platform. CD8 has been shown to have multiple roles including enhancing effects on early T-cell activation events and also in controlling the level of T-cell cross-reactivity. The pMHCI/CD8 interaction is classified as having a very weak binding affinity and very fast kinetics. I discovered that this low solution binding affinity is essential in maintaining homeostasis as dramatically increasing the strength of this interaction resulted in total loss of T-cell specificity and activation independent of TCR engagement. This led me to examine the possibility that anti-CD8 antibodies could also bypass the normal requirements for T-cell activation. I identified one specific clonotype of antibody capable of this phenomenon but simultaneously discovered multiple effector phenotypes of other anti-CD8 antibodies. These included both enhancing and inhibitory effects on pMHCI tetramer binding and $CD8^+$ T-cell activation. Subsequently, I explored the possibility of using these inhibitory anti-CD8 antibodies to block T-cell function in systems which are highly dependent on CD8 such as autoreactive $CD8^+$ T-cells. I demonstrated that targeting CD8 can be used as a strategy to block autoreactive $CD8^+$ T-cell activation in the absence of any effect on pathogen specific immunity. This highlights a novel therapeutic strategy that warrants further investigation. Finally, I demonstrated that CD8 can alter the functional avidity of a $CD8^+$ T-cell for its agonists and act to re-arrange the relative potencies of each of its potential agonists, a novel "focussing mechanism" for CD8 in T cell activation. These results provide new insight to the biological role of CD8 in T-cells and even predict a novel mechanism for CD8 in controlling T-cell function. My results also highlight the potential of targeting CD8 for immunotherapeutic design in autoimmune disorders.

LIST OF PUBLICATIONS

As a direct result of work from this thesis;

- **M. Clement,** L. Wooldridge, A. Lissina, E. S. J. Edwards, K. Ladell, J. Ekeruche, R. E Hewitt, E. Gostick, D. K. Cole, R. Debets, C. Berrevoets, J. J. Miles, S. R. Burrows, D. A. Price and A. K Sewell. Major Histocompatability Complex class I molecules with super-enhanced CD8 binding properties bypass the requirement for cognate TCR recognition and non-specifically activate cytotoxic T lymphocytes. *J Immunology*, (2010), 184, 3357 -3366
- **M. Clement**, K. Ladell, J. Ekeruche-Makinde, J. J. Miles, E. S. J. Edwards, G. M. Dolton, T. Williams, A. J. A. Schauenburg, D. K. Cole, S. N. Lauder, A. M. Gallimore, A. J. Godkin, S. R. Burrows, D. A. Price, A. K. Sewell, and L.Wooldridge. Anti-CD8 antibodies can trigger $CD8^+$ T-cell effector function in the absence of TCR engagement and improve pMHCI tetramer staining. *J Immunology* (July 15, 2011), 187(2): 654-663.
- B. Laugel, D. K. Cole, **M. Clement**, L. Wooldridge, D. A. Price, A. K. Sewell. The multiple roles of the CD8 coreceptor in T cell biology: opportunities for the selective modulation of self-reactive cytotoxic T cells. *J Leukoc Biol*, 90, 6 (December 2011) pp.1089-1099
- D. K. Cole, B. Laugel, **M. Clement**, L. Wooldridge, D. A. Price, A. K. Sewell. The molecular parameters that govern CD8 co-receptor function. *Immunology* (October 2012), 137(2): 139-48

Manuscripts in preparation

- **M. Clement**, D. Kronenberg, S. Llewellyn-Lacey, J. Ekeruche-Makinde, G. Dolton, A. K. Sewell, D. A. Price, M. Peakman, A. Skowera, L. Wooldridge. Specific blockade of autoreactive $CD8^+$ T-cell attack by targeting the MHCI/CD8 interaction.
- **M. Clement**, J. Ekeruche-Makinde, B. Szomolay, S. Llewellyn-Lacey, A. J. A. Schauenburg, A. K. Sewell, D. A. Price, B. Laugel, D. K. Cole, H. A. van den Berg, L. Wooldridge. CD8 focussing: a novel role for CD8 in T-cell activation

As a direct result of work outside of this thesis;

- Lissina, K. Ladell, A. Skowera, **M**. **Clement**, E. S. J. Edwards, R. Seggewiss, H. A. van den Berg, E. Gostick, K. Gallagher, E. Jones, J. J. Melenhorst, A. J. Godkin, M. Peakman, D. A. Price, A. K. Sewell, L. Wooldridge. Protein kinase inhibitors substantially improve the physical detection of T-cells with peptide-MHC tetramers. *J Immunol Methods*. (2008 Oct 14).
- D. K. Cole, E. S. J. Edwards, K. Wynn, **M. Clement**, J. J. Miles, K. Ladell, J. Ekeruche, E. Gostick, K. J. Adams, A. Skowera, M. Peakman, L. Wooldridge, D. A. Price, A. K. Sewell. Modification of MHC anchor residues generates heteroclitic peptides that alter TCR binding and T cell recognition. *J Immunology* (Aug 15, 2010)
- L. Wooldridge, B. Laugel, J. Ekeruche, **M. Clement**, H. A. van den Berg, D. A. Price, and A. K. Sewell. CD8 Controls T Cell Cross-Reactivity. *J Immunology* (September 15, 2010), doi:10.4049
- M. C. Iglesias, J. R. Almeida, S. Fastenackels, D. J. van Bockel, M. Hashimoto, V. Venturi, E. Gostick, A. Urrutia, L. Wooldridge, **M. Clement**, S. Gras, P. G. Wilmann, B. Autran, A. Moris, J. Rossjohn, M. P. Davenport, M. Takiguchi, C. Brander, D. C. Douek, A. D. Kelleher, D. A. Price, V. Appay. Escape from highly effective public CD8(+) T-cell clonotypes by HIV. *Blood,* 118, 8 (August 2011) pp.2138-2149.
- L. Wooldridge, J. Ekeruche-Makinde, H. A. van den Berg, A. Skowera, J. J. Miles, M. P. Tan, G. M. Dolton, **M. Clement**, S. Llewellyn-Lacey, D. A. Price, M. Peakman, A. K. Sewell. A single autoimmune T cell receptor recognizes more than a million different peptides. *J Biol Chem*, 287, 2 (January 2012) pp.1168-1177.
- **M. Clement**, J. Ekeruche, D. K. Cole, K. Ladell, E. S. J. Edwards, J. J. Miles, K. Wynn, A. Fuller, K. Lloyd, G. M. Dolton, J. M. Pentier, A. Lissina, E. Gostick, T. K. Baxter, B. M. Baker, P. Rizkallah, D. A. Price, A. K. Sewell, L. Wooldridge. TCR optimized peptide skewing of the T-cell repertoire. *J Biol Chem*. (October 2012) 26;287 (44) :37269-812012
- J. Ekeruche-Makinde, J. J. Miles, H. A. van den Berg, A. Skowera, G.M. Dolton, A. J. A. Schauenburg, M. P. Tan, J. M. Pentier, S. Llewellyn-Lacey, K. M. Miles, A. M. Bulek, **M. Clement**, T. Williams, M. Bailey, D. K. Cole, J. Rossjohn, M. Peakman, D. A. Price, S. R. Burrows, A. K. Sewell, L. Wooldridge. T-cell receptors exhibit explicit

major histocompatibility complex class I-peptide length recognition footprints. *Blood*. (December 18 2012) Epub ahead of print.

TABLE OF CONTENTS

LIST OF FIGURES

LIST OF ABBREVIATIONS

Ab	Antibody
APC	Antigen Presenting Cell
APL	Altered Peptide Ligand
AP-1	Activator protein 1
A-loop	Activating loop
α-CPM	α-chain connecting peptide motif
BCR	B-cell Receptor
β2m	β_2-microglobulin
Ca^{2+}	Calcium
CBA	Cytometric Bead Array
CD number	Cluster of Differentiation
CK	Cellkine
CMV	Cytomegalovirus
Csk	C-terminal kinase
CDR	Complementarity Determining Loop
CTL	Cytotoxic T Lymphocyte
^{51}Cr	Chromium
DC cells	Dendritic cells
DMSO	Dimethyl Sulfoxide
DNA	Deoxyribonucleic acid
DNA-PK	Dependent Protein Kinase Complex
DTT	Dithiothreitol
DP	Double positive
DMEM	Dulbecco modified Eagle's medium
EBV	Epstein Barr virus
EDTA	Ethylenediaminetetraacetic acid
ELISA	Enzyme Linked immunosorbant assay
ELISpot	Enzyme linked immunospot assay
ER	Endoplasmic Reticulum
ERK	Extracellular signal-regulated kinase
FACS	Fluorescence activated cell sorting
FCS	Foetal calf serum

FPLC	Fast Performance Liquid Chromatography
FRET	Forster Resonance Energy Transfer
HBS-EP	Biacore buffer
Th cells	Helper T-cells
HLA	Human Leukocyte Antigen
HIV-1	Human Immunodeficiency Virus Type-1
HEK cells	Human Embryonic Kidney
HTLV-1	Human T-cell Leukaemia Virus
IFN-γ	Interferon-gamma
Ig	Immunoglobulin
IL number	Interleukin
ITAM	Immune Receptor Tyrosine based Activation Motifs
IS	Immunological Synapse
IEL	Intra-Epithelial Lymphocytes
IMDM	Iscove`s Modified Dulbecco medium
IPTG	Isopropyl-1-thio-β-D-galactopyranoside
LAT	Linker for Activation in T-cells
MFI	Mean Fluorescence Intensity
mab	Monoclonal antibody
MES	2-[N-Morpholino]ethanesulfonic acid
MIP-1α	Macrophage Inflammatory Protein-1α
MIP-1β	Macrophage Inflammatory Protein-1β
MHCI	Major Histocompatability Class I
MHCII	Major Histocompatability Class II
MS	Multiple Sclerosis
NK cells	Natural Killer cells
NFAT	Nuclear factor of activated T-cells
NFκB	Nuclear Factor Kappa B
NOD	Non-obese diabetic
OD	Optical Density
PRR	Pattern Recognition Receptor
PBS	Phospho Buffered Saline
PBMC	Peripheral Blood Mononuclear Cell
PEP	PEST-domain enriched tyrosine phosphatase

PHA	Phytohemagglutinin
pMHC	peptide–MHC
PMA	Phorbol Myristate Acetate
PTK	Protein Tyrosine Kinase
PTPN22	protein tyrosine phosphatase non-receptor type 22
RANTES	Regulated on Activation, Normal T Expressed and Secreted
T_{reg} cells	Regulatory T-cells
RAG number	Recombinase Activating Gene
RU	Response Unit
RPMI	Roswell Park Memorial Institute Medium
RSV	Rous sarcoma virus
SAGE	Serial analysis of gene expression
SDS-PAGE	Sodium Dodecyl Sulphate-Polyacrylamide Gel Elecrophoresis
SP	Single Positive
SH number	Single Src Homology domains
SHP-1	Src homology region 2 domain-containing phosphatase-1
SMAC	Supramolecular Activation Clusters
SPR	Surface Plasmon Resonance
TAP	Transporter associated with Antigen Processing complex
TCR	T-cell Receptor
TCR-MC	T-cell Receptor Microclusters
TdT	Terminal deoxynucleotidyl Transferase
TL	Thymic Leukaemia Antigen
TNF-α	Tumour Necrosis Factor-alpha
TSA	Tissue specific antigens
Tyr	Tyrosine
T1D	Type-1 diabetes
VDJ	Variable, Diversity, and Joining gene segments

LIST OF FLUOROPHORES

FITC	Fluorescein Isothiocyanate
PE	R-phycoerythrin (including PE-Cy5 and PE-Cy7)
7-AAD	7-Amino-Actinomycin D
PerCP	Peridinin-Cholorophyll proteins (including PerCP-Cy5.5)
APC	Allophycocyanin (including H7-APC)
BV421	Brilliant Violet 421
PB	Pacific Blue
AmCyan	AmCyan
QDot 605	Quantum Dot Q605
QDot 800	Quantum Dot Q800

LIST OF AMINO ACIDS

A	Alanine	M	Methionine
C	Cysteine	N	Asparagine
D	Aspartic Acid	P	Proline
E	Glutamic Acid	Q	Glutamine
F	Phenylalanine	R	Arginine
G	Glycine	S	Serine
H	Histidine	T	Threonine
I	Isoleucine	V	Valine
K	Lysine	W	Tryptophan
L	Leucine	Y	Tyrosine

Chapter 1

1

INTRODUCTION

1. Introduction

1.1 Overview of the Immune system

The primary role of the immune system is the eradication of pathogens and tumours to protect against disease. The immune system is a diverse network of cell types, lymphoid organs and many other factors involved in immune control. The immune system can be divided into two arms, determined by the speed and specificity of the response to pathogen attack: (i) innate (natural) immunity, which provides the first line of anti-microbial defence (Tosi 2005), and; (ii) acquired (adaptive) immunity, which acts in concert with innate immunity in order to eliminate the invading pathogen.

1.1.1 Innate Immunity

The innate immune system provides the first line of defence. If pathogens breach physical barriers such as skin, mucosal surfaces and the respiratory tract then the innate immune response is activated and recognizes pathogens through 'pattern recognition receptors' (PRR) (Medzhitov 2007). PRRs concentrate on the recognition of highly conserved structures expressed by large groups of micro-organisms (Suzuki, Kurihara et al. 1997; Fraser, Koziel et al. 1998; Thomas, Li et al. 2000). The major cellular effectors of the innate immune system are dendritic cells (DC), neutrophils, monocytes and macrophages (which are all involved with phagocytosis) (Janeway and Medzhitov 2002), and natural killer cells (NK) (which are involved with removal of virally infected and transformed cells) (Smyth, Cretney et al. 2005). In addition, mast cells, eosinophils and basophils are involved in the release of inflammatory mediators and molecular components. Another important cellular effector of the innate immune system is the complement system. The activated complement system recognizes and

eliminates invading microorganisms. In addition, complement facilitates the elimination of dead or modified self cells, such as apoptotic particles and cellular debris. The alternative pathway of complement forms a spontaneously and constantly activated immune surveillance system as reviewed in (Zipfel and Skerka 2009). Effector function of the innate immune system is activated immediately on exposure to antigen and occurs to the same extent even on repeated exposure to the same antigen (Medzhitov and Janeway 2000).

1.1.2 Acquired Immunity

Aquired or 'Adaptive' immunity can be separated into either humoral or cell-mediated responses. Humoral immunity is mediated by the secretion of antibodies by B-cells. Antibodies bind to antigens present at the surface of invading pathogens (such as viruses or bacteria), which identifies them for removal via cell-mediated immunity. Cell-mediated immunity does not involve antibodies or complement but involves the activation of T-cells (Delves and Roitt 2000; Delves and Roitt 2000). Both B-cells and T-cells are derived from progenitor hematopoietic stem cells in the bone marrow (Janeway, Murphy et al. 2008). B and T-cells express receptors that are generated by somatic re-arrangement during T-cell development, as a result approximately 10^{14} B-cell receptors (BCRs) and 10^{18} T-cell receptors (TCRs) can be generated. B and T-cells express only one clonal antigen receptor and on recognition of specific antigen proliferate by a process called 'clonal expansion' which can take 3-5 days (Pancer and Cooper 2006). The adaptive response improves on repeated antigen exposure, a property called 'immunological memory'.

1.2 T-cell antigen recognition, processing and activation

1.2.1 T-cell activation and antigen recognition

T-cells are characterized by the surface expression of the lymphocyte marker CD45 and more specifically by the expression of the T-cell marker CD3. Approximately 95% of circulating T-cells will express a unique αβ T-Cell Receptor (TCR) at their cell surface (Lefranc and Lefranc 2001). These αβ T-cells are able to recognize short peptide fragments presented at the cell surface of an antigen presenting cell (APC) in association with the Major Histocompatability complex molecule (MHC) known as Human Leukocyte antigen (HLA) in humans (Engelhard 1994) (Rudensky, Preston-Hurlburt et al. 1991) (Davis, Boniface et al. 1998). T-cells can also exclusively express a γδ TCR. These cells are far less in number than αβ T-cells, i.e. <5% circulating T-cells will express a γδ TCR (Kabelitz, Wesch et al. 2007) (Lefranc and Lefranc 2001). The γδ T-cells role is less well understood in immunity than the αβ T-cells. It is believed that they can recognize specific microbial and viral antigens, and may play a role in tumor immunology (Kabelitz, Wesch et al. 2007).

MHC Class I (MHCI), molecules in complex with short peptides (8-13 amino acids) are expressed at the surface of all nucleated cells as peptide-MHCI (pMHCI). These presented peptides are mostly derived from endogenously processed intracellular proteins. In a healthy cell the peptides that are presented are host-derived. Intracellular infection or tumourigenesis results in presentation of foreign pMHCI at the cell surface. Foreign pMHCI molecules are recognised by $CD8^+$ T-cells which eradicate the target cell. Therefore, $CD8^+$ T-cells are important mediators of immunity to intracellular pathogens such as viruses, protozoa and

parasites, and play an important role in the elimination of tumour transformed cells (Harty, Tvinnereim et al. 2000).

MHC Class II (MHCII), molecules are expressed by 'professional' or 'bone marrow derived' APCs (dendritic cells, macrophages, B-cells and in the human T-cells) and present small peptide fragments (13-25 amino acids) processed from extracellular pathogens. Foreign peptide-MHCII is recognised by $CD4^+$ helper T-cells (Th). Activated $CD4^+$ helper T-cells exist as three types: (i) Type 1 (Th1) helper T-cells secrete cytokines that facilitate cell-mediated immunity such as macrophage activation and T-cell mediated cytotoxicity; (ii) Type 2 (Th2) helper T-cells secrete cytokines that help B-cells produce antibodies (Delves and Roitt 2000; Delves and Roitt 2000); and, (iii) Th17 T-cells which produce IL-17 and are involved with autoimmune disorders but their precise role is still unknown (Veldhoen and Seddon 2010). There are also regulatory forms of $CD4^+$ T-cells (T_{reg}) that are important in immune regulation. My work focused on $CD8^+$ T-cells so these Th cell types will not be discussed further here.

1.2.2 Antigen processing and presentation

In the cytosol, proteins become polyubiquitinated which targets them for proteasomal degradation (Ciechanover 1994). The proteasome is a central cytoplasmic processing unit and is required for the generation of the majority of MHCI-associated peptides (Rock, Gramm et al. 1994). Peptide fragments generated by the proteasome are translocated into the Endoplasmic Reticulum (ER) via the transporter associated with antigen processing complex (TAP), where they bind to newly synthesised MHCI molecules (Pamer and Cresswell 1998). These new pMHCI molecules associate with a number of chaperone proteins, including

tapasin, calnexin, calreticulin and ERp57 to form the peptide-loading complex. This complex then facilitates the loading of peptides into the MHCI peptide binding groove (Capps and Zuniga 1994; Sadasivan, Lehner et al. 1996; Peaper and Cresswell 2008; Purcell and Elliott 2008; Sadegh-Nasseri, Chen et al. 2008). The pMHCI complex then traverses the ER and Golgi apparatus, before transport to the plasma membrane and expression on the APC surface (Figure 1.1). The co-factor tapasin additionally edits the peptide repertoire that is loaded onto MHCI molecules in favour of those with slow dissociation kinetics (Howarth, Williams et al. 2004; Thirdborough, Roddick et al. 2008). Recognition of pMHCI is mediated by the αβ TCR which is expressed by $CD8^+$ T-cells (Antoniou, Powis et al. 2003). Alternatively, specialised professional antigen-presenting cells (including dendritic cells, B-cells, and macrophages) might have taken up exogenous antigen by endocytosis. Exogenous antigen is processed via a different pathway to endogenous antigen, and presented at the cell surface in complex with MHCII molecules (Figure 1.2). Briefly antigens are derived from extracellular pathogens and proteins internalised by phagocytosis or endocytosis. Internalised protein antigens are degraded in acidic endosomes. MHCII molecules in the endoplasmic reticulum are exported in vesicles. Vesicles fuse in cell cytoplasm so that MHCII molecules can bind antigen peptides. Antigenic peptides presented at the cell surface by MHCII molecules are recognised by $CD4^+$ T-cells (Parkin and Cohen 2001).

1.3 Structural and Molecular features of MHC and the TCR

1.3.1 MHC class I and II structure

MHCI and MHCII are cell surface glycoproteins with distinct subunit structures. The MHCI molecule is a membrane bound heterodimer consisting of two polypeptide chains, i.e. an α

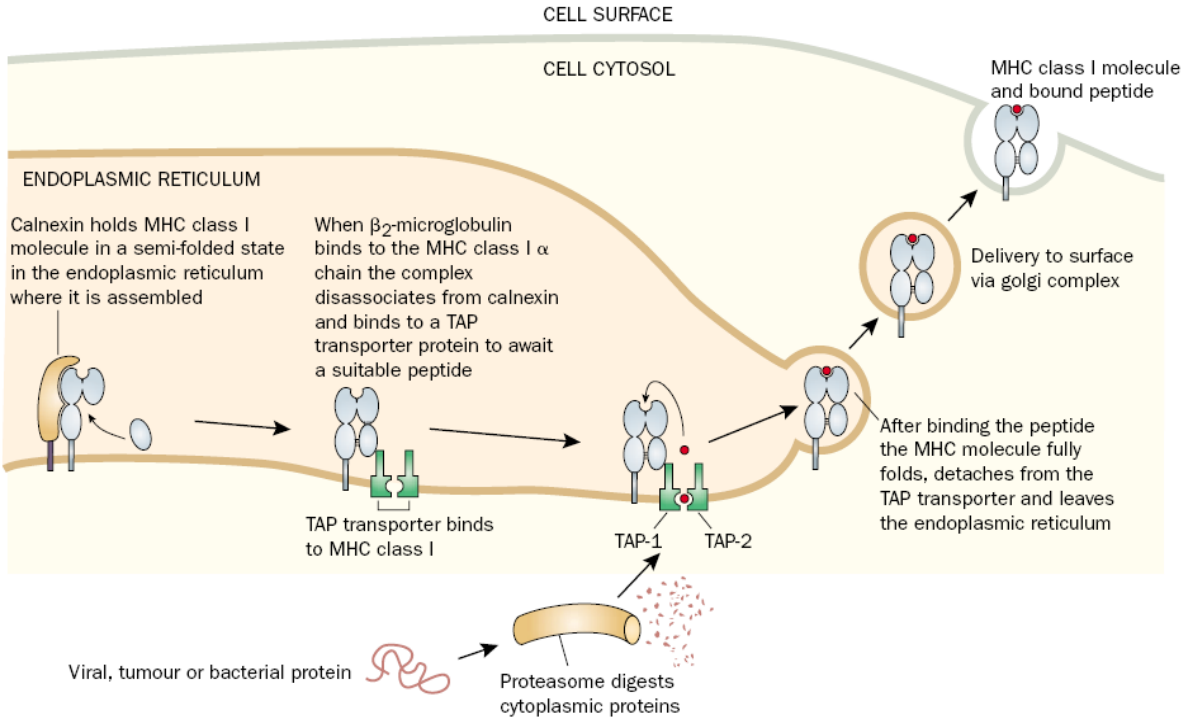

Figure 1.1: MHCI processing and presentation pathway. Peptides fragments are generated via proteasome digestion of bacterial, viral and tumour associated proteins, then transported into the endoplasmic reticulum (ER) where they associate with MHC molecules using TAP, peptide loading complex, and other chaperone proteins. Upon release from the ER, the pMHCI complex is transported to the cell surface by the Golgi apparatus where it is expressed, figure reprinted from The Lancet, **357**(9270): 1777-89, Parkin and Cohen, An overview of the immune system, © 2001, with permission from Elsevier.

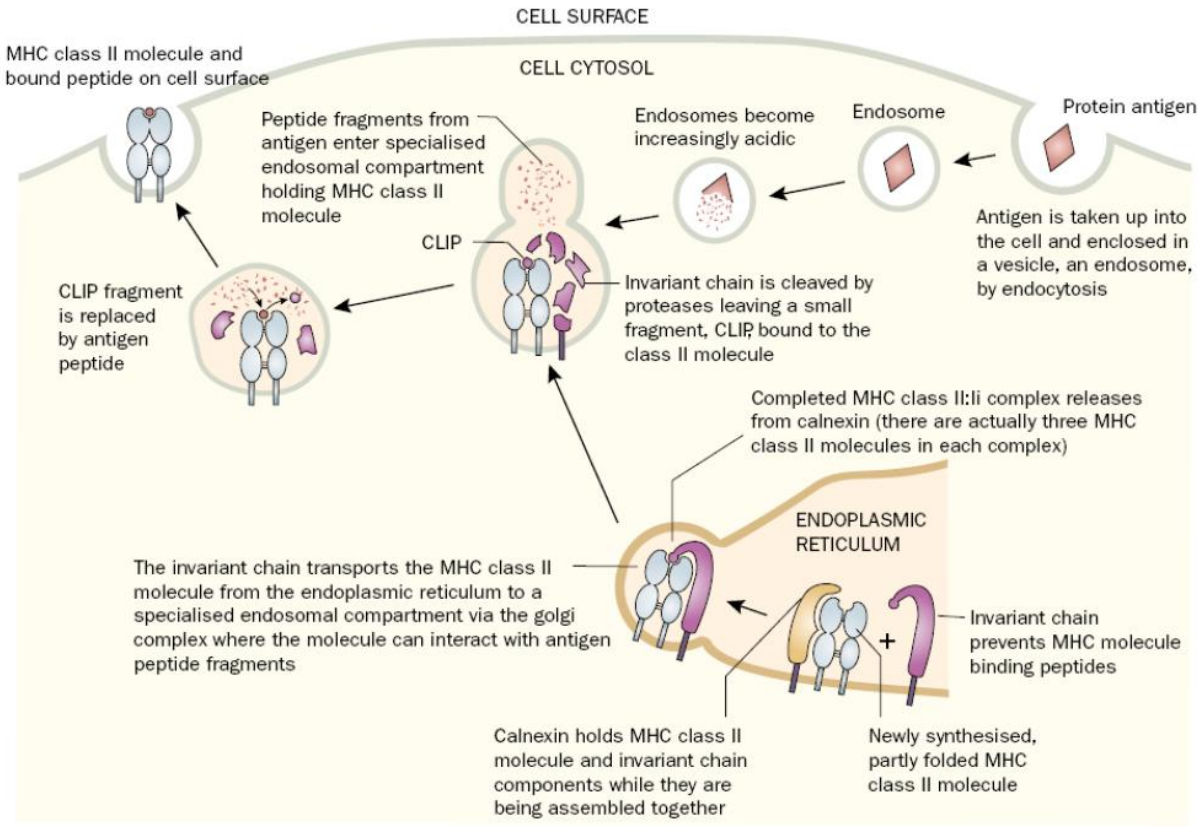

Figure 1.2: MHCII processing and presentation pathway. Antigens are internalised by phagocytosis or endocytosis where they are degraded in increasing acidic conditions and subsequently fuse to MHCII molecules preformed in the ER. Once released from the ER pMHCII molecules are presented on the cell surface and are recognised by $CD4^+$ T-cells, figure reprinted from The Lancet, **357**(9270): 1777-89, Parkin and Cohen, An overview of the immune system, © 2001, with permission from Elsevier.

chain, which is non-covalently associated with the smaller β_2-microglobulin light chain (Figure 1.3 A). The α chain contains three globular domains, α1, α2 and α3 and it is only this chain that spans the cell membrane. The α3 domain and β_2-microglobulin are membrane proximal whereas the α1 and α2 domains form the peptide binding groove. The MHCII molecule consists of two non-covalently associated chains, α and β chain (Figure 1.3 B). Both these chains span the cell membrane, and consist of a transmembrane domain and cytoplasmic tail. The α2 and β2 domains are membrane proximal domain whereas the α1 and β1 domains form the peptide binding groove. These subtle yet important differences between the MHC molecules do not deter from the fact that they both have similar structures and functions. The walls of the peptide binding groove are formed by 2 α-helices, whilst the base of the groove consists of 8 anti-parallel β-pleated sheets (Wolf and Ploegh 1995).

MHC molecules are unstable in the absence of peptide. Polymorphic amino acids in MHC molecules are mainly found and clustered in the peptide binding groove. These amino acids contribute to the formation of peptide binding pockets and side chains that project from certain amino acid residues into these binding pockets can stabilise the MHC molecule. The amino acid residues of the peptide epitope that sit in the pockets of the binding groove are known as the MHC anchor residues. These peptide binding pockets differ between MHC allelic variants in their spatial and chemical characteristics (Nielsen, Lundegaard et al. 2004). MHC molecules are known to be highly polymorphic at the peptide binding site and subsequently different MHC alleles will be able to bind different peptides.

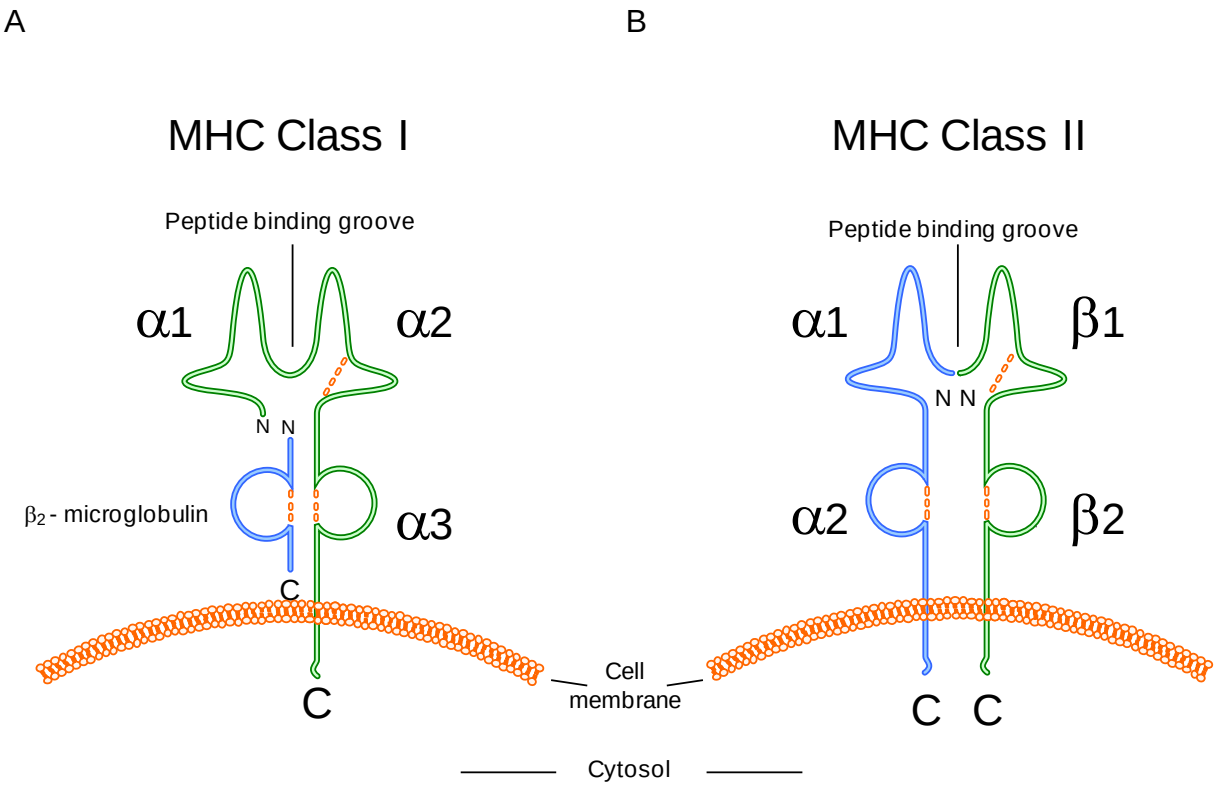

Figure 1.3: Structure of MHCI and MHCII molecules. (**A**) The MHCI molecule consists of an α domain (α1, α2 and α3) and β_2-microglobulin. The α1 and α2 domain form the peptide binding groove. The α chain also contains a transmembrane domain and a short cytoplasmic tail. (**B**) The MHCII molecule consists of non-covalently linked α and β chains. The α2 and β2 chains form the membrane proximal domain whereas the α1 and β1 chain form the peptide binding groove. Both α and β chains contain a transmembrane domain and a cytoplasmic tail.

MHCI restricted peptides are normally 8-13 amino acids in length (Rammensee 1995), where residues at position 2 and the C- terminus act as MHCI anchor residues (Rammensee, Bachmann et al. 1999). The ends of the peptide binding groove are closed (Bjorkman, Saper et al. 1987) restricting the length of the peptide that can be accommodated, therefore the longer peptides must adopt a bulged conformation. MHCII molecules can bind peptides that range from 13-25 amino acids in length (Rammensee 1995) although the most commonly found length ranges from 13-17 amino acids (Rudensky, Preston-Hurlburt et al. 1991). In contrast to the MHCI molecules, the peptide binding groove is open. As a consequence, anchor residue positions can vary (Brown, Jardetzky et al. 1993) and the peptide sits in a universally flat conformation.

The MHC encoding region is located on chromosome 6 and extends to over four million base pairs of DNA (Marsh 2000). It is divided into different gene encoding regions, i.e. (i) MHCI -A, -B, -C, -E, -F and -G genes. (ii) MHC class II -DP, -DQ and -DR genes, as well as -DM. MHC genes can be highly polymorphic allowing the presentation of a large range of potential peptide epitopes. In humans, there are over 5518 MHCI alleles and 1612 MHCII alleles known to exist to date (EMBL-EBI 2012).

1.3.2 TCR structure and pMHC recognition

Recognition of peptide-MHC (pMHC) molecules is mediated by T-cells bearing an αβ TCR (Unanue 1984; Townsend and Bodmer 1989). The TCR α and β chain are covalently linked by disulphide bonds (van der Merwe and Davis 2003). Each TCR chain consists of a membrane distal variable region (Vα or Vβ) and a membrane proximal immunoglobulin like

constant region (Cα or Cβ). The chains also contain a transmembrane region and a cytoplasmic tail (Bentley and Mariuzza 1996). The TCR chains are glycoproteins, with the α chain containing between four and five N-linked oligosaccharides and the β chain containing up to two N-linked glycans (Lefranc and Lefranc 2001) (Figure 1.4). The Vα and Vβ domains each contain three hypervariable regions known as the complementarity determining loops (CDR1, CDR2 and CDR3) which are involved in the recognition of the pMHC complex (Lefranc and Lefranc 2001). The CDR3 loops of the Vα and Vβ chains interact with the peptide-binding region of the MHC whereas the CDR1 and CDR2 loops make contacts with the MHC molecule (Figure 1.5). Data suggests that the CDR1 loop may also be making contact with the peptide (Tynan, Burrows et al. 2005; Cole, Yuan et al. 2009). Approximately 28 human class I and class II TCR/pMHC co-crystal structures have been solved to date. This comprises of 21 TCR/pMHCI and 7 TCR/pMHCII structures, whereas as of 2006 only 10 structures had been solved (Bulek, Madura et al. 2012; Rudolph, Stanfield et al. 2006). Data suggests that the TCR binds in a diagonal conformation to pMHC with the Vα domain of the TCR positioned over the N-terminus of the peptide and the Vβ domain over the C-terminus (Hennecke and Wiley 2001; Rudolph and Wilson 2002). A docking angle of approximately 35° is most often observed and classed as within the normal range of binding when referring to other classified TCR/pMHC complexes previously solved. There are extremes which are known including A6 TCR-A2-Tax complex which binds with an angle of 32° (Garboczi, Ghosh et al. 1996) and 1G4 TCR-A2-NY-ESO complex which binds with an angle of 62° (Chen, Stewart-Jones et al. 2005), highlighting the variation that can occur between different complexes.

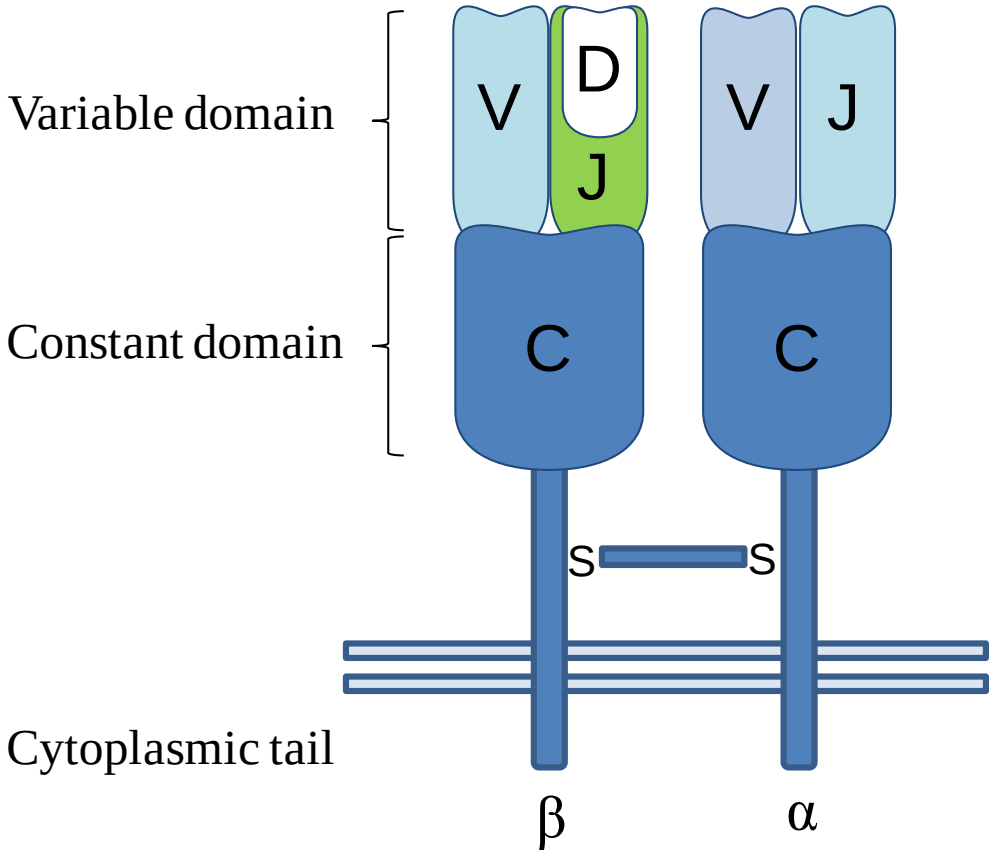

Figure 1.4: Structure of αβ TCR chains. The TCR α and β chain are covalently linked by disulphide bonds. Each TCR chain consists of an N-terminal region which consists of a membrane distal variable region (Vα or Vβ) and a membrane proximal immunoglobulin like constant region (Cα or Cβ). Each chain also contains a transmembrane region and a cytoplasmic tail.

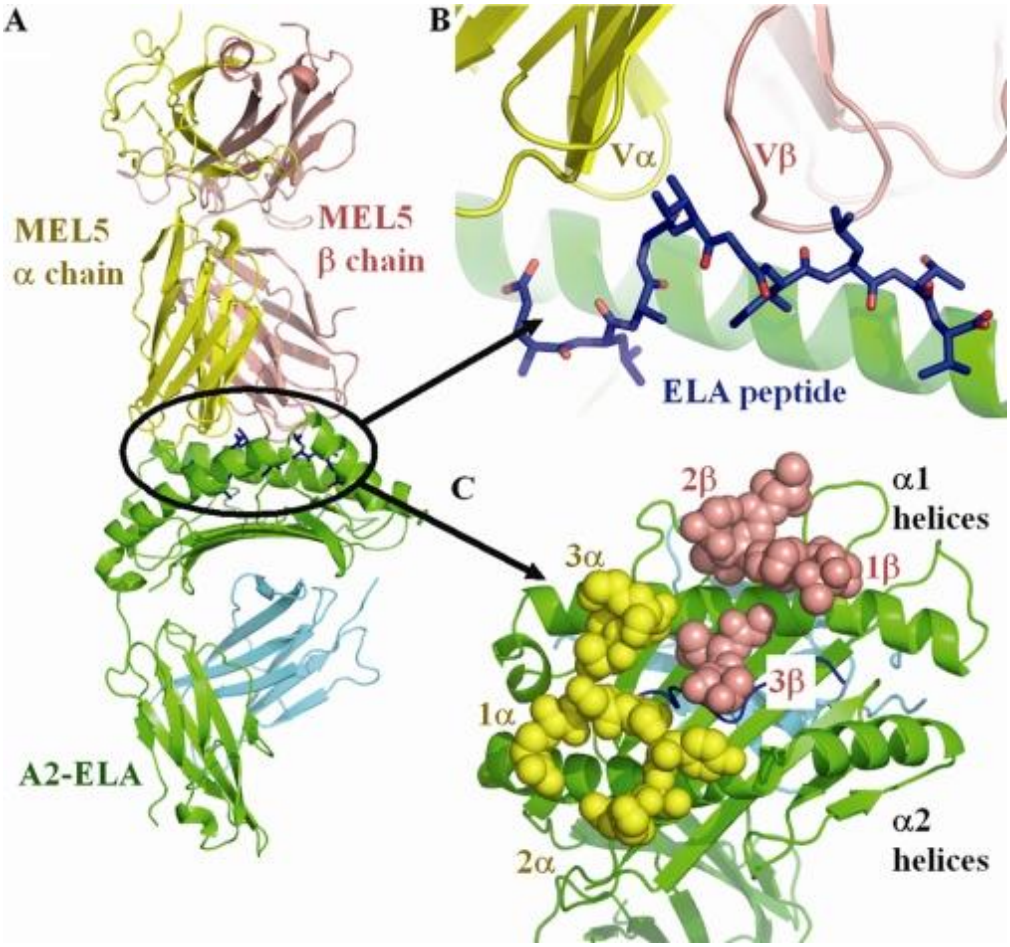

Figure 1.5: Crystal structure of TCR binding to pMHCI molecule. (**A**) The co-crystal structure of MEL5 (α chain shown as a yellow schematic diagram, β chain shown as a salmon schematic diagram) bound to the HLA-A*0201 (shown as green and blue schematic diagrams) molecule complexed with the ELAGIGILTV peptide (shown as blue sticks). (**B**) Expanded view of the interface between the MEL5 variable domain bound to the A2-ELA surface (colours as in **A**). The overall conformation of the ELAGIGILTV peptide (N to C terminus, left to right), including the central peptide bulge, is displayed. (**C**) View from above of the MEL5 CDR loops bound to the A2-ELA surface (colors as in **A**; MEL5 CDR loops shown as spheres). The MEL5 TCR binds toward the N terminus of the peptide, making contacts with the peptide via its CDR1 and CDR3 loops and contacts with the MHC surface via its CDR1 and CDR2 loops. This figure was originally published in The Journal of Biological Chemistry, (Cole, Yuan et al. 2009), © The American Society for Biochemistry and Molecular Biology.

1.3.3 T-cell generation and thymic selection

The initial stages of T-cell development involves the migration of bone marrow progenitor stem cells to the thymus where they undergo a selection process before maturing into different T-cell subsets. During thymocyte development the TCR α and β chains undergo a sequence of ordered somatic recombination events giving rise to T-cells with functional TCRs. These recombination events of the Variable (V), Diversity (D), and Joining (J), gene segments, known as VDJ recombination are mediated by VDJ recombinase enzymes such as Recombinase activating genes 1 and 2 (RAG1 and RAG2) (Schatz, Oettinger et al. 1992; Agrawal and Schatz 1997). These enzymes associate with each other and bring the V, D and J segments together cleaving the DNA at specific sites. DNA repair has to occur after RAG1 and RAG2 activity, which is achieved using DNA repair enzymes such as the DNA-dependent protein kinase complex (DNA-PK) that repairs double stranded DNA. (Ma, Pannicke et al. 2002). DNA-PK, among other enzymes, aligns the two DNA ends together and then recruits another enzyme, terminal deoxynucleotidyl transferase (TdT), which adds nucleotides randomly to the DNA ends. This process provides junctional diversity which can subsequently lead to TCR diversity. The process of VDJ recombination leads to an extremely diverse TCR repertoire and determines the antigen binding specificity of individual TCRs.

Double positive (DP) thymocytes, i.e. thymocytes that express both the CD4 and CD8 co-receptors are the first cells in the T-cell developmental pathway to express fully assembled successfully genetically rearranged αβ TCR on their cell surface. These DP thymocytes will then undergo positive selection, which is a process during which TCRs with minimal affinities for self-pMHC convey survival signals that permit continued thymocyte development (Huesmann, Scott et al. 1991). At the DP and single positive (SP) stages, cells

that express TCRs with high affinities for self-pMHC are deleted by the process of negative selection (Kappler, Roehm et al. 1987). The T-cell clonotypes that exist in the periphery post-thymic development therefore express TCRs with weak/intermediate affinities to self pMHC whilst ensuring a strong affinity for foreign pMHCI antigen. This reduces the potential for autoreactivity (Werlen, Hausmann et al. 2003). During the final stages in thymocyte development, immature DP thymocytes shut off expression of either one of their co-receptors. This gives rise to single positive mature $CD8^+$ and $CD4^+$ thymocytes as reviewed in (Basson and Zamoyska 2000). Van Laetham and colleagues showed that the MHC specificity of αβ TCRs is ultimately controlled by the CD4 and CD8 co-receptors during thymic development. Co-receptor deficient thymocytes can differentiate into mature αβ T-cells that can recognise antigenic ligands independently of MHC. The co-receptors can therefore control MHC specificity of αβ T-cells by preventing thymocytes from being signalled by non-MHC ligands. This data is consistent with the sequestration of intra-cellular Lck by CD4 and CD8, which would ensure that co-engagement of MHCI or MHCII by both the TCR and CD8 or CD4, respectively, is required to trigger the signals that elicit positive or negative selection in the thymus (Van Laethem, Sarafova et al. 2007).

Multiple models for CD4/CD8 lineage choice have been proposed (as reviewed in (Singer, Adoro et al. 2008). These include classical models such as stochastic or instructive, whereby termination of co-receptor transcription is either random or instructed, respectively. In addition, Singer *et al* suggest that lineage choice can be best described using a kinetic signalling model, which is a non-classical model. This postulates that the CD4/CD8 lineage choice is determined by TCR-signal duration and that cytokines such as IL-7 serve as sensors that detect the duration of the TCR signal. Singer *et al* suggest that CD8 gene expression is

terminated to create a $CD4^+CD8^-$ intermediate thymocyte in which lineage choice is made. Persistence of TCR signalling blocks IL-7R signal transduction and thymocytes differentiate into $CD4^+$ T-cells. Cessation or disruption to the TCR signalling allows IL-7R mediated signalling enabling the $CD4^+CD8^-$ intermediate thymocytes to undergo co-receptor reversal and differentiate into $CD8^+$ T-cells (Singer, Adoro et al. 2008). Indeed, CD8 lineage choice has recently been shown to be controlled by the intrathymic signalling by IL-7 and other γ-chain cytokines (Park, Adoro et al. 2007).

1.3.4 Kinetics of TCR/pMHCI interaction

The flexibility of antigenic peptide (ligand) recognition is essential for the function and development of T-cells (Kersh and Allen 1996). Some peptide ligands can partially activate the cell (partial agonists), others can inhibit activation (antagonists) and others will fully activate the cell to send a complete signal to the T-cell (agonists) (Sloan-Lancaster and Allen 1996). The affinity and kinetics of the TCR/pMHCI interaction can be studied using a technique known as Surface Plasmon Resonance (SPR). Typical antibody-antigen interactions have fast association rates of 10^5-10^6 M^{-1} x s^{-1} with dissociation rates of 10^{-5}-10^{-3} s^{-1} (Mason and Williams 1980). However, compared with conventional cell-cell recognition molecules the TCR has a relatively low affinity for peptide-MHC ligand (values range K_D= 0.13-278 μM, with typical values from 1-50 μM) (Mason and Williams 1980; Gao and Jakobsen 2000; Bridgeman, Sewell et al. 2011) (Figure 1.6). In contrast to other cell-cell recognition molecules the low affinity of the TCR/pMHC interaction is due to slow association rate constants (10^{-2}-10^{-4} M^{-1} x s^{-1}) rather than as a consequence of fast dissociation rates. The slow TCR/pMHC association rates are a consequence of the flexibility at the TCR/pMHC interface (Willcox, Gao et al. 1999). TCR/pMHC off rates fall into a

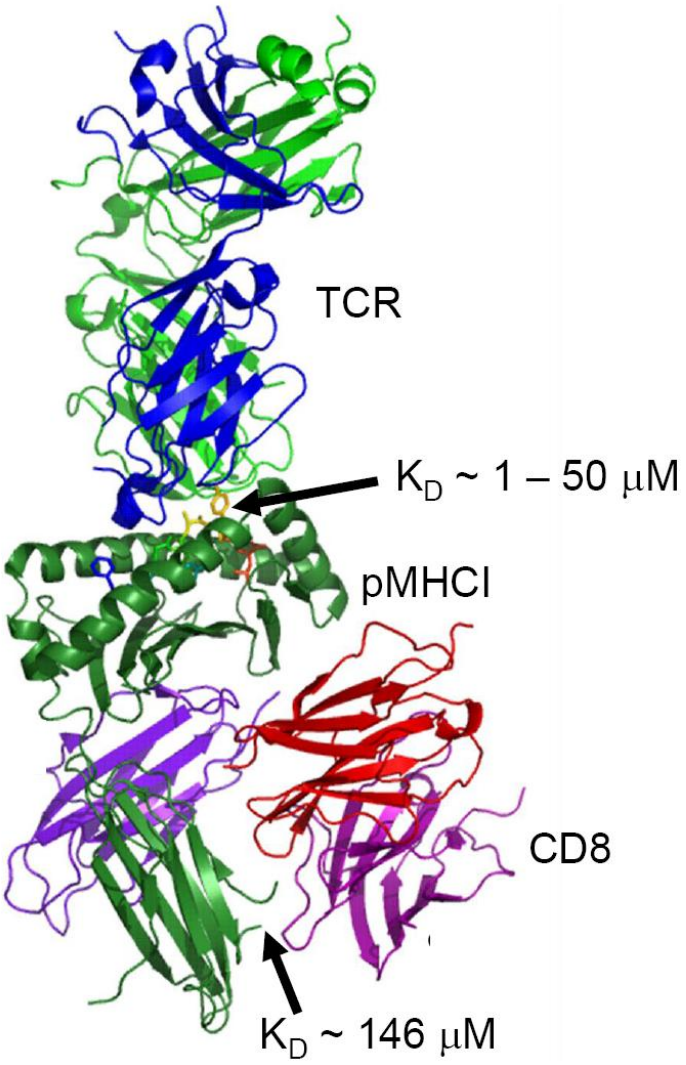

Figure 1.6: Typical wild-type affinity constants measured for TCR/pMHCI and pMHCI/CD8 interactions as measured via SPR. TCR/pMHCI interaction kinetics have been characterised using SPR and are typically of low affinity, i.e. typical wild-type values from 1-50 μM. Biophysical analysis has revealed that the pMHCI/CD8 interaction is much weaker than the TCR/pMHCI, i.e. typical wild-type values ~146 μM.

relatively narrow window (K_{off} = 0.63-0.01 s^{-1} with a mean of 0.24 s^{-1}) or a $t_{1/2}$ of 12-30 secs at 25°C (Davis, Boniface et al. 1998; Bridgeman, Sewell et al. 2011). In its simplest reversible form, the interaction of the TCR and pMHC can be described by the reaction;

$$\text{TCR} + \text{pMHC} \underset{k_{off}}{\overset{k_{on}}{\rightleftharpoons}} \text{TCR:pMHC}$$

involving an association rate (k_{on}) and a dissociation rate (k_{off}). The half-life of the interaction ($t_{1/2}$) is derived from the dissociation rate. At equilibrium, a binding constant ($K_D = 1/K_A$) can activate the cell to send a complete signal to the T-cell (agonists) (Sloan-Lancaster and Allen 1996). This binding constant can be determined for the interaction using standard Scatchard approaches (or the kinetic parameters, $K_D = k_{off}/k_{on}$), K_D = [TCR][pMHC]/[TCR:pMHC] (Rudolph, Stanfield et al. 2006).

1.4 T-cell activation

1.4.1 TCR/CD3 interaction

The αβ TCR transmembrane domains are non-covalently associated with the CD3 invariant polypeptide complex (-γ, -δ, -ε, and –ζ) (Kersh, Shaw et al. 1998). The transmembrane domains of the αβ TCR chains contain charged residues that maintain ionic interactions with the CD3 chains. Each TCR is associated with CD3-δε, CD3-γε heterodimeric and CD3-ζζ homodimeric signalling chains (Weiss and Littman 1994). Recent data also suggest that extracellular loops of the TCR α and β constant domains can interact with CD3-δε and CD3-γε heterodimers (Kuhns and Davis 2007). An additional CD3-η domain has also been identified. The CD3-η chain is a splice variant of CD3-ζ lacking the C-terminal signalling

motif and is believed to be involved in thymic selection (Blumberg, Alarcon et al. 1990; Love, Shores et al. 1994; Yamamoto, Isobe et al. 2005). The TCR-CD3 complex is assembled in the ER in a series of defined steps that begins with a CD3 core of CD3-δεγ (Alarcon, Berkhout et al. 1988). The CD3 chains contain signalling motifs called immune receptor tyrosine based activation motifs (ITAMs) which contains the consensus sequence $YXX(L/I)X_{6-8}YXXL/I$. The γ, δ and ε chains each contain 1 ITAM and the CD3ζ chain contains 3 ITAMs. Phosphorylation of these multiple ITAMs is sufficient to transduce and amplify signals from the TCR (Samelson, Harford et al. 1985; Reth 1989; Chan and Shaw 1996; Wange and Samelson 1996). The CD3-ζ subunits are important in stable accumulation of the TCR/CD3 complex at the immunological synapse. The CD3ζ chain contains clusters of arginine and lysine residues enabling the chain to complex to phosphoinositides. Elimination of the phosphoinositide binding function of CD3-ζ impaired the CD3-ζ to stabilise at the immunological synapse during T-cell/pMHC interaction (DeFord-Watts, Dougall et al. 2011).

After the TCR binds to pMHC antigen, one of the first intracellular events observed is the phosphorylation of the CD3-ζζ homodimer (Samelson, Patel et al. 1986; Koyasu, McConkey et al. 1992). This phosphorylation is induced by $p56^{lck}$ (a member of the Src tyrosine kinase family) (Barber, Dasgupta et al. 1989). The CD3-ζ polypeptide contains three ITAM motifs with a total of six tyrosines. CD3-ζ is phosphorylated in resting T-cells in the 21 kD isoform and upon full phosphorylation gives rise to the 23 kD isoform (Kersh, Shaw et al. 1998). The CD3-ζ ITAMs become phosphorylated in an ordered manner after recognition of a strong agonist ligand (Kersh, Kersh et al. 1998). Recognition of a less potent ligand leads to phosphorylation of a partial subset of tyrosines and non-complete ITAM phosphorylation (Kersh, Kersh et al. 1998).

The complete phosphorylation events are therefore controlled by the potency of the TCR/pMHC interaction. It is these phosphorylation events that determine the thresholds that are required for T-cell activation (Kersh, Kersh et al. 1998). A recent study has provided new data on the events that lead to CD3-ζζ phosphorylation on TCR ligation. Using optical tweezer experiments Kim *et al* suggest that the TCR is an anisotropic mechanosensor which upon specific pMHCI ligation, converts mechanical energy into biochemical signals. In this study a tangential force is applied to the TCR complex post-ligation which exerts a torque effect on CD3 as a consequence of the cell surface molecular movements. This change is thought to convert ectodomain ligation into the earliest intracellular signalling events (Kim, Shin et al. 2012).

1.4.2 Protein tyrosine kinases

The immediate result of specific TCR/pMHC engagement is the phosphorylation and subsequent activation of protein tyrosine kinases (PTKs). At the early stages of signal transduction two families of PTKs exist: (i) Src PTK and, (ii) Syk PTK (Chan, Iwashima et al. 1992; Chan, Desai et al. 1994; Iwashima, Irving et al. 1994). These PTKs are able to phosphorylate a range of substrates which signal multiple downstream targets. Upon phosphorylation of these targets, combined with appropriate signals from the T-cell co-receptors, T-cell activation will then commence (Iwashima, Irving et al. 1994). The Src family of kinases includes the family members $p56^{lck}$ (Lck) and Fyn (Wange and Samelson 1996). Both of these PTKs are co-localised to membranes as a result of myristoylation and palmitoylation modifications (Resh and Ling 1990; Kabouridis, Magee et al. 1997). Lck contains a di-cysteine motif which mediates association to the CD4 and CD8 co-receptors

(Turner, Brodsky et al. 1990; Kim, Sun et al. 2003). The Lck molecule contains single Src homology domains, (SH1, SH2 and SH3). The SH1 domain is a kinase domain which contains an ATP binding site and an autophosphorylation site at position Tyr394 (Abraham and Veillette 1990; Luo and Sefton 1990). Both SH2 and SH3 domains mediate intra and inter molecular protein to protein interactions via recognition of polyproline and phosphotyrosine motifs, respectively (Fantl, Escobedo et al. 1992; Zamoyska, Basson et al. 2003) (reviewed in (Salmond, Filby et al. 2009). The C-terminus of Lck contains a regulatory tyrosine residue at position Tyr505 which is specifically targeted by the Src C-terminal kinase (Csk) which will inhibit Lck function (Bergman, Mustelin et al. 1992). This is caused when Tyr505 becomes phosphorylated by the kinase Csk, resulting in a molecular association with the SH2 domain rendering Lck inactivated and non-functional (Weiss and Littman 1994; Sicheri and Kuriyan 1997), highlighting the importance of Tyr505 in T-cell activation and its requirement for full Lck activation (Caron, Abraham et al. 1992). Lck Tyr394 is another tyrosine residue required for T-cell activation which is also involved in enzymatic activity and is commonly referred to as the activating Tyr residue (reviewed in (Salmond, Filby et al. 2009). This Tyr residue is located in the activating loop (A-loop) of the kinase (Xu, Doshi et al. 1999). Upon activation of the Src family kinases via interactions through their SH2 and SH3 domains, the A-loop becomes exposed due to displacement by the now open kinase domains which contain the activating Tyr^{394} promoting enzymatic activity (Veillette and Fournel 1990).

Activated Lck phosphorylates the CD3-ζ ITAMs resulting in the recruitment of the ζ chain-associated protein ZAP-70 kinase via its SH2 domain (van Oers, Killeen et al. 1994; van Oers, Killeen et al. 1996; Wange and Samelson 1996). ZAP-70 is a member of the Syk

family of kinases which contain two tandemly arranged SH2 domains (Chan, Iwashima et al. 1992; Weiss and Littman 1994). It is believed the ZAP-70 only associates with diphosphorylated ITAMS (Mustelin and Tasken 2003) and once associated, ZAP-70 is phosphorylated at Tyr493 by Lck resulting in activation (Chan, Dalton et al. 1995). Studies have shown that point mutations in the ZAP-70 molecule can lead to autoimmune disorders such as rheumatoid arthritis and IgE-hyper autoimmune syndrome highlighting the impact that these defects can have on TCR driven T-cell signalling (Sakaguchi, Takahashi et al. 2003; Siggs, Miosge et al. 2007).

1.4.3 Role of CD45 in T-cell activation

CD45 is one of the most abundant cell surface glycoproteins comprising up to 10% of the cell surface (Thomas 1989). CD45 has a constant domain consisting of two tyrosine-specific phosphatase domains in tandem. In resting cells CD45 has been shown to associate with Lck (Guttinger, Gassmann et al. 1992). It is thought that CD45 activates Lck by its ability to selectively dephosphorylate the negative regulatory tyrosine at position 505 (Ostergaard, Shackelford et al. 1989; Ostergaard and Trowbridge 1990). Indeed, studies of CD45 deficient cell lines demonstrate that CD45 is required for the induction of PTK activity and TCR signal transduction. Csk, a cytoplasmic PTK acts to phosphorylate the inhibitory carboxyl-terminal tyrosine of Lck and is therefore a potent inhibitor of TCR signalling (Chow and Veillette 1995). Therefore Lck activity is thought to be regulated by the opposing phosphorylation effects of CD45 and Csk on the inhibitory Tyr505. Csk phosphorylates Tyr505 therefore inactivating Lck whereas CD45 de-phosphorylates Lck at this site thus priming PTK activity. CD45 is also thought to have an inhibitory effect which is mediated by the dephosphorylation of the activatory Tyr394 residue of Lck which subsequently suppresses kinase activity and T-

cell activation (D'Oro and Ashwell 1999; Palacios and Weiss 2004; Zhao, Yang et al. 2004) . It is known that other phosphatases act at the same site as CD45 such as PEST-domain enriched tyrosine phosphatase (PEP) which is also referred to as protein tyrosine phosphatase non-receptor type 22 (PTPN22) (Hasegawa, Martin et al. 2004; McNeill, Salmond et al. 2007), and Src homology region 2 domain-containing phosphatase-1 (SHP-1) (Chiang and Sefton 2001) thereby exerting an inhibitory effect. This inhibition leads to a severe block in T-cell differentiation and profound impairment of activation in mature T-cells (Ashwell and D'Oro 1999; Hermiston, Xu et al. 2003; Zamoyska, Basson et al. 2003). Therefore, CD45 has a role as both a positive and negative regulator of T-cell signalling and acts as a 'rheostat' which regulates the threshold of activation of T-cells (McNeill, Salmond et al. 2007; Zamoyska 2007).

1.4.4 T-cell transduction signalling

As previously mentioned activated Lck phosphorylates the CD3-ζ ITAMs resulting in the recruitment of the CD3ζ chain associated protein ZAP-70 kinase (Chan, Dalton et al. 1995). ZAP-70 becomes phosphorylated and recruits adaptor proteins which will propagate the signal transduction pathway (Zhang, Sloan-Lancaster et al. 1998). One of the substrates of phosphorylated ZAP-70 is the adaptor molecule LAT (linker for activation in T-cells). LAT consists of a short extracellular domain, a transmembrane region and a long cytoplasmic tail. When the cytoplasmic tail becomes phosphorylated at conserved tyrosine residues by activated ZAP-70, this then recruits various signalling molecules to the plasma membrane including PLC-γ1, Grb2, Grap, Gads, SLP-76, Vav-1, Cbl and the regulatory subunit of PI3K forming a multi-protein complex known as the "LAT signalasome" (Malissen, Aguado et al. 2005; Brownlie and Zamoyska 2009). Gads uses the LAT adaptor protein to form a complex

with SLP-76, Vav-1 and Itk which will mediate the phosphorylation of PLC-γ1 (Beach, Gonen et al. 2007; Bogin, Ainey et al. 2007; Seet, Berry et al. 2007) (Figure 1.7). LAT is an important adaptor protein in linking the TCR to downstream signalling events including activation of the transcription factor NFAT and ultimately proliferation and expression of cytokine genes (Brownlie and Zamoyska 2009). Subsequent tyrosine kinase phosphorylation activates downstream secondary messenger pathways through the cytoplasm directly into the cell nucleus activating multiple transcription factors. These include Activator protein 1 (AP-1), Nuclear factor of activated T-cells (NFAT) and Nuclear factor Kappa B (NFκB) which are three transcription factors important for the regulation of cytokine production including IL-2. The activation of the Ras/MAPK pathway by Grb2 is another important pathway that plays an important role in T-cell development and activation by activating the Extracellular signal-regulated kinase (ERK) (Salojin, Zhang et al. 2000; Werlen and Palmer 2002). Sustained signalling required for complete T-cell activation is thought to be achieved by a positive feedback loop activating ERK. ERK will phosphorylate serine residues in Lck barring the recruitment of the SHP-1 (a phosphatase used to dephosphorylate Lck and inhibit activation). Lck is no longer de-phosphorylated and the T-cell signalling cascade can continue (Stefanova, Hemmer et al. 2003).

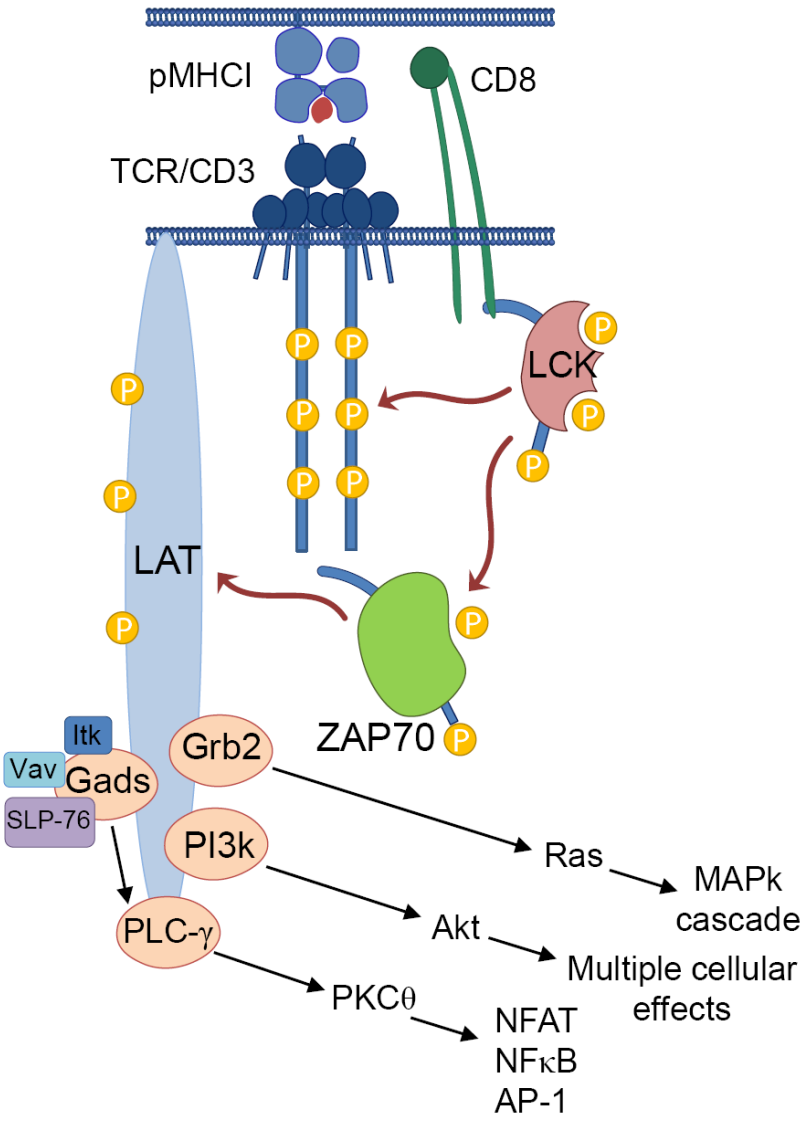

Figure 1.7: A model of T-cell activation. TCR stimulation via pMHCI results in phosphorylation of CD3 chain ITAMs by kinases such as Lck. Diphosphorylated ITAMs recruit ZAP-70 which is in turn phosphorylated by Lck. ZAP-70 then phosphorylates LAT. LAT recruits various adaptor molecules which in turn activates multiple protein cascades and transcription factors.

1.4.5 Cytoskeletal rearrangement

The Vav-1 protein which interacts with ZAP-70 contains a domain known to be involved in binding to the actin cytoskeleton. TCR/pMHC engagement leads to recruitment of Vav-1 and adaptor proteins that stimulate the polymerisation of filamentous actin. Once actin is polymerised, cytoskeletal movement takes place that facilitates the coalescence of membrane rafts, TCR clustering and Supramolecular activation clusters (SMAC) formation providing a dynamic scaffold for TCR signalling (Mak and Saunders 2005). Actin polymerisation promotes the assembly of signalling microclusters at the periphery of the immunological synapse and drives their centripetal flow toward the central-supramolecular activation cluster (c-SMAC) (see section 1.6) (Burkhardt, Carrizosa et al. 2008).

1.5 Plamsa membrance lipid rafts

The plasma membrane of T-cells is made up of a combination of phospholipids and proteins organised as glycolipoprotein microdomains termed lipid rafts. These phospholipids are rich in glycosphingolipids and protein receptors (Thomas, Kumar et al. 2004). These lipid rafts are specialised membrane microdomains which have important roles in T-cell signalling events. The post-translational addition of lipids by myristylation, palmitoylation or farnesylation can target proteins to lipid rafts within the plasma membrane (Viola 2001). It has been suggested that one way to consider a lipid raft is that they form concentrating platforms for individual receptors activated by ligand binding (Simons and Toomre 2000). Evidence from several studies have suggested that lipid rafts will cluster upon T-cell activation and that this is an essential feature in the formation of an immunological synapse (Janes, Ley et al. 2000; Langlet, Bernard et al. 2000). Several kinase molecules are recruited

to lipid rafts which are essential for T-cell activation. These include Lck and Csk (Resh 1994). Upon T-cell activation Csk is dephosphorylated and is removed from the lipid rafts (Cary and Cooper 2000; Latour and Veillette 2001). Also removed from lipid rafts on T-cell activation is CD45 molecule which would otherwise be inhibitory to full T-cell activation (Hermiston, Xu et al. 2003). Cytoplasmic proteins including ZAP-70, Vav-1, PLC-γ1, Grb2, PI3K and also LAT are also associated with lipid rafts upon T-cell activation (Xavier, Brennan et al. 1998; Harder and Kuhn 2000; Simons and Toomre 2000). Therefore raft binding recruits proteins to a new microenvironment where the phosphorylation state can be modified by local kinases and phosphatases and thus are acting as specialised membrane microdomains which are preferential sites for T-cell signalling.

1.6 Formation of the immunological synapse

The interface or contact zone between the T-cell and the APC where membrane protein re-organisation occurs is referred to as the immunological synapse (IS), a site which favours T-cell signalling (Lee, Holdorf et al. 2002). Rapid polarisation of molecules by the accumulation of stabilised lipid rafts and triggered TCR/pMHC complexes to the centre of the contact zone is observed (as reviewed in (Delon and Germain 2000; Bromley, Burack et al. 2001). This structure is also referred to as being the SMAC. This structure becomes highly stable which can explain the long TCR/pMHC contact time (Monks, Freiberg et al. 1998). SMACs have two discrete zones. The innermost ring, known as the central zone (c-SMAC) contains the TCR, MHC and co-receptors (CD4 or CD8) and also accessory molecules such as CD28 and CD2. The c-SMAC also contains the lipid rafts, which include additional enzymes and molecules required for signal transduction and co-stimulation (section 1.5). There are multiple changes to the actin cytoskeleton that are established by adhesive contacts

and extended by co-stimulatory molecules. Surrounding the central zone is a second zone, the peripheral-SMAC (p-SMAC) which is enriched for the integrin LFA-1 (Monks, Freiberg et al. 1998; Grakoui, Bromley et al. 1999). The p-SMAC contains outer and inner p-SMAC layers and it is these layers that ensure the T-cell and APC remain in prolonged contact sufficient to complete signal transduction.

The full and precise role of the IS is still unclear. Freiberg and colleagues suggested that pre-SMAC signals are sufficient to activate cell adhesion but not productive T-cell responses which require orchestrated signalling in SMACs (Freiberg, Kupfer et al. 2002). However data suggests that T-cells can still activate intracellular kinase signalling prior to the formation of the IS suggesting that many hours of T-cell signalling are not required for T-cell activation (Davis and van der Merwe 2001; Lee, Holdorf et al. 2002). This is further supported by data suggesting that immediately after pMHC recognition and prior to formation of the c-SMAC, hundreds of T-cell receptor microclusters (TCR-MC), containing the TCR and signalling molecules (kinases and adaptor proteins) are generated and function as a signalasome to transduce the initial signals for T-cell activation (Bunnell, Hong et al. 2002; Campi, Varma et al. 2005; Yokosuka, Kobayashi et al. 2008). After their generation, TCR-MCs move toward the centre of the IS and generate the c-SMAC. TCRs are internalised at the c-SMAC and TCR signalling is terminated. TCR-MCs are generated continuously at the periphery resulting in a sustained activation signal. Therefore the translocation of TCR-MCs from the periphery maintains the balance between the generation of new TCR-MCs and their degradation at the c-SMAC and is critical in sustaining T-cell activation (Varma, Campi et al. 2006; Yokosuka, Kobayashi et al. 2008).

1.7 T-cell co-stimulation

Accessory signals generated during TCR/pMHCI engagement leads to enhanced survival and proliferation signals. The signal generated through the TCR/CD3 complex is termed signal 1 whereas the signal generated through co-stimulatory molecules is termed signal 2 (Baxter and Hodgkin 2002). There is also evidence of a signal 3 which is provided by IL-12 cytokine stimulation in $CD8^+$ T-cells and by the cytokine IL-1 in $CD4^+$ T-cells (Curtsinger, Schmidt et al. 1999). The absence of necessary accessory signals upon T-cell activation results in T-cell death and apoptosis (Kabelitz and Janssen 1997). Multiple co-stimulatory molecules are associated with full T-cell activation including CD28 (Thompson, Lindsten et al. 1989) and CD2 (Howard, Moingeon et al. 1992). Other co-stimulatory molecules do exist but are less well studied such as the TNF receptor superfamily and CD27.

1.8 Co-receptors CD8 and CD4

The CD4 and CD8 molecules were initially identified as phenotypic markers on T lymphocytes restricted by MHCII and MHCI proteins, respectively. Treatment of T-cells with anti-CD4 or anti-CD8 antibodies resulted in the blockade of Th-cell and $CD8^+$ T-cell activation, respectively (MacDonald, Glasebrook et al. 1982). Subsequent data suggested that CD4 and CD8 were functional components of the T-cell antigen recognition machinery. CD4 and CD8 physically engage the same ligand as the TCR and thereby "co-receive" this ligand (Meuer, Schlossman et al. 1982). This unique role resulted in these glycoproteins being called "co-receptors" (Janeway 1992). CD4 or CD8 binding to MHC facilitates downstream proximal signalling events triggered by TCR ligation through interaction with the Lck (Rudd, Trevillyan et al. 1988; Veillette, Bookman et al. 1988). Both CD4 and CD8 are involved in

thymic development and selection of either $CD4^+$ or $CD8^+$ T-cells by their association with Lck (Fung-Leung, Schilham et al. 1991; Rahemtulla, Fung-Leung et al. 1991).

1.8.1 CD8 and CD4 structure

CD4 and CD8 both interact with structurally homologous sites on their respective MHC ligands using basic immunoglobulin domains. These domains are arranged quite differently in the two molecules (Zamoyska 1998). CD8 is a transmembrane, disulfide-linked glycoprotein that exists on the cell surface in either αα homodimeric or αβ heterodimeric form (Ledbetter, Seaman et al. 1981; Norment and Littman 1988; Terry, DiSanto et al. 1990). Each chain consists of a short cytoplasmic region, a single transmembrane domain, a long glycosylated stalk region and a globular variable Immunoglobulin-like domain. The αβ isoform of CD8 is exclusively expressed by conventional MHCI-restricted αβ T-cells. In contrast, the CD8αα homodimer has a more promiscuous expression pattern in both humans and rodents; distinct lymphoid cells, such as intra-epithelial lymphocytes (IELs), γδ T-cells and NK cells, and also certain myeloid cell types, all express the αα isoform of CD8 (Zamoyska 1994; Gangadharan and Cheroutre 2004; Gibbings and Befus 2009). The CD8 α and β chains are encoded by distinct genes that are physically linked and are predicted to show conserved overall structural topology although they share only approximately 20% residue identity (Parnes 1989). Both chains have an immunoglobulin like amino terminal domain. This domain is linked by an extended polypeptide region which contains a number of O-linked sugars to the transmembrane domain (Zamoyska 1998). Crystal structures currently solved reveal that the amino-terminal immunoglobulin like domains fold very similarly to an Fv-like homodimer (Zamoyska 1998). CD4 however is a single polypeptide

which consists of four external immunoglobulin-related domains D1 to D4 (Wang, Yan et al. 1990; Lange, Lewis et al. 1994; Brady and Barclay 1996; Wu, Kwong et al. 1997). There is a unique strand topology between domains 1 and 2 (D1 and D2) and between domains 3 and 4 (D3 and D4) (Zamoyska 1998) and due to interactions between adjacent D4 domains, this may allow for CD4 to dimerise on the cell surface (Wu, Kwong et al. 1997). There is also a hydrophobic transmembrane domain, and a highly basic cytoplasmic tail which contains three serine residues which can be phosphorylated (Mak and Saunders 2005).

1.8.2 pMHCI/CD8 interaction

The involvement of CD8 in the recognition of target cells by $CD8^+$ T-cells was appreciated prior to the identification of the TCR. Early reports showed that antibodies recognizing either the α or β sub-unit of CD8 were able to block the killing of target cells by $CD8^+$ T-cells *in-vitro* (Nakayama, Shiku et al. 1979; Ledbetter, Seaman et al. 1981). This hinted that CD8 was involved in the molecular process of antigen recognition. CD8 binds MHCI molecules via interactions with largely non-polymorphic amino acid residues situated in the α3 and to a lesser extent the α2 domain of the heavy chain and β_2-microglobulin (Salter, Norment et al. 1989; Salter, Benjamin et al. 1990). Gao and colleagues solved the co-crystal structure of the human pMHCI/CD8αα interaction confirming the binding interactions that had been classified previously (Figure 1.8). Similarly to the TCR, CD8 contains a number of flexible complementarity determining loops (CDR) that are involved in MHCI binding. Gao *et al* showed that the interaction between the CDR3 loops of human CD8αα (residues 51-55) and a finger-like loop in the α3-domain of HLA-A*0201 (residues 223-229) form the main contact zone of the complex by clamping asymmetrically, with each dimer contributing differently to the overall binding (Gao, Tormo et al. 1997). Although murine CD8αα binds to H2-K^b in a

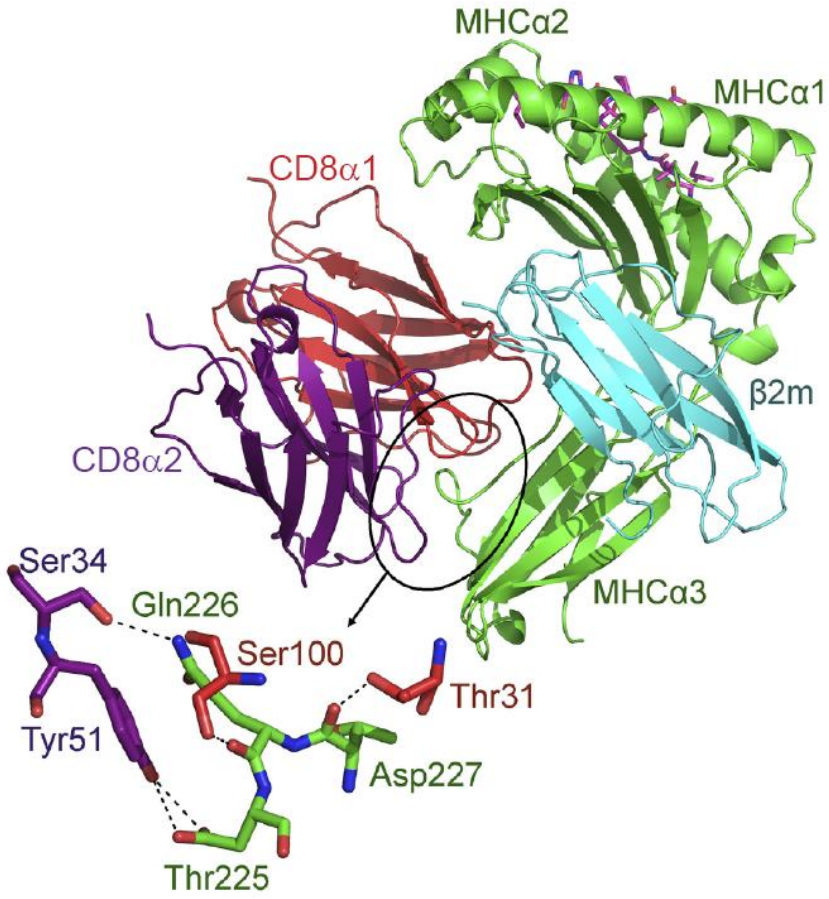

Figure 1.8: Overview of the molecular interactions between human CD8αα and MHCI molecule. CD8αα is shown in red (α1) and purple (α2), binding mainly to the α3 domain of MHCI (green). The CDR like loops of the CD8 molecule binds the MHCI α3 domain at residues 223–227 forming the main binding interface. When enlarging this interface between CD8 and MHCI the two CDR like loops of the CD8 molecule form a "clamp" - like topology around the MHCI loop encompassing residues 223–227 of the α3 domain. The most important contacts are made between the CD8 α1 chain Thr31/Ser100 and the MHCI α chain Gln226/Asp227 and between the CD8 α2 chain Ser34/Tyr51 and the MHCI α chain Thr225/Gln226. Figure taken from (Laugel et al 2011). © 2013 by the Society for Leukocyte Biology.

similar overall fashion compared to human CD8αα/HLA-A*0201 interaction (Kern, Teng et al. 1998), there are some key differences in the fine specificity of the two interactions. For example, in the murine system; more contacts are made between CD8 and the MHCI α3-domain, at the interface between CD8 and the MHCI α2-domain a number of unique bonds are formed between the interface between CD8 and β_2m. These differences may explain the higher binding affinity of murine CD8 compared human CD8 for their species specific MHCI (Purbhoo, Boulter et al. 2001).

Gao *et al* predicted, based on electrostatic surface analysis of the human pMHCI/CD8αα, that the CD8β chain would replace the CD8α2 subunit (Gao, Tormo et al. 1997). This was also supported by data suggesting that mutating the CD8α chain severely impaired binding whereas a similar mutation in the CD8β chain did not (Devine, Sun et al. 1999). The orientation of the human CD8αβ heterodimer in complex remained speculative until Wang and colleagues solved the co-crystal structure of the murine CD8αβ in complex with H-2D^d (Wang, Natarajan et al. 2009). This study demonstrated that the binding mode of the CD8αβ heterodimer was largely homologous with CD8αα (Wang, Natarajan et al. 2009). The CDR-like loops of the CD8αβ predominantly bound to the conserved H-2D^d α3 domain Importantly, the H-2D^d/CD8αβ co-complex also revealed that CD8αβ adopted a single orientation, with the β chain in the equivalent position of the CD8α1-chain proximal to the T-cell membrane, and the CD8α chain in the equivalent position of the CD8α2 chain in the T-cell distal position (Wang, Natarajan et al. 2009), in contrast to the prediction made by Gao *et al*. However, it is important to note that Gao *et al* had made that hypothesis based on the human pMHCI/CD8αα interaction. Key differences exist between the murine pMHCI/CD8αα and pMHCI/CD8αβ complexes. For example, CD8αβ does not make contact with the α2 and

β_2m domains of H-2D^d which reduces the buried surface area of this complex compared to murine pMHCI/CD8αα (Wang, Natarajan et al. 2009).

1.8.3 Low solution binding affinity of the pMHCI/CD8 interaction

The average human pMHCI/CD8αα interaction exhibits very low solution binding affinities (K_D ~146 μM) (Table 1.1) and is characterised by extremely rapid kinetics (K_{off} ~18 s^{-1}) (Wyer, Willcox et al. 1999; Gao, Willcox et al. 2000; Cole, Dunn et al. 2008). Despite these seemingly unfavourable binding characteristics, the engagement of MHCI molecules by CD8 at the cell surface both enhances the association rate of pMHCI complexes with TCRs and increases the half-life of cognate TCR/pMHCI interactions (Gakamsky, Luescher et al. 2005; Wooldridge, van den Berg et al. 2005; Laugel, van den Berg et al. 2007). It seems unlikely that the striking biophysical characteristics of the pMHCI/CD8 interaction have occurred by accident and it has been hypothesised that the kinetics are essential for maintaining antigen specificity. However, to date there has been no study to probe the significance of the low solution binding affinity that characterises the pMHCI/CD8 interaction. This will be addressed in chapter 3.

It is interesting to note that the average murine pMHCI/CD8 interaction is significantly stronger (K_D ~ 30μM) (Table 1.2 A&B) than the equivalent human interaction (K_D ~ 146μM) (Purbhoo, Boulter et al. 2001). Murine studies have concluded that CD8αα and CD8αβ bind murine pMHCI with similar affinity (Sun and Kavathas 1997) (Arcaro, Gregoire et al. 2001; Wang, Natarajan et al. 2009).

1.8.4 MHCII/CD4 interaction

The N-terminal immunoglobulin-like domains of CD4 interact with the non-polymorphic α2 and β_2 domains of MHCII. This interaction mediates both recognition and adhesive functions of the CD4 Th-cell. The cytoplasmic tail of the CD4 has sites that facilitate the physical association with Lck (Mak and Saunders 2005).

1.8.5 CD8/CD4 T-cell activation profiles

On recognition of specific pMHCI, $CD8^+$ T-cells become activated, as outlined above, then subsequently kill the target cell. The principal mechanism of killing is through the release of pre-formed cytotoxic granules which contain perforin and granzyme

Table 1.1: Binding affinities of human CD8αα to pMHCI using surface plasmon resonance. # values are averages from cited studies

Human pMHCI/human CD8αα	K_D (μM)
HLA-A*0201-GILGFVFTL (Wyer, Willcox et al. 1999; Cole, Dunn et al. 2008)	166#
HLA-A*0201-FIDSYICQV (Wyer, Willcox et al. 1999)	173
HLA-A*0201-VLHDDLLEA (Wyer, Willcox et al. 1999)	107
HLA-A*0201-ILKEPVHGV (Wyer, Willcox et al. 1999)	126
HLA-A*0201-ILAKFLHWL (Cole, Dunn et al. 2008)	183
HLA-A*0201-SLLMWITQC (Cole, Dunn et al. 2008)	125

HLA-A*0201-YLEPGPVTV (Cole, Dunn et al. 2008)	144
HLA-A*0201-LLFGYPVYV (Cole, Rizkallah et al. 2007; Cole, Dunn et al. 2008)	149[#]
HLA-A*1101-AIFQSSMTK (Gao, Willcox et al. 2000)	100
HLA-A*2402-PYLFWLAAI (Cole, Rizkallah et al. 2007; Cole, Dunn et al. 2008)	154[#]
HLA-B*0801-FLRGRAYGL (Cole, Dunn et al. 2008)	135
HLA-B*3501-TPEGIIPTL (Gao, Willcox et al. 2000)	130
HLA-C*0702-KYFDEHYEY (Gao, Willcox et al. 2000)	220
Average CD8αα K_D (μM)	146

Table 1.2 A: Binding affinities of murine CD8αα to pMHCI using surface plasmon resonance. [#] values are averages from cited studies.

Murine pMHCI/murine CD8αα	K_D (μM)
H-2K[b]-SIINFEKL (Leishman, Naidenko et al. 2001)	91.6
H-2K[b]-IFSK8 (Wang, Natarajan et al. 2009)	34.7
H-2K[b]-VSV8 (Kern, Hussey et al. 1999)	64[#]
H-2K[b]-RGYVYQGL (Garcia, Scott et al. 1996)	39.3
H-2K[b]-OVA (Garcia, Scott et al. 1996)	30.4
H-2K[d]-P18I10 (Wang, Natarajan et al. 2009)	6.7

Average CD8αα K_D (μM)	44

Table 1.2 B: Binding affinities of murine CD8αβ to pMHCI using surface plasmon resonance. # values are averages from cited studies.

Murine pMHCI/murine CD8αβ	K_D (μM)
H-2K^b-SIINFEKL (Leishman, Naidenko et al. 2001)	135
H-2K^b-IFSK8 (Wang, Natarajan et al. 2009)	38.4
H-2K^b-VSV8 (Kern, Hussey et al. 1999)	40$^{\#}$
H-2K^b-RGYVYQGL (Garcia, Scott et al. 1996)	11.8
H-2D^b-FAGHNLDLI (Garcia, Scott et al. 1996)	14.1
H-2K^b-OVA (Garcia, Scott et al. 1996)	14
H-2K^d-SYIPSAEK (Arcaro, Gregoire et al. 2001)	99
H-2K^d-P18I10 (Wang, Natarajan et al. 2009)	8.2
H-2L^d-p2Ca (Garcia, Scott et al. 1996)	11.2
Average CD8αβ K_D	41

(Podack, Konigsberg et al. 1985). Perforin creates pores in the membrane of the target cell which can allow the transition of granzymes into the target cell inducing apoptosis (Heusel, Wesselschmidt et al. 1994). A new model of killing was suggested by Pipkin *et al*. Here perforin creates pores in the membrane of the target cell which allow an influx of Ca^{2+}, then granzymes are endocytosed by the target cell and induce apoptosis (Pipkin and Lieberman 2007). $CD8^+$ T-cells can also induce killing through the interaction between the Fas-death receptor on the target cell (CD95), and its counterpart on the T-cell surface FasL (CD95L) (Bossi and Griffiths 1999). The Fas-FasL interaction allows for dimerisation of procaspases which induce apoptosis (Thorburn 2004). Activated $CD8^+$ T-cells can differentiate into two effector phenotypes (Tc1 and Tc2) each with different cytokine profiles and both of which are cytotoxic. The cytokine profile expressed by $CD8^+$ effector Tc1 cells is similar to that seen of the Th1 subset of $CD4^+$ T-cells (Kelso and Glasebrook 1984; Fong and Mosmann 1990). These include IFN-γ, TNF-α and IL-2 (Mosmann, Li et al. 1997). $CD8^+$ T-cells also release a broad profile of chemokines, including Macrophage Inflammatory Protein-1α (MIP-1α), Macrophage Inflammatory Protein-1β (MIP-1β) and Regulated on Activation, Normal T Expressed and Secreted (RANTES) among others. Data does suggest the some $CD8^+$ T-cells, Tc2 cells, have been shown to release IL-4, IL-5 and IL-10, common Th2 response cytokines, when patients are infected with leprosy (Salgame, Abrams et al. 1991; Mosmann, Li et al. 1997).

$CD4^+$ Th-cells play an important role in the activation and co-ordination of $CD8^+$ T-cell and B-cell responses. $CD4^+$ Th-cells can be classified into different subsets which have different roles and are characterised by different cytokine and chemokine profiles. Th1 responses are characterised by the secretion of IL-2, IFN-γ and lymphotoxin. IL-2 is a T-cell growth factor

and is important for the proliferation of activated $CD8^+$ T-cells (Morgan, Ruscetti et al. 1976). IFN-γ release by a Th1 response is believed to activate the anti-microbial activity of macrophages (Taylor, Martinez-Pomares et al. 2005). Th2 responses are characterised by the production of IL-4, IL-5, IL-6 and IL-13 which results in the activation of the B-cell antibody response (Salgame, Abrams et al. 1991) and influences the isotype switching of antibodies (Tangye, Ferguson et al. 2002). Another Th subset known as Th17 are characterised by the production of IL-17, IL-21 and IL-23 which result in the activation and migration of neutrophils (Weaver, Harrington et al. 2006). This thesis is concerned with the role of CD8 in $CD8^+$ T-cell activation and the introduction from this point will concentrate on aspects of CD8 roles and functions.

1.8.6 The co-receptor model of CD8 function

It was initially suggested that CD8 binds to MHCI independently of the TCR/pMHCI interaction subsequently increasing the binding affinity of the T-cell for the target cell and allowing T-cells to respond to lower numbers of antigen. This was also known as the accessory molecule hypothesis (Marrack, Endres et al. 1983; Gay, Coeshott et al. 1986; Bierer, Sleckman et al. 1989). The accessory molecule theory was replaced by Janeway et al who proposed the co-receptor model for CD8 function. The co-receptor model suggested that CD8 is a physical component of the TCR complex contributing directly to signal transduction on T-cell activation, and for optimal T-cell activation both CD8 and the TCR must bind to the same pMHCI molecule at the APC surface. Hence, Janeway suggested that it would be more appropriate to describe CD8 as a co-receptor rather than accessory molecule (Janeway 1988; Janeway 1989). The existence of a physical association between the TCR and CD8 on the T-cell surface was first suggested by studies using co-modulation (Takada and Engleman 1987),

co-precipitation (Beyers, Spruyt et al. 1992; Suzuki, Kupsch et al. 1992) and affinity chromatography (Gallagher, Fazekas de St Groth et al. 1989). One study actually suggests that the majority of TCRs are associated with CD8 (~90%) even in non-activated cells (Suzuki, Kupsch et al. 1992). Data also suggested that the TCR and CD8 can engage a single pMHCI molecule simultaneously because both bind at distant non-overlapping sites. In addition, studies demonstrated that when peptide is presented by targets bearing point mutations in the MHC Class I α3 domain loop mutations that knock out the pMHCI/CD8 interaction in a CD8-dependent setting, $CD8^+$ T-cell activation is lost (Potter, Rajan et al. 1989; Purbhoo, Boulter et al. 2001). $CD8^+$ T-cell antigen responsiveness is not restored by the presence of non-cognate pMHCI with intact CD8 binding sites in both human (Salter, Benjamin et al. 1990) or murine systems (Potter, Rajan et al. 1989; Connolly, Hansen et al. 1990; Schott and Ploegh 2002). Furthermore, the conserved α-chain connecting peptide motif (α-CPM), located on the membrane proximal domain of the TCR α-chain, facilitates the recruitment of CD8 in close proximity to the TCR/CD3 complex (Naeher, Luescher et al. 2002; Mallaun, Naeher et al. 2008) (Figure 1.9). All of this data highlighted that CD8 can form a physical part of the TCR complex and that CD8 and TCR could engage the same pMHCI complex at the same time which is critical for optimal T-cell activation.

1.8.7 Roles of CD8 in T-cell activation

Multiple roles for CD8 in T-cell activation have been highlighted. It was originally proposed that CD8 played the role of an adhesion molecule ensuring that the $CD8^+$ T-cell and the APC would bind together (Norment and Littman 1988). However, the weak solution binding affinity of the pMHCI/CD8 interaction excludes the possibility that CD8 plays a major role in T-cell/target cell adhesion.

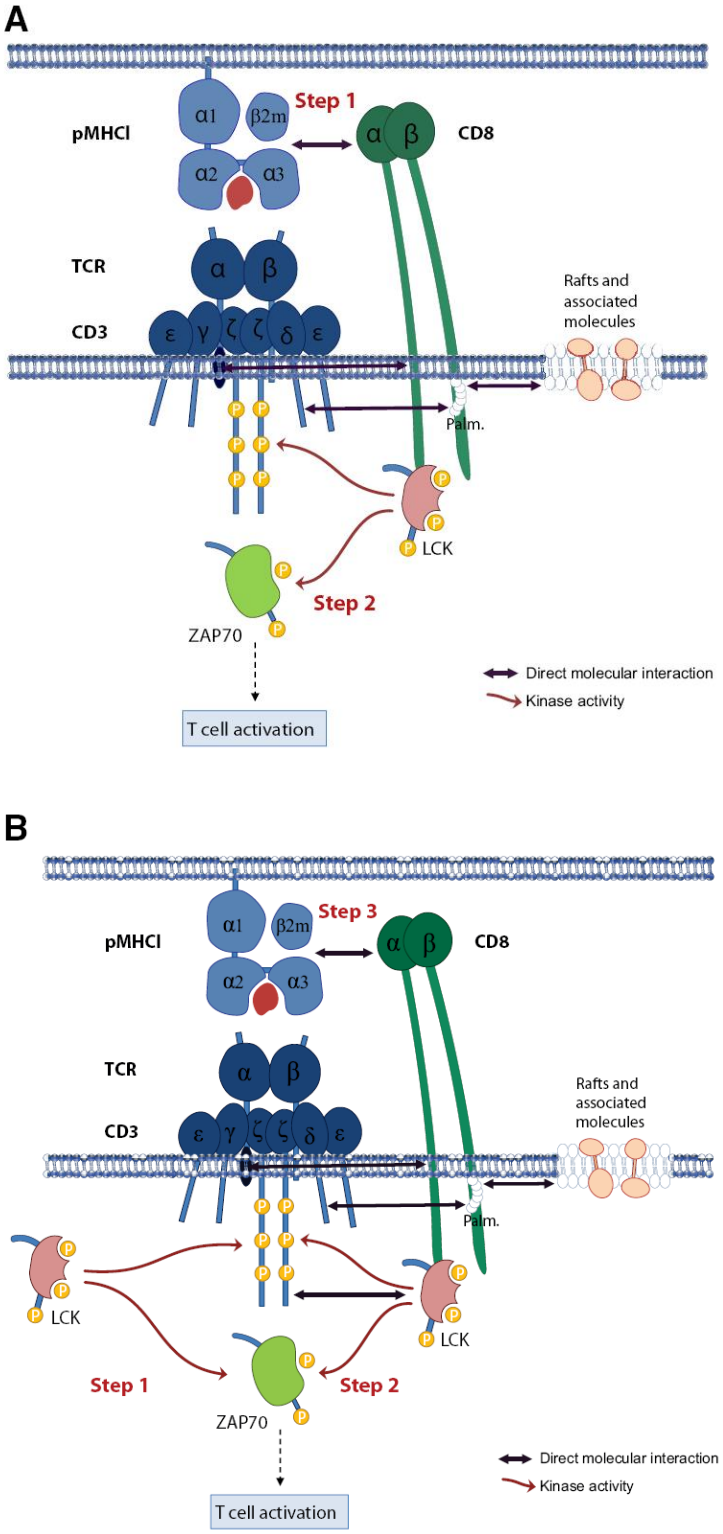

Figure 1.9: Schematic representation of CD8 co-receptor functions in early T-cell activation events. (**A**) The classical view of T-cell activation is that CD8 is recruited to the TCR complex before phosphorylation takes place and that Lck bound to the CD8α cytoplasmic tail catalyses the initial CD3-ζ ITAM phosphorylation events which then allow

for the recruitment of additional Lck molecules and signal amplification. (**B**) Alternatively recent experimental data favour a model whereby free Lck is responsible for the initial phosphorylation events. Phosphorylated CD3-ζ ITAMs then allow for the recruitment of Lck bound to CD8α in close proximity to CD3. In this scenario, the interaction between the TCR and CD8 occurs after the initial phosphorylation events and is driven intra-cellularly by interactions between CD3 and CD8α bound Lck. Figure taken from (Laugel, Cole et al. 2011).

Subsequently, it was suggested that CD8 plays a major role in stabilising the TCR/pMHCI interaction. Initial data suggested that the TCR/pMHCI off rate was significantly reduced in the presence of CD8 which led the authors to posit that CD8 may induce conformational changes to favour the TCR/pMHCI interaction (Garcia, Scott et al. 1996). However crystal structures of pMHCI/CD8αα revealed that there is no change in the TCR/pMHCI binding platform (Gao, Tormo et al. 1997) and also the presence of CD8 does not affect the TCR binding to the same pMHCI when analysed via SPR (Wyer, Willcox et al. 1999). More recent data using mutated pMHCI tetramers with altered CD8 binding have shown that CD8 has a role in altering TCR/pMHCI avidity at the T-cell surface (Wooldridge, Hutchinson et al. 2003; Wooldridge, van den Berg et al. 2005; Wooldridge, Scriba et al. 2006; Laugel, van den Berg et al. 2007). By abrogating the pMHCI/CD8 interaction both the tetramer association rate and the half-life of binding decreased compared to wild-type tetramers (Laugel, van den Berg et al. 2007). This study also showed that the intensity of steady-state tetramer binding was substantially reduced using CD8 null tetramers compared to wild-type reagents. These data highlight that, despite the weak pMHCI/CD8 interaction, pMHCI/CD8 binding has an important role in stabilizing the TCR/pMHCI complex at the cell surface. In support of this notion, a recent investigation by Jiang *et al*, using a novel approach for measuring the 2D binding affinity between TCR, pMHCI and CD8, demonstrates that the TCR and CD8 bind cooperatively to pMHCI which modulates antigen discrimination (Jiang, Huang et al. 2010).

CD8 has also been shown to play an extremely important role in T-cell signalling. The binding of CD8 to pMHCI drives the recruitment of CD8-associated Lck to the vicinity of an engaged TCR/CD3 signalling complex, resulting in phosphorylation of the CD3ζ ITAMs (Purbhoo, Boulter et al. 2001). This role is achieved through the association of the CD8 α

chain with Lck, via two vicinal cysteines, that interact through a zinc chelate complex to produce a co-activation signal (Veillette, Bookman et al. 1988; Turner, Brodsky et al. 1990). This interaction leads to a signalling cascade, which recruits ZAP-70 to the CD3/TCR complex leading to the amplification or enhancement of T-cell activation signals. Further studies into the nature of the TCR/CD8 interaction were revealed by the finding that the signalling role of the CD8 α chain can be enhanced by palmitoylation of the CD8 β chain at a membrane-proximal cysteine. This enables the co-receptor to interact directly with CD3δ and recruit TCR/CD3 complexes to membrane microdomains that promote signalling through the exclusion of inhibitory phosphatase proteins (Arcaro, Gregoire et al. 2000; Arcaro, Gregoire et al. 2001; Doucey, Goffin et al. 2003).

These lipid rafts are made up of ordered microdomains, enriched with sphingolipids and cholesterol which exclude molecules such as phosphatases (CD45), but recruit Lck and LAT; molecules vital to T-cell activation. Lipid raft formation is thought to allow Lck phosphorylation, mobilization of intracellular calcium and ZAP-70/CD3 activation to occur more efficiently, leading to a stronger co-activation signal (Zhang, Trible et al. 1998; Bosselut, Zhang et al. 1999; Bosselut, Kubo et al. 2000). Thus, the tripartite interaction between the TCR and CD8 with the same pMHCI molecule (Figure 1.9) allows the intracellular signalling domains of CD8 and the TCR/CD3 complex to interact, leading to T-cell activation (Grakoui, Bromley et al. 1999).

A recent study demonstrated a new role for CD8 in controlling levels of crossreactive peptide recognition by $CD8^+$ T-cells by examining recognition of combinatorial peptide libraries in the presence of altered MHC/CD8 interaction. This study made use of APCs that express

HLA-A2*0201 molecules mutated to interact with CD8 at slightly enhanced (K_D = 85 μM) (Wooldridge, Lissina et al. 2007), decreased (K_D = 500 μM) (Hutchinson, Wooldridge et al. 2003), normal (K_D = ~146 μM) or abrogated interaction with CD8 (K_D < 10,000 μM). A direct positive correlation between the pMHCI/CD8 binding affinity and the number of ligands eliciting T-cell activation was identified (Wooldridge, Laugel et al. 2010). These findings revealed that CD8 extends the range of pMHCI ligands that can be recognised by an individual cell surface-bound TCR, a feature that is essential for effective immune coverage.

In a recent study, Chervin *et al* found that activation of $CD8^+$ T-cells that expressed high and intermediate affinity TCRs (K_D 14 nM and 1.5 μM respectively) to pMHCI that lacked the ability to bind CD8 was greatly reduced compared to CD8-negative T-cells. The authors proposed that mechanism of CD8 inhibition is likely due to the sequestration of Lck. Even though the TCR has high-affinity for the pMHCI, engagement of the TCR alone without colocalisation of CD8 and associated Lck leads to impairment of T-cell activation (Chervin, Stone et al. 2009). This identifies a novel role for CD8 in T-cell activation where the ability of CD8 to sequester Lck maintains appropriate TCR-mediated MHC restriction in peripheral T-cell activity.

Despite recent advances in understanding CD8 biology, there are still aspects of CD8 function that we do not understand. For example, it is possible that CD8 can exert a novel focussing mechanism on T-cell recognition of antigen which has never been tested experimentally before (van den Berg and Rand 2007). A combination of all the described roles above are all important for T-cell activation, however which precise role dominates for successful T-cell activation is still unclear. In addition, we have failed to harness the potent

ability of CD8 to tune the antigen specific CD8 T-cell response which has immense therapeutic benefit. This thesis aims to address some of the remaining gaps in our knowledge.

1.8.8 Distinct functions of CD8αα versus CD8αβ

CD8αβ is exclusively expressed on Cytotoxic T-Lymphocytes (CTLs). The binding of the co-receptor to the pMHCI molecule drives the recruitment of CD8α cytoplasmic tail associated Lck (Veillette, Bookman et al. 1988). As a result of this association early hybridoma studies demonstrated that CD8αα was enough to restore co-receptor function leading Gabert *et al.* (Gabert, Langlet et al. 1987) to question the role of the CD8β chain. However subsequent studies demonstrated that CD8αβ functions as a more efficient co-receptor than CD8αα (Wheeler, von Hoegen et al. 1992; Renard, Delon et al. 1996; Holler and Kranz 2003) and can actually broaden the range of T-cell antigen recognition (Karaki, Tanabe et al. 1992). At first the exact mechanism by which CD8β endows CD8 with efficient co-receptor function was unclear. Initially, it was thought that the CD8β chain contributed this increased function by increasing the strength of the pMHCI/CD8 interaction however cell-cell adhesion assays and SPR studies found that MHCI molecules interact with CD8αα and CD8αβ with similar affinities (Garcia, Scott et al. 1996; Sun and Kavathas 1997). It was then posited that the CD8β chain increased co-receptor function by increasing TCR/pMHCI binding which would enhance the association of the CD8α chain with essential signalling molecules such as Lck and LAT (Irie, Ravichandran et al. 1995; Renard, Romero et al. 1996; Bosselut, Zhang et al. 1999). Arcaro *et al* then provided key data showing that these effects are mediated by palmitoylation of the CD8β chain which allows association with membrane microdomains called lipid rafts. Interaction between CD3δ and CD8 ensures that palmitoylation of the CD8β also enriches TCR in these domains. Lipid rafts act as privileged sites T-cell signal

transduction because they are enriched in signalling machinery and exclude negative phosphatases such as CD45. Thus, CD8β-mediated enrichment of TCR in lipid rafts has an important positive effect on TCR-mediated signal transduction (Arcaro, Gregoire et al. 2000; Arcaro, Gregoire et al. 2001; Doucey, Goffin et al. 2003).

In contrast, CD8αα is expressed on a specialised subset of IELs associated with the gut, γδ T-cells, NK cells (Gangadharan and Cheroutre 2004) or memory αβ T-cells (Madakamutil, Christen et al. 2004). CD8αα has also been shown to possess a strong preference to interact with the thymic leukaemia antigen (TL), a β_2M independent non-classical MHCI expressed by epithelial cells of the small intestine. This interaction modifies signalling via the TCR which results in reduced proliferation and cytotoxicity but enhanced IEL cytokine production. As a result CD8αα T-cells can provide protection without destroying the epithelial cell layer. This suggests that CD8αα may play more of an immunomodulatory role (Leishman, Naidenko et al. 2001; Liu, Xiong et al. 2003). CD8αα has also been shown to be up-regulated when a subset of conventional CD8αβ T-cells are activated and survive and differentiate into memory precursor cells (Madakamutil, Christen et al. 2004). Therefore CD8αα and CD8αβ have distinct functions. CD8αβ functions as a more efficient co-receptor than CD8αα (Holler and Kranz 2003), allowing for a wider range of agonists available for recognition by the TCR (Karaki, Tanabe et al. 1992). In contrast, CD8αα has been suggested to play a more immunomodulatory role. (Leishman, Naidenko et al. 2001) (Liu, Xiong et al. 2003).

1.8.9 Models of co-receptor function

The timing of the co-receptor activity during pMHCI recognition is crucial for a full understanding of the mechanics involved in this process. CD8 and TCR have been shown to be constitutively associated on resting primary $CD8^+$ T-cells suggesting that pre-existing bi-specific receptors might engage pMHCI agonist ligands in a co-ordinate manner (Beyers, Spruyt et al. 1992; Suzuki, Kupsch et al. 1992; Doucey, Goffin et al. 2003; Demotte, Stroobant et al. 2008). Studies of the interaction between CD8 and TCR/CD3 using forster resonance energy transfer (FRET) technique suggest a chronological binding event. It was shown that the TCR binds to the pMHCI molecule first followed by the recruitment of the CD8 molecule subsequently (Yachi, Ampudia et al. 2005; Yachi, Ampudia et al. 2006). This data suggests that the TCR will perform an antigen-specific proof reading event. This will then ensure that signalling cascades activated by the CD8 co-receptor will only occur when the TCR will bind the pMHCI with suitable affinity and kinetics. This serves to discriminate between agonist and non-agonist pMHCI complexes with the recruitment of the CD8 only being enabled on encounter of TCR with agonist pMHCI.

1.9 T-cell receptor triggering

The process by which TCR binding to pMHCI molecules leads to phosphorylation events in the cytoplasmic tail of the TCR/CD3 complex is referred to as TCR triggering. Considerable controversy about the mechanisms of TCR triggering still exist with multiple mechanisms proposed to explain the process (van der Merwe and Dushek 2011). To evaluate possible models of TCR triggering, it is important to consider some unique features that distinguish it from other cell-surface receptor recognition events. First, TCR triggering is highly sensitive

allowing T-cells to sense a single pMHCI (Sykulev, Joo et al. 1996; Irvine, Purbhoo et al. 2002; Purbhoo, Irvine et al. 2004). Second, the TCR is able to discriminate between very similar ligands and binds to self peptide-MHC molecules or altered peptides with a range of affinities to produce different responses. Third, the TCR differs from other receptors due to the enormous structural diversity that exists between the interface of a TCR and pMHCI complex (van der Merwe and Dushek 2011). Several mechanisms to explain TCR triggering have been proposed:

1.9.1 Aggregation model

This model can be separated into two models that account for aggregation of the TCR/CD3 complex following TCR engagement: (i) The co-receptor *heterodimerisation* model suggests that CD4 and CD8 co-receptor can bind to the same agonist pMHCI complex as the TCR which will recruit co-receptor associated Lck into close proximity with the CD3 associated ITAMs to mediate phosphorylation as reviewed in (Trautmann and Randriamampita 2003). (ii) The *pseudodimer* model suggests a role for self pMHCI molecules in TCR triggering (Irvine, Purbhoo et al. 2002; Krogsgaard, Li et al. 2005). According to this model, one TCR can bind an agonist pMHCI molecule and a second TCR binds a self pMHCI molecule. Dimerisation is enhanced when the co-receptor associated with the TCR that is complexed with self pMHC binds to the agonist pMHCI molecule. A pseudodimer is then formed by the dual interaction of a second TCR with the self pMHC and its co-receptor with the agonist. This model then predicts that self pMHCI molecules would enhance TCR triggering as reviewed in (van der Merwe and Dushek 2011).

1.9.2 Conformational change model

Several models have been proposed which suggest conformational change as a mechanism for TCR triggering. Conformational change models describe the changes in the CD3 cytoplasmic domains upon TCR/pMHCI interaction. Recent data suggests that differences in mechanical effects of the TCR/pMHCI interaction such as a pulling or shearing forces can induce TCR triggering (Li, Chen et al. 2010; Sun, Kim et al. 2001; Choudhuri and van der Merwe 2007). This could be generated as a result of the small size of the TCR/pMHCI complex which would generate a force as large molecules are either compressed or removed from the contact area (van der Merwe 2001). It has been proposed that TCR/pMHCI binding could push and/or twist the TCR (Davis 2002; Kuhns, Davis et al. 2006). Mechanical pulling is suggested when TCR/pMHCI binding leads to a piston like movement of the CD3 cytoplasmic tails, relative to the plasma membrane that could alter the conformation. Also the pulling could induce a conformational change in the structure of the CD3 ecto-domains and/or transmembrane domains that leads to clustering of the engaged TCR/CD3 complex with other TCR/CD3 complexes (van der Merwe and Dushek 2011) which in turn would enhance kinase activity. The conformational change in the cytoplasmic region of the TCR/CD3 complex is determined by the dissociation of ITAMs from phospholipids in the cell membrane exposing them to phosphorylation (reviewed in (van der Merwe and Dushek 2011).

1.9.3 Segregation and redistribution model

The kinetic segregation model predicts that upon TCR/pMHCI recognition TCR/CD3 complexes are trapped in close contact zones, which exclude larger inhibitory tyrosine

phosphatases such as CD45, leading to stable phosphorylation of TCR/CD3 ITAMs by Lck. The lipid raft model predicts that TCR/pMHCI recognition leads to an association of TCR/CD3 complex with lipid rafts which are privileged sites for phosphorylation.

Van der Merwe and Dushek suggest that TCR triggering can be induced by any mechanism that aids the complex in favour of phosphorylation. They suggest that, aggregation, segregation, conformational change and clustering of TCR are all involved in the TCR triggering event (van der Merwe and Dushek 2011). A recent study by Manz and colleagues provide new data on TCR triggering. They show that T-cell triggering thresholds are modulated by the number of activating ligands available to individual TCR clusters, not by the total amount encountered by the cell. They also demonstrated that the minimal triggering unit is at least four pMHC in a single cluster when measuring activity by Ca^{2+} (Manz, Jackson et al. 2011). Overall, the precise mechanism of this initial triggering event still remains elusive.

1.9.4 TCR triggering/kinetics and co-receptor dependency

To achieve efficient T-cell signalling then the TCR/pMHCI interaction must be of long enough duration to allow for a series of ordered phosphorylation events of the CD3-ζ chains (McKeithan 1995; Rabinowitz, Beeson et al. 1996; Kersh, Shaw et al. 1998). It has been postulated previously that the TCR is a T-cell signalling unit which can trigger T-cell activation in the complete absence of CD8 suggesting that the co-receptor is not required for TCR triggering to occur (Janeway 1992). Recent work by Van der Merwe and Dushek, support this theory by demonstrating that TCR triggering can occur in the complete absence

of co-receptors and agonist pMHCI monomers cannot induce TCR triggering. As a result they state that the co-receptor heterodimerisation model is not sufficient for TCR triggering (Locksley, Reiner et al. 1993; Schilham, Fung-Leung et al. 1993; van der Merwe and Dushek 2011). Kinetic models of TCR triggering such as kinetic segregation model also suggest that the co-receptor only plays a role in amplifying signals from already triggered TCRs and not in the primary initial signalling event (van der Merwe and Davis 2003).

Data does suggest however that CD8 may indeed be playing a role in the TCR triggering event. The off-rate (k_{off}) of the TCR/pMHCI interaction and hence its half life, is the principal kinetic feature that determines the feature of biological outcome. CD8 has been shown to generate a stabilising factor that preferentially increases the predicted TCR triggering rate suggesting an important role for CD8 in T-cell triggering and controlling T-cell crossreactivity (Wooldridge, van den Berg et al. 2005). When further studying the kinetics of the CD8 molecule, Gakamsky *et al* found that the CD8 molecule kinetically promotes ligand binding to the TCR (Gakamsky, Luescher et al. 2005). It is important that we undertake further studies to define the role of CD8 in TCR triggering (discussed in chapter 6).

1.10 The physiological importance of CD8 in $CD8^+$ T-cell biology

The biochemical mechanisms involved during $CD8^+$ T-cell responses and activation to antigens have been extensively studied and provide a wealth of data. However the only firmly proven physiological role for CD8 is with regards to the events that transpire during thymic development and T-cell selection in the thymus (see section 1.3.3).

Evidence however does suggest that CD8 helps in driving the priming and expansion of $CD8^+$ T-cell clonotypes with low functional avidities for cognate antigen which will enhance the clonotypic diversity of $CD8^+$ T-cell responses to microbial and potentially against self determinants in an autoimmune system. This was supported by Price *et al* where they showed that *ex-vivo* activation of sub-dominant $CD8^+$ T-cell clonotypes specific for epitopes derived from Epstein-Barr virus and human cytomegalovirus relied more heavily on CD8 engagement compared to numerically dominant clonotypes with the same antigen specificity. This suggests that CD8 is augmenting clonotypic diversity within the antigen-specific $CD8^+$ T-cell pool during chronic viral infections (Price, Brenchley et al. 2005). Surh and Sprent demonstrated that sub-optimal TCR engagement by self-ligands, resulted in low level signalling without associated activation, and is required for the survival of naïve $CD8^+$ T-cells in the periphery (Surh and Sprent 2008). However memory $CD8^+$ T-cell persistence only requires the presence of homeostatic cytokines and does not rely on sub-optimal TCR stimuli which suggest that CD8 is required for the survival of naïve, but not memory, $CD8^+$ T-cells. It is clear that more studies are required in the future to define the role that CD8 plays *in-vivo*.

1.11 Research Aims

Despite major advances in terms of understanding the multiple roles of CD8 in T-cell activation, important questions still remain unanswered. Overall, the aim of this thesis was to further our understanding of the role that CD8 plays in T-cell activation and also the therapeutic potential of targeting CD8 for the treatment of $CD8^+$ T-cell mediated diseases such as autoimmunity.

My specific aims were to:

1. Probe the biological significance of the low solution binding affinity of the pMHCI/CD8 interaction for the first time.

2. Examine the possibility that anti-CD8 antibodies can trigger $CD8^+$ T-cell effector function in the absence of TCR engagement. In addition, the aim of this study was to phenotype a panel of anti-CD8 antibodies and classify antibodies that have either an activatory or inhibitory function.

3. Examine the possibility that anti-CD8 antibodies with an inhibitory phenotype can be used to block T-cell activation that is highly dependent on CD8. This could be potentially useful for blocking autoreactive $CD8^+$ T-cells which are characterized by low affinity TCR/pMHCI interactions and are highly dependent on CD8.

4. Finally, examine the possibility that CD8 can alter the functional avidity of a $CD8^+$ T-cell for its agonists and act to re-arrange the relative potencies of each of its potential agonists. If so this would suggest a novel "focussing mechanism" for CD8 in T-cell activation.

2

MATERIALS AND METHODS

2.1 Reagents and consumables

2.1.2 Mammalian Cell culture and reagents

The following media were used to culture the cells required for this thesis:

R10: Roswell Park Memorial Institute medium-1640 (RPMI-1640) supplemented with 10% heat inactivated foetal calf serum (FCS), 2 mM L-glutamine, 100 units/ml penicillin and 100 μg/ml streptomycin.

PSG: RPMI-1640 medium supplemented with 2 mM L-glutamine, 100 units/ml penicillin and 100 μg/ml streptomycin.

R2: RPMI-1640 medium supplemented with 2% heat inactivated foetal calf serum (FCS), 2 mM L-glutamine, 100 units/ml penicillin and 100 μg/ml streptomycin.

CK media: R10 supplemented with 2.5% Cellkines (Helvetica Healthcare, Geneva), 200 IU/ml IL-2 and 25 ng/ml IL-15 (PeproTech, London, U.K.).

D10: 293T cell culture media, Dulbecco modified Eagle's medium (DMEM), supplemented with 2 mM L-glutamine, 100 units/ml penicillin, 100 μg/ml streptomycin, 1% sodium pyruvate and 10% heat inactivated FCS.

I10: Iscove`s Modified Dulbecco medium (IMDM), supplemented with 2 mM L-glutamine, 100 units/ml penicillin, 100 μg/ml streptomycin, 1% sodium pyruvate and 10% heat inactivated IgG low FCS.

I0: IMDM media supplemented with 2 mM L-glutamine, 100 units/ml penicillin, 100 μg/ml streptomycin and 1% sodium pyruvate.

Freezer mix: FCS supplemented with 10% sterile dimethyl sulfoxide (DMSO; Sigma-Aldrich, Poole, U.K.).

RPMI-1640, DMEM, IMDM, FCS, L-glutamine, penicillin, streptomycin, and sodium pyruvate were purchased from Gibco, Life Technologies (Paisley, U.K.).

2.2 Mammalian Cell culture

2.2.1. Preparation of peripheral blood mononuclear cells (PBMC)

Typically 50 ml of peripheral blood, obtained from the Welsh Blood Transfusion Service or healthy donors, was collected into a sterile 50 ml Falcon tube (BD Biosciences) containing the anti-coagulant heparin (Unihep Leo) at 1000 units/ml. PBMC were generated by Ficoll-Hypaque density gradient centrifugation. Peripheral blood was gently layered onto an equal volume of Ficoll-Hypaque solution (Lymphoprep, Nycomed) and centrifuged for 20 minutes at 693 x g (Heraeus megafuge 1.0 R, Bucks, UK) with the break off. The buffy coat layer was gently removed from the gradient interface using a sterile Pasteur pipette. Cells were washed twice in PSG by centrifugation at 561 x g for 10 minutes followed by 561 x g for 6 minutes with maximum break. After the final wash, cells were re-suspended in R10 and kept in the incubator at 37°C/5% CO_2 prior to use for the generation of human CD8 T-cell lines/clones or kept at 4°C prior to use as human γ-irradiated (30Gy) allogeneic feeders.

2.2.2 Counting cells with Trypan blue

Cells were counted and analysed for viability by combining 10 µl of cell suspension with an equal volume of 0.1% Trypan blue in PBS (w/v) (Sigma-Aldrich) and loaded on to an improved Neubauer haemocytometer (Weber Scientific International Limited, Lancing, U.K.). Viable cells remain colourless, whilst non-viable cells appear blue at 100 times

magnification on a light microscope (Nikon Eclipse TS100). The percentage of total cells counted that remained white equates to the viability of the cell culture.

2.2.3 Generation of Human $CD8^+$ T-cell peptide specific lines

Blood from HLA A*0201 (HLA A2 from hereon) positive donors was used to generate $CD8^+$ T-cell lines. $CD8^+$ T-cells specific for (i) Melan-A derived epitope ELAGIGILTV (residues 26-35) (Laugel, van den Berg et al. 2007; Purbhoo, Li et al. 2007); and (ii) EBV BMLF1-derived epitope GLCTLVAML (residues 259-267) (Lissina, Ladell et al. 2009) were generated by pulsing 6 x 10^6 PBMC from a HLA A2 individual with cognate peptide at concentrations of 1 μM, 10 μM or 100 μM for 1 hour at 37°C. Cells were subsequently washed and resuspended in R10 only. After 3 days, increasing amounts of Interleukin-2 (IL-2) (Peprotech) were gradually added to the media, reaching a maximum concentration of 20 IU/ml by day 14. Expansion of antigen specific $CD8^+$ T-cells was assessed by FACS staining with cognate HLA A2/peptide tetramers and anti-CD8 antibody conjugated to a fluorochrome (see section 2.7.8).

2.2.4 Generation of human T-cell clones by limiting dilution

Clones were all generated by limiting dilution culture from peptide-specific T-cell lines. Cloning mix consisting of 2 x 10^6 PBMCs and 2 x 10^5 peptide-pulsed allogeneic B cells (optional) per ml of R10 supplemented with T-STIM (BD Biosciences) and 200 IU/ml IL-2 was made then γ-irradiated (30 Gy). Cells to be cloned were added to the cloning mix at a concentration of 1 cell per 600 μl mix, then plated out at 200 μl per well of a round-bottomed 96 well plate (i.e. 1 cell per 3 wells). Control wells at 10 and 100 cells per well were

included. Plates were cultured at 37°C/5% CO_2 and after 14-21 days examined for clones. Clones were re-stimulated as necessary, transferring them first to a 48 well plate, then at a second re-stimulation to a 24 well plate. Since the discontinuation of T-STIM in 2007, all clones and lines were subsequently cultured in CK media (ZeptoMatrix, NY, USA).

2.2.5 Human $CD8^+$ and $CD4^+$ T-cell clones used in this thesis

The following HLA A2 restricted $CD8^+$ T-cell clones were used in this study (Table 2.2.6); (i) ILA1, specific for the human telomerase reverse transcriptase (hTERT)-derived epitope ILAKFLHWL (residues 540-548) (Laugel, van den Berg et al. 2007; Purbhoo, Li et al. 2007); (ii) ALF3, specific for the influenza A matrix protein (M1)-derived epitope GILGFVFTL (residues 58-66) (Cole, Edwards et al. 2010); (iii) MEL5 and MEL187.c5, specific for the Melan-A-derived epitope ELAGIGILTV (residues 26-35) (Laugel, van den Berg et al. 2007; Purbhoo, Li et al. 2007); (iv) 003 specific for the HIV-1 p17 Gag-derived epitope SLYNTVATL (residues 77–85) (Sewell, Harcourt et al. 1997; Choi, Chen et al. 2003; Gostick, Cole et al. 2007); (v) 1E6 and 3F2 specific for the restricted autoantigen preproinsulin peptide ALWGPDPAAA ($PPI_{15–24}$) (Skowera, Ellis et al. 2008); and (vi) NLV2 specific for the CMV-pp65 derived epitope NLVPMVATV (residues 495-503). In addition, the following non-HLA A2–restricted $CD8^+$ T-cell clones were used: (i) HLA A*6801-restricted clone c23, specific for the HIV-1 Tat-derived epitope ITKGLGISYGR (residues 38–48) (Gostick, Cole et al. 2007); (ii) HLA B*0702-restricted clone KD4, specific for the EBV EBNA3A-derived epitope RPPIFIRRL (residues 379–387) (Burrows, Silins et al. 1995; Kjer-Nielsen, Clements et al. 2003); (iii) HLA B*0801-restricted clone LC13, specific for the EBV EBNA3A-derived epitope FLRGRAYGL (residues 339–347); (iv) HLA B*3508-restricted clones SB27, SBS1 specific for the EBV BZLF1-derived epitope

LPEPLPQGQLTAY (residues 52–64) and SB10 specific for the EBV BZLF1-derived epitope CPSQEPMSIYVY (Green, Miles et al. 2004; Tynan, Borg et al. 2005; Tynan, Burrows et al. 2005; Wynn, Fulton et al. 2008); (v) HLA A*2402-restricted clone 4C6, specific for the restricted autoantigen preproinsulin peptide LWMRLLPLL (PPI_{3-11}) (Knight, Kronenberg et al. 2012),; and (vi) The HLA DR*0101-restricted $CD4^+$ T-cell clone C6 recognizes the influenza A hemagglutinin (HA)-derived epitope PKYVKQNTLKLAT (residues 307-319) was generated as described previously (Lissina, Ladell et al. 2009).

Table 2.2.6 Human $CD8^+$ and $CD4^+$ T-cell clones

Clone name	MHCI restriction	Epitope	Residue number	Origin
ILA1	HLA*0201	ILAKFLHWL	540-548	hTERT
ALF3	HLA*0201	GILGFVFTL	58-66	Influenza
ALF8	HLA*0201	GILGFVFTL	58-66	Influenza
MEL5	HLA*0201	ELAGIGILTV	26-35	Melan-A
MEL187.c5	HLA*0201	ELAGIGILTV	26-35	Melan-A
1E6	HLA*0201	ALWGPDPAAA	15–24	Type-1 diabetes
3F2	HLA*0201	ALWGPDPAAA	15–24	Type-1 diabetes
4C6	HLA*2402	LWMRLLPLL	3-11	Type-1 diabetes
003	HLA*0201	SLYNTVATL	77–85	HIV-1 Gag p17-18
NLV2	HLA*0201	NLVPMVATV	495-503	CMV
c23	HLA A*6801	ITKGLGISYGR	38–48	HIV-1 Tat
KD4	HLA B*0702	RPPIFIRRL	379–387	EBV
LC13	HLA B*0801	FLRGRAYGL	339–347	EBV
SB27	HLA B*3508	LPEPLPQGQLTAY	52–64	EBV
SBS1	HLA B*3508	LPEPLPQGQLTAY	52–64	EBV
SB10	HLA B*3508	CPSQEPMSIYVY	103-111	EBV
C6	HLA DR*0101	PKYVKQNTLKLAT	307-319	Influenza

Table 2.2.7 Human $CD8^+$ and $CD4^+$ T-cell lines

Name	MHCI restriction	Epitope	Residue number	Origin
MEL5	HLA*A0201	ELAGIGILTV	26-35	Melan-A
EBV	HLA*A0201	GLCTLVAML	259-267	EBV

Table 2.2.8 Murine $CD8^+$ transgenic T-cell lines

Name	MHCI restriction	Epitope	Residue number	Origin
F5	H2-D^b	ASNENMDAM	Influenza H17	Influenza

2.2.9 Culture of human $CD8^+$ T-cell lines and clones

$CD8^+$ T-cells were grown from cryopreserved stocks in 24-well tissue culture plates in 2.5% CK media following re-stimulation using 1 µg/ml PHA with 5 x 10^6 irradiated allogeneic PBMC from 2-3 different individuals in 2 ml of media per well of a 24 well tissue culture plate. Following this, the cells were maintained in 2.5% CK media for several months without the need for re-stimulation with antigen and/or irradiated autologous PBMC feeders.

2.2.10 Generation of Murine $CD8^+$ T-cell peptide specific lines

Naïve mouse $CD8^+$ T-cells were obtained by harvesting splenocytes from transgenic F5 mice. A significant percentage of $CD8^+$ T-cells within the splenic population of these mice express the F5 TCR, which recognizes the H-2D^b-restricted influenza H17 nucleoprotein-derived epitope ASNENMDAM.(Table 2.2.8) (Mamalaki, Elliott et al. 1993). Naïve mouse $CD8^+$ T-

cells were obtained by harvesting splenocytes from Balbc mice (Mosier 1974). Cells were also stimulated with 10 μg/ml anti-mouse CD3 (clone 500A2, eBioscience) and 0.5 μg/ml anti-mouse CD28 antibodies (clone 37.51, eBioscience) and cultured in D10 media for 7 days.

2.2.11 Cryopreservation storage of cells

2 – 10 x 10^6 lymphocytes were centrifuged at 389 x g for 5 minutes then re-suspended in 1 ml freezer mix and transferred to a cryovial (Nunc). Cryovials were stored in 100% Propan-2-ol (Mr.Frosty™, ThermoScientific, UK) storage containers at -80°C for 48 hours before being transferred to liquid nitrogen containers for long term storage. When required, cell stocks were rapidly thawed at 37°C to minimize cell death, washed once in PSG to remove the DMSO and resuspended in appropriate culture media.

2.2.12 Generation and culture of C1R B cell clones expressing HLA A*0201

Endotoxin free pcDNA3.1 mammalian expression vectors (Life Technologies) with inserts encoding either full length HLA A2 or one of the following mutants: HLA A2 DT227/8KA (Purbhoo, Boulter et al. 2001), HLA A2 Q115E (Wooldridge, Lissina et al. 2007), HLA A2 K^b/245V and chimeric HLA A2/K^b were generated then linearised before transfection into the C1R B cell line by electroporation. The C1R B cell line is a Class I A and B allele negative, Epstein-Barr virus (EBV) transformed B cell line (Storkus, Howell et al. 1987) that can be cultured in R10. C1R cells were split and fed 24 hours before transfection as transfection efficiency is increased if C1R B cells are actively dividing and the population is >90% viable. For each transfection 10 x 10^6 C1R B cells were washed twice in PSG (ensuring all absence

of serum), by centrifuging at 292 x g for 6-7 minutes at room temperature, and subsequently resuspended in 500 µl of PSG then transferred to a sterile 0.4 cm electroporation cuvette (Bio-Rad, Herts, UK) with 10 µg endotoxin free linearalised DNA (10 µl of 1 µg/µl). After gently mixing the cell suspension and DNA using a pasteur pipette the cuvette was placed on ice for 5 minutes. Electroporation was performed using the following conditions for each DNA construct; Voltage = 250 V, Capacitance = 400 µF.

Electroporation was performed using a GenePulser Xcell electroporator (Bio-Rad). The electroporated cells were then rested at room temperature for 10 minutes. After the addition of 500 µl warm R10, the suspension was gently transferred into a T25 flask with a further 12 ml R10 and subsequently cultured at 37°C/5% CO_2. Stable transfectants were selected by adding 0.5 mg/ml G418 (Sigma-Aldrich) 72 hours after transfection. Significant cell death occurred within the first 5 days (>90% death) following G418 addition but cell viability began to recover at 10 days. The transfected C1R cell lines were cloned by limited dilution. The clones were then regularly tested for HLA A2 expression by staining with Fluorescein Isothiocyanate (FITC) conjugated anti-human HLA A2 conformation specific antibody clone BB7.2 (Serotec; Oxford, U.K.) and analysed by flow cytometry. All clones showed 100% HLA A2 expression, with equal Mean Fluorescence Intensities (MFI`s) in the FL1 channel.

2.2.13 293T (HEK 293) lentiviral packaging cell line

The 293T cell line was originally derived from human embryonic kidney (HEK) cells by transformation of cultured cells with sheared adenovirus-5 DNA (Graham, Smiley et al. 1977). Cultures reaching 100% confluency were removed from the tissue culture plastic by

incubation with 0.5% trypsin in HBSS (Life Technologies) due to the fact that 293T cells are an adherent cell line then washed with 293T culture media to remove the trypsin and split. Cells were cultured in DMEM supplemented with 20% FCS, 1 mM sodium pyruvate, 100 units/ml penicillin, 100 mg/ml streptomycin and 2 mM L-glutamine. The 293T CD8α transfected cells used in this study (a kind gift from Dr Reno Debets) were manufactured by introducing pBullet-human CD8α into 293T cells using vesicular stomatitis virus-pseudotyped Moloney murine leukaemia virus particles (Willemsen, Ronteltap et al. 2005; Willemsen, Sebestyen et al. 2006).

2.2.14 Generation of whole antibody IgG from hybridomas

The following hybridomas were used in this study: anti-human CD8 antibody clone OKT8 IgG2a (MRC cooperative facility, ATCC), anti-human CD3 antibody clone OKT3 IgG2a (MRC cooperative facility ATCC) and anti-mouse CD8 antibody clone KT112 IgG2a (a kind gift provided by Professor Rose Zamoyska). OKT8 hybridoma was originally generated by three separate fusions between CAF mice which were immunised intraperitoneally at 2 to 3 week intervals with either 2 x 10^7 thymocytes, ConA activated sheep red blood cell rosetting (E^+) cells or ConA activated E^+ cells depleted of $OKT4^+$ cells by OKT4 and rabbit complement. Four days after the third injection splenocytes were fused with P3 x 63 Ag8U1 myeloma cells (Kung, Goldstein et al. 1979; Biddison, Rao et al. 1984). KT112 hybridomas were originally generated from a fusion between NSO myeloma cells and spleen from a Spraque-Dawley rat hyperimmunised with cells from the T-cell clone AK1 (specific for the non H2 antigen plus D^k) (Tomonari and Spencer 1990). OKT3 hybridomas were originally generated by female mice of strain BALBcJ or CAF mice were immunised intraperitoneally with 2 x 10^7 E rosette-purified peripheral T cells in PBS at 14-day intervals. Four days after

the third immunization the spleens were removed and a suspension of single cells was prepared. For each fusion, 1 x 10^8 splenocytes were fused in 35% PEG in 5% DMSO and RPMI 1640 with 2 x 10^7 P3 x 63 Ag8U, myeloma cells. After cell fusion, the cells were distributed into 100 to 400 wells and cultured in selective medium. The wells were observed regularly under an inverted phase microscope and as cells grew up supernatants from those wells were harvested and tested for binding to human peripheral lymphocytes separated into E rosette-positive (E^+) and E rosette-negative (E^-) populations. Binding was detected both by radioimmunosassay and indirect immunofluorescence techniques (Kung, Goldstein et al. 1979).

Hybridomas were cultured in I10 media (FCS IgG low) within the main compartment of a two compartment Celline flask (Integra, NH, USA). In the large body of the flask I0 media was used. Every 7-10 days the hybridoma was harvested for antibody and both compartments of the flasks were cultured in fresh media, i.e. in the main compartment of the flask, approximately 20 mls of hybridoma supernatant was harvested and fresh I10 media was added. This 20 mls was then centrifuged at 693 x g for 10 minutes at 4°C. The subsequent antibody in the supernatant was removed and stored at -20°C prior to purification. To the large body compartment, fresh I0 media was added.

2.2.15 Purification of whole antibody IgG from hybridomas

Whole IgG antibody was purified by first filtering whole antibody generated as above through a 0.4 μM filter. Antibody was then loaded to a protein G column (GE healthcare) with the use of a peristaltic pump. Once this had been completed the antibody was eluted

with the use of Elution buffer (0.1 M Glycine/HCl pH 2.5 (both Fisher Scientific, Loughborough, UK) and neutralised immediately with Neutralising buffer (1 M Tris pH 10.5 Fisher Scientific). Antibody purity was then checked by SDS-PAGE electrophoresis (section 2.5.6).

2.2.16 Generation of OKT8 and OKT3 Fab, F(ab´)$_2$ and Fc´ fragments

250 µg of the anti-human CD8 antibody OKT8 or anti-human CD3 antibody OKT3 (IgG) was digested to yield Fab and Fc´ fragments using a Pierce Fab micro preparation kit (Thermo scientific, Rockford IL, USA) or digested to yield F(ab´)$_2$ fragments using a Pierce F(ab´)$_2$ micro preparation kit (Thermo scientific). IgG fragmentation was performed according to the manufacturer's instructions and purity was checked via SDS-PAGE electrophoresis.

2.3 Bacterial Cell culture

2.3.1 Bacterial culture media

Agar plates: 15 g Bacto-agar in 1 litre milliQ d.$H_2$0 (Fisher Scientific) supplemented with 100 µg/ml ampicillin/carbenicillin or Kanamycin (Fisher Scientific).

LB low salt media: 1% Bacto-tryptone (Difco), 0.5% NaCl (Sigma-Aldrich), 0.5% yeast extract (Difco).

TYP media: 1.6% yeast extract (Difco), 1.6% Bacto-tryptone (Difco), 0.5% NaCl, 0.25% K_2HPO_4 (Sigma-Aldrich).

(All media was autoclaved on a liquid cycle at 121°C for 60 minutes and supplemented with 100 µg/ml ampicillin/carbenicillin (Fisher Scientific) prior to use).

Table 2.3.2 Bacterial strains

Strain	Description/Application	Antibiotic Resistance	Supplier
Top10	Plasmid amplification for transformation, sequencing or transfection.	Ampicillin/Carbenicillin	Life Technologies
XL10-Gold	Plasmid amplification for transformation, sequencing or transfection.	Ampicillin/Carbenicillin	Agilent Technologies
BL21 (DE3) pLysS	High stringency expression in bacterial cell culture under the control of the T7 promoter.	Ampicillin/Carbenicillin	Life Technologies

2.3.3 Transformation of competent bacterial cells by heat shock method

Aliquots of competent bacteria were thawed slowly on ice. 50 - 100 ng of plasmid DNA (quantified by absorbance at 260 nm) was added to 50 µl thawed competent bacteria, kept on ice for 5 minutes, before being transferred to 42°C for 90 seconds then replaced on ice for 2 minutes. Following this heat shock procedure, 100 µl of SOC media (Life Technologies) was added to the bacteria, and the mixture placed in an orbital incubator (Sanyo, Leics, UK) at 37°C for 60 minutes. Cells were then streaked out on LB agar plates supplemented with 100 µg/ml ampicillin/carbenicillin or kanamycin (Fisher Scientific) and incubated overnight at 37°C. A negative control tube containing bacteria alone was plated out for every transformation.

2.3.4 Target gene expression in bacterial cell culture

A single colony from a plate of freshly transformed BL21 bacteria was used to inoculate 30 ml of TYP media supplemented with 100 µg/ml ampicillin/carbenicillin and agitated overnight in an orbital incubator at 37°C. The following morning 1 litre of TYP media (supplemented with 100 µg/ml ampicillin/carbenicillin) was inoculated with 2 - 5 ml of the starter culture and agitated at 37°C until the OD_{600} reaches between 0.4 and 1 (ideally 0.6) as measured by a spectrophotometer (Biochrom, Cambridge, UK). A 1 ml pre-induction sample was collected, microfuged at 17,900 x g (Eppendorf 5417 R, Cambridge, UK) for 1 minute and 1 ml of glycerol added then the pellet stored at -80°C. Protein expression was induced by adding 0.5 mM dioxin free isopropyl-1-thio-β-D-galactopyranoside (IPTG; Melford Laboratories). Flasks were agitated for a further 4 - 6 hours post induction. A 1 ml post-induction sample was taken and stored as for the pre-induction sample. The remaining culture was centrifuged at 2122 x g for 20 minutes at 4°C (Heraeus) and the supernatant discarded. The bacterial pellet was either resuspended in lysis buffer for immediate preparation of inclusion bodies (section 2.5.1), or in 10 - 15 ml d.H_2O and stored at -20°C.

2.4 Molecular Biology

2.4.1 Plasmid DNA miniprep

A single transformed bacterial colony was placed in 5 ml LB media supplemented with 100 µg/ml ampicillin/carbenicillin or 100 µg/ml kanamycin and incubated overnight in an orbital incubator at 37°C. Bacterial cells were pelleted by centrifugation at 2772 x g for 15 minutes at room temperature and the supernatant discarded. Plasmid DNA was extracted using a commercially available miniprep kit (Miniprep 250 kit; Qiagen or Zyppy plasmid miniprep

kit; Zymo Research, CA, USA) based on the alkaline lysis method. Extracted DNA was resuspended in milliQ d.H_2O or elution buffer and stored a -20°C.

2.4.2 Plasmid DNA maxiprep (Endotoxin free)

A single bacterial colony previously transformed with plasmid DNA was used to inoculate a starter culture of 5 ml LB media (supplemented with 100 µg/ml ampicillin/carbenicillin) and shaken for 8 hours in an orbital incubator at 37°C. 0.5 - 2 ml of starter culture was used to inoculate between 100 and 500 ml of LB media (dependent on DNA yield output) which was subsequently shaken overnight in an orbital incubator at 37°C. The cultures were centrifuged at 2772 x g for 20 minutes at 4°C and the supernatant discarded. The bacterial pellet was treated using a commercial endotoxin-free maxi-prep kit (Qiagen, UK) to extract the plasmid DNA. Ethanol precipitated and dried DNA pellets were resuspended in 200 - 500 µl TE buffer or endotoxin free water and the concentration of eluted DNA quantified as outlined below. A maxi-prep typically yielded 700 µg of plasmid DNA.

2.4.3 DNA quantification

2 µl of eluted DNA following either a mini or maxiprep procedure was diluted in 198 µl milliQ d.H_2O. The absorbency of this solution was then measured using a spectrophotometer (Biomate, Thermo Scientific, MA, USA) or 1 µl of DNA was measured using a nano-drop (Thermo Scientific) set to record at 260 nm wavelength. MilliQ d.H_2O was used as a blank reference. An absorbency of 1 at 260 nm was assumed to indicate a DNA concentration of 50 ng/µl (after the extinction coefficient for DNA and the dilution factor were taken into account).

2.4.4 DNA sequencing

After each step of cloning strategy, the construct (500 ng total) was sent for sequencing by the DNA sequencing facility, Central Biotechnology Services, Cardiff University. For all samples, forward and reverse primers were also sent (MWG 50 pmol/µl). DNA was sequenced using ABI PRISM 3100-Avant Genetic Analyser (Applied Biosystems, UK) using silver sequencing and analysed using CLG Genomics workbench (Swansea, UK).

2.4.5 Linearisation of DNA

For the generation of stable cell transfectants, plasmid DNA that had been generated via the methods outlined above must be linearised in order for it to successfully integrate with C1R cell DNA. 25 µl of plasmid DNA (of 50 µg @ 2 µg/µl) was digested with 10 µl BglII (New England Biolabs), 20 µl of 10 x NEB buffer and 145 µl RNAse/DNAse free water (200 µl total). Plasmid DNA was digested for 18 hours at 37°C and digestion efficiency was measured by running the sample on a 1% agarose gel (see section 2.4.7).

2.4.6 Ethanol precipitation

200 µl of the linearised plasmid DNA was precipitated using ethanol to allow the removal of any remaining restriction enzymes that remained post overnight digestion. 400 µl of 100% ethanol (Sigma-Aldrich) was added, and the mixture incubated at room temperature for 10 minutes. The reaction was centrifuged at 292 x g for 10 minutes and the supernatant carefully aspirated then discarded. 500 µl of 70% ethanol was used to resuspend the DNA pellet for washing. The same centrifugation step was repeated and the supernatant again discarded. The pellet was allowed to dry before being resuspended in 50 µl of endotoxin free water.

2.4.7 Agarose gel electrophoresis and extraction

Agarose gels were generated by the addition of 1% agarose (W/V) with 50 ml of 1 x TAE buffer (10 x buffer: 48.4 g Tris base, 10.9 g glacial acetic acid, 2.92 g EDTA, 1.0 Litre d.H_2O, pH 8.2). This was heated to dissolve all agarose and once cool either 5 µl of 10,000 x SYBR® Safe DNA gel stain or 10 ng/ml Ethidium Bromide (Life Technologies) were added and the gel was cast. Samples were mixed with 5 x loading buffer (Bioline, London, UK) before being loaded then run on the gel alongside gel loading marker (Bioline) at 75 V, 200 mA for 40 minutes. Subsequently gels were analysed using a UV transilluminator (UVP, Cambridge, UK). For extraction, DNA bands were excised from agarose gels using an UV transilluminator and the DNA subsequently extracted from the gel fragment using a QIAquick gel extraction kit (Qiagen), according to the manufacturer's instructions.

2.4.8 Plasmid restriction digestion

Restriction digestion enzymes were used to specifically target a restriction site of choice: 2 µl of miniprep was added to 1 µl of restriction enzyme of choice (New England Biolabs) and 2 µl of the appropriate enzyme buffer (New England Biolabs) then made up to a final volume of 20 µl DNAse free water (adding BSA if required for buffer (New England Biolabs)).

2.4.9 Vector/insert ligation

Vectors and inserts were ligated by mixing insert and vector at different ratios with 1U DNA ligase (T4 DNA ligase Promega, Southampton, UK) and 3 µl DNA ligase buffer (Promega) and made to a final volume of 30 µl DNAse free water. Ligation reactions were left overnight at 16°C.

2.5 Protein Chemistry

2.5.1 Inclusion body preparation

Biotin-tagged MHCI heavy chains (wild type and mutant HLA A2), α and β TCR chains, human CD8α and β_2m were all expressed under the control of the T7 promoter as insoluble inclusion bodies in the *Escherichia coli* strain BL21 (DE3) pLys (Life Technologies) (section 2.3.2). To prepare inclusion bodies from IPTG-induced *E. Coli* the bacterial pellet from 1 litre culture was re-suspended in 20 ml of lysis buffer (10 mM Tris pH8.1 (Sigma-Aldrich), 10 mM $MgCl_2$ (Sigma-Aldrich), 150 mM NaCl (Sigma-Aldrich) and 10% Glycerol (Fisher Scientific)). The bacterial suspension was then transferred to a 50 ml centrifuge tube (Falcon) and lysed by sonication to release the inclusion bodies. Inclusion bodies were purified by adding 5 volumes of Triton wash buffer (0.5% Triton X-100 (Sigma-Aldrich), 50 mM Tris pH8.1 (Sigma-Aldrich), 100 mM NaCl (Sigma-Aldrich), 10 mM EDTA (Sigma-Aldrich) and 2 mM DTT (Sigma-Aldrich), pelleted by centrifugation at 2772 x g for 20 minutes at 4°C and the supernatant containing the bacterial cell debris discarded. This step was repeated 2 - 3 times (a homogenizer was used each time to resolubilise the pellet in the Triton buffer). To check purity of the inclusion body preparation, a small sample was analysed via SDS-PAGE electrophoresis. Once purity had been achieved, the inclusion body pellet was denatured into 8 M guanidine buffer (8 M guanidine (Sigma-Aldrich), 50 mM Tris pH8.1 (Sigma-Aldrich), 100 mM NaCl (Sigma-Aldrich), 10 mM EDTA pH8 (Sigma-Aldrich) and 10 mM DTT (Sigma-Aldrich)). The concentration of the inclusion body preparation was determined using spectrophotometry (Biomate, Thermo Scientific) then stored in 1 ml aliquots at -80°C.

2.5.2 Production of soluble human biotinylated peptide-MHCI monomers

For the manufacture of pMHCI monomers, 30 mg of HLA A2 heavy chain with a biotin tag and 30 mg of β_2m inclusion body preparations were denatured separately in 10 ml 8 M urea buffer (8 M urea (Sigma-Aldrich), 50 mM Tris pH8.1 (Sigma-Aldrich), 100 mM NaCl (Sigma-Aldrich), 10 mM EDTA pH8 (Sigma-Aldrich) and 10 mM DTT (Sigma-Aldrich)) for 30 minutes at 37°C. Refolding was initiated by adding (in the order described) 1 ml peptide (4 mg/ml in DMSO), 30 mg denatured β_2m, 30 mg denatured heavy chain in 1 litre of a pre-chilled cysteamine/cystamine redox buffer (100 mM Tris pH8.1 (Sigma-Aldrich), 400 mM L-arginine HCL (Sigma-Aldrich), 2 mM EDTA (Sigma-Aldrich), 2.3 mM cysteamine and 3.7 mM cystamine (Sigma-Aldrich) at 4°C while stirring vigorously. After stirring for 4 hours at 4°C the refold was transferred into 12 KD cut-off dialysis tubing (Sigma-Aldrich), dialysed against 12 litres of d.H_2O overnight then against 12 litres 10 mM Tris pH8.1 for 8 hours followed by another overnight dialysis in fresh 10 mM Tris pH8.1. Following equilibration of a 5 ml anion exchange column (Hi Trap Q HP; GE healthcare) with 10 mM Tris pH8.1, the refold was loaded onto the column and the protein eluted with a salt gradient (0 - 500 mM NaCl in 10 minutes/10 mM Tris pH8.1) (Figure 2.1 A). The eluted fractions were collected and 1 x protease inhibitors (500 μM AEBSF, 1 μg/ml Aprotinin, 1 μM E-64, 500 μM EDTA and 1 μM Leupeptin; Calbiochem, UK) added to prevent biotin tag cleavage, stored at 4°C and analysed by SDS-PAGE. If fractions contain correctly refolded pMHCI then SDS-PAGE shows two main bands: a band at ~35 KD (pMHCI heavy chain) and a band at ~12 KD (β_2m). The pMHCI band is typically more prominent than the β_2m (Figure 2.1 B). After analysis of the collected fractions by SDS-PAGE, the fractions containing the two correctly folded proteins were pooled, concentrated down to 500 μl using 10 KD cut off Ultrafree centrifugal filter (Millipore) and desalted using a 5 ml Hi Trap desalting column (GE

healthcare) equilibrated with 10 mM Tris pH8.1 (Sigma-Aldrich). Desalted pMHCI monomer fractions were collected, pooled and biotinylated in a 1 ml biotinylation reaction ~700 µl pooled protein, 100 µl BioMix A, 100 µl BioMix B and 1 µl (2.5 µg), Bir A enzyme (Avidity, Denver, USA) overnight at room temperature. The removal of excess biotin and buffer exchange into PBS or HBS-EP BIAcore buffer (BIAcore AB, UK) was performed by gel filtration (size exclusion) chromatography using either a Superdex HR 75 10/30 column or a Superdex HR 200 column (Amersham Pharmacia) equilibrated in PBS or HBS-EP BIAcore buffer (Figure 2.2). Fractions were collected, pooled and 1 x protease inhibitors added (Calbiochem). The final concentration of the pMHCI monomer was determined by spectrophotometry (Biomate, Thermo Scientific), aliquoted and stored at -80°C.

2.5.3 Manufacture of soluble human T-cell receptor (TCR)

For a 1 litre refold: 30 mg TCRα chain and 30 mg TCRβ were denatured separately by incubating at 37°C for 30 minutes in 10 mls of 6 M guanidine buffer (6 M guanidine, 50 mM Tris pH 8.1, 100 mM NaCl, 10 mM EDTA pH 8 and 10 mM DTT) (Sigma-Aldrich). Refolding was initiated by simultaneously adding denatured TCRα and β chains to 1 litre of refold buffer (5 M urea, 100 mM Tris pH8.1, 400 mM L-arginine HCL, 2.3 mM cysteamine and 3.7 mM cystamine) (Sigma-Aldrich) previously chilled to 4°C whilst stirring vigorously. After 3 - 4 hours the refold mixture was transferred to dialysis tubing (12 KD cut off; Sigma-Aldrich) and dialysed overnight against 12 litres of d.H_2O which had been pre-chilled (4°C). The refold was then dialysed twice against 12 litres pre-chilled 10 mM Tris pH8.1 (4°C) for 8 hours. After equilibrating a HiTrapQ HP column (GE healthcare) in 10 mM Tris pH8.1 the TCR refold was loaded at a flow rate of 5 ml/minute. Protein was then eluted using a salt

A

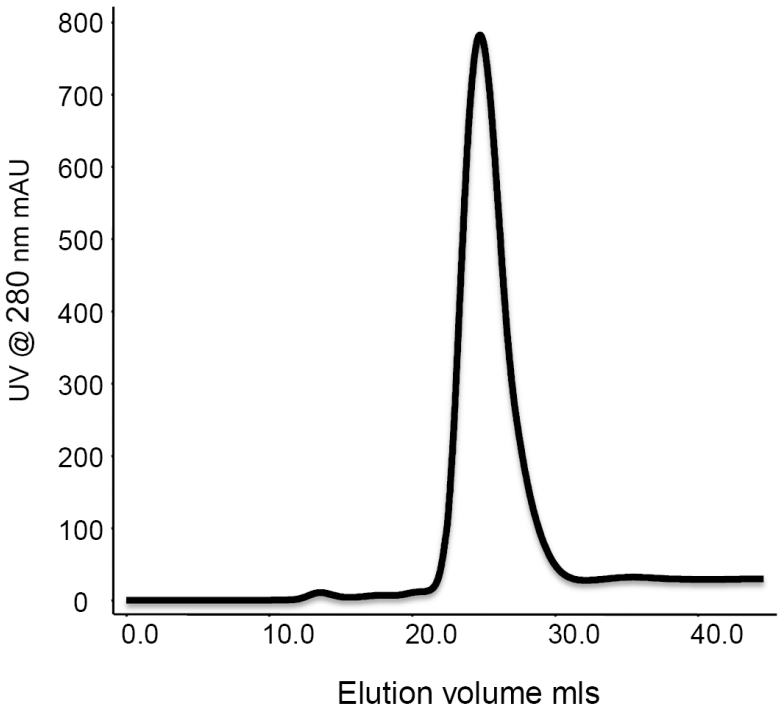

B

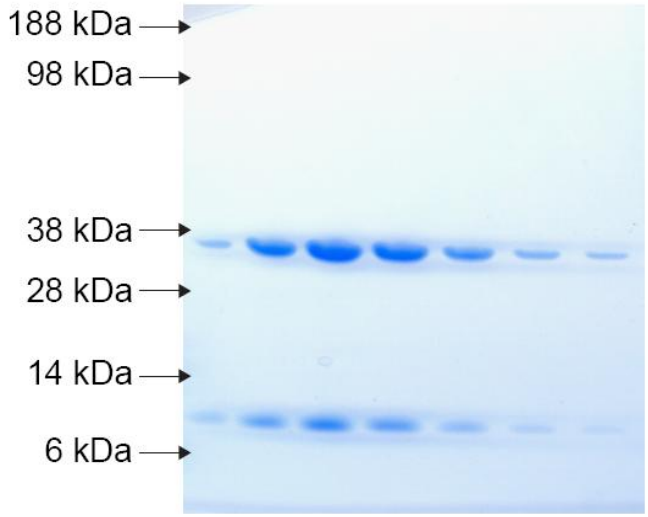

Figure 2.1: (**A**) Typical anion exchange trace for pMHCI monomer refold eluted from column using a salt gradient. (**B**) Protein quality measured by loading 1µg of refold protein from eluted fractions (**A**) using SDS-PAGE (section 2.5.6) and visualised using Coomassie brilliant blue stain (section 2.5.6).

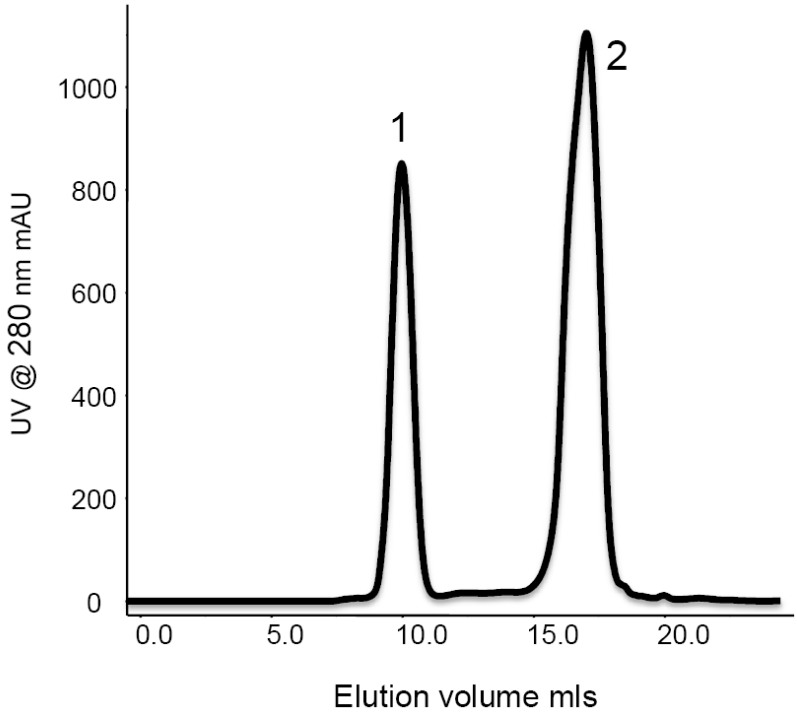

Figure 2.2: A typical gel filtration trace. Post anion exchange, correctly folded pMHCI protein is biotinylated. Post-biotinylation, using a size exclusion chromatography column, biotinylated protein (peak 1) is separated from excess biotin (peak 2). Correctly folded biotinylated pMHCI monomer is pooled, the concentration of protein determined and stored @ -80 °C.

A

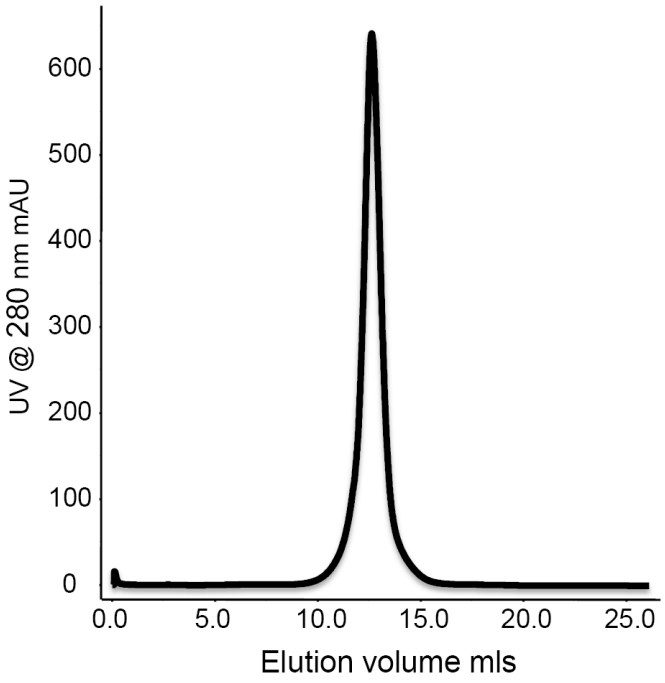

B

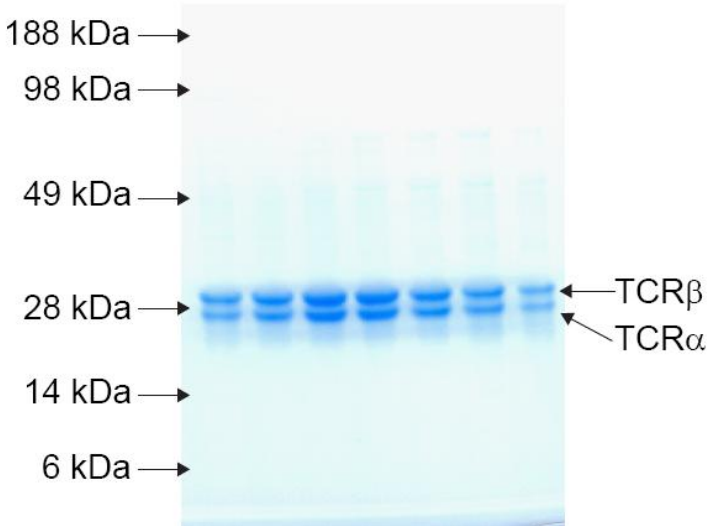

Figure 2.3: (**A**) Typical anion exchange trace for TCR refold eluted from column using a salt gradient (section 2.5.3). (**B**) Protein quality measured by loading 1μg of refold protein from eluted fractions (**A**) using SDS-PAGE (section 2.5.6) and visualised using Coomassie brilliant blue stain (section 2.5.6).

gradient (0 - 500 mM NaCl in 10 minutes/10 mM Tris pH 8.1) (Figure 2.3 A) and fractions containing correctly folded TCR were identified by SDS-PAGE (Figure 2.4 B), pooled and stored at 4°C.

2.5.4 Manufacture of soluble human CD8αα.

4 litres of redox refolding buffer (0.2 M Tris pH8.1 (Sigma-Aldrich), 0.5 M L-arginine hydrochloride (Sigma-Aldrich), 10 mM EDTA pH8 (Sigma-Aldrich), 2.3 mM cysteamine, 3.7 mM cystamine (both Sigma-Aldrich) was pre-chilled to 4°C. 240 mg of human sCD8α inclusion bodies were denatured in 60 ml 6 M Guanidine buffer (6 M guanidine (Sigma-Aldrich), 50 mM Tris pH8.1 (Sigma-Aldrich), 100 mM NaCl (Sigma-Aldrich), 10 mM EDTA pH 8 (Sigma-Aldrich) and 10 mM DTT (Sigma-Aldrich)) at 37°C for 30 minutes. Refolding was initiated by adding 20 ml of the denatured sCD8α solution to pre-chilled redox buffer whilst stirring at 4°C. At 10 minutes intervals the second and third 20 ml volume of denatured sCD8α was added. After stirring for 1 - 3 hours in the cold room the refold mixture was concentrated to 200 ml with a MasterFlex L/S (Cole/Palmer, London, UK) concentrator using a VivaFlow 200 filter (Sartorius, Goettingen, Germany) using a 10 KD cut off filter and placed in 12 KD cut off dialysis tubing. The 200 ml refold was first dialysed against 8 litres of d.H_2O overnight, then for 6 hours against 8 litres of 10 mM MES (2-[N-Morpholino]ethanesulfonic acid) pH 6 (Sigma-Aldrich) and finally against 8 litres of 10 mM MES pH 6 (Sigma-Aldrich) overnight. After dialysis the refold was filtered through a 0.45 μM filter, diluted to a final volume of 1 litre with 10 mM MES pH6 (Sigma-Aldrich) and loaded onto a 5 ml Hi Trap SP cation exchange column (GE healthcare) pre-equilibrated in 10 mM MES pH6 (Sigma-Aldrich). Protein was eluted from the column with a salt gradient

(0 – 500 mM NaCl in 10 minutes/10 mM Mes pH6) (Figure 2.4 A). The correctly folded sCD8αα was identified by SDS-PAGE (Figure 2.4 B), fractions collected, pooled, 1 x cocktail of protease inhibitors added (Calbiochem) then concentrated using an ultrafree 10 KD cut off centrifugal filter (Millipore). Buffer exchange into PBS or HBS-EP BIAcore buffer and removal of aggregates was achieved by size exclusion using a Superdex HR 200 column (Amersham Pharmacia).

Table 2.5.5 FPLC (Fast protein liquid chromatography)

The table outlines some of the properties of the Amersham Pharmacia columns used in this thesis. All the columns were used by attaching them to an automated FPLC system (Amersham Pharmacia).

Column	Description	Use	Column volume (mls)	Flow rate (ml/min)	Volume of sample added (mls)	Volume of collected fractions (mls)
HiTrap Q HP	Anion exchange	Purification of pMHCI monomers or TCR	5	5	500 - 1000	1
HiTrap SP	Cation exchange	Purification of sCD8αα	5	5	500 - 1000	1
HiTrap desalting	Gel filtration	Salt removal prior to biotinylation	5	5	1	1
Superdex HR 75	Gel filtration	Removal of excess biotin after biotinylation	23	0.5	1	0.5
Superdex HR 200	Gel filtration	Removal of excess biotin after biotinylation	23	0.5	1	0.5

A

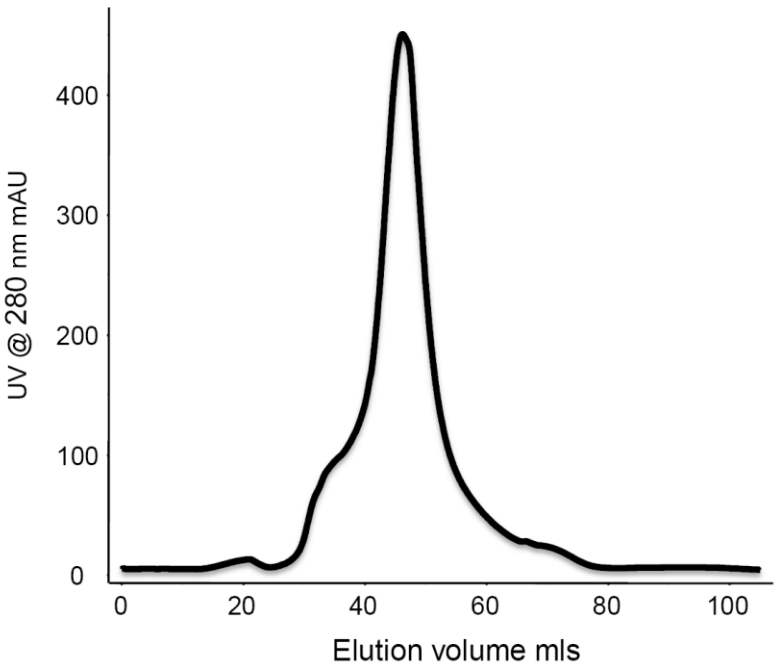

B

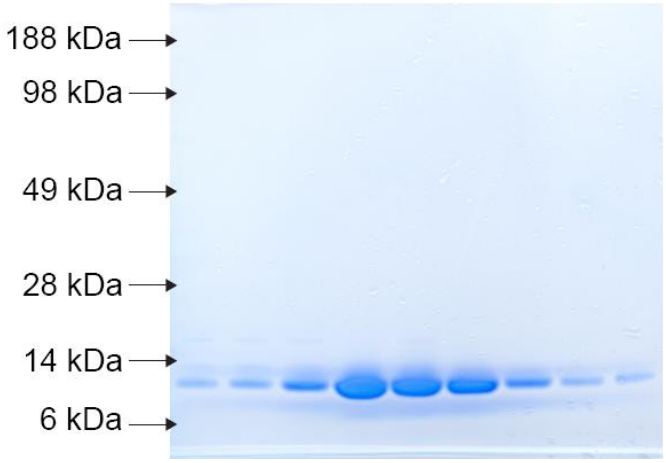

Figure 2.4: (**A**) Typical cation exchange trace for human CD8αα refold eluted from column using a salt gradient (section 2.5.4). (**B**) Protein quality measured by loading 1µg of refold protein from eluted fractions (**A**) using SDS-PAGE (section 2.5.6) and visualised using Coomassie brilliant blue stain (section 2.5.6).

2.5.6 Sodium dodecyl sulphate-polyacrylamide gel elecrophoresis (SDS-PAGE)

Proteins were separated by SDS-PAGE using the Life Technologies X-Cell SureLock™ system. Pre-cast gels, 4-12% Bis/Tris gels were removed from storage packaging and cleaned. The gel was locked in place using the XCell SureLock™ running chamber. The chamber was filled using 1 x NuPage® MES SDS running buffer (Life Technologies). Samples were prepared by diluting 1:4 in 5 x non reducing sample buffer (125 mM Tris pH6.8, 4% SDS, 20% glycerol, 20 μg/ml bromothenol blue) or 5 x reducing buffer with the addition of 10% DTT then incubated at 95°C for 5 minutes. The samples and the molecular weight marker (Seeblue Plus2 marker, Life Technologies) were loaded into separate lanes on the gel. Gels were run at 180 V for 45 minutes at 200 mA and stained by agitating them for 1 hour with Coomassie Blue staining solution (40% methanol (BDH), 7% acetic acid (BDH), 0.025% Brilliant Blue G) (Life Technologies). The gels were destained by further agitation for a minimum of 1 hour with miliQ d.H_2O for visualisation.

2.5.7 Estimating protein concentration by spectrophotometry

To determine the concentration of pMHCI, samples were diluted 1/100 in PBS or HBS-EP BIAcore buffer. Inclusion bodies were diluted 1 in 100 in 6 M guanidine buffer. Using a spectrophotometer (Biomate, Thermo Scientific) the machine was blank referenced using the buffers that the protein had been made in, i.e. guanidine buffer for inclusion bodies and either PBS or HBS-EP BIAcore buffer for refolded protein by FPLC. Readings at 280 nm wavelength were recorded and the protein concentration was calculated using the dilution factor and extinction co-efficient for each protein previously calculated from the amino acid

sequence. For example the extinction co-efficient for monomeric pMHCI is approximately 0.46 (with some variation between different pMHCI).

2.5.8 Surface Plasmon Resonance

Prior to surface plasmon resonance, proteins to be flowed over the sensor chip surface were gel filtrated through a Superdex 75 or 200 column to remove any aggregates and to buffer exchange into HBS-EP buffer (BIAcore AB, UK) containing 10 mM HEPES pH 7.4, 150 nM NaCl, 3.4 mM EDTA and 0.005% Surfactant P20. Proteins were then concentrated to an absorbency of at least 10 (measured @ 280 nm) using a 10 KD cut off Ultrafree centrifugal filter (Millipore). A standard amine coupling kit (BIAcore AB) was used to activate the surface of a research grade CM5 sensor chip (BIAcore AB). Streptavidin was covalently coupled to the chip surface by injecting a 0.2 mg/ml streptavidin solution (Sigma-Aldrich) diluted in 10 mM sodium acetate pH 4.5 over the surface. Biotinylated pMHCI monomers diluted in HBS-EP buffer (BIAcore AB) were immobilized onto the chip surface at approximately 1000 response units (RU) in each flow cell. Serial dilutions of either sCD8αα or soluble TCR were flowed over the chip to generate kinetic data. Data was analysed using BIAeval, Excel and Origin version 6.1 (Microcal software). K_D values were calculated both by linear Scatchard plots and non-linear analysis assuming 1:1 Langmuir binding ($A + B \leftrightarrow AB$) using non-linear curve fitting to the equation: $AB = B \times AB_{max}/(K_D + B)$.

2.6 Tetramer technology

2.6.1 Manufacture of pMHCI tetramers

Streptavidin has four binding sites for biotin therefore pMHCI tetramers can be constructed by adding streptavidin to a solution of biotinylated pMHCI monomers in a 1:4 molar ratio. Tetramers were conjugated to R-phycoerythrin (PE) (Life Technologies), Allophycocyanin (APC) (Prozyme, CA, USA), Quantum Dot Q605 or Quantom Dot Q800 (Life Technologies), Brilliant Violet 421 (BV421) (Biolegend, San Diego, CA, USA) or unconjugated Streptavidin alone for use in flow cytometry. The volume of conjugated streptavidin required for each tetramer preparation was calculated and added in 5 aliquots of equal volume at 20 minutes intervals at 4°C, mixing the contents well each time. By adding streptavidin in aliquots as described the complete saturation of all four biotin binding sites for streptavidin is ensured with each addition. The tetramers were stored at 4°C for a period of up to four weeks or until the tetramer showed signs of degradation.

2.6.2 pMHCI Tetramer decay experiments

HLA A*0201 pMHCI tetramers and 1 x 10^6 $CD8^+$ T-cells were stained in 100 µl azide buffer (PBS, 0.1% NaN_3/0.5% FCS (Sigma-Aldrich)) for 20 minutes on ice with a concentration of tetramer, previously determined by titration, that gave a starting mean fluorescence intensity (MFI) of 200; 5 µl of 7-Amino-actinomycin D (7-AAD, Viaprobe; BD Biosciences) was included so that dead cells could be gated out of the analysis. After washing twice in ice cold azide buffer, $CD8^+$ T-cells were resuspended in azide buffer, split into 2 separate aliquots, and placed at room temperature. To one sample, an excess of unconjugated anti-HLA A2 mAb (clone BB7.2, Serotec, UK) at 100 µg/ml was added to block tetramer rebinding. 10 µl

of cells were then taken at time points 0, 2, 5, 8, 10, 15, 20, and 30 minutes, resuspended in PBS and analysed using a FACSCalibur flow cytometer. The remaining sample was left without BB7.2 and used as a control. Decays were repeated for all tetramers on the same day and data analysed with FlowJo software (TreeStar, Ashland, OR).

2.6.3 pMHCI tetramer association experiments

1 x 10^6 $CD8^+$ T-cells were washed twice in PSG and resuspended in 200 µl PBS with or without unconjugated anti-human CD8 antibody. 5 µg/ml of pMHCI tetramer was applied to the cell suspension, and at indicated time points 10 µl aliquots were taken out and placed in individual FACS tubes containing 100 µl PBS. The aliquots were removed from the master mix at the following time points; 0, 1, 2, 4, 6, 8, 10, 12, 15, 18, 20, 25, 28, and 30 minutes. Data was acquired using a FACSCalibur flow cytometer (BD) and analysed with FlowJo software (TreeStar).

2.7 Flow cytometry

2.7.1 Antibodies

2.7.2 Activating antibodies

Anti-human CD3 antibodies (clone OKT3 or UCHT1) were purchased from Pharmingen, BD Biosciences (San Jose, CA). The following anti-human CD8 antibodies were used in this study;

Table 2.7.3. Unconjugated anti-human CD8 antibodies

Antibody clone	CD8 α or β	Purchased from
OKT8	α	eBioscience, Hatfield, UK
SK1	α	BD Biosciences, New Jersey, USA
MCD8	α	IqProducts, Groningen, The Netherlands
32/M4	α	Santa Cruz Biotechnology Inc., Heidelberg, Germany
C8/144B	α	Santa Cruz Biotechnology Inc.
DK25	α	DAKO, Stockport, UK
2ST8.5H7	β	Abcam, Cambridge, UK

For experiments with mouse cells, the following anti-mouse CD8 antibodies were used in this study;

Table 2.7.4. Unconjugated anti-mouse CD8 antibodies

Antibody clone	CD8 α or β	Purchased from
CT-CD8a	α	Caltag-Medsystems, Buckingham, UK
53.6.7	α	Biolegend, Cambridge, UK
CT-CD8b	β	Caltag-Medsystems
KT112	β	hybridoma kindly provided by Prof. Rose Zamoyska

2.7.5 Fluorescent conjugated anti-human antibodies for detection of cell surface protein expression

Anti-CD3$^{FITC,\ PerCP,\ PE\text{-}Cy7,\ H7APC}$, anti-CD4$^{PE,\ PE\text{-}Cy\text{-}5.5,\ APC}$, anti-CD8α$^{FITC,\ PE,\ PerCP,\ PE\text{-}Cy7,\ APC}$, anti-CD8β^{PE}, anti-TCRαβ^{FITC}, pan-TCRγδ$^{FITC,\ PE}$, anti-CD19$^{Pacific\ Blue}$, anti-CD14$^{Pacific\ Blue}$, anti-CD56$^{FITC,\ APC}$, anti-CD107a^{FITC}, Violet Live/Dead stain ViViD$^{Pacific\ Blue}$, Aqua Live/Dead stain^{AmCyan}, Anti-HLA-A2 BB7.2^{FITC}, Violet Live/Dead stain^{PacificBlue} and Viaprobe^{TM}. All antibodies were purchased from either BD Pharmingen, BD Biosciences (Oxford, UK), Caltag-Medsystems (CA, USA), AbD Serotec (Oxford, UK), Beckman Coulter (High Wycombe, UK), eBioscience (Hatfield, UK), DakoCytomation (Stockport, UK) or Miltenyi Biotec (Surrey, UK). For full antibody source, see below methods.

2.7.6 Fluorescent conjugated anti-mouse antibodies for detection of cell surface protein expression

Anti-CD4$^{Pacific\ Blue}$, anti-CD45R/B220^{FITC}, anti-CD3$^{PerCP\text{-}Cy5.5}$.were purchased from BD Pharmingen, and BD Biosciences.

2.7.7 Fluorescent conjugated anti-human antibodies for detection of intracellular protein expression

Anti-IFN-γ$^{PE\text{-}Cy7}$, anti-TNF-α^{APC}, anti-MIP-1β^{PE} were purchased from BD Pharmingen and BD Biosciences.

2.7.8 pMHCI tetramer staining of $CD8^+$ T-cells clones and PBMC

5 x 10^4 $CD8^+$ T-cells clones (unless otherwise stated) were re-suspended in 40 µl PBS and stained with 1 µg PE, BV421, QDot605 or QDot800-conjugated pMHCI tetramer (final concentration of 25 µg/ml) for 15 minutes at 37°C. Cells were then stained with either 3 µl Peridinin-Cholorophyll proteins (PerCP)-conjugated anti-human CD3 (clone SK7, BD Biosciences), 3 µl APC-conjugated anti-human CD8 (clone SK1, BD Biosciences) and 5 µl 7-AAD for 20 minutes on ice or stained with 3 µl PE-Cy7 anti-human CD3 (clone SK7, BD Pharmingen), 3 µl FITC-conjugated anti-human CD8 (clone SK1, BD Biosciences) and 3 µl APC-conjugated anti-human CD4 (clone RPA-T4, BD Biosciences) and with LIVE/DEAD fixable violet for 20 minutes on ice. After washing twice in PBS, cells were resuspended in 200 µl of PBS. Data was acquired using either a FACSCalibur, FACSCanto II or a modified FACSAria II flow cytometer (all BD Biosciences) and analysed with FlowJo software (TreeStar).

2.5 x 10^5 PBMC`s from an HLA A2 donor (unless otherwise stated) were re-suspended in 40 µl PBS and stained with 0.5 µg PE-conjugated pMHCI tetramer (final concentration of 10 µg/ml) for 15 minutes at 37°C. Cells were then stained with 3 µl Fluorescein Isothiocyanate (FITC)-conjugated anti-human γδ-TCR (clone YB5.B8; BD Biosciences) or 3 µl FITC-conjugated anti-human CD56 (clone MEM188; Caltag-Medsystems, CA, USA) and 5 µl 7-AAD for 20 minutes on ice. In parallel experiments, cells were also stained with 3 µl PerCP-conjugated anti-human CD3 (clone SK7; BD Biosciences), 3 µl APC-conjugated anti-human CD8 (clone SK1; BD Biosciences) and 3 µl FITC-conjugated αβ-TCR (clone BMA 031; Serotec). After washing twice in PBS, cells were resuspended in 200 µl of PBS. Data was

acquired using a FACSCalibur flow Cytometer and analysed with FlowJo software (TreeStar).

2.7.9 Anti-CD8 antibodies and pMHCI tetramer staining of $CD8^+$ T-cells clones, lines and PBMC

5 x 10^4 $CD8^+$ T-cell clones were resuspended in 20 µl PBS and pre-incubated with or without unconjugated anti-human CD8 antibodies at a final concentration of 100 µg/ml of clone OKT8, 32/M4, C8/144B and 2ST8.5H7, 50 µg/ml of clone MCD8, 6.25 µg/ml SK1 or 25 µg/ml DK25 on ice for 20-25 minutes. Cells were also pre-incubated with 12.5, 6.25, 3.125 and 1 µg/ml DK25 and 6.25, 3.125 and 1 µg/ml SK1 on ice for 20-25 minutes. Following antibody pre-incubation, PE, APC, or BV421 conjugated pMHCI tetramers folded around peptides specific for each $CD8^+$ T-cell clone were added at a final concentration of 25 µg/ml and incubated at 37°C for 15 minutes prior to staining with 5 µl 7-AAD at 4°C for 30 minutes. Data was acquired using either a FACSCalibur or FACSCantoII flow cytometer and analysed with FlowJo software (TreeStar).

For human $CD8^+$ T-cell lines, 5 x 10^4 cells were pre-incubated with unconjugated anti-human CD8 antibodies at concentrations indicated above for 25 minutes on ice and then stained with cognate PE-conjugated tetramer (25 µg/ml) at 37°C for 15 minutes prior to staining with 5 µl amine-reactive fluorescent dye LIVE/DEAD Fixable Aqua (Life Technologies), 1 µl Pacific Blue-conjugated anti-human CD14 (clone Tuk4; Caltag-Medsystems), 1 µl Pacific Blue-conjugated anti-human CD19 (clone SJ25-C1; Caltag-Medsystems), 3 µl PE-Cy5.5–conjugated anti-human CD4 (clone S3.5; Caltag-Medsystems) and 3 µl FITC-conjugated anti-human CD8 (clone SK1; BD Biosciences) at 4°C for 20 minutes.

For human PBMCs directly *ex-vivo*, 1 x 10^5 cells were pre-incubated with anti-human CD8 antibodies at concentrations as indicated above for 25 minutes on ice and then stained with 1 μg HLA A2 APC-conjugated tetramer (25 μg/ml) at 37°C for 15 minutes prior to staining with 5 μl LIVE/DEAD Fixable Aqua (Life Technologies), 1 μl Pacific Blue-conjugated anti-human CD14 (clone Tuk4, Caltag-Medsystems), 1 μl Pacific Blue-conjugated anti-human CD19 (clone SJ25-C1, Caltag-Medsystems), 3 μl FITC-conjugated anti-human CD3 (clone HIT3a, BD Biosciences), 3 μl PE-Cy5.5-conjugated anti-human CD4 (clone S3.5 Caltag-Medsystems) and 3 μl PE-Cy7-conjugated anti-human CD8 (clone RPA-T8, BD Biosciences) at 4°C for 20 minutes. Data was acquired using either a FACSCanto II (BD Biosciences) and analyzed with FlowJo software (TreeStar).

2.7.10 pMHCI tetramer staining of murine F5 transgenic T-cells

5 x 10^4 cells were pre-incubated with 100 μg/ml anti-mouse CD8 antibody (clone CT-CD8a; Caltag-Medsystems, clone 53.6.7; BioLegend, clone KT112; in-house, or clone CT-CD8b; Caltag-Medsystems) for 20-25 minutes on ice and then stained with cognate PE-conjugated H-2D^b tetramer (25 μg/ml) at 37°C for 15 minutes prior to staining with 5 μl LIVE/DEAD FixableAqua (Life Technologies), 1 μl Pacific Blue-conjugated anti-mouse CD4 (clone RM4-5; BD Biosciences), 1 μl FITC-conjugated anti-mouse CD45R/B220 (clone RA3-6B2; BD Biosciences), and 1 μl PerCP-Cy5.5–conjugated anti-mouse CD3 (clone 17A2; BD Biosciences) at 4°C for 20 minutes. Data was acquired using either a FACSCanto II or a modified FACSAria II flow cytometer (both BD Biosciences) and analyzed with FlowJo software (TreeStar).

2.7.11 pMHCI tetramer staining of 293T CD8α

2 x 10^5 transfected 293T CD8α T-cells were incubated with 10 μg/ml of PE-conjugated tetramers for 15 minutes at 37°C, then stained with 5 μl 7-AAD and either 3 μl FITC-conjugated anti-human CD8 (clone SK1; BD Biosciences) or 3 μl PE-conjugated anti-CD8β (clone 2ST8.5H7; Beckman-Coulter, High Wycombe, UK) for 30 minutes on ice, washed twice, and resuspended in PBS. Data was acquired using a FACSCalibur flow cytometer (BD Biosciences) and analyzed with FlowJo software (TreeStar).

2.7.12 Antibody staining of PBMC

2.5 x 10^5 PBMC`s were stained with 3 μl PerCP-conjugated anti-human CD8 (clone SK1; BD Biosciences), 5 μl 7-AAD and either 3 μl FITC-conjugated anti-human αβ-TCR (clone BMA031; Serotec, UK), APC-conjugated anti-human CD56 (clone AF12-7H3; Miltenyi, CA, USA) or PE-conjugated anti-human γδ-TCR (clone YB5.B8; BD Biosciences) for 30 minutes on ice, washed twice, and resuspended in PBS. Data was acquired using a FACSCalibur flow cytometer (BD Biosciences) and analyzed with FlowJo software (TreeStar).

2.8 $CD8^+$ T-cell effector function assays

2.8.1 Intracellular Cytokine staining (ICS)

PBMCs were harvested from a healthy donor and cultured with or without 1 mg/ml Phytohemagglutinin (PHA) (Alere, Cheshire, U.K.) and 25 ng/ml IL-15 (Promega, Hampshire, U.K.) for 7 days then washed and cultured overnight in R2 medium. A total of 5 x 10^4 PBMCs (un-stimulated or stimulated with PHA/IL-15) were resuspended in the

presence of 1 µl/ml brefeldin A (GolgiPlug; Sigma-Aldrich), 0.7 µl/ml monensin (GolgiStop; BD Biosciences) and 5 µl/ml FITC-conjugated anti-human CD107a (clone H4A3; BD Biosciences) then incubated with unconjugated anti-human CD8 antibodies at previously indicated concentrations for 18 hours at 37°C in a 5% CO_2 atmosphere. After washing with PBS, cells were stained with 5 µl LIVE/DEAD Fixable Violet (ViViD; LifeTechnologies) at room temperature for 15 minutes. Subsequently, cells were washed and stained with 1 µl Pacific Blue-conjugated anti-human CD14 (clone Tuk4; Caltag-Medsystems), 1 µl Pacific Blue-conjugated anti-human CD19 (clone SJ25-C1; Caltag-Medsystems), 4 µl H7-APC-conjugated anti-human CD3 (clone SK7; BD Biosciences) and 3 µl PE-Cy5.5-conjugated anti-human CD4 (clone S3.5; Caltag-Medsystems) at 4°C for 20 minutes. Cells were then washed an additional three times, resuspended in 200 µl BD Cytofix/Cytoperm and incubated at 4°C for 20 minutes. After three additional washes in 1 x Perm/Wash (BD Biosciences; diluted with d.H_2O) cells were stained with 3 µl PE-Cy7-conjugated anti-human IFN-γ (clone B27; BD Biosciences), 3 µl APC-conjugated anti-human TNF-α (clone MAb11; BD Biosciences) and 3 µl PE-conjugated anti-human MIP-1β (clone D21-1351; BD Biosciences) at 4°C for 20 minutes. Cells were washed again three more times and resuspended in 200 µl Perm/Wash. Data was acquired using a modified FACSAria II flow cytometer (BD Biosciences) and analyzed with FlowJo software (Tree Star).

2.8.2 Peptide activation assays

3 x 10^4 rested $CD8^+$ T-cells were mixed with either HLA A*0201 wild-type, HLA A*0201 227/8, HLA A*0201 QE, HLA A*0201 K^b expressing C1R B cells which have been previously pulsed with or without cognate peptide titrated from 10^{-5} M to 10^{-11} M for 1 hour or with unconjugated anti-CD8 antibodies as stated. Cells were either washed twice prior to

the addition of $CD8^+$ T-cells to remove excess peptide or remained unwashed and incubated with or without secondary crosslinking by the addition of 5 µl anti-mouse IgG antibody (Beckman-Coulter) in a total volume of 100 µl in duplicate. Cells were then and incubated for 4 hours for antibody blocking assays where stated or for 18 hours at 37°C in a 5% CO_2 atmosphere. Positive controls included: (i) target cells pulsed with 10^{-7} M cognate peptide; (ii) 10 µg/ml unconjugated anti-human CD3 antibody (UCHT1; BD Biosciences); (iii) 1 µg/µl PHA (Alere-technologies, UK); or when using F5 transgenic mice (iv) 50 ng/ml phorbol myristate acetate (PMA) and 1 µg/ml ionomycin (Sigma-Aldrich). Negative controls included rested $CD8^+$ T-cells alone and $CD8^+$ T-cells incubated with target cells. Supernatants were harvested and assayed for MIP-1α, MIP-1β and RANTES using a Quantikine duoset ELISA kit (R&D Systems, Abingdon, UK).

2.8.3 ELISA (Enzyme-linked immunosorbent assay for MIP-1α, MIP-1β, IFN-γ, and RANTES

All ELISAs were performed according to the manufacturer's instructions using the advised reagents (Wash buffer, Regent diluents, Streptavidin HRP, Chromogen, Peroxide and Stop solution (all R&D systems)). Briefly 96 well ELISA microplates (R&D systems) were coated with 50 – 100 µl diluted capture antibody. Plates were incubated overnight at room temperature and washed three times using an AquaMax 2000 microplate washer (MDS analytical technologies, Sunnyvale, USA). Plates were then blocked for a minimum of 60 minutes using reagent diluent. Plates were washed again and 50 – 100 µl of cell supernatant was added including 50 – 100 µl of serially diluted standard solution. Plated were incubated for 75 minutes and washed again and 100 µl of diluted detection antibody was added to each

well. Plates were incubated as recommended and washed prior to the addition of diluted Streptavidin-horseradish peroxidise. After a further incubation, plates were washed and 50 – 100 µl of 1:1 solution of chromogen and peroxide added. Plates were incubated for 20 minutes avoiding exposure to the light. 50 µl of stop solution (sulphuric acid) was then added and plates were read at 450 nm with a reference filter set at 570 nm (Bio-rad iMark microplate reader, Bio-rad, UK).

2.8.4 Tetramer activation assays

2.5 x 10^4 $CD8^+$ T-cell clones were incubated with HLA A2 or HLA A2 variant tetramers conjugated to QDot605 or QDot800, at 1 µg/ml overnight at 37°C. Supernatant was then harvested and assayed for MIP-1β production by ELISA (R&D). 2.5 x 10^4 $CD8^+$ T-cell clones were incubated with HLA A2 or HLA A2 variant tetramers conjugated to PE at 1 and 5 µg/ml for 4 hours at 37°C. $CD8^+$ T-cell clones were also incubated with 5 µl/ml FITC-conjugated anti-human CD107a (clone H4A3, BD Biosciences) and 0.7 µl/ml monensin (Golgi-Stop BD Biosciences) (Betts, Brenchley et al. 2003). Cells were then stained with APC-conjugated anti-human CD8 (Clone SK1, BD Biosciences) for 20 mins on ice. Data was acquired using a FACSCalibur flow cytometer and analyzed with FlowJo software (Tree Star).

2.8.5 Chromium Release Assay

2 x 10^3 $CD8^+$ T-cell clones were treated with unconjugated anti-human CD8 antibodies at varying concentrations in 100 µl R2 medium. 2 x 10^3 C1R-HLA A2 target cells (100 µl), labelled with 30 µCi of ^{51}Cr (PerkinElmer, Cambridge, UK) per 10^6 cells for 1 hour

previously, were subsequently added. Targets were also cultured alone (target spontaneous release) and with TritonX-100 (Sigma-Aldrich) at a final concentration of 5% (target total release). Cells were incubated at 37°C for 18 hours in a 5% CO_2 atmosphere. For each sample, 20 µl supernatant was harvested and mixed with 150 µl OptiPhase Supermix Scintillation Cocktail (PerkinElmer). Plates were analyzed using a liquid scintillator and luminescence counter (MicroBeta TriLux; PerkinElmer) with Microbeta Windows Workstation software (PerkinElmer). Specific lysis was calculated according to the following formula: (experimental release - target spontaneous release/target total release - target spontaneous release) x 100. Each value was calculated as the average of triplicates and shown with SEM.

2.8.6 CBA (Cytometric bead array)

The supernatants that were generated from the experiments referred to in section 2.8.3, were assayed using the human Th1/Th2 Cytokine kit specific for IL-2, IL-4, IL-5, IL-10, TNF-α and IFN-γ (BD Biosciences) according to the manufacturer's instructions. Briefly, 25 µl of cell supernatant was incubated with diluted R-phycoerythrin (PE)-conjugated detection antibodies and beads coated with the relevant capture antibodies at room temperature for three hours, after which the beads were washed twice with wash buffer (BD), and resuspended in PBS (Oxoid). The samples were acquired using a FACSCalibur (BD Biosciences) flow cytometer and the results analysed using the CBA 6 Bead analysis software (BD Biosciences).

3

THE LOW SOLUTION BINDING AFFINITY OF THE pMHCI/CD8 INTERACTION IS ESSENTIAL FOR THE MAINTENANCE OF CD8$^+$ T-CELL ANTIGEN SPECIFICITY

(Clement et al 2010 & Appendix 1)

3.1 Introduction

CD8 has the potential to engage all pMHCI complexes, both self and foreign, because it binds to largely non-polymorphic regions of the MHCI molecule. Recent publications suggest that the ability of CD8 to interact with non-stimulatory pMHCI complexes lowers T-cell activation thresholds and enables $CD8^+$ T-cells to respond to low copy numbers of specific pMHCI (Yachi, Ampudia et al. 2005; Anikeeva, Lebedeva et al. 2006). It therefore remains unclear how the specificity of TCR recognition is maintained despite the potential for multiple pMHCI/CD8 interactions at the cell surface. One possibility resides in the fact that the binding of CD8 to MHCI is characterized by very low affinities and extremely rapid kinetics. In this chapter, I intend to probe the functional significance of the low solution affinity pMHCI/CD8 interaction using pMHCI molecules with super-enhanced CD8 binding properties.

3.1.1 T-cell recognition of antigen involves the binding of two receptors (TCR and CD8) to a single ligand (pMHCI): implications for $CD8^+$ T-cell activation

The exquisite specificity of the TCR/pMHCI interaction is the critical factor in permitting specific T-cell activation. The TCR must be able to recognise a large number of different peptides presented at the cell surface whilst ensuring that it does not recognise self peptides. Whilst stimulation of the TCR is required for T-cell activation, stimulation through this receptor alone is inadequate for full and sustained T-cell activation. Signals provided by the co-receptor and other accessory molecules provide an extra stimulus that leads to activation of anti-apoptotic proteins and supporting cytokines (Watts and DeBenedette 1999). As previously discussed, the MHCI binding site for CD8 is physically distinct from the peptide-

binding domains that are recognized by the TCR (Rudolph and Wilson 2002) and this spatial segregation allows both TCR and CD8 to bind a single MHCI molecule simultaneously (Gao, Tormo et al. 1997). Thus, T-cell recognition of antigen could involve the binding of two receptors (TCR and CD8) to a single ligand (pMHCI), a *modus operandi* that is unique to αβ T-cell biology. Indeed, a large proportion of CD8 and TCR molecules are constitutively associated on $CD8^+$ T-cells in the absence of TCR engagement by agonist ligands suggesting that the TCR and CD8 pre-exist as bi-specific receptors that can engage pMHCI agonist ligands in an ordered manner (Beyers, Spruyt et al. 1992; Suzuki, Kupsch et al. 1992; Doucey, Goffin et al. 2003; Demotte, Stroobant et al. 2008).

Fluroesence Energy Resonance Transfer techniques (FRET) studies investigating the interaction of CD8 and TCR/CD3 with specific pMHCI suggest that TCR binding to pMHCI occurs first, thereby satisfying the antigen-specific component of the interaction, and that the recruitment of CD8 occurs subsequently (Yachi, Ampudia et al. 2005; Yachi, Ampudia et al. 2006). Using T-cell hybridomas, this data pointed to a chronological sequence according to which the pivotal antigen specific proofreading event provided by the TCR occurs prior to the association of CD8 with the TCR/CD3 complex. This is often referred to as the 'sequential engagement model'. This mechanism would ensure that CD8 recruitment only results in the amplification of downstream signalling cascades for ligands that engage the TCR with favourable kinetics. In this scenario, the TCR could also discriminate between agonist and non-agonist pMHCI complexes, with CD8 recruitment being enabled only in the context of agonist-ligand interactions with the TCR. Indeed data by Yachi *et al* demonstrated that the kinetics of CD8 recruitment to the TCR ensures that the TCR can specifically distinguish between structurally similar peptides (Yachi, Ampudia et al. 2006). This was further

supported by Jiang *et al* who proposed that the induced recruitment of CD8 following TCR/pMHCI engagement serves to stabilize molecular contact between the $CD8^+$ T-cell and the antigen presenting cell, thereby unveiling another potential role for CD8 (Jiang, Huang et al. 2010). This data further supports the importance of CD8 in allowing the TCR to specifically distinguish between self and non-self peptides, thus highlighting the importance of CD8 in controlling T-cell specificity.

3.1.2 Biophysical measurements of the TCR/pMHCI and pMHCI/CD8 interaction

Surface plasmon resonance (SPR) has provided a reliable way of measuring very weak receptor-ligand interactions in real time. SPR uses soluble molecules therefore the technique can be used to measure the affinity and kinetics of the TCR/pMHCI interaction and pMHCI/CD8 interaction in the absence of cell surface effects. The results of these SPR studies are quite striking. The pMHCI/CD8 interaction is characterized by very low solution binding affinities (K_D ~146 μM) (Table 1.1) and rapid kinetics (K_{off} ~18 s^{-1}) (Wyer, Willcox et al. 1999; Gao, Willcox et al. 2000). Indeed, the affinity of the pMHCI/CD8 interaction is even lower than the corresponding values measured for conventional molecular binding events involved in cell-cell recognition, such as the CD2/CD48 interaction (K_D = 60-90 μM) (Dustin, Golan et al. 1997; Wyer, Willcox et al. 1999).

In stark contrast, the TCR/pMHCI interaction can be more than 1000-fold stronger than the pMHCI/CD8 interaction (K_D range for agonists from 0.14 μM, the strongest natural TCR/pMHCI interaction measured to date) (Table 3.1) and exhibits considerably slower kinetics (K_{off} range for agonists from 0.01 to 1 s^{-1}) (Davis, Boniface et al. 1998; Cole,

Pumphrey et al. 2007; Laugel, van den Berg et al. 2007; Varela-Rohena, Molloy et al. 2008; Stone, Chervin et al. 2009). Typical TCR/pMHCI interaction are characterised by K_{Ds} of between 0.1 and 50 µM (Table 3.1) as measured using surface plasmon resonance (SPR) (Bridgeman, Sewell et al. 2011). Although, recent data suggests that alloreactive and autoreactive TCR/pMHCI interactions may be outliers and can be characterised by a much weaker affinity (K_D > 180 µM). It seems extremely unlikely that the striking biophysical characteristics of the pMHCI/CD8 interaction have occurred by accident. Indeed, this conclusion is strengthened by the finding that the pMHCI/CD8 interaction is capable of exerting the vast majority of its biological function when weakened even further (Hutchinson, Wooldridge et al. 2003), which suggests that CD8 has specifically evolved to operate at very low solution affinities.

Table 3.1: Binding affinities of human TCR to pMHCI using SPR (Bridgeman, Sewell et al. 2011)

Autoreactive, alloreactive, anti-cancer and anti-pathogen TCR/pMHC binding affinity measurements are shown in blue, green, red and black, respectively.

TCR/pMHCI	K_D (µM)
PP1 TCR/A*0201-ALW (Cole, Edwards et al. 2010)	270 ± 40
LC13 TCR/B*4402-allo (Macdonald, Chen et al. 2009)	189 ± 7
LC13 TCR/B*4405-allo (Macdonald, Chen et al. 2009)	49 ± 0.2
A6 TCR/A*0201-HuD (Borbulevych, Piepenbrink et al. 2009)	48 ± 4
MEL187.c5/A*0201-EAA (Cole, Edwards et al. 2010)	42 ± 0.3
TEL TCR/A*0201-ILA (Cole, Pumphrey et al. 2007)	34 ± 2
MEL187.c5/A*0201-ELA (Cole, Edwards et al. 2010)	18 ± 0.3
MEL5 TCR/A*0201-ELA (Cole, Pumphrey et al. 2007; Cole, Edwards et al. 2010)	18 ± 1
IG4 TCR/A*0201-NYESO (Chen, Stewart-Jones et al. 2005)	13.3 ± 0.4

gp100 TCR/A*0201-YLE (Cole, Pumphrey et al. 2007)	11 ± 0.5
MEL5 TCR/A*0201-EAA (Cole, Edwards et al. 2010)	6.4 ± 0.04
A6 TCR/A*0201-Tel1p (Laugel, Boulter et al. 2005; Borbulevych, Piepenbrink et al. 2009)	41 ± 2
RA14 TCR/A*0201-NLV (Gras, Saulquin et al. 2009)	27.7 ± 2.3
AM3 TCR/A*2402-EBV (Cole, Pumphrey et al. 2007)	21 ± 0.8
DM1 TCR/B*4403-EENL (Archbold, Macdonald et al. 2009)	9.4 ± 0.2
LC13 TCR/B*0801-EBNA (Borg, Ely et al. 2005; Cole, Pumphrey et al. 2007)	9 ± 0.4
CF34 TCR/B*0801-EBNA (Gras, Burrows et al. 2009)	8.9 ± 1.3
AS01 TCR/A*0201-GLC (Miles, Bulek et al. 2010)	8.1 ± 1
TCR_{CMV}/A*0201-pp65 (Gakamsky, Lewitzki et al. 2007)	6.3 ± 1
DM1 TCR/B*4402-EENL (Archbold, Macdonald et al. 2009)	6.3 ± 0.3
GRB TCR/B*2702-Flu (Cole, Pumphrey et al. 2007)	6 ± 0.1
JM22 TCR/A*0201-GIL (Willcox, Gao et al. 1999; Cole, Pumphrey et al. 2007)	5 ± 0.2
TK3 TCR/B*3501-HPVG (Gras, Chen et al. 2010)	2.2 ± 0.2
G10 TCR/A*0201-SL9 (Lee, Stewart-Jones et al. 2004)	2.2 ± 0.5
A6 TCR/A*0201-Tax (Ding, Baker et al. 1999; Cole, Pumphrey et al. 2007)	2 ± 0.7
B7 TCR/A2-Tax (Davis-Harrison, Armstrong et al. 2005)	1.35 ± 0.04
DM1 TCR/B4405-EENL (Archbold, Macdonald et al. 2009)	0.3 ± 0.1
868 TCR/A*0201-SL9 (Varela-Rohena, Molloy et al. 2008)	0.13 ± 0.01

3.1.3 Summary and Aims

It has been proposed that the stronger TCR/pMHCI interaction dominates thereby maintaining $CD8^+$ T-cell specificity and that CD8 can only initiate its effects on signal transduction if the TCR/pMHCI interaction is of sufficient duration. This is consistent with the sequential engagement model of co-receptor function which proposes that the co-receptor is only recruited to the TCR once a stable TCR/pMHCI interaction has been established (Hampl, Chien et al. 1997; Madrenas, Chau et al. 1997). This led me to hypothesise that the

pMHCI/CD8 interaction must remain substantially weaker than the TCR/pMHCI interaction in order to maintain $CD8^+$ T-cell specificity and efficient co-receptor function.

Here I intend to probe the functional significance of the low solution binding affinity of the pMHCI/CD8 interaction in maintaining the specificity of TCR/pMHCI binding at the T-cell surface and pMHCI induced T-cell activation. In order to do this, I will use chimeric pMHCI molecules with super-enhanced affinities for CD8 that lie within the typical range for agonist TCR/pMHCI interactions (K_D ~10 μM).

3.2 Results

3.2.1 Generation of MHCI molecules with super-enhanced CD8 binding affinity

Tetrameric fusion molecules comprising the α1/α2 peptide binding platform of HLA A*0201 (A2 from hereon) and the α3 domain of H2-K^b (A2/K^b from hereon) enable the monitoring of $CD8^+$ T-cell responses in A2 transgenic mice (Choi, Palmowski et al. 2002). This reflects a requirement for the murine MHCI α3 domain to engage murine CD8 (Purbhoo, Boulter et al. 2001), thus enabling A2/K^b reagents to stain murine $CD8^+$ T-cells with lower affinity TCR/pMHCI interactions (so-called 'low avidity' $CD8^+$ T-cells) (Choi, Chen et al. 2003). The A2/K^b heavy chain folded with human β2m interacts strongly with human CD8 (K_D ~10 μM; compared to HLA A2 which binds to CD8 with a K_D ~ 146 μM) but exhibits faithful HLA A2-restricted TCR binding properties (Choi, Chen et al. 2003; Wooldridge, van den Berg et al. 2005). Thus, fusing the murine α3 domain with A2 α1/α2 domains increases the strength of the pMHCI/CD8 interaction by approximately 15-fold without affecting the TCR/pMHCI interaction (Figure 3.1).

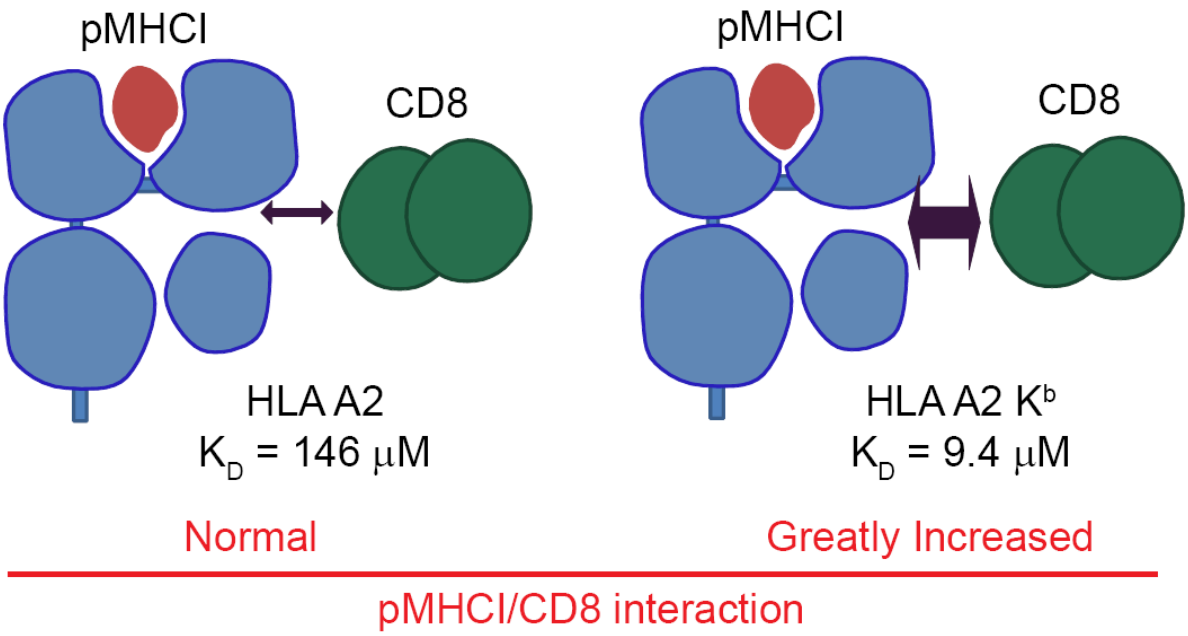

Figure 3.1: Wild-type and super enhanced pMHCI/CD8 binding affinity. A2/ K^b binding affinity to CD8 is increased to approximately 15 times the normal A2/CD8 binding when analysed by Surface Plasma Resonance.

3.2.2 Super-enhanced CD8 binding results in non-specific TCR/pMHCI interactions

Monomeric pMHCI complexes cannot be used to examine TCR/pMHCI binding at the cell surface due to the extremely short half-life of such interactions. Increasing the valency of these molecules by avidin/biotin-based tetramerization overcomes this limitation and produces reagents that are invaluable for the identification and characterization of antigen-specific $CD8^+$ T-cells (Altman, Moss et al. 1996; Wooldridge, Lissina et al. 2009). Indeed, it is well established that wild-type tetrameric pMHCI reagents bind to cell surface TCR with exquisite specificity (Altman, Moss et al. 1996; Burrows, Kienzle et al. 2000). Thus, I generated $A2/K^b$ tetrameric reagents to study the effect of super enhanced CD8 binding on the specificity of pMHCI ligand interactions at the cell surface.

Wild-type pMHCI tetrameric reagents bearing cognate peptide stained an HLA A2 restricted $CD8^+$ T-cell clone (MEL5) specific for the Melan-A-derived epitope ELAGIGILTV (residues 26-35) (Figure 3.2 A). Non-cognate A2 tetramers folded around the human telomerase reverse transcriptase (hTERT)-derived epitope ILAKFHWL (residues 540-548) failed to stain the MEL5 $CD8^+$ T-cell clone. However, $A2/K^b$ ILAKFLHWL tetramers stained all ELAGIGILTV specific $CD8^+$ T-cells. To examine this effect in more detail, I stained fresh human PBMC with HLA A2 and $A2/K^b$ tetramers. Antigen-specific $CD8^+$ T-cell populations were not identified in PBMC from healthy donors with either the A2 ELAGIGILTV or A2 ILAKFLHWL tetramers (Figure 3.2 B). In contrast, both the $A2/K^b$ ELAGIGILTV and $A2/K^b$ ILAKFLHWL tetramers stained >85% of $CD8^+$ T-cells in PBMC (Figure 3.2 B). Taken together, these data indicate that the exquisite specificity of tetrameric pMHCI reagents is lost when the strength of the pMHCI/CD8 interaction is increased by ~15-fold.

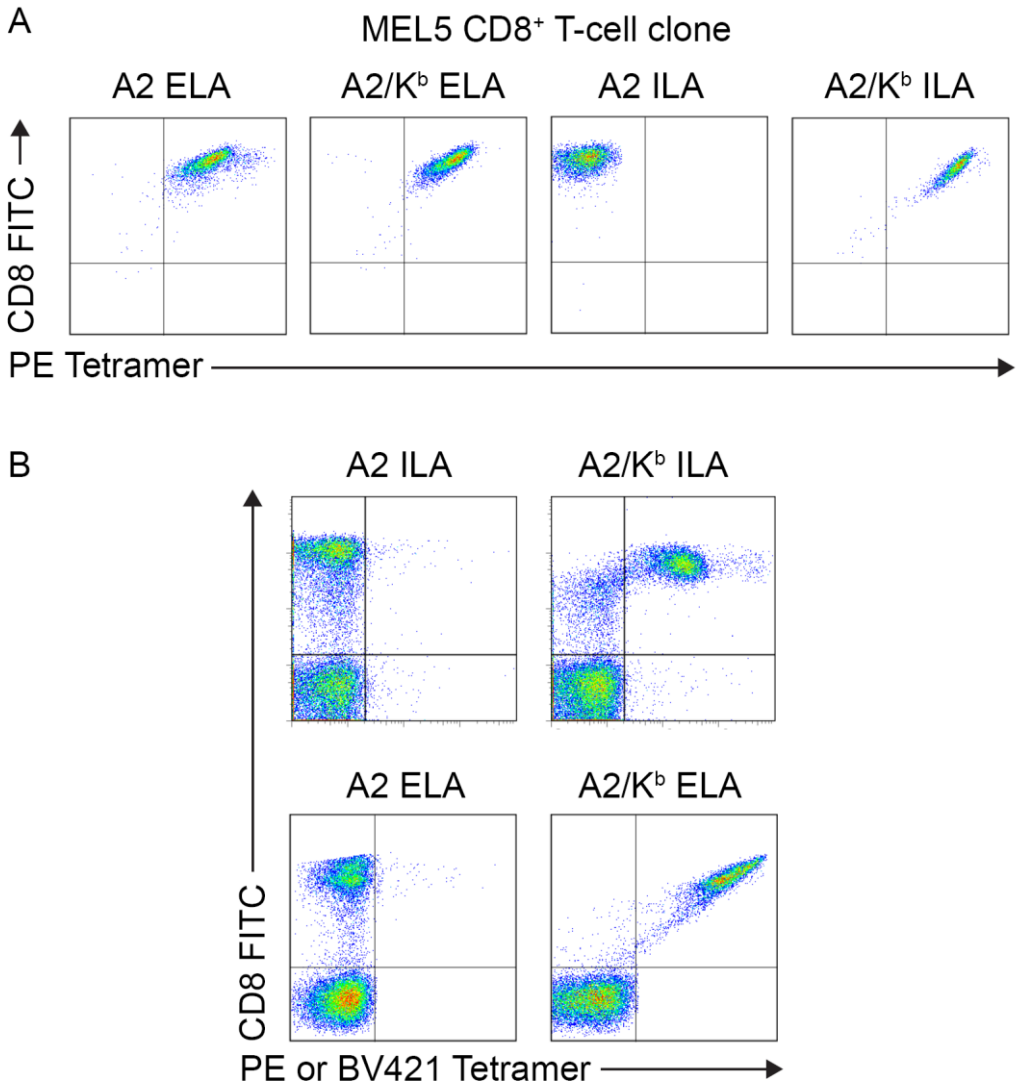

Figure 3.2: The exquisite specificity of pMHCI tetramer staining is lost when the strength of the pMHCI/CD8 interaction is increased by ~15-fold. (**A**) 5 x 10^4 of the MEL5 $CD8^+$ T-cell clone specific for the Melan-A-derived epitope ELAGIGILTV (residues 26-35) was stained with 1 µg of the PE-conjugated tetramers A2 ELAGIGILTV, A2/K^b ELAGIGILTV, A2 ILAKFLHWL or A2/K^b ILAKFLHWL in 40 µl PBS for 15 minutes at 37°C. Cells were then stained with either FITC-conjugated anti-human CD8, and 7-AAD for 30 minutes on ice, washed twice and resuspended in PBS. Data were acquired using a FACSCalibur flow cytometer and analyzed with FlowJo software. (**B**) 2.5 x 10^5 PBMC were resuspended in 40 µl PBS, then stained with 1 µg of either PE-conjugated tetramers A2 ILAKFLHWL, A2/K^b ILAKFLHWL, or BV421-conjugated tetramers A2 ELAGIGILTV, or A2/K^b ELAGIGILTV for 15 minutes at 37°C. Each sample was subsequently stained with FITC-conjugated anti-human CD8, PerCP or PE-Cy7-conjugated anti-human CD3, APC-conjugated anti-human CD4 and 7-AAD or LIVE/DEAD fixable Aqua for 30 minutes on ice, washed twice and resuspended in PBS. Data were acquired using a FACSCanto II flow cytometer and analysed with FlowJo software by gating on the live $CD3^+$ population.

Therefore, the low solution affinities of the wild-type pMHCI/CD8 interaction are essential in maintaining pMHCI binding specificity at the cell surface.

3.2.3 A2/K^b tetramers bind the majority of CD8$^+$ T-cells in peripheral blood

Non-cognate A2/K^b tetramers bind ~80% of the CD8α$^+$ population in peripheral blood (Figure 3.2 B). Although CD8α is predominantly found on the surface of αβ TCR$^+$ CD8$^+$ T-cells, it is also found on the surface of other lymphocytes, most notably some γδ T-cells and natural killer (NK) cells. Therefore, it was necessary to determine the identity of the CD8α$^+$ cells that stained with A2/K^b tetramers. Staining of fresh *ex-vivo* PBMC isolated from healthy HLA A2$^+$ donors revealed that CD8α was expressed on approximately 39%, 54% and 32% of the αβ TCR$^+$, NK cell and γδ TCR$^+$ populations respectively, with some variation between donors (Figure 3.3 A). The majority of γδ TCR$^+$ (~93.6%) and NK cells (~77%) failed to stain with the A2/K^b ILAKFLHWL tetramer and no significant binding was observed with the corresponding HLA A2 tetramer (Figure 3.3 B). However, the vast majority of αβ TCR$^+$/CD8$^+$ cells within the lymphocyte population stained non-specifically with the A2/K^b ILAKFLHWL tetramer (Figure 3.3 C). I hypothesised that most γδ TCR$^+$ cells and NK cells might fail to bind A2/K^b tetramers because they express the CD8αα homodimer rather than the CD8αβ heterodimer, which is expressed exclusively on the surface of αβ TCR$^+$/CD8$^+$ T-cells. Thus, a 293T cell line that expressed CD8αα was generated (Figure 3.4 A) to examine the ability of A2/K^b tetramers to bind this homodimeric form of the CD8 co-receptor on the cell surface. In contrast to both HLA A2 and HLA A2 D227K/T228A tetramers, which exhibit normal and abrogated interactions with CD8 respectively, A2/K^b tetramers bound to most (74.3%) of the CD8αα$^+$ 293T cell transfectants (Figures 3.4 A&B); no binding was

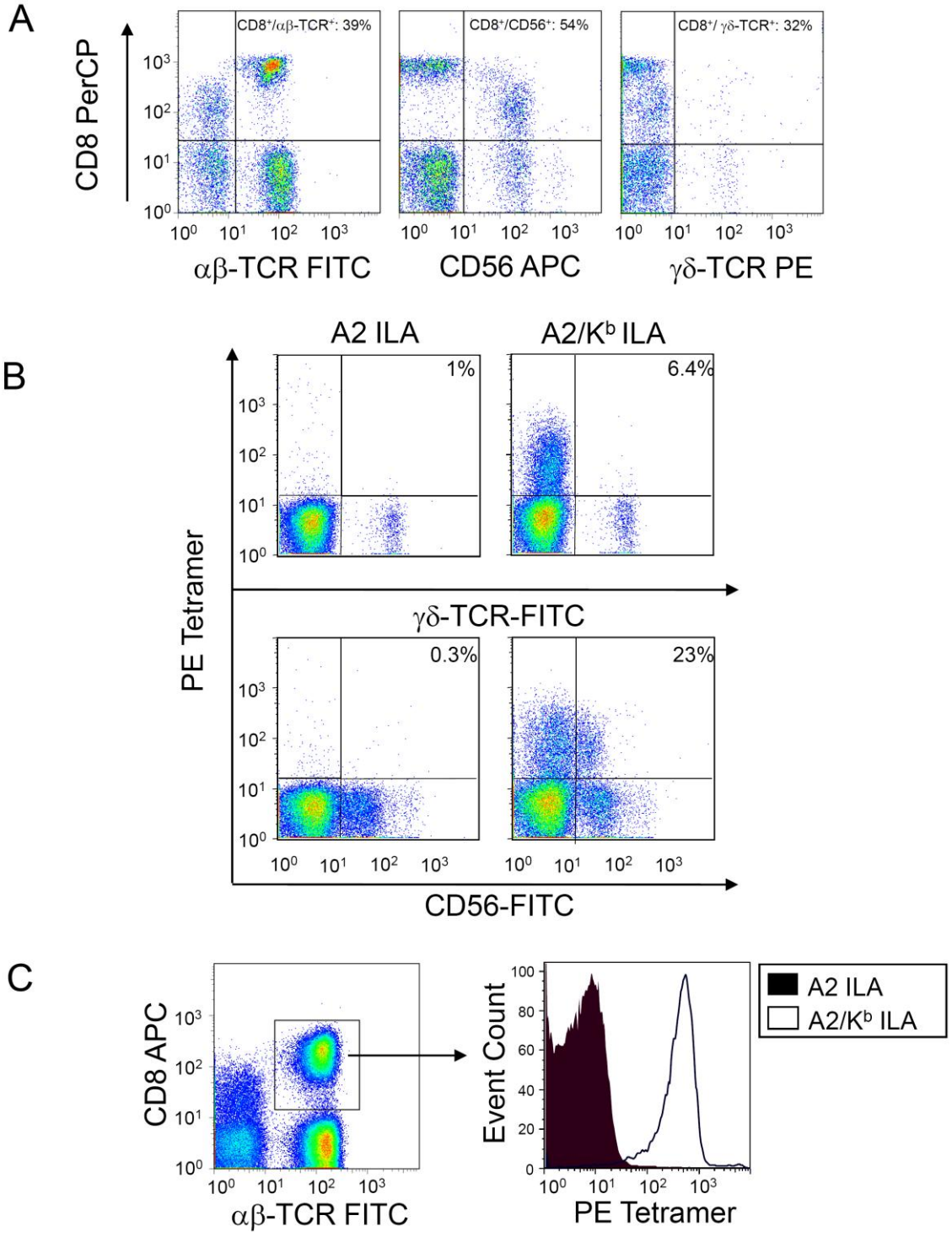
A
CD8 PerCP
CD8+/αβ-TCR+: 39%
CD8+/CD56+: 54%
CD8+/ γδ-TCR+: 32%
αβ-TCR FITC
CD56 APC
γδ-TCR PE
B
A2 ILA
A2/Kb ILA
1%
6.4%
0.3%
23%
PE Tetramer
γδ-TCR-FITC
CD56-FITC
C
CD8 APC
αβ-TCR FITC
Event Count
PE Tetramer
A2 ILA
A2/Kb ILA

Figure 3.3: A2/K^b tetramers bind the majority of αβ TCR$^+$/CD8$^+$ T-cells in peripheral blood. (**A**) 2.5 x 10^5 PBMC from an A2$^+$ donor were stained with PerCP-conjugated anti-human CD8, 7-AAD and either FITC-conjugated anti-human αβ TCR, APC-conjugated anti-human CD56 or PE-conjugated anti-human γδ TCR for 30 minutes on ice, washed twice and resuspended in PBS. (**B**) 2.5 x 10^5 A2$^+$ PBMC were stained with 10 μg/ml of the PE-conjugated tetramers A2 ILAKFLHWL or A2/K^b ILAKFLHWL for 20 minutes at 37°C. After washing, cells were subsequently stained with 7-AAD and either FITC-conjugated anti-human γδ TCR or FITC-conjugated anti-human CD56 for 30 minutes on ice, washed twice and resuspended in PBS. (**C**) 2.5 x 10^5 A2$^+$ PBMC were stained with 10 μg/ml of the PE-conjugated tetramers A2 ILAKFLHWL or A2/K^b ILAKFLHWL for 20 minutes at 37°C. After washing, cells were stained with APC-conjugated anti-human CD8, FITC-conjugated anti-human αβ TCR and 7-AAD for 30 minutes on ice, washed twice and resuspended in PBS. In **A**, **B** and **C**, data were acquired using a FACSCalibur flow cytometer and analyzed with FlowJo software.

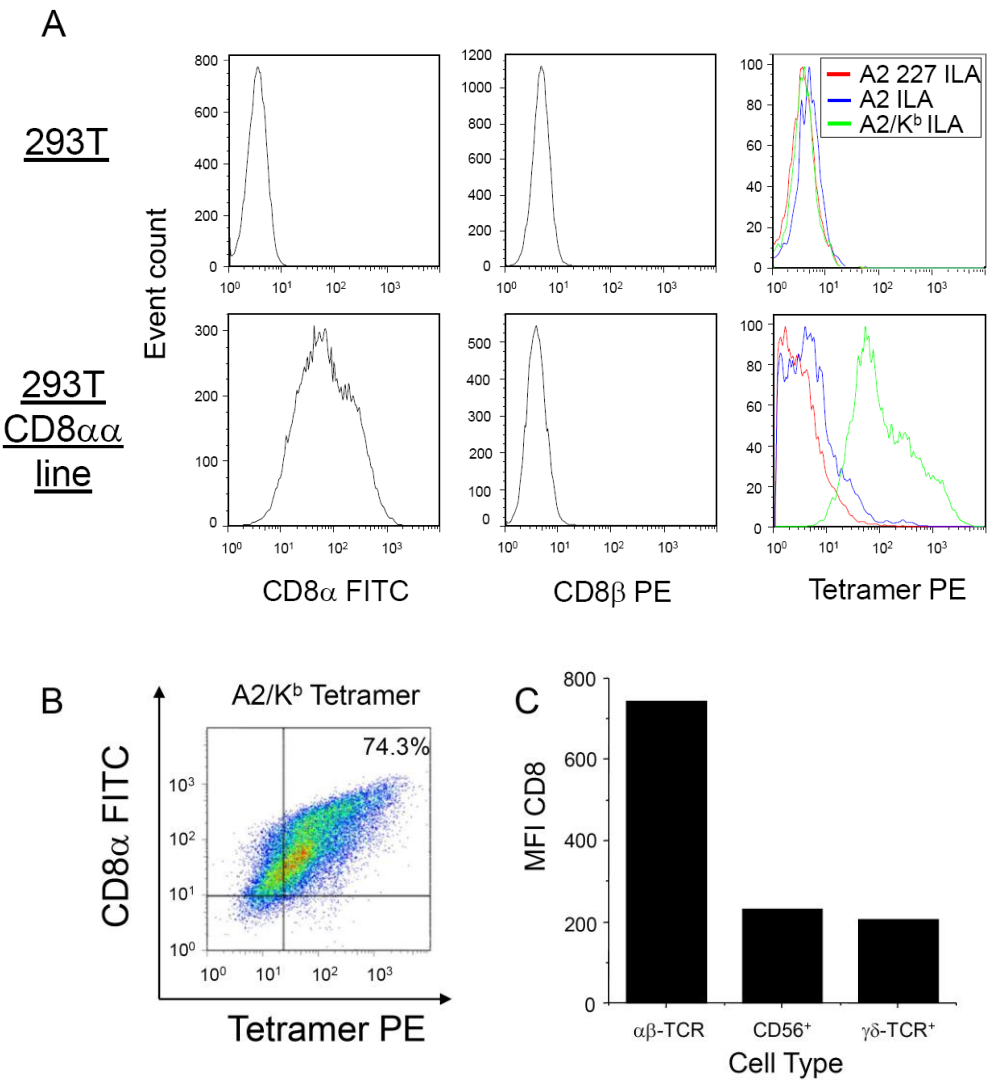

Figure 3.4: Non-specific A2/K^b tetramer binding is influenced by CD8 cell surface density. (**A&B**) 2 x 10^5 non-transfected or CD8αα transfected 293T cells were incubated +/- 10 μg/ml of the PE-conjugated tetramers A2 D227K/T228A ILAKFLHWL, A2 ILAKFLHWL or A2/K^b ILAKFLHWL for 20 minutes at 37°C, then stained with 7-AAD and either FITC-conjugated anti-human CD8 or PE-conjugated anti-human CD8β for 30 minutes on ice, washed twice and resuspended in PBS. (**C**) 2.5 x 10^5 PBMC were stained with PerCP-conjugated anti-human CD8, 7-AAD and either FITC-conjugated anti-human αβ TCR, APC-conjugated anti-human CD56 or PE-conjugated anti-human γδ TCR for 30 minutes on ice, washed twice and resuspended in PBS. In **A**, **B** and **C**, data were acquired using a FACSCalibur flow cytometer and analyzed with FlowJo software.

observed in the absence of CD8αα surface expression (Figure 3.4 A). Thus, A2/K^b tetramers are capable of binding to cell surface CD8αα. The question still remained as to why A2/K^b tetramers bind predominantly to the αβ $TCR^+/CD8^+$ T-cell population in peripheral blood and not to other cells that express CD8. Figure 3.4 B shows that A2/K^b tetramer staining is directly proportional to the level of CD8αα expression, such that only cells with a higher level of CD8αα expression stain with this reagent. Examination of PBMC from healthy donors revealed that αβ $TCR^+/CD8^+$ T-cells express high levels of CD8, whereas NK and γδ TCR^+ cells express substantially lower levels (Figure 3.4 C). Therefore, increasing the strength of the pMHCI/CD8 interaction allows pMHCI ligand binding at the cell surface that can be mediated through the engagement of either CD8αα or CD8αβ. However, this result suggests that binding is only observed when cells express CD8 at levels above a certain threshold. Importantly, these data demonstrate that TCR expression is not required for cell surface binding of A2/K^b tetramers.

3.2.4 A2/K^b tetramers activate $CD8^+$ T-cell clones irrespective of TCR specificity

It is well established that pMHCI tetramers can activate $CD8^+$ T-cell clones bearing cognate TCR (as reviewed in (Wooldridge, Lissina et al. 2009). However, previous studies have shown that pMHCI tetrameric binding at the cell surface does not necessarily equate with activation by cell surface antigen (Purbhoo, Boulter et al. 2001; Schott and Ploegh 2002). To determine whether non-specific A2/K^b tetramer binding at the cell surface (Figures 3.2 - 3.4) could activate human $CD8^+$ T-cell clones, ALF3 A2 restricted $CD8^+$ T-cell clone specific for the Influenza A virus $MP1_{58-66}$ epitope GILGFVFTL was used (Cole, Edwards et al. 2010). Consistent with the findings above, when staining the ALF3 $CD8^+$ T-cell clone with tetramers A2 ILAKFLHWL or A2/K^b ILAKFLHWL conjugated with either streptavidin-

QDot605 or streptavidin-QDot800, no staining was observed with the A2 ILAKFLHWL whereas non–specific staining was observed with the A2/K^b ILAKFLHWL (Figure 3.5 A). On ligation, it is known that TCRs are down-regulated from the cell surface (Valitutti, Muller et al. 1995). This TCR down-regulation correlated with various functional readouts typical of $CD8^+$ T-cell effector activity where both QDot 605 and QDot 800 A2/K^b ILAKFLHWL tetramers induced the release of MIP-1β non-specifically (Figure 3.5 B). Results similar to Figure 3.5 A&B were also obtained with tetramers conjugated to fluorochromes other than QDots (Appendix 1 Figure 4 A-F). This then eliminated the possibility of the tetramer fluorochrome being the cause for the non-specific activation by fluorochrome aggregation. Similar results were observed with SLYNTVATL-specific $CD8^+$ T-cell clones 003 and 868 bearing alternative cognate TCRs where non-cognate A2/K^b tetramers can induce release of IFN-γ, RANTES and CD107a (Appendix 1 Figure 4 D-F). Consistent with the staining patterns, the activation of $CD8^+$ T-cells by non-cognate A2/K^b tetramers was less efficient than that induced by tetramers bearing the agonist peptide (Appendix 1 Figure 4 C-E). Thus, at least to some extent, the strong interaction between A2/K^b and CD8 can bypass the requirement for a specific TCR/pMHCI interaction and non-specifically activate human $CD8^+$ T-cells.

3.2.5 Cell surface-expressed A2/K^b activates $CD8^+$ T-cells in the absence of cognate antigen

To extend the investigation to the more natural situation of cell surface pMHCI presentation, C1R B-cells transfected with either HLA A2 or A2/K^b at similar cell surface MHCI densities were selected as targets for further experiments. Target cells expressing either HLA A2 or

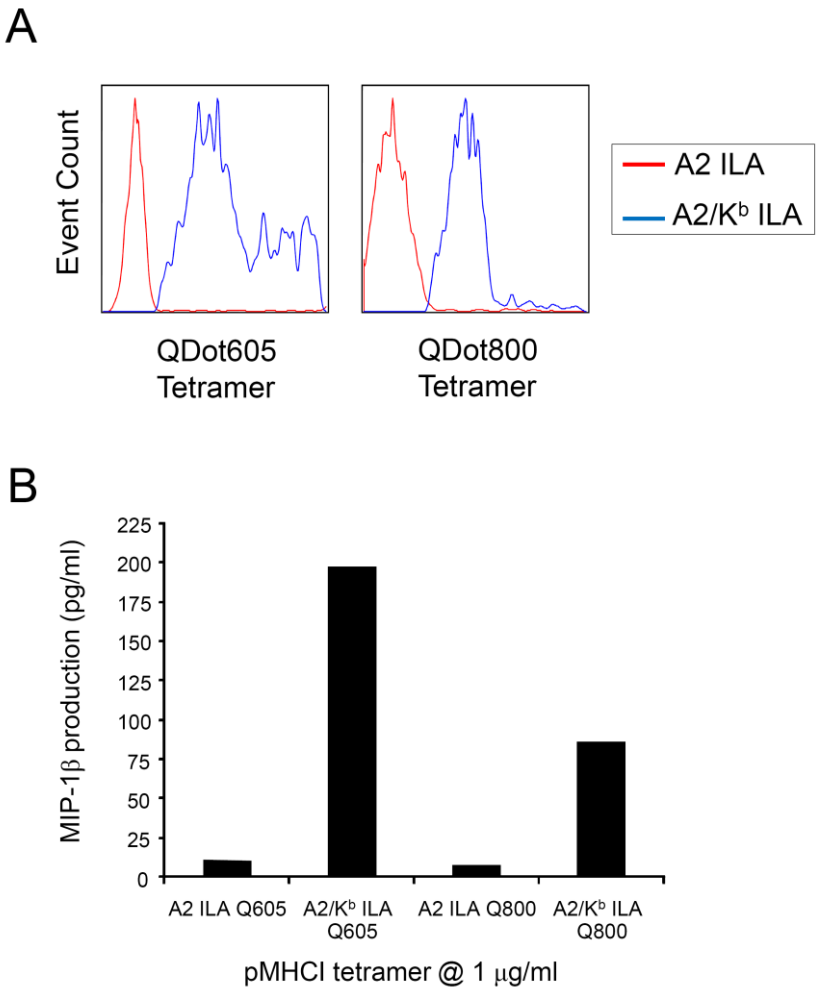

Figure 3.5: Non-cognate A2/K^b tetramer induced activation is not influenced by flurochrome aggregation. (**A**) 5 x 10^4 A2 restricted CD8$^+$ T-cell clone ALF3 specific for the Influenza A virus $MP1_{58-66}$ epitope GILGFVFTL were stained with 10 μg/ml HLA A2 ILAKFLHWL or A2/K^b ILAKFLHWL tetramer conjugated with either streptavidin-QDot605 or streptavidin-QDot800 for 30 minutes at 37°C. After 2 washes with PBS, data were acquired using a modified FACSAria II and analysed with FlowJo software. (**B**) 2.5 x 10^4 ALF3 CD8$^+$ T-cell clone were incubated with either HLA A2 ILAKFLHWL-Q605, A2/K^b ILAKFLHWL-Q605, HLA A2 ILAKFLHWL-Q800 or A2/K^b ILAKFLHWL-Q800 tetramer at 1 μg/ml overnight at 37°C. Supernatant was then harvested and assayed for MIP-1β production by ELISA (R&D). The mean ± SD of two replicate assays is shown.

A2/K^b were incubated overnight with three HLA A2-restricted $CD8^+$ T-cell clones (MEL5, 003 and ILA1) with different peptide specificities (ELAGIGILTV, SLYNTVATL and ILAKFLHWL respectively). Targets that expressed HLA A2 failed to activate any of the $CD8^+$ T-cell clones significantly above background (Figure 3.6 A). Remarkably, however, the A2/K^b targets stimulated MEL5, 003 and ILA1 $CD8^+$ T-cell clones to produce significant amounts of MIP-1β in the absence of specific peptide (Figure 3.6 A). A2/K^b targets also elicited substantial levels of TNF-α and IFN-γ at titratable E:T ratios (Figure 3.6 B) and induced degranulation (Figure 3.6 C) in the absence of specific TCR/pMHCI interactions.

3.2.6 Cell surface-expressed A2/K^b primes non-cognate $CD8^+$ T-cell expansions

Thymic output in healthy HLA $A2^+$ individuals is known to generate a high frequency of naïve $CD8^+$ T-cells that can recognize the self-antigen Melan-A_{26-35} (Zippelius, Pittet et al. 2002); this system can be used to examine the priming of $CD8^+$ T-cells directly *ex-vivo* (Salio, Palmowski et al. 2004). These observations were exploited to investigate the effect of super-enhanced pMHCI/CD8 binding on $CD8^+$ T-cell priming. In priming experiments conducted with C1R target cells, the percentages of $CD8^+$ T-cells specific for Melan-A_{26-35} that were present after 10 days in culture were related to the context of the pMHCI/CD8 interaction in which the cognate ELAGIGILTV peptide was presented. Thus, in the absence of a pMHCI/CD8 interaction (HLA A2 D227K/T228A C1R targets), only 1.5% of the $CD8^+$ T-cell population was specific for Melan-A_{26-35}; in contrast, 5.6% and 5.7% of the $CD8^+$ population bound the HLA A2 ELAGIGILTV tetramer in the same experiment when priming was conducted with HLA A2 and A2/K^b C1R targets, respectively (Figure 3.7). Exposure to A2/K^b C1R targets also resulted in substantial expansions of the total $CD8^+$ population (Figure 3.7). Similar results were obtained with multiple donors. Thus, target cells that

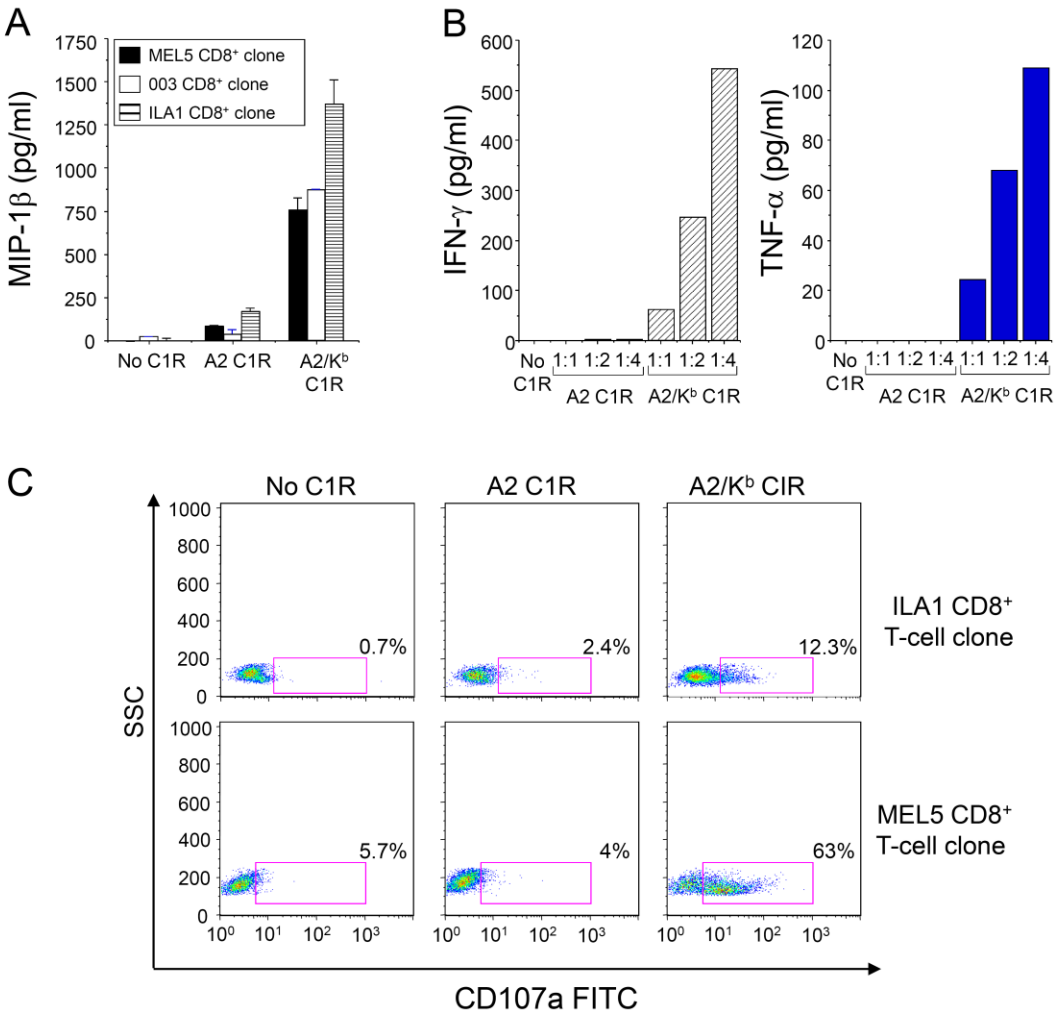

Figure 3.6: Cell surface-expressed A2/K^b activates CD8$^+$ T-cell clones in the absence of cognate antigen. (**A**) 2.5 x 10^4 MEL5, 003 or ILA1 CD8$^+$ T-cell clones were incubated for 12 hours at 37°C with 1 x 10^5 C1R cells stably transfected to express equal levels of either A2 or A2/K^b at the cell surface. Supernatant was subsequently assayed for MIP-1β content by ELISA. The mean ± SD of two replicate assays is shown. (**B**) 2.5 x 10^4 MEL5 were incubated for 12 hours at 37°C with 1 x 10^5 C1R cells stably transfected to express either A2 or A2/K^b at the cell surface. Supernatant was assayed for IFN-γ and TNF-α content by cytokine bead array. (**C**) CD107a expression by ILA1 and MEL5 following a 12 hour incubation at 37°C with C1R cells stably transfected to express either A2 or A2/K^b on the cell surface. For (**A-C**), C1R cells were not previously pulsed with peptide. The mean ± SD of two replicate assays is shown.

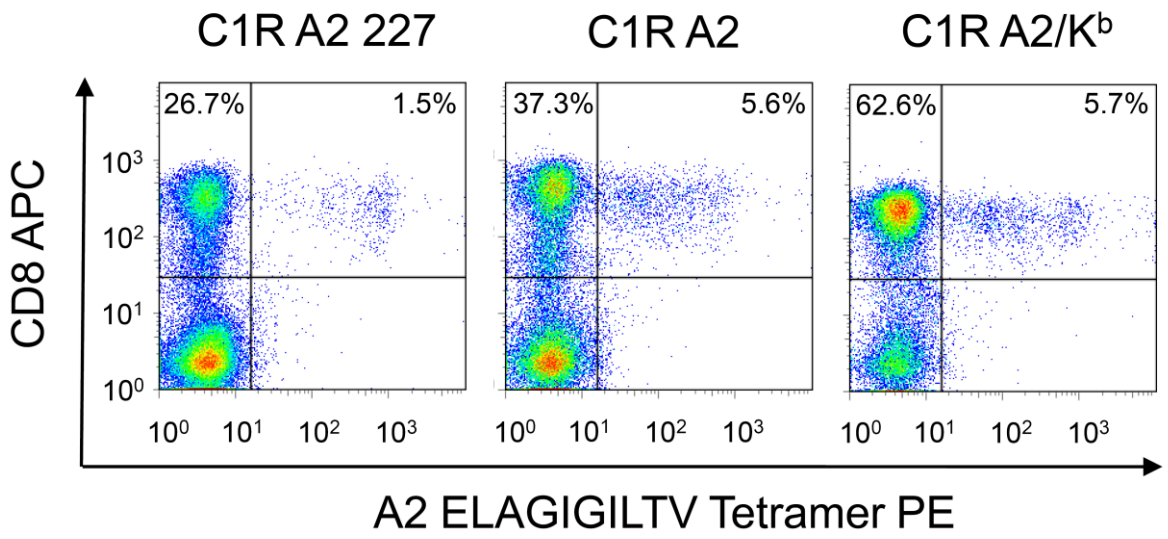

Figure 3.7: Cell surface-expressed A2/K^b primes non-specific expansion of CD8$^+$ cells. 1 x 10^6 A2$^+$ PBMC were incubated with 2 x 10^5 irradiated HLA A2 D227K/T228A, HLA A2 or A2/K^b C1R cells that had previously been pulsed with 1 μM ELAGIGILTV (Melan-$A_{26\text{-}35}$) peptide in R10. From day 3, IL-2 was added in increments to reach a maximum concentration of 200 IU/ml by day 10. Lines were subsequently stained with PE-conjugated HLA A2 ELAGIGILTV tetramer followed by APC-conjugated anti-human CD8 and 7-AAD. Data were acquired using a FACSCalibur flow cytometer and analyzed with FlowJo software.

express MHCI molecules with super-enhanced CD8 binding properties can induce non-specific expansions of $CD8^+$ cells in the absence of cognate antigen.

3.2.7 Non-specific A2/K^b-mediated $CD8^+$ T-cell activation and tetramer staining are not dependent on TCR restriction

In earlier experiments, I demonstrated that A2/K^b tetramers bound to the majority of αβ TCR^+CD8^+ cells in PBMC derived from HLA $A2^+$ donors (Figure 3.3). To exclude the possibility that this phenomenon was dependent on the presence of HLA A2-restricted TCRs, I performed staining experiments with HLA $A2^-$ PBMC. As previously described, the A2/K^b ILAKFLHWL tetramer bound non-specifically to the majority of $CD8^+$ cells (Figure 3.8 A). Furthermore, A2/K^b tetramer binding favoured $CD8^{high}$ cells and was abrogated by pre-treatment with the anti-human CD8 mAb (clone DK25) (Figure 3.8 A). Thus, consistent with the data shown in Figure 3.4, non-specific A2/K^b tetramer binding is a CD8-mediated effect that is not dependent on the presence of HLA A2-restricted TCRs. In addition, I demonstrated in earlier experiments that A2/K^b, both in soluble and cell-associated form, non-specifically activated HLA A2-restricted $CD8^+$ T-cell clones (Figures 3.5 & 3.6). To confirm that these functional correlates of non-specific binding were similarly independent of HLA A2-restricted TCR expression, the study was extended to test $CD8^+$ T-cell clones restricted by other HLA molecules. Cell surface expressed A2/K^b activated all $CD8^+$ T-cell clones regardless of restriction element (Figure 3.8 B).

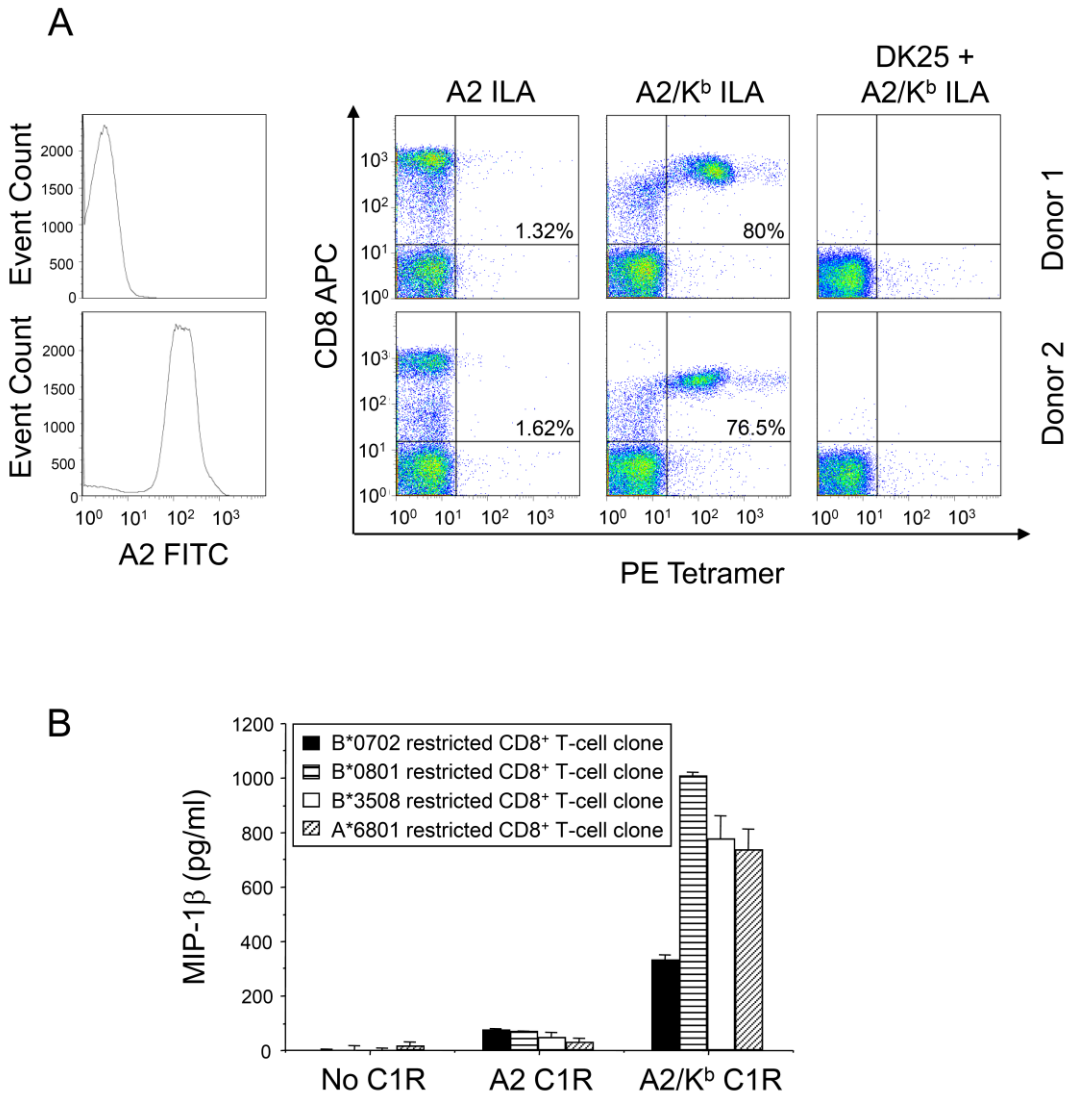

Figure 3.8: Non-cognate A2/K^b-mediated CD8$^+$ T-cell clone activation and tetramer binding is not influenced by MHCI restriction. (**A**) 2.5 x 10^5 PBMC were suspended in 250 µl FACS buffer (2% FCS/PBS) and stained with FITC-conjugated anti-human A2 and 7-AAD for 30 minutes on ice, then washed twice and resuspended in PBS. For pMHCI tetramer staining experiments, 2.5 x 10^5 PBMC were suspended in 50 µl FACS buffer (2% FCS/PBS) and incubated +/- 10 µg/ml unconjugated anti-human CD8 for 20 minutes on ice, then stained with 10 µg/ml of the PE-conjugated tetramers HLA A2 ILAKFLHWL or A2/K^b ILAKFLHWL for 45 minutes on ice. After washing, cells were subsequently stained with APC-conjugated anti-human CD8 and 7-AAD, washed again and resuspended in PBS. Data were acquired using a FACSCalibur flow cytometer and analyzed with FlowJo software. (**B**) 2.5 x 10^4 CD8$^+$ T-cell clones were incubated for 12 hours at 37°C with 1 x 10^5 unpulsed C1R cells expressing either HLA A2 or A2/K^b on the cell surface. The following CD8$^+$ T-cell clones were used: (i) the HLA A*6801-restricted clone c23, specific for the HIV-1 Tat-derived epitope ITKGLGISYGR (residues 38-48); (ii) the HLA B*0702-restricted clone KD4, specific for the Epstein-Barr virus (EBV) EBNA3A-derived epitope RPPIFIRRL

(residues 379-387); (iii) the HLA B*0801-restricted clone LC13, specific for the EBV EBNA3A-derived epitope FLRGRAYGL (residues 339-347); and, (iv) the HLA B*3508-restricted clone SB27, specific for the EBV BZLF1-derived epitope LPEPLPQGQLTAY (residues 52-64). Supernatant was subsequently assayed for MIP-1β content by ELISA. The mean ± SD of two replicate assays is shown.

3.3 Discussion

$CD8^+$ T-cells must be able to discriminate between very small numbers of foreign pMHCI within a sea of structurally related self peptide-MHCI molecules presented at the cell surface. CD8 binds to the non-polymorphic regions of the MHCI molecule (Gao, Tormo et al. 1997) and as a result has the potential to interact with any pMHCI molecule regardless of the peptide it presents. If the pMHCI/CD8 interaction was capable of independently initiating cell-cell recognition then the high density of pMHCI molecules on the nucleated cell surface would constantly initiate T-cell recognition. This is clearly not the case and it has been suggested that it is the low solution affinity of the pMHCI/CD8 interaction that prevents such non-specific activation (Wyer, Willcox et al. 1999). This led me to hypothesise that the pMHCI/CD8 interaction must remain substantially weaker than the TCR/pMHCI interaction in order to maintain $CD8^+$ T-cell specificity and efficient co-receptor function.

Here, I generated chimeric $A2/K^b$ MHCI tetramers that increase the strength of the pMHCI/CD8 interaction by ~15-fold to probe the biophysical and functional significance of the low solution binding affinities observed for the pMHCI/CD8 interaction. Initially, I examined the effect of super-enhanced CD8 binding on pMHCI tetramer binding at the cell surface. Increasing the strength of the pMHCI/CD8 interaction by ~15-fold resulted in the total loss of pMHCI tetramer binding specificity. Thus, irrespective of restriction element and the presented peptide, $A2/K^b$ tetramers bound to the surface of all $CD8^+$ T-cell clones examined in this study and to the majority of $CD8^+$ T-cells present within PBMC (Figures 3.2, 3.3 & 3.8 A). In addition, $A2/K^b$ tetramers bound to the cell surface in the absence of TCR expression (Figure 3.4) and non-specific binding was abrogated by pre-treatment with an anti-human CD8 antibody (Figure 3.8 A), thereby demonstrating that the observed loss of

pMHCI tetramer binding specificity was CD8-mediated and TCR-independent. These findings indicate that the low solution binding affinities observed for the pMHCI/CD8 interaction are essential for the preservation of pMHCI ligand binding specificity at the cell surface.

It has previously been documented that pMHCI tetramers are efficient activators of cognate $CD8^+$ T-cell clones (reviewed in (Wooldridge, Lissina et al. 2009). However, pMHCI tetramer staining does not necessarily equate with cellular activation. Therefore, I examined the ability of $A2/K^b$ to activate $CD8^+$ T-cell clones. Notably, $A2/K^b$ tetramers activated $CD8^+$ T-cell clones in a non-specific manner (Figure 3.5). Activation resulted in a full range of effector functions, including cytokine/chemokine release, degranulation and killing. Flow cytometric assessment of degranulation by analysis of CD107a mobilization revealed that $CD8^+$ T-cell clones with higher surface expression of CD8 were the cells most likely to activate in response to $A2/K^b$ molecules. These findings led me to examine the effects of cell-surface presented antigen. Strikingly, exposure of PBMC to C1R target cells bearing $A2/K^b$ molecules caused a general non-specific expansion of $CD8^+$ cells during the course of the experiment (Figure 3.7). Furthermore, $A2/K^b$ C1R cells, unlike their wild-type HLA A2 counterparts, were capable of stimulating effector function in all $CD8^+$ T-cell clones tested regardless of specificity and MHCI restriction (Figure 3.6 & 3.8 B). These findings cannot exclude the possibility that inclusion of the murine α3 domain induces conformational changes at the T-cell surface on binding to CD8 that favour non-cognate activation. However this seems unlikely as the TCR binding site is shown to be unaltered (Choi, Chen et al. 2003; Wooldridge, van den Berg et al. 2005). In addition, murine and human pMHCI/CD8αα co-crystals exhibit similar binding orientations (Gao, Tormo et al. 1997; Kern, Teng et al. 1998).

These results are consistent with the observation that thymus leukaemia antigen (TL), which interacts strongly (K_D = 12 μM) with cell surface CD8αα expressed by intraepithelial lymphocytes (IELs), can modulate T-cell responses independently of the TCR (Kern, Teng et al. 1998; Leishman, Naidenko et al. 2001; Tsujimura, Obata et al. 2003).

The question still remained as to how does a super-enhanced pMHCI/CD8 interaction result in non-specific $CD8^+$ T-cell activation? It has previously been demonstrated that an incremental increase in the pMHCI/CD8 interaction (HLA A2 Q115E) results in enhanced immunogenicity of cognate antigens and that this effect is mediated by enhanced early intracellular signal transduction (Cole and Gao 2004; Wooldridge, van den Berg et al. 2005). In contrast, the stimulatory properties of $A2/K^b$ molecules exhibited no peptide specificity requirements whatsoever; indeed, cell surface-expressed $A2/K^b$ was shown to activate even non-HLA A2-restricted $CD8^+$ T-cell clones (Figure 3.8 B), thereby confirming that cognate TCR/pMHCI interactions are not required. Combined with the ability of $A2/K^b$ to engage multiple CD8 molecules at the cell surface, these results suggest that $A2/K^b$ cross-links CD8 and induces activation in an 'antibody-like' manner. Indeed, this is consistent with previous studies demonstrating that antibody-induced CD8 cross-linking can induce T-cell signalling (Grebe, Clarke et al. 2004; Wooldridge, Lissina et al. 2007) and elicit downstream effector functions such as chemokine release (Wooldridge, Hutchinson et al. 2003); such effects are predictable given that the CD8α tail is coupled to $p56^{lck}$, an essential component of the early intracellular signalling pathway (Veillette, Bookman et al. 1988). It is interesting to note that the murine pMHCI/CD8 interaction is significantly stronger (K_D ~ 30 μM) than the equivalent human interaction (K_D ~ 150μM) (Purbhoo, Boulter et al. 2001) but does not result in non-cognate $CD8^+$ T-cell activation. It is therefore likely that a pMHCI/CD8 interaction

affinity threshold exists for the maintenance of $CD8^+$ T-cell activation specificity. The strength of the murine pMHCI/CD8 interaction is 3-fold weaker than the strength of the interaction measured between $A2/K^b$ and human CD8, thereby still operates at a level below this threshold.

In summary, I have utilized chimeric MHCI molecules that exhibit a super-enhanced interaction with CD8 to probe the physical and functional significance of the low solution binding affinities previously described for the pMHCI/CD8 interaction. I found that increasing the strength of the pMHCI/CD8 interaction by ~15-fold resulted in: (i) total loss of pMHCI binding specificity at the cell surface; (ii) non-cognate pMHCI tetramer mediated activation; and, (iii) non-specific activation and proliferation triggered by cell surface-expressed pMHCI molecules. Thus, the low solution binding affinity of the pMHCI/CD8 interaction is essential for the preservation of pMHCI ligand binding specificity at the cell surface. Notably, my work highlights that pMHCI molecules with affinities for CD8 that lie within the typical range for agonist TCR/pMHCI interactions (K_D ~10 μM) are able to activate $CD8^+$ T-cells in the absence of a specific TCR/pMHCI interaction. Thus, the biophysical characteristics of the pMHCI/CD8 interaction are essential for the maintenance of $CD8^+$ T-cell antigen specificity and T-cell homeostasis.

4

ANTI-CD8 ANTIBODIES CAN TRIGGER T-CELL EFFECTOR FUNCTIONS IN THE ABSENCE OF TCR ENGAGEMENT AND IMPROVE pMHCI TETRAMER STAINING

(Clement et al 2011 & Appendix 2)

4.1 Introduction

As previously discussed in Chapter 3, it is possible to induce $CD8^+$ T-cell activation in the absence of a cognate TCR/pMHCI interaction using chimeric $A2/K^b$ that exhibits a super-enhanced affinity for CD8. The results presented in chapter 3 suggest that $A2/K^b$ cross-links CD8 and induces activation in an "antibody-like" manner. As such I hypothesized that it would be possible to induce $CD8^+$ T-cell activation independently of the TCR/pMHCI interaction using anti-CD8 antibodies. Anti-CD8 antibodies have been used extensively to examine the role of CD8 in $CD8^+$ T cell activation. However, as previous studies have yielded conflicting results, it is unclear from the literature whether anti-CD8 antibodies *per se* are capable of inducing effector function. Here I intend to examine the effects of multiple anti-CD8 antibodies on a panel of $CD8^+$ T-cell clones with different specificities to address the apparent incongruity in the literature.

4.1.1 Use of anti-CD8 antibodies to study the role of CD8 in T-cell activation

Monoclonal antibodies recognise and bind to defined 'epitopes' with high affinity ($K_D < 10^{-9}$ M) and specificity. In early studies, examining the behaviour of cells after the binding of specific antibody became a widely accepted method of studying the function of T cell surface antigens. Early studies showed that pre-incubation with anti-CD8 antibodies can block conjugate formation between effector and target cells (Norment and Littman 1988) and inhibit $CD8^+$ T-cell activation in response to cognate pMHCI presented on the target cell surface (Nakayama, Shiku et al. 1979; Shinohara and Sachs 1979; Janeway 1992; Miceli and Parnes 1993). By cross-linking anti-CD8 antibodies using a secondary anti-IgG antibody, this resulted in the rapid phosphorylation of $p56^{lck}$ thereby suggesting that cross-linking CD8 may

contribute directly to TCR triggering (Veillette, Bolen et al. 1989; Veillette, Zuniga-Pflucker et al. 1989; Luo and Sefton 1990). These findings provided key evidence that CD8 was important in the process of $CD8^+$ T-cell activation. However, considerable heterogeneity between different $CD8^+$ T-cells was apparent in terms of their ability to activate in the presence of anti-CD8 antibodies and, as a result, these reagents were used as tools to classify $CD8^+$ T-cells as either CD8-dependent or CD8-independent (MacDonald, Glasebrook et al. 1982). MacDonald *et al* suggested that the variations they observed were related to TCR/pMHCI affinity (as discussed in Chapter 5). In summary, anti-CD8 antibodies have been used to demonstrate that CD8 plays an important role in $CD8^+$ T-cell activation and as tools to describe $CD8^+$ T-cells as either 'CD8-dependent' or 'CD8-independent'.

4.1.2 Caveats of using anti-CD8 antibodies in the study of CD8

Many studies have been performed using anti-CD8 antibodies and different tetrameric pMHCI complexes to study the role of CD8 in stabilising the TCR/pMHCI complex. These studies demonstrated that anti-CD8 antibodies can block the stable binding of tetrameric reagents to the cell surface (Daniels and Jameson 2000; Denkberg, Cohen et al. 2001; Campanelli, Palermo et al. 2002). However studies have been performed in the human and murine system that also highlight an enhancing effect of anti-CD8 antibodies on pMHCI tetramer binding (Murali-Krishna, Altman et al. 1998; Busch and Pamer 1999; Daniels and Jameson 2000; Devine, Hodsdon et al. 2004). To date, the precise mechanism of how anti-CD8 antibodies may elicit varying effects when studying T-cells is not known. Anti-CD8 antibodies are a rather blunt tool for dissecting the role of CD8 as these reagents are likely to affect all roles of the molecule. My laboratory has preferred to use point mutated MHCI with altered CD8 binding as these reagents specifically target the MHCI/CD8 interaction. Indeed

systems involving the use point mutated MHCI molecules were developed that fail to interact with CD8 (Potter, Rajan et al. 1989; Purbhoo, Boulter et al. 2001) and have allowed in-depth investigations into the role of CD8 in $CD8^+$ T-cell activation.

4.1.3 Can anti-CD8 antibodies induce $CD8^+$ T-cell effector function?

Antibody-mediated ligation of T-cell surface molecules, such as CD2, CD3 and CD28 (Clark, Law et al. 1988; Luhder, Huang et al. 2003), can result in effector function. In contrast, studies of antibody-mediated CD8 ligation in the absence of TCR engagement have yielded conflicting results. As previously discussed, early studies demonstrated that the induction of CD8 cross-linking at the cell surface can result in $p56^{lck}$ phosphorylation similar to that seen with anti-CD3 antibodies (Veillette, Zuniga-Pflucker et al. 1989) and further studies showed that this cross-linking could elicit downstream effector functions, such as chemokine release (Wooldridge, Hutchinson et al. 2003) ERK1/2 phosphorylation and cytokine function (Kim, Billard et al. 2010) and potent cytotoxicity (Tomonari and Spencer 1990). However, in conflict with these data, more recent studies suggest that CD8 ligation alone may actually deliver a negative signal (Grebe, Clarke et al. 2004; Abidi, Dong et al. 2008). Indeed Abidi *et al* studied specific serial analysis of gene expression (SAGE) genotypic analysis and highlighted that an anti-CD8 antibody can induce transcription in a $CD8^+$ T-cell clone which is ultimately inhibitory to T-cell activation as it fails to induce NFAT-dependent transcription. However, the major caveat of this study was that the authors only studied a single $CD8^+$ T-cell clone using a single anti-CD8 antibody (Abidi, Dong et al. 2008). These heterogeneous effects question the suitability of anti-CD8 antibodies for use in the characterisation of CD8 function (Jonsson, Boyce et al. 1989) and it is important that we understand these observations in more detail.

4.1.4 Summary and Aims

To date, a cohesive explanation for these widely disparate findings with anti-CD8 antibodies has remained elusive. Furthermore, there has been no systematic study of the effects of multiple different anti-human CD8 antibodies on $CD8^+$ T-cells with different TCR/pMHCI specificities. The aim of this study was to investigate the effect of cross-linking CD8 using anti-CD8 antibodies on T-cell function and the TCR/pMHCI interaction. I aimed to undertake a thorough study of the effects of anti-CD8 antibodies using multiple antibody clones and many different $CD8^+$ T-cells. I hoped that a comprehensive study might explain the wide variation in the results from other groups that have used these tools.

4.2 Results

4.2.1 Anti-CD8 antibodies can trigger T-cell effector function in the absence of TCR engagement

Several studies suggest that antibody-mediated ligation of CD8 in the absence of TCR engagement can elicit downstream effector function (Veillette, Zuniga-Pflucker et al. 1989; Tomonari and Spencer 1990; Wooldridge, Hutchinson et al. 2003); however, others have reported the delivery of negative signals with this manipulation (Grebe, Clarke et al. 2004; Abidi, Dong et al. 2008). To reconcile these apparently disparate findings, I conducted a systematic study of the effects of multiple different anti-human CD8 antibodies on $CD8^+$ T-cells with several different specificities. For this purpose, I assembled a panel of anti-human CD8 antibodies that comprised six anti-CD8α antibodies (OKT8, SK1, MCD8, 32/M4, C8/144B and DK25) and one anti-CD8β antibody (2ST8.5H7). Six out of seven anti-human CD8 antibodies from the panel (SK1, MCD8, 32/M4, C8/144B, DK25 and 2ST8.5H7) did

not elicit any chemokine production when incubated with four different HLA A2-restricted $CD8^+$ T-cell clones (ILA1, ALF3, MEL5 and MEL187.c5) with a total of three different specificities in the absence of specific pMHCI antigen (Figure 4.1 A-D). However, the anti-CD8α antibody OKT8 induced MIP-1α, MIP-1β and RANTES release from all four HLA A2-restricted $CD8^+$ T-cell clones (Figure 4.1 A-D) even when titrated down to a low concentration (1-100 µg/ml) (Figure 4.2 A&B).

I extended my studies by measuring chemokine release by two non-HLA A2-restricted $CD8^+$ T-cell clones following incubation with each anti-human CD8 antibody. Both of these non-HLA A2-restricted $CD8^+$ T-cell clones produced MIP-1α, MIP-1β and RANTES in response to OKT8 but did not activate in the presence of the other antibodies tested (Figure 4.3). Remarkably, the highly antigen sensitive HLA B*3508-restricted EBV BZLF1-specific $CD8^+$ T-cell clone SB10 released >2000 pg/ml of each chemokine in response to OKT8 (Figure 4.3 B). OKT8 was also incapable of staining the HLA DR*0101-restricted $CD4^+$ T-cell clone C6 (Figure 4.4 A) and failed to induce chemokine release from this clone (Figure 4.4 B-D). Thus, the stimulatory effects of OKT8 appear to be $CD8^+$ T-cell-specific.

The panel of seven anti-human CD8 antibodies was further tested in cytotoxicity assays with 4 different $CD8^+$ T-cell clones (MEL187.c5, ALF3, LC13 and SB10). Anti-human CD8 antibodies incapable of inducing chemokine release failed to elicit cytotoxic activity in any of these four $CD8^+$ T-cell clones (Figure 4.5). In contrast, SB10 $CD8^+$ T-cell exhibited

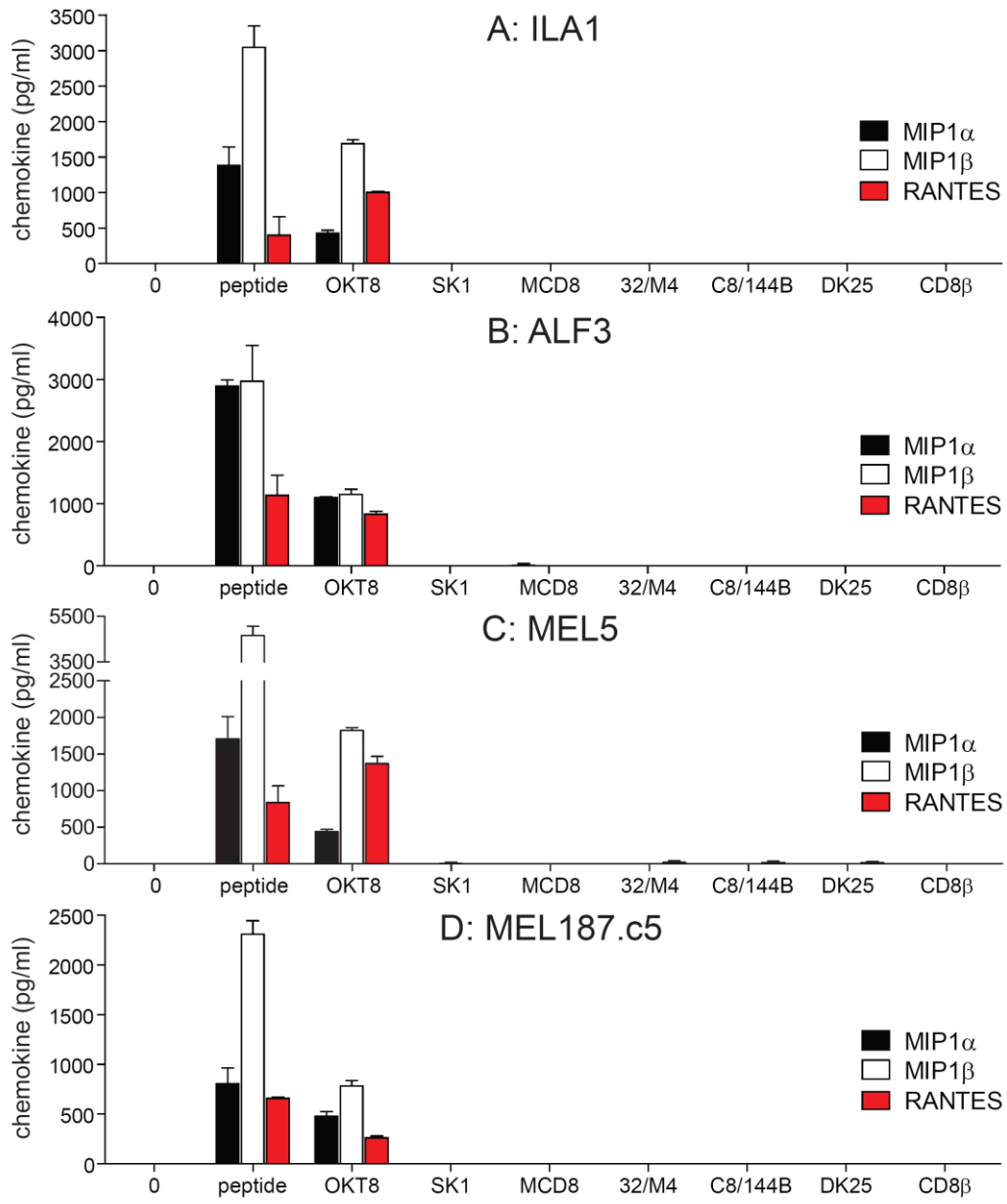

Figure 4.1: Antibody-mediated CD8 ligation can trigger chemokine release from HLA A2-restricted CD8$^+$ T-cells. 3 x 10^4 ILA1 CD8$^+$ T-cells (**A**), ALF3 CD8$^+$ T-cells (**B**), MEL5 CD8$^+$ T-cells (**C**) or MEL187.c5 CD8$^+$ T-cells (**D**) were incubated for 18 hours with each of the following individual anti-human CD8 antibodies in parallel: 100 μg/ml OKT8, 6.25 μg/ml SK1, 50 μg/ml MCD8, 100 μg/ml 32/M4, 100 μg/ml C8/144B, 25 μg/ml DK25 and 100 μg/ml 2ST8.5H7 (CD8β). The maximum possible antibody concentrations were used, determined by the concentration of the commercially available preparation in each case. For each CD8$^+$ T-cell clone, 3 x 10^4 C1R-A2 B-cells pulsed with cognate peptide at 10^{-7} M were used as positive controls. Supernatant was harvested and assayed for MIP-1α, MIP-1β and RANTES by ELISA. The mean ± SD of two replicate assays is shown.

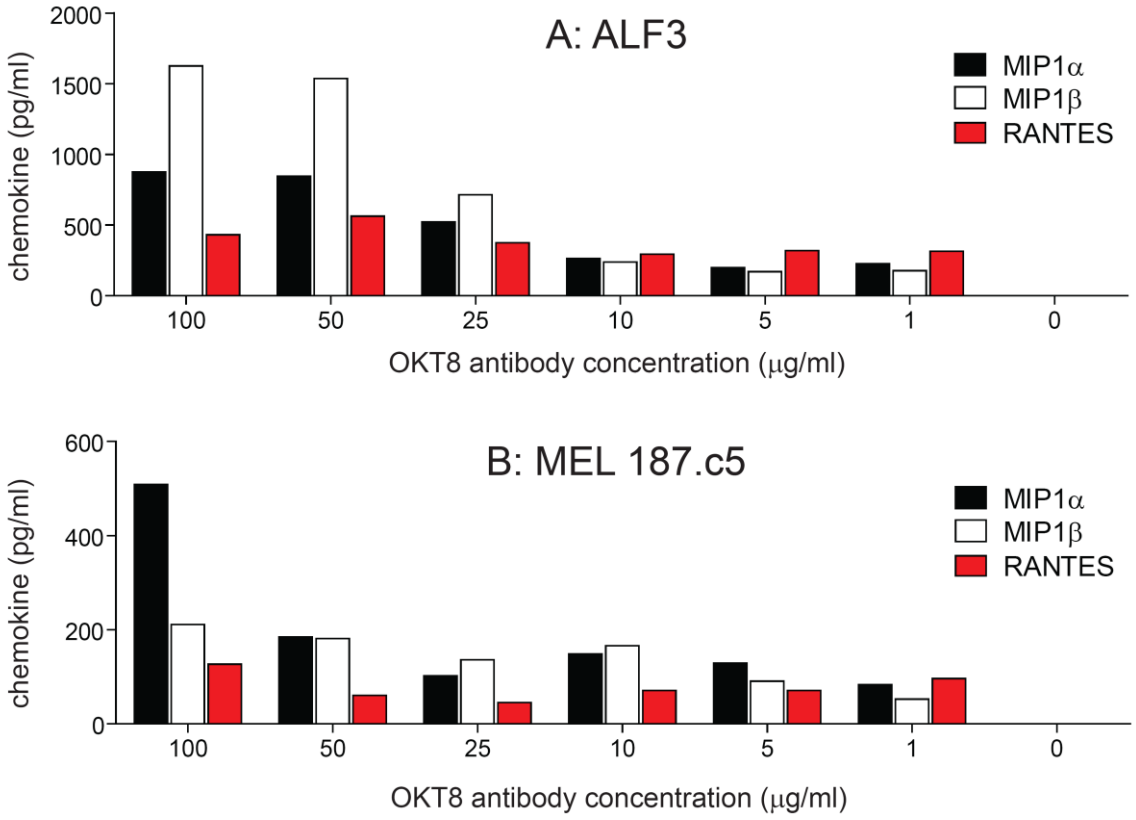

Figure 4.2: OKT8 activity is still detectable at low antibody concentrations. 3 x 10^4 (**A**) ALF3 or (**B**) MEL187.c5 were incubated with various concentrations of anti-human CD8 antibody OKT8 (0-100 μg/ml) for 18 hours @ 37°C. For each $CD8^+$ T-cell clone, 3 x 10^4 C1R-A2 B-cells pulsed with cognate peptide at 10^{-7} M were used as positive controls. Supernatant was harvested and assayed for MIP-1α, MIP-1β and RANTES by ELISA. Similar data was obtained for ILA1 and MEL5. The mean ± SD of two replicate assays is shown.

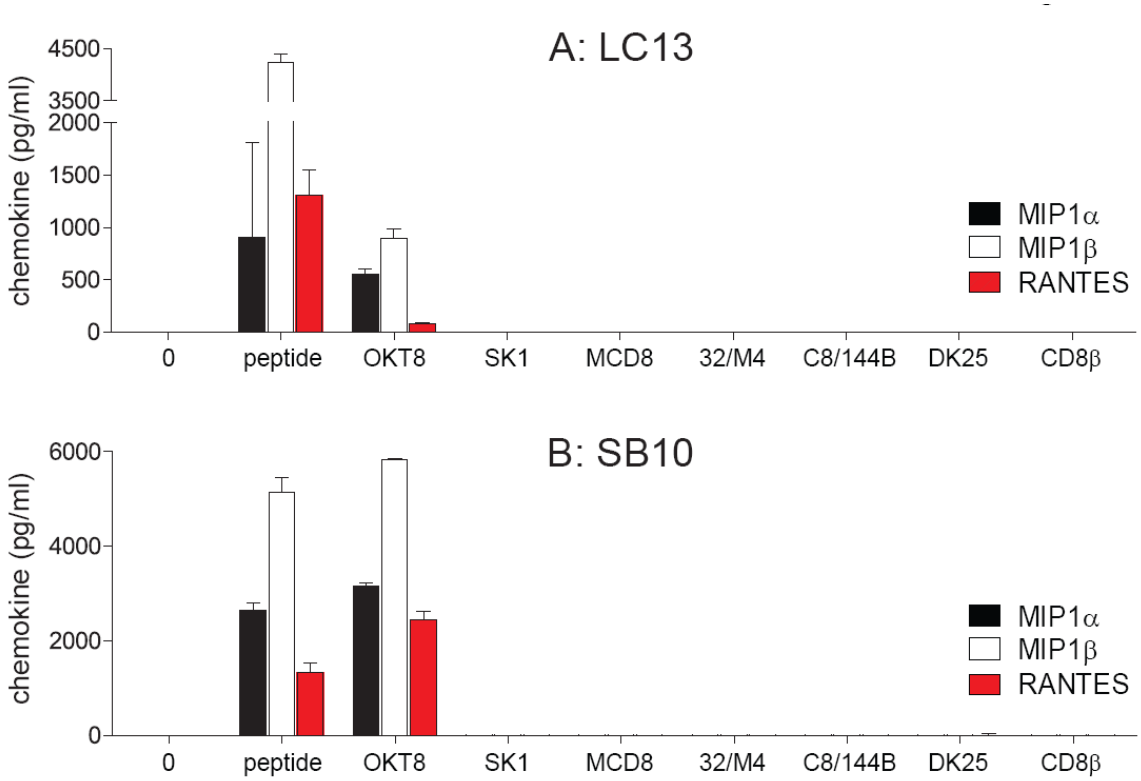

Figure 4.3: Antibody-mediated CD8 ligation can trigger chemokine release from non-HLA A2-restricted CD8$^+$ T-cells. 3 x 10^4 LC13 CD8$^+$ T-cells (**A**) or SB10 CD8$^+$ T-cells (**B**) were incubated for 18 hours @ 37°C with each of the following individual anti-human CD8 antibodies in parallel: 100 μg/ml OKT8, 6.25 μg/ml SK1, 50 μg/ml MCD8, 100 μg/ml 32/M4, 100 μg/ml C8/144B, 25 μg/ml DK25 and 100 μg/ml 2ST8.5H7 (CD8β). For each CD8$^+$ T-cell clone, 3 x 10^4 HLA-matched B-cells pulsed with cognate peptide at 10^{-7} M were used as positive controls. Supernatant was harvested and assayed for MIP-1α, MIP-1β and RANTES by ELISA. The mean ± SD of two replicate assays is shown.

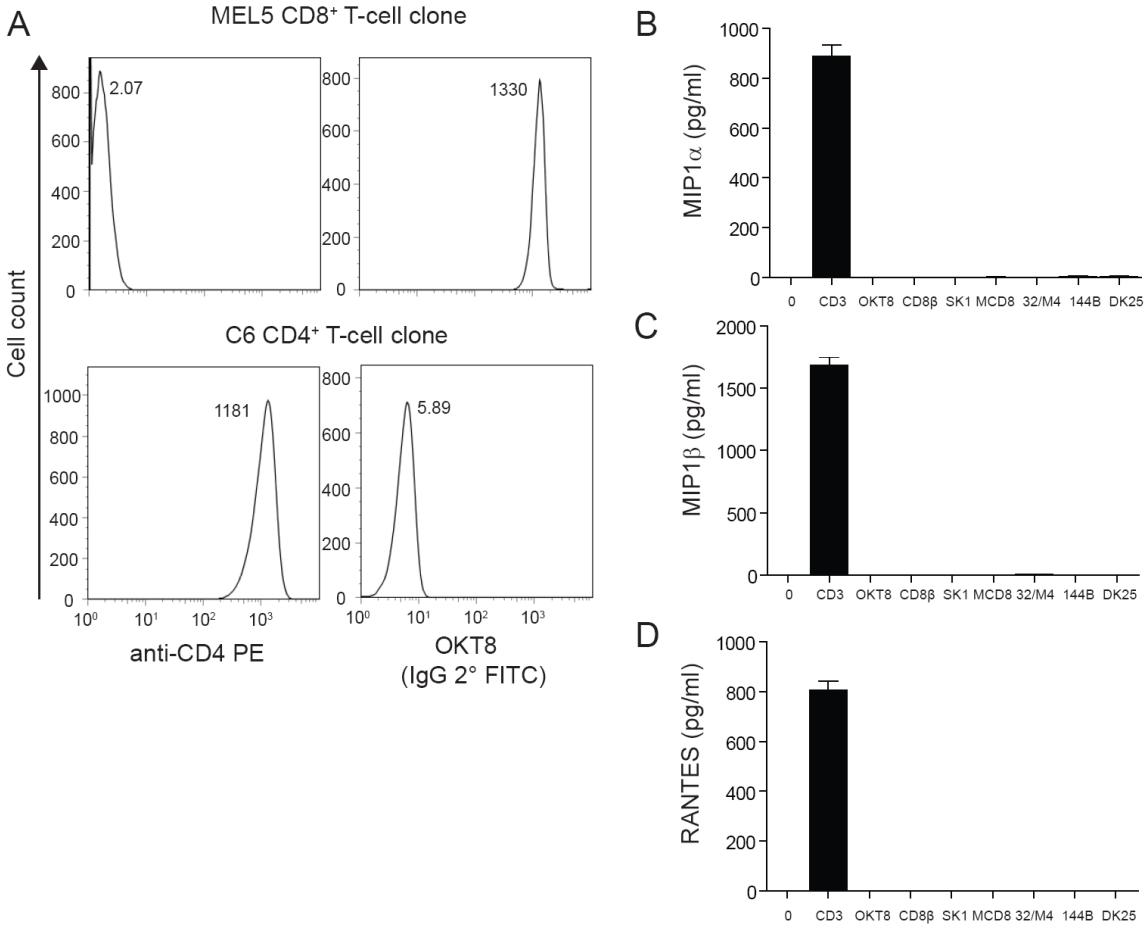

Figure 4.4: OKT8 activity is specific for CD8$^+$ T-cells. (**A**) 5 x 10^4 MEL5 CD8$^+$ T-cells or C6 CD4$^+$ T-cells were stained with PE-conjugated anti-human CD4 (clone L200) at 4°C for 25 minutes or incubated with 100 μg/ml unconjugated OKT8 at 4°C for 25 minutes, washed twice and incubated with FITC-conjugated anti-mouse IgG (serum IgG) at 4°C for a further 25 minutes. Data were acquired using a FACSCalibur flow cytometer and analyzed using FlowJo software. (**B-D**) 3 x 10^4 CD4$^+$ C6 T-cells were incubated for 18 hours @ 37°C with each of the following individual anti-human CD8 antibodies in parallel: 100 μg/ml OKT8, 6.25 μg/ml SK1, 50 μg/ml MCD8, 100 μg/ml 32/M4, 100 μg/ml C8/144B (144B), 25 μg/ml DK25 and 100 μg/ml 2ST8.5H7 (CD8β). The maximum possible antibody concentrations were used, determined by the concentration of the commercially available preparation in each case; the anti-human CD3 antibody UCHT1 (10 μg/ml) served as a positive control. Supernatant was harvested and assayed for MIP-1α (**B**), MIP-1β (**C**) and RANTES (**D**) by ELISA. The mean ± SD of two replicate assays is shown.

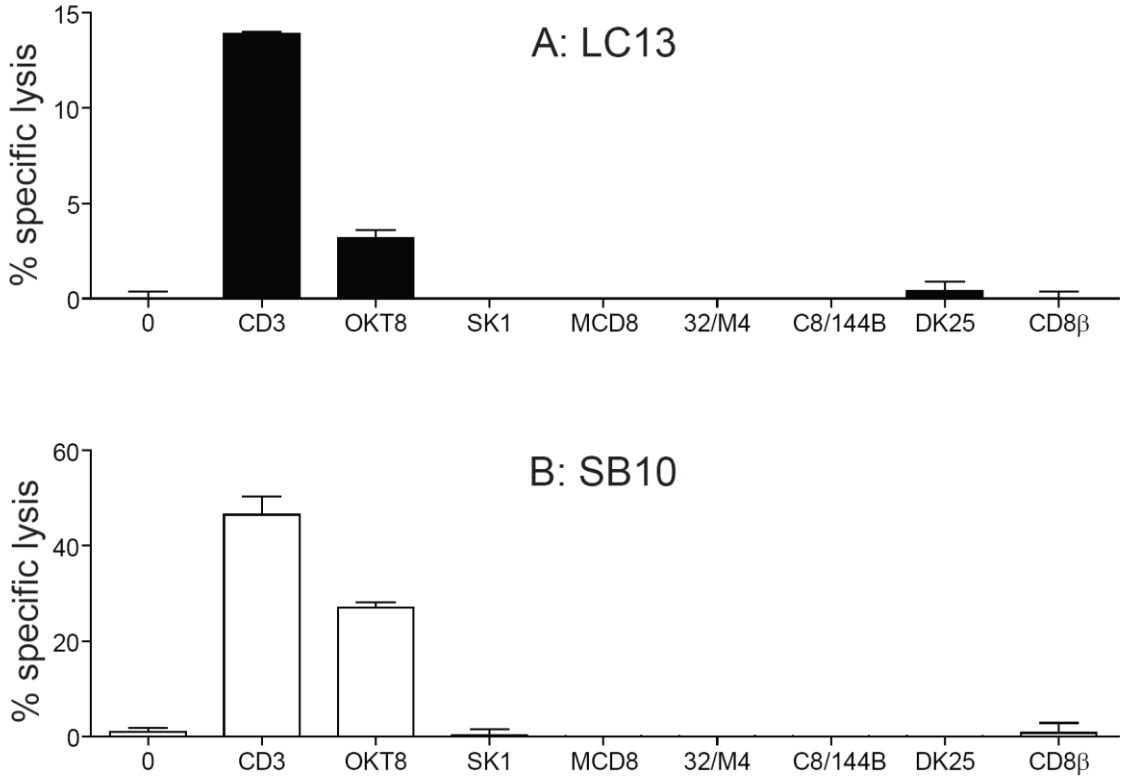

Figure 4.5: Cytotoxic activity triggered by the anti-human CD8 antibody OKT8. 2 x 10^3 LC13 $CD8^+$ T-cells (**A**) or SB10 $CD8^+$ T-cells (**B**) were incubated with each of the following individual anti-human CD8 antibodies in parallel: 100 μg/ml OKT8, 6.25 μg/ml SK1, 50 μg/ml MCD8, 100 μg/ml 32/M4, 100 μg/ml C8/144B, 25 μg/ml DK25 and 100 μg/ml 2ST8.5H7 (CD8β). The anti-human CD3 antibody UCHT1 (10 μg/ml) was used as a positive control. Cytotoxicity assays were then performed over a period of 18 hours @ 37°C as described in the Materials & Methods using ^{51}Cr-labelled C1R-A2 B-cells as targets. The mean ± SD of three replicate assays is shown.

substantial cytotoxicity in response to stimulation with OKT8; lower levels of specific lysis were also induced in $CD8^+$ T-cell clones LC13 (3.18%), ALF3 (5.1%) and MEL187.c5 (3.8%) (Figure 4.5). These results are consistent with a previous study that describes an anti-mouse CD8 antibody, KT112, capable of inducing cytotoxicity (Tomonari and Spencer 1990). Collectively, these data indicate that considerable heterogeneity exists in the ability of anti-CD8 antibodies to activate $CD8^+$ T-cells.

4.2.2 OKT8 induces chemokine secretion in the absence of cytokine secretion

Next, I examined the ability of antibody-mediated CD8 ligation to elicit cytokine release by $CD8^+$ T-cells in the absence of TCR engagement. As expected, the anti-human CD8 antibodies that did not elicit chemokine release or cytotoxic activity (SK1, MCD8, 32/M4, C8/144B, DK25 and 2ST8.5H7) also failed to induce IFN-γ, TNF-α or IL2 release (Figure 4.6). Interestingly, OKT8 similarly failed to elicit cytokine production from the majority of $CD8^+$ T-cell clones tested (Figure 4.6). Importantly, chemokine and cytokine assays were performed using the same supernatant, thereby confirming that OKT8 stimulated $CD8^+$ T-cells to secrete chemokines in the absence of cytokine production; one exception to this dichotomy occurred with $CD8^+$ T-cell clone SB10, which released IFN-γ in response to treatment with OKT8. These data suggest that OKT8-mediated CD8 ligation delivers a signal that falls below the threshold required for cytokine production in most $CD8^+$ T-cells.

4.2.3 Neither secondary antibody cross-linking nor PHA/IL-15 treatment alters the functional phenotype of anti-human CD8 antibodies

To probe the possibility that the degree of cross-linking mediated by each of the anti-human

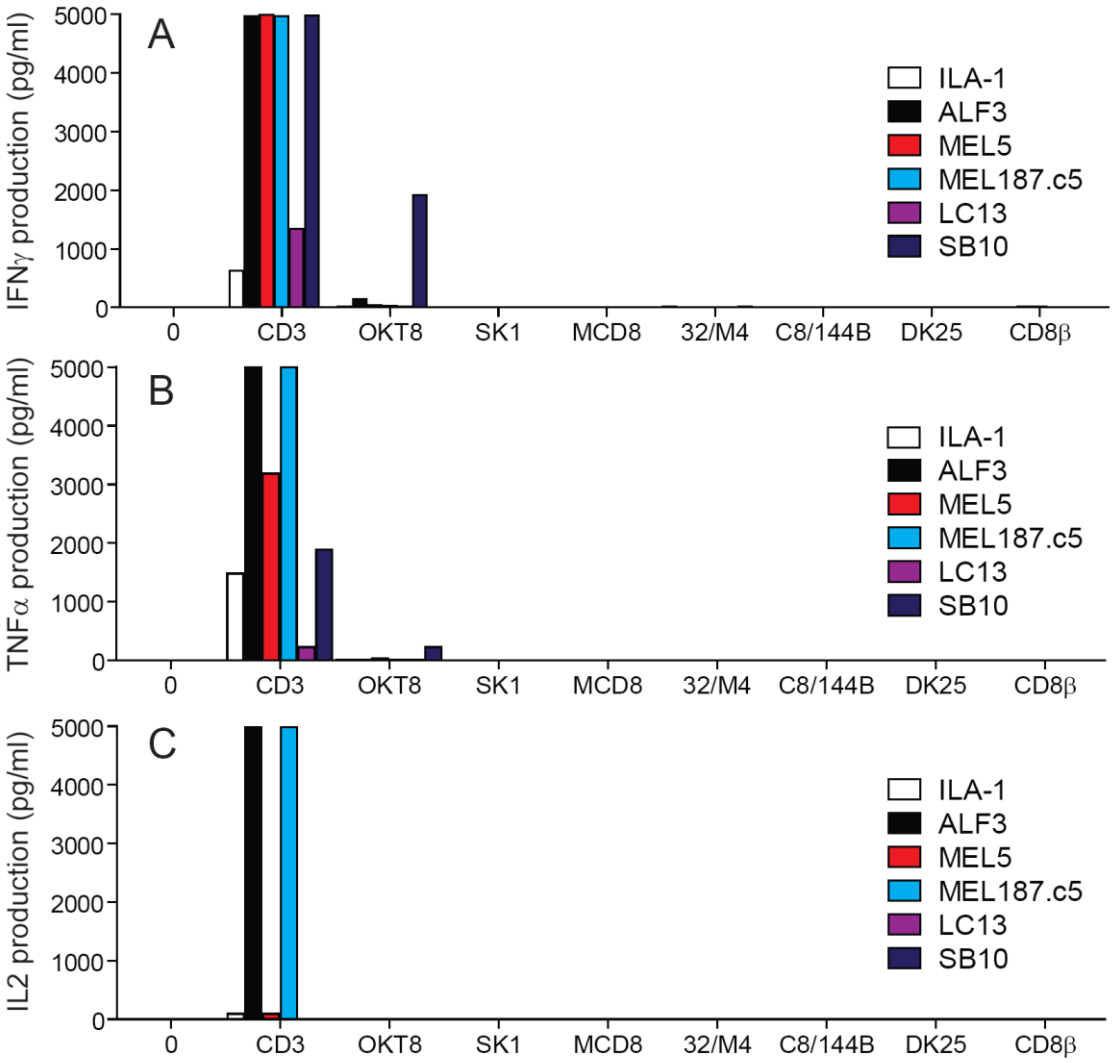

Figure 4.6: Antibody-mediated chemokine release occurs in the absence of cytokine release. 3 x 10^4 ILA1, ALF3, MEL5, MEL187.c5, LC13 or SB10 $CD8^+$ T-cells were incubated for 18 hours @ 37°C with each of the following individual anti-human CD8 antibodies in parallel: 100 µg/ml OKT8, 6.25 µg/ml SK1, 50 µg/ml MCD8, 100 µg/ml 32/M4, 100 µg/ml C8/144B, 25 µg/ml DK25 and 100 µg/ml 2ST8.5H7 (CD8β). The anti-human CD3 antibody UCHT1 (10 µg/ml) was used as a positive control. Supernatant was harvested and assayed for IFN-γ (**A**), TNF-α (**B**) and IL2 (**C**) by CBA. The mean ± SD of two replicate assays is shown.

CD8 antibodies tested could explain the functional heterogeneity observed between these reagents, I performed activation experiments with the addition of secondary antibodies. Secondary cross-linking of OKT8 increased the level of MIP-1α, MIP-1β and RANTES release by ILA1, ALF3, MEL187.c5, MEL5, LC13 and SB10 $CD8^+$ T-cells above that observed with OKT8 alone (Figure 4.7 and data not shown). However, secondary antibody-mediated cross-linking did not reverse the phenotype of the non-activating anti-human CD8 antibodies (Figure 4.7).

I also examined the effect of PHA/IL-15 treatment on the ability of anti-human CD8 antibodies to elicit effector function from $CD8^+$ T-cells in healthy donor PBMCs. PHA is capable of cross-linking glycosylated proteins at the T-cell surface. The seven anti-human CD8 antibodies tested did not elicit significant levels of effector function from $CD8^+$ T-cells in untreated PBMCs (Figure 4.8 A). The six non-activating anti-human CD8 antibodies also failed to induce significant levels of $CD8^+$ T-cell activation in PBMCs cultured for 7 days in PHA/IL-15 (Figure 4.8 B). In contrast, OKT8 activated $CD8^+$ T-cells in PHA/IL-15-stimulated PBMCs to release MIP-1β and degranulate as measured by surface mobilization of CD107a. Interestingly, OKT8 also induced IFN-γ and TNF-α production by $CD8^+$ T-cells in PHA/IL-15-stimulated PBMCs, thereby suggesting that this treatment regimen synergistically lowered the activation threshold of the responding cells. OKT8 failed to activate $CD4^+$ T-cells in PHA/IL-15-stimulated PBMCs (Figure 4.8 C) consistent with previously discussed data (Figure 4.4).

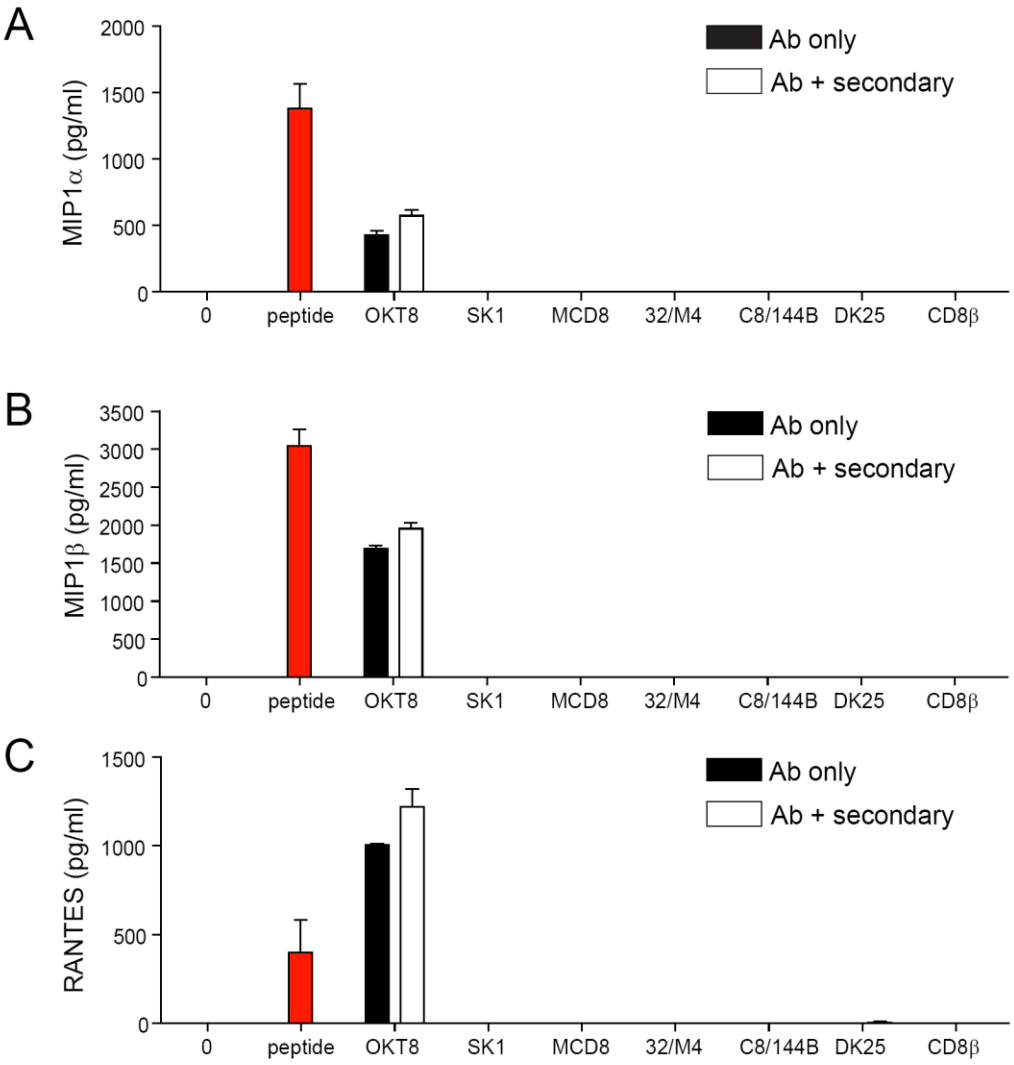

Figure 4.7: Secondary cross-linking does not alter the functional phenotype of anti-human CD8 antibodies. 3 x 10^4 ILA1 $CD8^+$ T-cell clone were incubated with each of the following individual anti-human CD8 antibodies in parallel: 100 µg/ml OKT8, 6.25 µg/ml SK1, 50 µg/ml MCD8, 100 µg/ml 32/M4, 100 µg/ml C8/144B, 25 µg/ml DK25 and 100 µg/ml 2ST8.5H7 (CD8β). The positive control comprised 3 x 10^4 C1R-A2 B-cells pulsed with cognate peptide at 10^{-7} M. Antibodies were then crosslinked with the addition of 5 µl anti-mouse IgG antibody (serum IgG) and incubated for 18 hours at 37°C in a 5 % CO_2 atmosphere. Supernatant was harvested and assayed for MIP-1α (**A**), MIP-1β (**B**) and RANTES (**C**) by ELISA. Secondary cross-linking of OKT8 increased the levels of all analytes measured and also increased the levels of anti-CD3 antibody induced chemokine release. Similar results were obtained with all other $CD8^+$ T-cell clones examined: ALF3, MEL5, MEL187.c5, LC13 and SB10. The mean ± SD of two replicate assays is shown.

4.2.4 OKT8 enhances pMHCI tetramer staining

I next tested the effects of anti-human CD8 antibodies on the staining of ILA1, ALF3, MEL187.c5 and MEL5 $CD8^+$ T-cells with cognate pMHCI tetramers. Three anti-human CD8 antibody clones (SK1, DK25 and 2ST8.5H7) inhibited tetramer staining; clones MCD8, 32/M4 and C4/144B had little or no effect on staining. In contrast, pre-incubation with OKT8 enhanced cognate pMHCI tetramer staining of all four $CD8^+$ T-cell clones (Figure 4.9). Thus, OKT8 can enhance the binding of pMHCI tetramers in a range of systems. These findings suggested that OKT8 might facilitate the identification of antigen-specific $CD8^+$ T-cells within mixed cell populations. To test this idea, I examined pMHCI tetramer staining of $CD8^+$ T-cell lines raised against the HLA A2-restricted EBV BMLF1-derived epitope GLCTLVAML (residues 259-267). OKT8 enhanced the staining intensity of cognate $CD8^+$ T-cells with HLA A2 tetramer folded around the GLCTLVAML peptide without concomitant increases in non-cognate tetramer binding (Figure 4.10 A&B). No increase in the percentage of $tetramer^+$ cells was observed in this viral system (Figure 4.10 A&B) which was thought to reflect the high affinity interaction with pMHCI which is typical of anti-viral TCRs (Cole, Pumphrey et al. 2007).

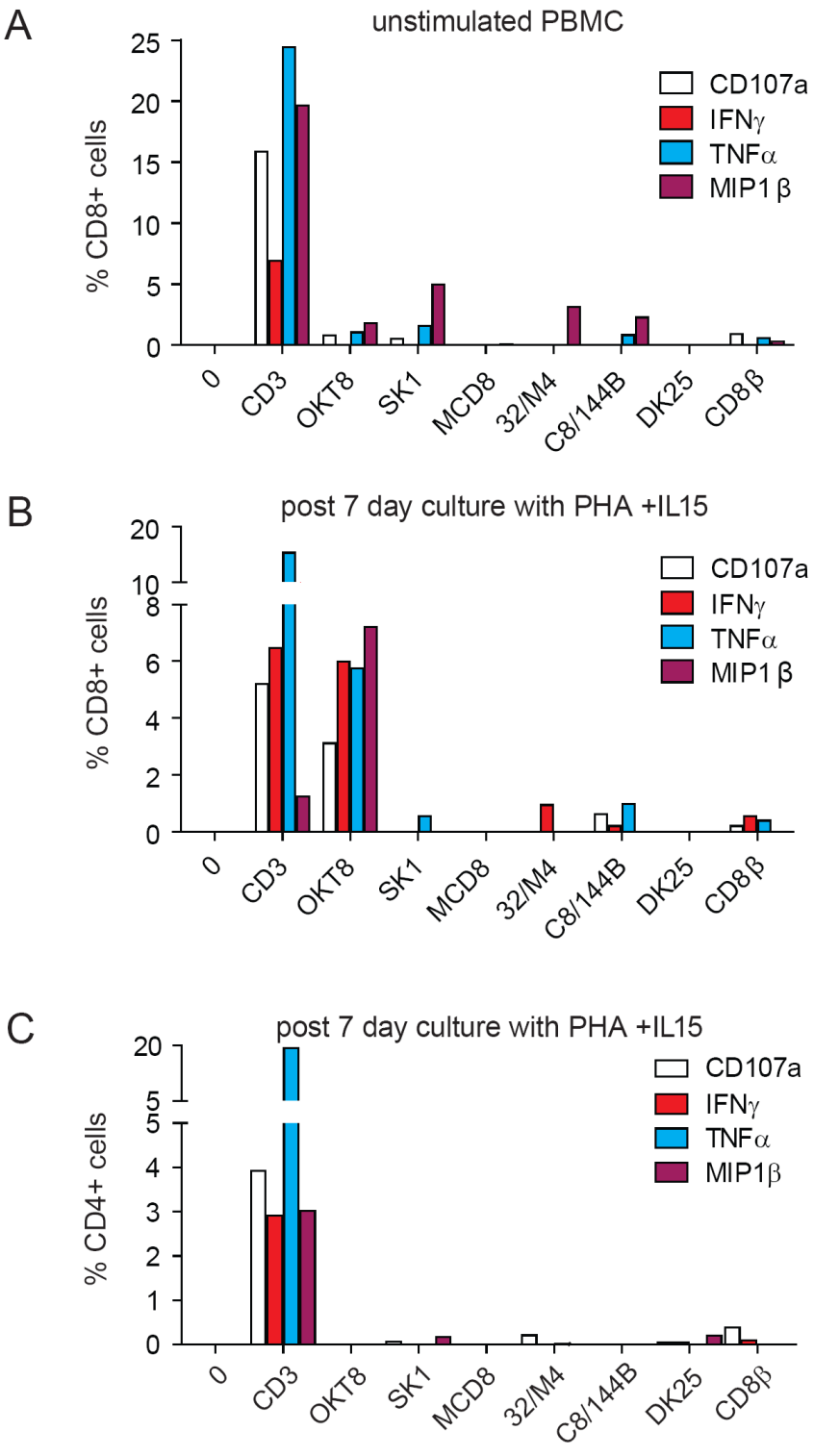

Figure 4.8: Functional phenotype of antibodies not affected by PHA/IL-15 treatment of cells. PBMCs were harvested from healthy donors and cultured either without (A) or with (B&C) 1 µg/ml PHA and 25 ng/ml IL-15 for 7 days, then washed and cultured overnight in R2 medium. 5 x 10^4 PBMCs were then incubated for 18 hours @ 37°C with each of the

following individual anti-human CD8 antibodies in parallel: 100 μg/ml OKT8, 6.25 μg/ml SK1, 50 μg/ml MCD8, 100 μg/ml 32/M4, 100 μg/ml C8/144B, 25 μg/ml DK25 and 100 μg/ml 2ST8.5H7 (CD8β). The anti-human CD3 antibody UCHT1 (10 μg/ml) was used as a positive control. $CD8^+$ T-cell effector functions were measured by intracellular cytokine staining and surface CD107a mobilization as described in the Materials & Methods. Data were acquired using a modified FACSAriaII™ flow cytometer and analyzed with FlowJo software. Results obtained by gating on either the $CD8^+$ (A&B) or $CD4^+$ (C) population are shown and are representative of two separate experiments. Differences in the background levels of $CD8^+$ T-cell activation were observed with the different anti-human CD8 antibodies tested in A&B which may reflect heterogeneity in $CD8^+$ PBMC population.

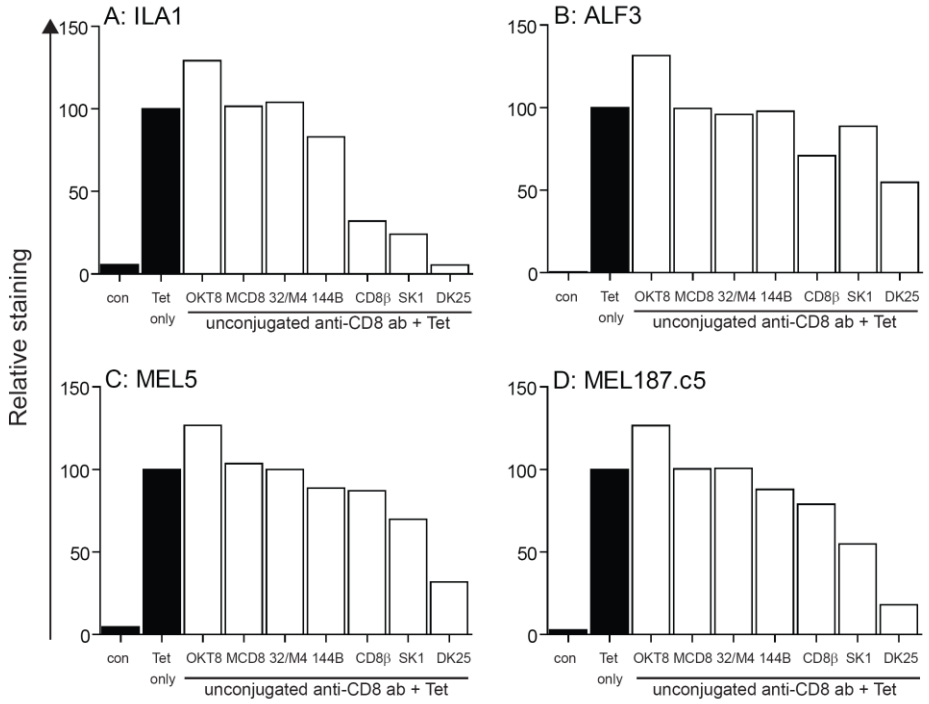

Figure 4.9: Anti-human CD8 antibodies can either enhance or inhibit the binding of pMHCI tetramers. 5 x 10^4 ILA1 (**A**), ALF3 (**B**), MEL5 (**C**) or MEL187.c5 (**D**) $CD8^+$ T-cell clones were preincubated at 4°C for 25 minutes with each of the following individual anti-human CD8 antibodies in parallel: 100 µg/ml OKT8, 6.25 µg/ml SK1, 50 µg/ml MCD8, 100 µg/ml 32/M4, 100 µg/ml C8/144B, 25 µg/ml DK25 and 100 µg/ml 2ST8.5H7 (CD8β). $CD8^+$ T-cells were subsequently stained with cognate PE-conjugated HLA A2 tetramers (25 µg/ml) and 5 µl 7-AAD at 37°C for 15 minutes, washed twice and resuspended in PBS. Data were acquired using a FACSCalibur flow cytometer and analyzed with FlowJo software. Relative MFI values with respect to pMHCI tetramer staining in the absence of pre-incubation with anti-CD8 antibody are shown. Fluorescence in the absence of added cognate tetramer (con) is shown in each case. Results shown are representative of four separate experiments using ILA1 and ALF3, and six separate experiments using MEL5 and MEL187.c5.

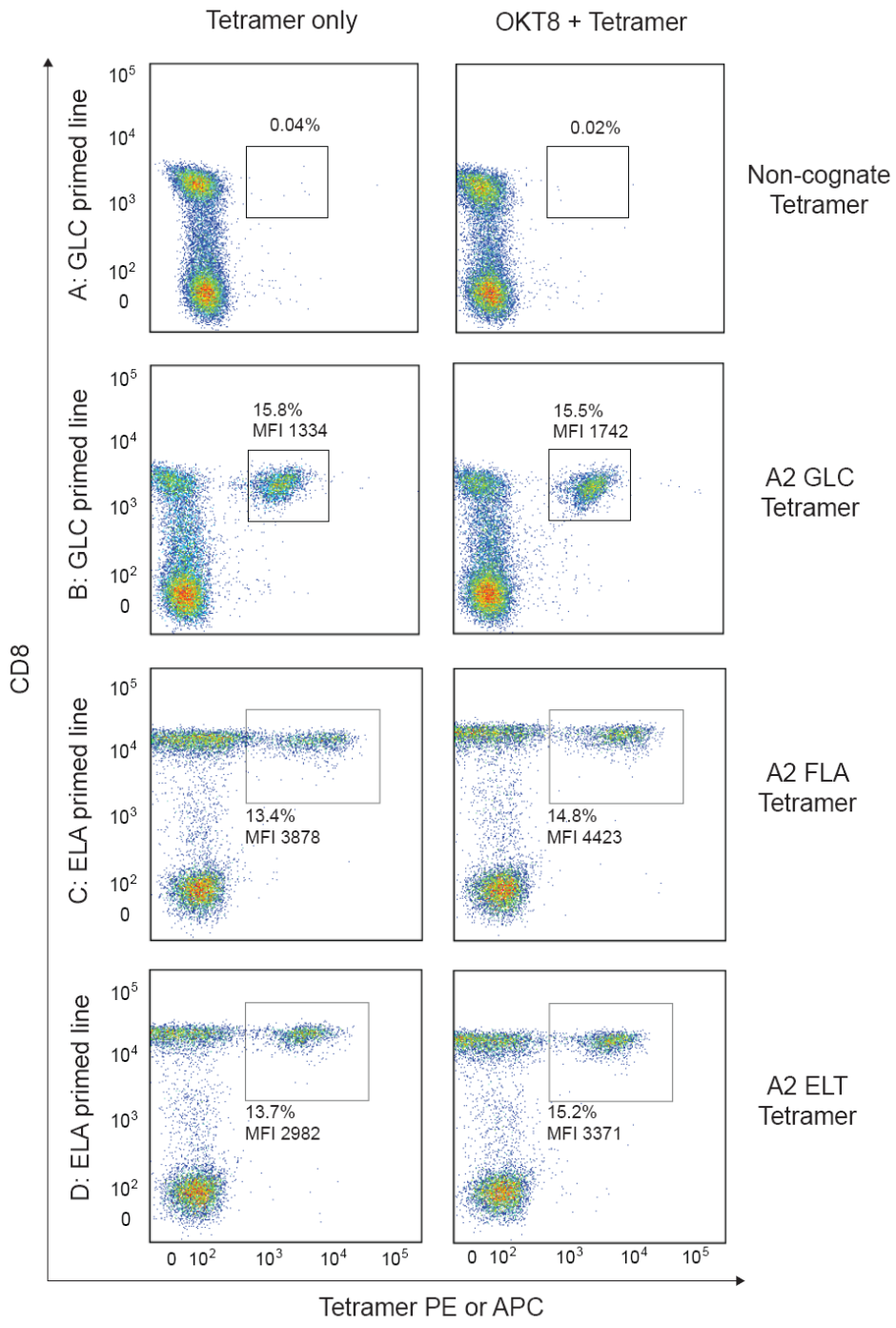

Figure 4.10: OKT8 enhances pMHCI tetramer staining in a mixed population. (**A&B**) 5 x 10^4 cells from a $CD8^+$ T-cell line primed with the EBV BMLF1-derived epitope GLCTLVAML (residues 259-267) were either mock treated or incubated with 100 µg/ml OKT8 at 4°C for 25 minutes, then stained with either (**A**) HLA A2-ELAGIGILTV (non-cognate) or (**B**) HLA A2-GLCTLVAML (cognate) APC-conjugated tetramer (25 µg/ml each) at 37°C for 15 minutes. (**C&D**) 5 x 10^4 cells from a $CD8^+$ T-cell line primed with the Melan-A/MART-1-derived epitope ELAGIGILTV (residues 26-35) were either mock treated or incubated with 100 µg/ml OKT8 at 4°C for 25 minutes, then stained with either (**C**) HLA A2-

FLAGIGILTV or (**D**) HLA A2-ELTGIGILTV PE-conjugated tetramer (25 μg/ml each) at 37°C for 15 minutes. Cells were then stained with 5 μl amine-reactive fluorescent dye LIVE/DEAD Fixable Aqua. 1 μl Pacific Blue-conjugated anti-human CD14, 1 μl Pacific Blue-conjugated anti-human CD19, 3 μl PE-Cy5.5–conjugated anti-human CD4 and 3 μl FITC-conjugated anti-human CD8 at 4°C for 20 minutes. Data were acquired using a FACSCantoII flow cytometer and analyzed with FlowJo software.

Next, I hypothesized that OKT8-mediated enhancement of TCR/pMHCI binding at the cell surface might have beneficial effects on pMHCI tetramer staining with low affinity ligands, an effect that could prove very useful for the detection of T-cells with TCRs that bind weakly to cognate antigen, such as those that appear to predominate in anti-cancer and autoimmune responses (Cole, Pumphrey et al. 2007; Cole, Edwards et al. 2010). To test this hypothesis, I used two monoclonal $CD8^+$ T-cell systems and a series of altered peptide ligands that vary in their affinity for cognate TCR by over 5-fold (Table 4.1 & Figure 4.11). Pre-incubation with OKT8 enhanced staining efficiency with all variant pMHCI tetramers, including low affinity variants (Table 4.1 & Figure 4.12). Consistent with this finding I also observed that OKT8 increased both the staining intensity and percentage of antigen specific $CD8^+$ T-cells detected when $CD8^+$ T-cell lines raised against the HLA A2-restricted Melan-A/MART-1-derived epitope ELAGIGILTV (residues 26-35) were stained with HLA A2 tetramers folded around the low affinity peptide variants **F**LAGIGILTV or EL**T**GIGILTV (Figure 4.10 C&D).

4.2.5 OKT8 enhances TCR/pMHCI on-rates at the cell surface

To examine how OKT8 enhances antigen binding at the $CD8^+$ T-cell surface in more detail, I examined the effects of this antibody on TCR/pMHCI kinetics using pMHCI tetramers. Differences in tetramer off-rates were minimal. However, pretreatment of $CD8^+$ T-cells with OKT8 resulted in a significant increase in the TCR/pMHCI on-rate at the cell surface in each $CD8^+$ T-cell clone tested (Figure 4.13). In contrast, DK25 inhibited pMHCI tetramer binding at the cell surface (Figure 4.13 B). OKT8 antibody-induced enhancement of pMHCI tetramer on-rates was also apparent with CD8-null tetramers (Figure 4.13 C). Collectively, these data

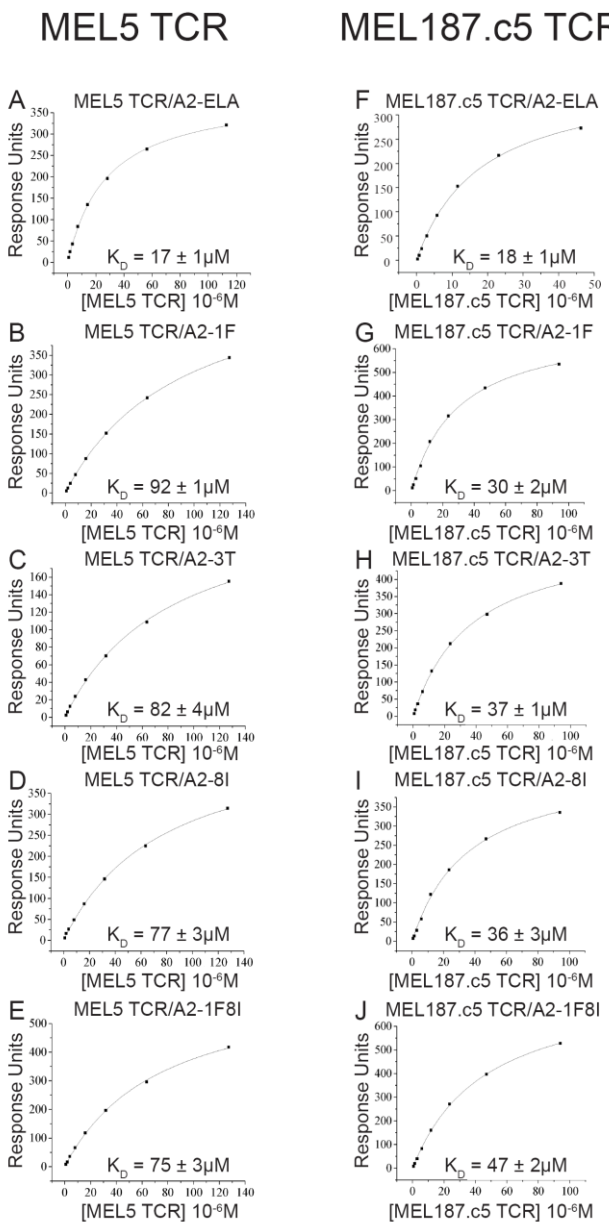

Figure 4.11: Surface plasmon resonance measurements of MEL5 and MEL187.c5 TCR binding to peptide variants complexed with HLA A2. (**A-E**) SPR equilibrium binding of soluble MEL5 TCR to HLA A2-ELAGIGILTV (**A**), HLA A2-FLAGIGILTV (**B**), HLA A2-ELTGIGILTV (**C**), HLA A2-ELAGIGIITV (**D**) and HLA A2-FLAGIGIITV (**E**). (**F-J**) SPR equilibrium binding of soluble MEL187.c5 to HLA A2-ELAGIGILTV (**F**), HLA A2-FLAGIGILTV (**G**), HLA A2-ELTGIGILTV (**H**), HLA A2-ELAGIGIITV (**I**) and HLA A2-FLAGIGIITV (**J**). The mean response for each concentration is plotted (n = 3). The equilibrium dissociation constant (K_D) values were calculated assuming 1:1 Langmuir binding and plotted using a nonlinear curve fit ($y = (P_1x)/(P_2 + x)$).

Peptide	MEL5 K_D (μM)	MEL5 Tetramer only (MFI)	MEL5 OKT8 + Tetramer (MFI)	MEL187.c5 K_D (μM)	MEL187.c5 Tetramer only (MFI)	MEL187.c5 OKT8 + Tetramer (MFI)
ELAGIGILTV	17 ± 1	855	917	18 ± 1	353	418
FLAGIGILTV	92 ± 1	194	227	30 ± 2	300	373
EL**T**GIGILTV	82 ± 4	36	87	37 ± 1	128	181
ELAGIGI**I**TV	77 ± 3	123	236	36 ± 3	195	257
FLAGIGI**I**TV	75 ± 3	367	426	47 ± 2	246	311

Table 4.1: OKT8 increases tetramer staining of MEL5 and MEL187.c5 $CD8^+$ T-cells with low affinity pMHCI variants. Summary of equilibrium binding analysis of MEL5 and MEL187.c5 TCRs with pMHCI variants, and the effect of OKT8 on HLA A2 tetramer staining. Raw SPR data are shown in Figure 4.11; flow cytometry data are shown in Figure 4.12.

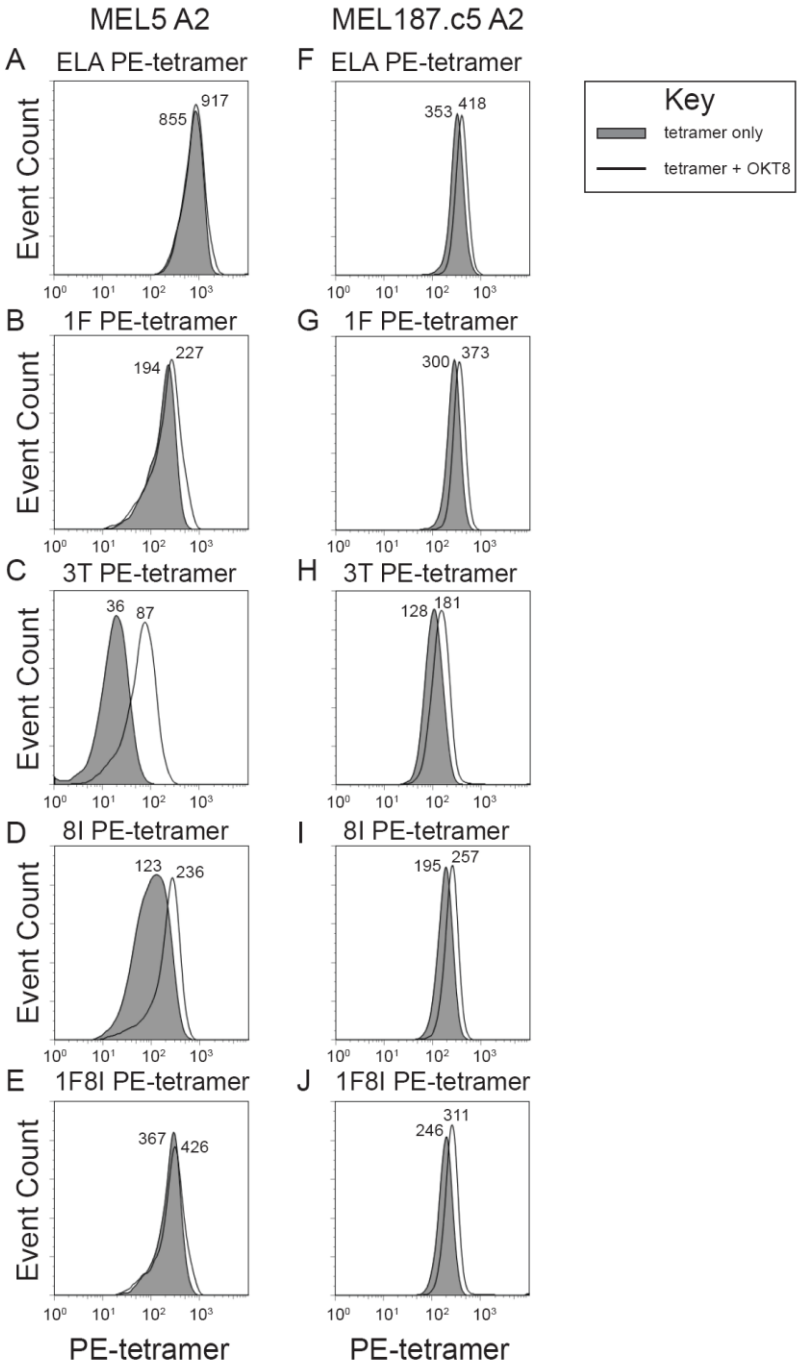

Figure 4.12: OKT8 increases tetramer staining with low affinity pMHCI variants. 5 x 10^4 MEL5 (**A-E**) or MEL187.c5 (**F-J**) $CD8^+$ T-cells were either mock treated or incubated with 100 µg/ml OKT8 at 4°C for 25 minutes, then stained with cognate or variant PE-conjugated HLA A2 tetramers (25 µg/ml) as indicated and 5 µl 7-AAD (BD Biosciences) at 37°C for 15 minutes. Data were acquired using a FACSCalibur flow cytometer and analyzed with FlowJo software.

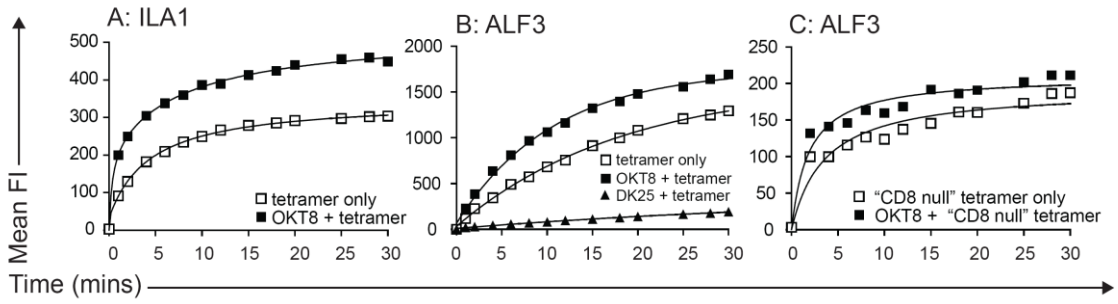

Figure 4.13: OKT8 increases TCR/pMHCI on-rates at the cell surface. 5 x 10^5/ml ILA1 (**A**) or ALF3 (**B&C**) $CD8^+$ T-cells were removed from culture, washed twice and resuspended in 100 µl PBS with or without 100 µg/ml OKT8 or 25 µg/ml DK25, then incubated at 4°C for 25 minutes. Cognate PE-conjugated HLA A2 tetramer was added in each case at 5 µg/ml; at various time points as indicated, 12 µl of cell suspension was removed and analyzed using a FACSCalibur flow cytometer with FlowJo software. In panel (**C**), the CD8-null (D227K/T228A) cognate HLA A2 tetramer was used (Purbhoo, Boulter et al. 2001).

indicate that OKT8 enhances pMHCI tetramer pMHCI tetramer staining by increasing the on-rate Furthermore, OKT8 antibody-mediated augmentation of antigen binding at the cell surface occurs independently of the pMHCI/CD8 interaction.

4.2.6 Stimulatory and Inhibitory anti-CD8 antibodies bind to different CD8 epitopes

I have thus far demonstrated that there is considerable heterogeneity in the ability of anti-CD8 antibodies to induce activation in the absence of TCR engagement, and in influencing subsequent pMHCI tetramer binding and $CD8^+$ T-cell sensitivity to pMHCI antigen. Monoclonal antibodies bind to 'defined' epitopes with high affinity (K_D $<10^{-9}$ M). Thus, I hypothesized that anti-CD8 antibodies might exert differential effects because they bind to distinct CD8 epitopes. To address this, I performed a series of antibody-blocking experiments. Pre-incubation with OKT8 was shown to block the binding of further OKT8 antibody demonstrating that the system can be used effectively to judge antibody binding sites (Figure 4.14)

Pre-incubation with OKT8 did not block the subsequent binding of SK1, DK25 or anti-CD8β antibody suggesting that OKT8 binds to a site that is distinct from the binding sites of these antibodies. Conversely, DK25, SK1 and anti-CD8β antibody did not significantly block the binding of OKT8 to the T-cell surface. Anti-CD8 antibodies that block pMHCI tetramer binding would appear to bind similar epitopes on CD8. This result is consistent with a previous report using a murine system (Devine, Hodsdon et al. 2004). Thus, antibody-blocking experiments suggest that the unique enhancing properties of OKT8 are a result of

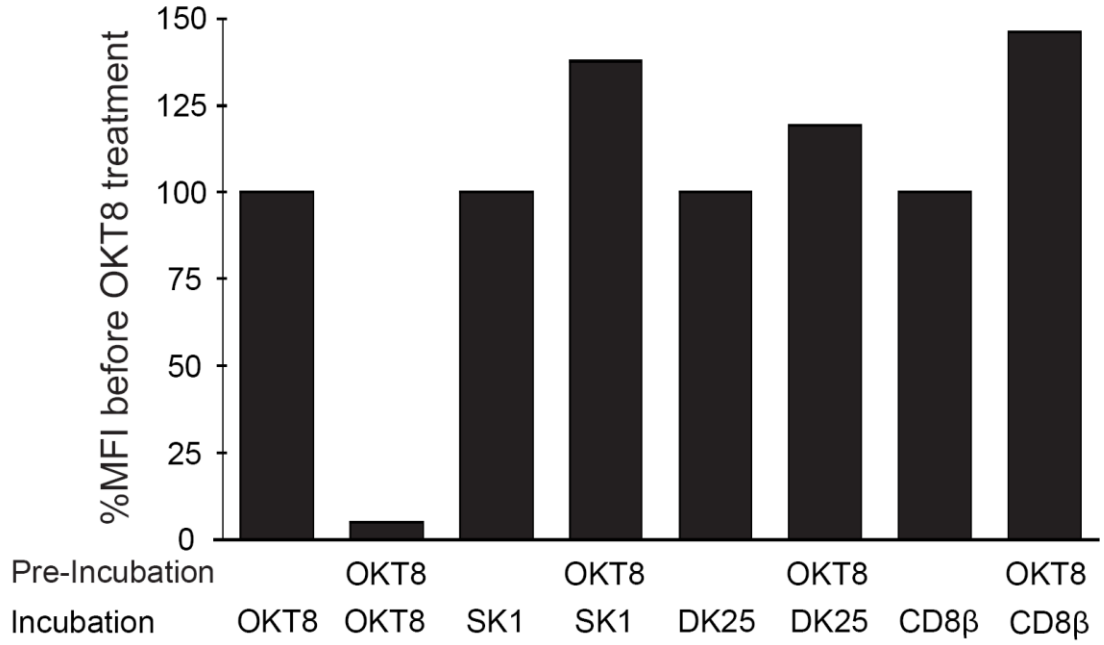

Figure 4.14: OKT8 binds to a distinct epitope compared to other CD8 antibodies. 5 x 10^4 ALF3 CD8+ T-cells were removed from culture, washed twice and resuspended in 40 µl PBS with or without 100 µg/ml OKT8, 6.25 µg/ml SK1, 25 µg/ml DK25 or 100 µg/ml 2ST8.5H7 (CD8β) then incubated at 4°C for 25 minutes. 3 µl of fluorochrome conjugated anti-human CD8 antibodies, APC-conjugated OKT8, PE-conjugated SK1, APC-conjugated DK25 or PE-conjugated CD8β, were then added and incubated at 4°C for 25 minutes along with LIVE/DEAD fixable violet, washed with PBS. Data were acquired using a FACSCantoII flow cytometer and analyzed with FlowJo software.

binding to a specific site on CD8, which is distinct from the site bound by blocking CD8 antibodies (Figure 4.15).

4.2.7 OKT8 F(ab´)$_2$ fragments can enhance tetramer staining and elicit T-cell effector function

Antibodies can be digested by papain or pepsin to produce Fab or F(ab´)$_2$ fragments, respectively. These enzymatically generated fragments have been used extensively in the past to study the structure and function of antibodies. I examined the ability of OKT8 Fab and F(ab´)$_2$ fragments to induce chemokine release in the absence of TCR engagement and enhance pMHCI tetramer staining. Fab fragments of OKT8 do not retain any ability to activate CD8$^+$ T-cells or have any significant effect on pMHCI tetramer staining (Figure 4.16 A&B). Interestingly, OKT8 F(ab´)$_2$ fragments do retain some ability to enhance pMHCI tetramer activation and elicit chemokine release (Figure 4.16 A&B). OKT8 mediated effects are diminished by pepsin digestion but this is consistent with similar observations when anti-human CD3 antibodies are digested by this enzyme (Figure 4.16 C) (Woodle, Thistlethwaite et al. 1991; Herold, Burton et al. 2003; Chatenoud and Bluestone 2007). Overall, it appears that whole OKT8 antibody is more efficient at exerting effects on pMHCI tetramer binding and CD8$^+$ T cell activation. However, the data suggests that F(ab´)$_2$ fragments are capable of cross-linking CD8 at the cell surface to some degree and that the ability of OKT8 to exert its effects are not entirely Fc´ dependant.

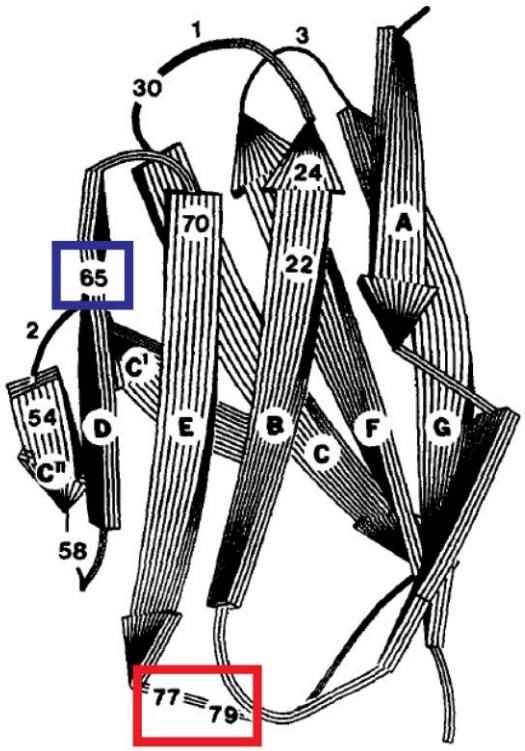

Figure 4.15: A schematic displaying binding sites of the enhancing anti-CD8 antibody OKT8. Mutational analysis of a single CD8 α chain reveals distinct distal binding site of OKT8 (red box) compared to other anti-CD8 antibodies (blue box) proximal to pMHCI (figure taken from © (Sanders, Fox et al. 1991)), originally published in the Journal of Experimental Medicine, **174**(2): 371-9.

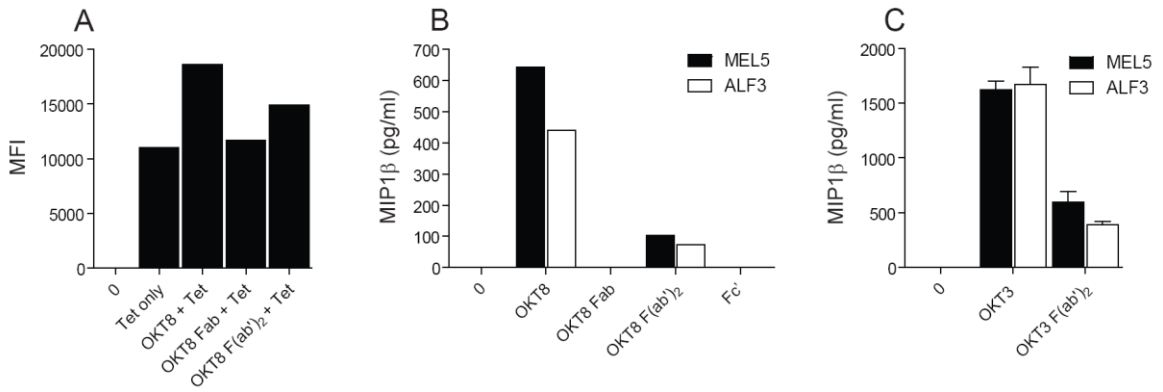

Figure 4.16: OKT8 F(ab´)$_2$ fragments can enhance tetramer staining and elicit T-cell effector function. (**A**) 5 x 10^4 MEL5 were either mock treated or incubated with 100 µg/ml OKT8, 100 µg/ml OKT8 Fab or 100 µg/ml OKT8 F(ab´)$_2$ then subsequently stained with PE-conjugated HLA A2 ELAGIGILTV tetramer (25 µg/ml) and stained with LIVE/DEAD® Fixable Aqua. Data were acquired using a FACSCantoII flow cytometer and analyzed with FlowJo software. (**B**) 3 x 10^4 MEL5 or ALF3 were incubated with either 100 µg/ml OKT8, 100 µg/ml Fab OKT8, 100 µg/ml F(ab´)$_2$ OKT8 or 100 µg/ml OKT8 Fc´ for 18 hours @ 37°C. Supernatant was harvested and assayed for MIP-1α, MIP-1β and RANTES by ELISA. (**C**) 3 x 10^4 MEL5 or ALF3 were incubated with either 10 µg/ml OKT3 or 10 µg/ml F(ab´)$_2$ OKT3 for 18 hours @ 37°C. Supernatant was harvested and assayed for MIP-1α, MIP-1β and RANTES by ELISA. The mean ± SD of three replicate assays is shown and only MIP-1β is shown.

4.2.8 Anti-mouse CD8 antibodies can trigger T-cell effector function in the absence of TCR engagement

To extend these findings beyond human systems, I examined the effect of the anti-mouse CD8α antibody CT-CD8a and the anti-mouse CD8β antibody CT-CD8b on pMHCI tetramer staining and $CD8^+$ T-cell activation in the absence of TCR engagement. I observed that CT-CD8a inhibited tetramer staining of mouse transgenic F5 $CD8^+$ T-cells, whereas CT-CD8b enhanced tetramer staining of the same antigen-specific population (Figure 4.17 A). These results are consistent with previous findings (Wooldridge, Hutchinson et al. 2003). Interestingly, despite exerting opposite effects on pMHCI tetramer staining, both of these anti-mouse CD8 antibodies were capable of inducing MIP-1β production in the absence of TCR engagement from both naïve and antigen-exposed F5 $CD8^+$ T-cells (Figure 4.17 B). This effect was shown to be CD8-specific and occurred in the absence of any concomitant IL2 release. The anti-mouse CD8 antibodies, 53.6.7 and KT112, were both shown to enhance pMHCI tetramer staining and induced small amounts of MIP-1β production (Figure 4.17 A&B). Therefore, I identified three different phenotypes (Table 4.2) within a panel of four different anti-mouse CD8 antibodies which further underscores the considerable heterogeneity in this group of reagents.

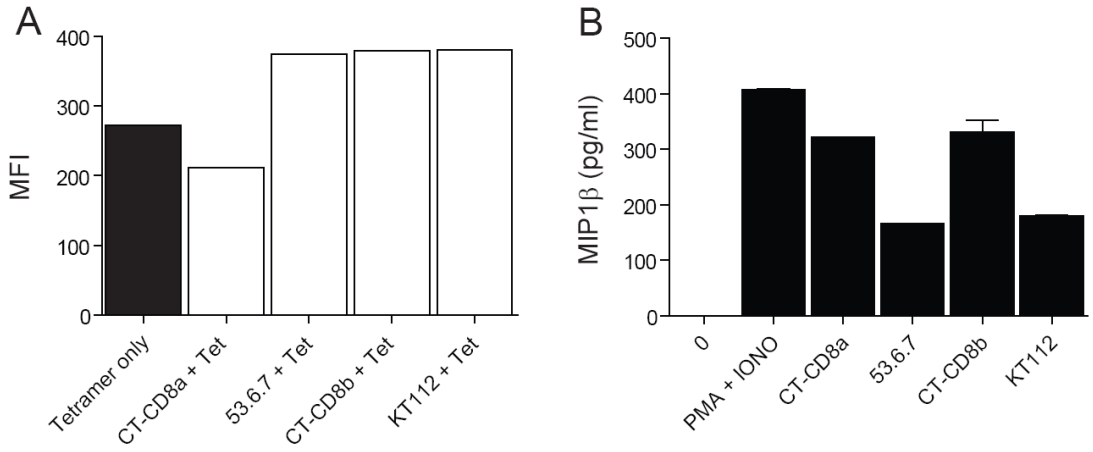

Figure 4.17: Anti-mouse CD8 antibodies can exhibit the same phenotype as OKT8. (**A**) 5 x 10^4 naïve mouse transgenic F5 T-cells were either mock treated or incubated with 100 μg/ml CT-CD8a, 100 μg/ml 53.6.7, 100 μg/ml CT-CD8b or 100 μg/ml KT112 at 4°C for 25 minutes, then stained with 25 μg/ml PE-conjugated H-2D^b tetramer folded around ASNENMDAM (cognate peptide) or KAVYNFATC (non-cognate peptide corresponding to the lymphocytic choriomeningitis virus GP1-derived epitope spanning residues 33-41) at 37°C for 15 minutes. Additional stains were conducted as described in the Materials and Methods. Data were acquired using a modified FACSAriaII flow cytometer and analyzed with FlowJo software. (**B**) 3 x 10^4 naïve mouse transgenic F5 T-cells were incubated at 37°C for 18 hours with either 100 μg/ml CT-CD8a, 100 μg/ml 53.6.7, 100 μg/ml CT-CD8b or 100 μg/ml KT112, or with PMA (50 ng/ml) and ionomycin (1 μg/ml). Supernatants were harvested and assayed for MIP-1β by ELISA. The mean ± SD of two replicate assays is shown.

Antibody Clone	α or β	Tetramer binding	MIP-1β	IFN-γ	IL-2
CT-CD8a	α	Inhibit	Yes	No	No
53.6.7	α	Enhance	Weak*	No	No
CT-CD8b	β	Enhance	Yes	No	No
KT112	β	Enhance	Weak	NT	NT

Table 4.2: The heterogeneity of anti-mouse CD8 antibodies. The effects exerted by anti-mouse CD8 antibodies on pMHCI tetramer binding and $CD8^+$ T-cell activation in the absence of TCR engagement. *53.6.7 elicited low levels of MIP-1β production from F5 naive $CD8^+$ T-cells, F5 $CD8^+$ T-cell lines and blasted BALB/c $CD8^+$ cells, but not from naive BALB/c $CD8^+$ cells. NT = Not Tested.

Antibody Clone	α or β	**Tetramer binding**	**MIP-1β**	**MIP-1α**	**RANTES**	**IFN-γ**	**TNF-α**	**IL-2**	**Cyto-toxicity**
OKT8	α	Enhance	Yes	Yes	Yes	No (Y*)	No (Y*)	No	Yes
SK1	α	Inhibit	No	No	No	No	No	No	No
MCD8	α	Neutral	No	No	No	No	No	No	No
32/M4	α	Neutral	No	No	No	No	No	No	No
C8/144B	α	Neutral	No	No	No	No	No	No	No
DK25	α	Inhibit	No	No	No	No	No	No	No
2ST8.5H7	β	Inhibit	No	No	No	No	No	No	No

Table 4.3: The heterogeneity of anti-human CD8 antibodies. The effects exerted by anti-human CD8 antibodies on pMHCI tetramer binding and $CD8^+$ T-cell activation in the absence of TCR engagement. *OKT8 was shown to elicit IFN-γ and TNF-α release by SB10 and PHA/IL-15 stimulated PBMC.

4.3 Discussion

Anti-CD8 antibodies are integral to the flow cytometric detection of pMHCI-restricted T-cells and have been used extensively in the past to identify an important role for CD8 in $CD8^+$ T-cell activation (Nakayama, Shiku et al. 1979; Shinohara and Sachs 1979; Norment, Salter et al. 1988; Miceli and Parnes 1993). Most studies have concluded that anti-CD8 antibodies inhibit the recognition of cognate antigen (MacDonald, Glasebrook et al. 1982; Janeway 1992). Furthermore, a recent study provided evidence that a single anti-CD8 antibody could deliver a negative signal to a $CD8^+$ T-cell clone in the absence of cognate antigen (Abidi, Dong et al. 2008). In contrast, however, earlier studies concluded that anti-CD8 antibodies could activate $CD8^+$ T-cells (Veillette, Zuniga-Pflucker et al. 1989; Tomonari and Spencer 1990). Thus, contradictory effects of antibody-mediated CD8 ligation have been reported and the overall picture remains unclear. To clarify this issue, I examined the ability of seven different monoclonal anti-human CD8 antibodies to activate six different human $CD8^+$ T-cell clones specific for a total of five different pMHCI antigens.

In the absence of cognate antigen, the anti-human CD8 antibody OKT8 induced chemokine release from all six human $CD8^+$ T-cell clones tested and cytotoxic activity in all four human $CD8^+$ T-cell clones tested (Figures 4.1-4.3 & 4.5). Interestingly, this activation appeared to occur in the absence of any detectable cytokine release, with the exception of $CD8^+$ T-cell clone SB10, which released IFN-γ (Figure 4.6). It is well established that a hierarchy of $CD8^+$ T-cell effector functions exists with respect to antigen sensitivity (Valitutti, Muller et al. 1996; Price, Sewell et al. 1998); thus, each function exhibits a distinct activation threshold that must be exceeded for triggering to occur. These findings suggest that OKT8 delivers a

positive signal to $CD8^+$ T-cells that is generally sufficient to exceed the activation threshold required for chemokine release and cytotoxic activity, but is not sufficient to trigger cytokine release in the majority of $CD8^+$ T-cells. In contrast to OKT8, the anti-human CD8α antibody clones SK1, MCD8, C8/144B, 32/M4 and DK25, and the anti-human CD8β antibody clone 2ST8.5H7, did not induce any measurable T-cell effector functions in the absence of cognate antigen. It was not possible to reverse the phenotype of the non-activating anti-human CD8 antibodies by secondary antibody-mediated cross-linking or PHA/IL-15 treatment (Figures 4.7 & 4.8). Thus, I conclude that anti-CD8 antibodies can exert differential effects on $CD8^+$ T-cells. These findings help to reconcile previous disparate observations and suggest that previous reports in the literature may not be intrinsically contradictory, but rather reflective of the considerable heterogeneity that characterizes the ability of anti-CD8 antibodies to induce $CD8^+$ T-cell effector function.

To examine the effects of OKT8 on antigen binding at the T-cell surface, I used soluble pMHCI tetramer technology. Pre-incubation with OKT8 enhanced the capture of cognate pMHCI tetramers from solution and produced higher intensity staining (Figure 4.9 & 4.10). Accordingly, OKT8 enhanced the identification of $CD8^+$ T-cells with low and high affinity TCR/pMHCI interactions (Figure 4.10 & 4.12 & Table 4.1), such as those that typically predominate in tumour-specific and autoimmune responses (Cole, Pumphrey et al. 2007). The other anti-CD8 antibodies in the panel either exerted inhibitory effects on pMHCI tetramer binding (SK1, DK25 and 2ST8.5H7) or displayed no biologically significant activity in this regard (MCD8, 32/M4 and C8/144B). Thus, OKT8 can be used as a tool to improve pMHCI tetramer staining; this property may be especially useful in the context of low avidity antigen-specific $CD8^+$ T-cell populations.

The findings described above suggest that OKT8 has properties that are distinct from other anti-human CD8 antibodies. To extend these results, I conducted additional experiments with the anti-mouse CD8α antibody CT-CD8a and the anti-mouse CD8β antibody CT-CD8b. CT-CD8a was shown to inhibit pMHCI tetramer staining, whereas CT-CD8b enhanced pMHCI tetramer binding, consistent with a previous report (Wooldridge, Hutchinson et al. 2003). Despite their differential effects on pMHCI tetramer binding, both of these anti-mouse CD8 antibodies activated $CD8^+$ T-cells efficiently (Figure 4.17). These results demonstrate that the ability of anti-CD8 antibodies to elicit $CD8^+$ T-cell effector function does not always correlate with their effect on pMHCI tetramer staining. In addition, a third phenotype was identified in the mouse system; the anti-mouse CD8α antibody 53.6.7 and the anti-mouse CD8β antibody KT112 both enhanced pMHCI tetramer staining but only induced the release of MIP-1β (Figure 4.17 & Table 4.2). Taken together, these data further underline the heterogeneity that exists within this group of reagents.

The mechanism by which anti-CD8 antibodies exert either inhibitory or stimulatory effects on pMHCI recognition remains elusive. Previous studies have shown that anti-CD8 antibodies retain their effects in the absence of a pMHCI/CD8 interaction (Van Seventer, Van Lier et al. 1986; Hoo and Kranz 1993; Campanelli, Palermo et al. 2002; Wooldridge, Hutchinson et al. 2003). Here, I confirmed that the enhancing effects of OKT8 on HLA A2 tetramer on-rate at the cell surface are still apparent in the context of CD8-null MHCI molecules (Figure 4.13); thus, these effects are independent of any interaction between pMHCI and CD8. Subtle local re-arrangements of the TCR relative to CD8 on pMHCI engagement are required for optimal $CD8^+$ T-cell activation (Block, Johnson et al. 2001; Lee and Kranz 2003). By extension, it seems likely that anti-CD8 antibodies exert their effects by

interfering with, or enhancing, this surface receptor topology. The observation that anti-CD4 antibodies can block cell surface intermolecular interactions essential for calcium flux and inhibit subsequent synapse formation is consistent with this hypothesis (Krummel, Sjaastad et al. 2000). Furthermore, it has been previously demonstrated that anti-CD4 antibodies can interfere with pMHCII tetramer binding despite the fact that the pMHCII/CD4 interaction does not stabilize TCR/pMHCII interactions (Wooldridge, Scriba et al. 2006). I have also shown that OKT8 binds to a site which is distinct from all of the other anti-human CD8 antibodies tested within this panel (Figure 4.14) which may provide an explanation for its unique phenotype.

In summary, I have shown that: (i) heterogeneity exists in the ability of anti-CD8 antibodies to activate $CD8^+$ T-cells; (ii) antibody-mediated ligation of CD8 in the absence of TCR engagement can induce chemokine release and cytotoxic activity, largely in the absence of cytokine release; (iii) the anti-human CD8 antibody OKT8 can enhance pMHCI tetramer staining; and, (iv) anti-murine CD8 antibodies (CT-CD8a and CT-CD8b) can activate $CD8^+$ T-cells in the absence of TCR engagement despite differential effects on pMHCI tetramer staining (Table 4.2 & 4.3). Thus, anti-CD8 antibodies can have potent effects on TCR/pMHCI binding kinetics and activation. These effects vary according to the antibody clone under investigation and should be taken into account when interpreting studies using these reagents. Furthermore, the ability of antibody-mediated CD8 engagement to activate $CD8^+$ T-cells underscores the importance of co-receptor function in $CD8^+$ T-cell signalling.

Chapter 5

5

TARGETING CD8 TO BLOCK AUTOREACTIVE CD8$^+$ T-CELL ATTACK

(Clement et al., manuscript in preparation)

5.1 Introduction

As a result of my findings in chapters 3 & 4, it is clear that CD8 has a potent ability to tune the antigen specific $CD8^+$ T-cell response. In chapter 4, I demonstrated that antibodies that target CD8 can have dramatic effects on pMHCI tetramer binding and $CD8^+$ T-cell activation. I was able to characterize anti-CD8 antibodies capable of blocking pMHCI tetramer binding and subsequent pMHCI-induced $CD8^+$ T-cell activation, suggesting that targeting CD8 may be useful in situations where blocking unwanted $CD8^+$ T-cell activation may be beneficial. It is beginning to emerge that $CD8^+$ T-cells play an important role in the pathogenesis of common autoimmune diseases such as type-1 diabetes (T1D from heron) and Multiple Sclerosis (MS from hereon). As such, therapies that target autoreactive $CD8^+$ T-cell attack are highly desirable.

5.1.1 Role of $CD8^+$ T-cells in the pathogenesis of common autoimmune diseases

It has been traditionally theorised that autoimmune disorders such as T1D, MS, and Rheumatoid Arthritis are attributed to $CD4^+$ T-cells. However there is growing evidence to suggest that $CD8^+$ T-cells also contribute to the disease processes, most notably in MS, T1D and also Psoriasis. MS is the most common neurological disorder of young adults affecting over 1 million adults worldwide. MS is an inflammatory disease of the central nervous system (CNS) which destroys oligodendrocytes, neurons and axons. MS patients harbour $CD8^+$ T-cells specific for multiple central nervous system antigens and $CD8^+$ T-cells have been shown to be enriched in MS plaques (Huseby, Huseby et al. 2012; Friese and Fugger 2009). T1D results in a total loss of self-tolerance and the destruction of insulin-producing β-cells in the islets of langerhans of the pancreas. This destruction is dominated by

lymphocytes, many of which are $CD8^+$ T-cells that specifically target epitopes derived from β-cell proteins (Roep and Peakman 2011; Coppieters, Dotta et al. 2012). Currently there is no known cure for T1D and the condition results in life-long insulin dependence, which is an expensive course of treatment. As of 2011 the incidence of T1D in the UK was ~0.3 million people at a cost of ~£0.3 billion to the NHS (www.diabetes.nhs.uk). It is of no doubt that there is a need for new treatments for autoimmune disorders. Therefore the timing of this study is very important as it may aid in the development of potential new treatments for these diseases.

5.1.2 Autoreactive TCR/pMHCI interactions are characterized by low affinity

Advances in understanding the molecular mechanisms which govern recognition of pMHCI antigen reveal key intrinsic differences between pathogen and autoreactive $CD8^+$ T-cells that could be exploited for therapeutic benefit. Extensive biophysical studies have revealed that pathogen specific $CD8^+$ T-cells display a high affinity for foreign pMHCI (range K_D 1 - 50 μM) (Bridgeman, Sewell et al. 2011). In contrast, TCRs with a high affinity for tissue specific antigens (TSAs) are eliminated from the repertoire during thymic selection. Autoreactive TCRs that escape negative selection are characterized by structural defects that reduce the overall stability of the complex and result in K_D values >100 μM (Yin, Li et al. 2012) Biophysical measurements of a further four diabetogenic MHCI restricted TCRs suggest that the average TCR/pMHCI affinity in this disease context may actually be characterised by K_Ds >200 μM (unpublished data). This then suggests that this activation pathway would be highly dependent on CD8 for activation. I decided to test the hypothesis

that targeting CD8 could be used to block autoreactive $CD8^+$ T-cell activation in the absence of any affect on pathogen specific $CD8^+$ T-cell immunity.

5.1.3 Low affinity TCR/pMHCI interactions are highly CD8 dependent

Previous studies using $CD8^+$ T-cell clones and hybridomas have demonstrated that the degree of CD8 dependency for efficient antigen recognition roughly correlates with the potency of the peptide ligand as defined by the concentration of peptide required to elicit half maximum activation in dose dependent titrations (as reviewed in (Laugel, Cole et al. 2011)). Indeed Holler *et al* showed that using the murine 2C TCR system, T-cell hybridomas were not fully activated in the absence of CD8 expression by agonist ligands with K_D > 100 nM (Holler, Holman et al. 2000; Holler and Kranz 2003). The same group also showed that with a TCR/pMHCI K_D > 3 μM antigen recognition became strictly dependent on the presence of the co-receptor. They posited that the majority of $CD8^+$ T-cells that express TCRs specific to antigen in a natural setting were likely to demonstrate a degree of dependence on the co-receptor. This theory was then further supported by studies showing that dependency on CD8 for $CD8^+$ T-cell activation by altered peptide ligands correlated well with the EC_{50} (Laugel, van den Berg et al. 2007; Wooldridge, Laugel et al. 2010). Ligands with a K_D > 35-40 μM displayed some degree of CD8 dependency in peptide titration assays (Laugel, van den Berg et al. 2007; Wooldridge, Laugel et al. 2010). It was also shown in these studies that recognition of TCR ligands with very low affinities (K_D values > 100-200 μM) are entirely CD8-dependent. It is important to note that the quantitative differences observed between the Holler and Laugel studies are likely due to the different systems being used in each study. The Holler study used the murine 2C TCR system which has a stronger TCR/pMHCI interaction than the human $CD8^+$ T-cell clones used in the Laugel study. It would therefore be

of interest to determine the range of TCR/pMHCI and their reliance on CD8 to respond adequately to cognate ligands in different systems. Overall there is a direct relationship between CD8 dependency of the $CD8^+$ T-cell for activation and the affinity of the TCR/pMHCI interaction, where very weak TCR/pMHCI affinity interactions are entirely CD8 dependent. Interestingly, the level of CD8 dependency exhibited by the $CD8^+$ T-cell has also been shown to be affected by the ligand density on the target cell. When using anti-CD8 antibodies to block $CD8^+$ T-cell activation, increasing levels of pMHCI density can bypass antibody blockade (Alexander, Damico et al. 1991; Hoo and Kranz 1993; Viola, Salio et al. 1997).

5.1.4 Exploiting CD8 dependency in pathological settings

On the basis of published literature, I predict that stronger pathogen specific TCR/pMHCI interactions will show little dependence on CD8 for activation. In stark contrast, autoreactive TCR/pMHCI interactions are very weak and likely to be highly CD8 dependent. As such, I hypothesise that the stark differences between typical pathogen specific and autoreactive TCR/pMHCI interactions can be exploited in order to preferentially target $CD8^+$ T-cell mediated autoimmune attack without interfering with pathogen specific immunity. Thus CD8 may be a desirable target in pathological scenarios where the TCR/pMHCI binding affinity is CD8 dependent, i.e. K_Ds > 100 μM such as autoimmune disorders.

I decided to study the effects of CD8 dependency and the effect of using inhibitory anti-CD8 antibodies where this weak interaction applies. The 1E6 $CD8^+$ T-cell clone specific for the autoantigen preproinsulin peptide ALWGPDPAAA ($PPI_{15–24}$) (Skowera, Ellis et al. 2008),

which has recently been measured biophysically using surface plasmon resonance, shows that this TCR binds to the cognate ligand ALWGPDPAAA with a K_D ~278 μM (Bulek, Cole et al. 2012). This provided an excellent candidate to examine the CD8 dependency of T-cell activation from a clinically relevant setting. In the human autoimmune disease type-1 diabetes, $CD8^+$ T-cells are focussed on the islets of Langerhans and destroy β cells via the recognition of β cell–specific peptides presented by HLA class I molecules, leading to a lifelong dependence on insulin (Skowera, Ellis et al. 2008). To date no study has been conducted to examine the possibility that targeting CD8 using anti-CD8 antibodies can preferentially block highly dependent autoreactive $CD8^+$ T-cells that recognise a defined epitope on the surface of pancreatic β cells.

5.1.5 Use of antibodies to inhibit $CD8^+$ T-cell activation

It has long been known that anti-CD8 antibodies can be used to block the activation of some $CD8^+$ T-cells (MacDonald, Glasebrook et al. 1982). MacDonald *et al* used a murine system to highlight the heterogeneity in the functional output of multiple anti-CD8 antibodies where some antibodies could inhibit T-cell activation whereas others were shown to have no effect. These heterogeneous effects have been further supported and observed in multiple subsequent studies including our own (see chapter 4). Importantly, it was suggested that heterogeneity in the ability of $CD8^+$ T-cells to activate in the presence of inhibitory anti-CD8 antibodies was thought to correlate with the strength of the TCR/pMHCI interaction. I will test this theory in this chapter and also investigate the possibility that this can be exploited for therapeutic benefit.

5.1.6 Summary and Aims

The aim of this chapter was to examine the potential use of anti-CD8 antibodies to preferentially block autoreactive $CD8^+$ T-cell activation.

Using multiple $CD8^+$ T-cell clones which vary in TCR/pMHCI binding affinities I aim:

- To investigate the relationship between TCR/pMHCI affinity and CD8 dependence.
- To investigate the possibility that targeting the CD8 co-receptor can be used to block autoreactive $CD8^+$ T-cell activation in the absence of any effect on pathogen specific $CD8^+$ T-cell responses.

5.2 Results

5.2.1 CD8 dependency is governed by TCR/pMHCI binding affinity

I examined how CD8 dependency is governed by the strength of the TCR/pMHCI interaction. Stable C1R B-cell (Storkus, Howell et al. 1987) transfectants expressing A2 wild-type and HLA A2 DT227/8KA (Purbhoo, Boulter et al. 2001) were used to study the effect of wild-type and abrogated pMHCI/CD8 interaction, respectively whilst not effecting the TCR/pMHCI interaction. When C1R wild-type and 227/8 B-cells were pulsed with cognate ligands for multiple HLA A2 restricted $CD8^+$ T-cell clones, each with varying TCR/pMHCI binding affinities, differences in levels of T-cell activation can be seen (Figure 5.1 A-H). $CD8^+$ T-cell clones which have a high TCR/pMHCI binding affinity are less dependent on CD8. The $CD8^+$ T-cell clone ALF8, specific for the Influenza A virus $MP1_{58-66}$ epitope GILGFVFTL, elicits a very sensitive and high level of T-cell activation. ALF8 is relatively

unaffected by the abrogation of CD8 using C1R 227/8 B-cells (Figure 5.1 A&B) which is not surprising given the relatively strong binding affinity of the TCR/pMHCI interaction K_D of 2.6 μM (Table 5.1 & Appendix 3).

I then examined more $CD8^+$ T-cell clones with varying TCR/pMHCI affinities (Table 5.1), i.e. MEL5, specific for the Melan-A-derived epitope ELAGIGILTV (residues 26-35) (K_D = 18 μM) (Cole, Pumphrey et al. 2007; Cole, Edwards et al. 2010), ILA1 specific for the human telomerase reverse transcriptase (hTERT)-derived epitope ILAKFLHWL (residues 540-548) (K_D = 36 μM) (Cole, Pumphrey et al. 2007) and 1E6, specific for the restricted autoantigen preproinsulin peptide ALWGPDPAAA ($PPI_{15–24}$) (K_D = 278 μM) (Cole, Edwards et al. 2010; Bulek, Cole et al. 2012). Decreasing the strength of the TCR/pMHCI interaction was accompanied by an increase in CD8-dependency and revealed an extremely high level of CD8-dependency in the autoimmune 1E6 $CD8^+$ T-cell clone (Figure 5.1 G&H). Activation of the 1E6 $CD8^+$ T-cell clone in the absence of CD8 engagement resulted in almost 100% impairment of MIP-1β release and no detectable production of IFN-γ (Figure 5.1 G&H). In summary, this data demonstrates that CD8 dependency is governed by the TCR/pMHCI binding affinity.

5.2.2 Anti-CD8 antibodies can efficiently block pMHCI tetramer binding when the TCR/pMHCI interaction is extremely weak

As previously discussed in chapter 4, there are multiple anti-CD8 antibody phenotypes including those that are capable of blocking tetramer binding at the cell surface. The two

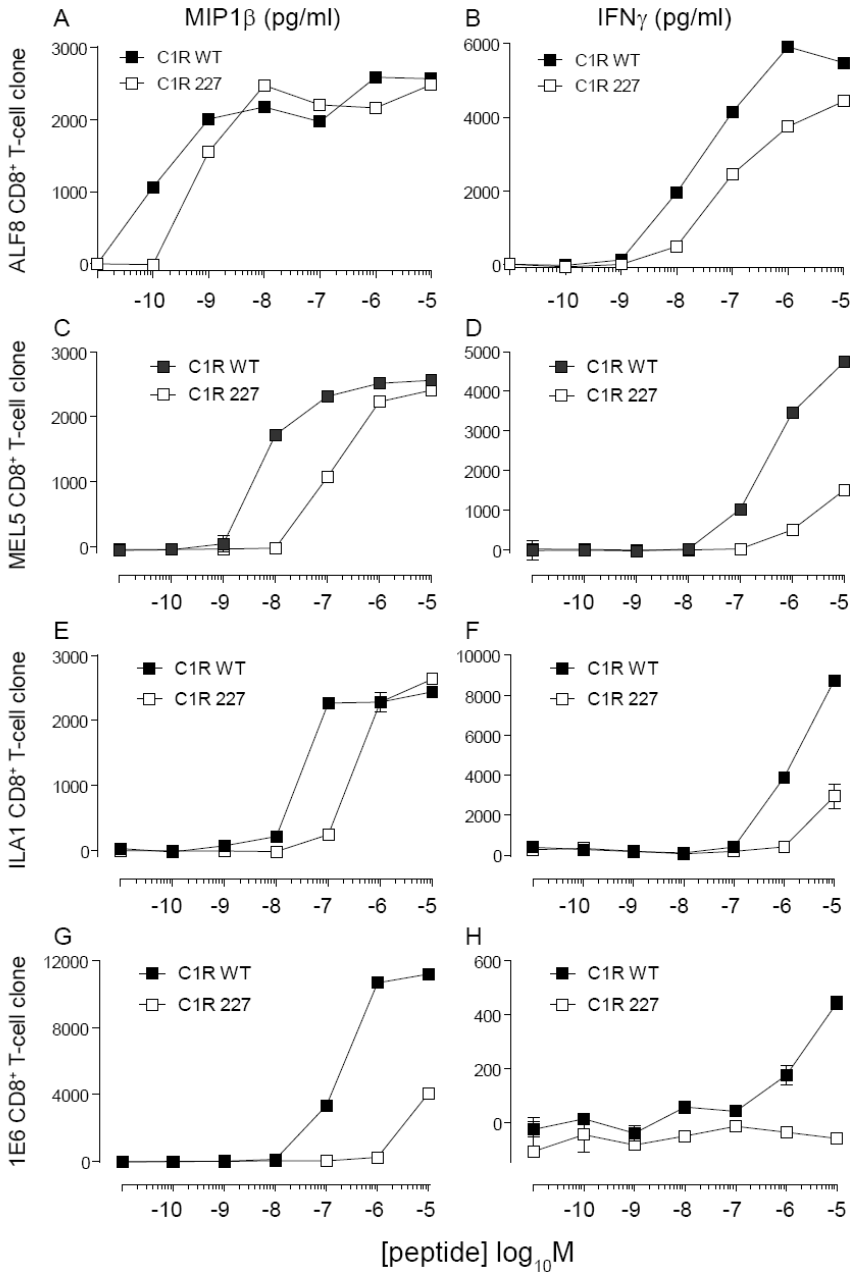

Figure 5.1: The level of CD8 dependency of CD8$^+$ T-cells increases as the TCR/pMHCI interaction decreases. (**A-H**) 6 x 10^4 C1R-A*0201 (CD8 wild-type) or C1R-A*0201 227/8 (CD8 abrogated) B-cells were pulsed with cognate peptide from 10^{-11} to 10^{-5} M in duplicate for 1 hour @ 37°C. Excess peptide was washed off twice with PSG. 3 x 10^4 ALF3, MEL5, ILA1 or 1E6 CD8$^+$ T-cell clones were incubated with pulsed C1R B-cells for 4 hours @ 37°C. Supernatant was harvested and assayed for MIP-1β and IFN-γ by ELISA. The mean ± SD of two replicate assays is shown.

$CD8^+$ T-cell clone	1E6	ILA1	MEL5	ALF3	ALF8
Epitope	ALWGPDPAAA	ILAKFLHWL	ELAGIGILTV	GILGFVFTL	GILGFVFTL
TCR/pMHCI K_D μM	278	36	18	5.4[1]	2.6[1]

Table 5.1: TCR/pMHCI binding affinities of different target restricted $CD8^+$ T-cell clones. Summary of the TCR/pMHCI binding affinities of different $CD8^+$ T-cell clones used. [1] See Appendix 3 for SPR Biophysical data.

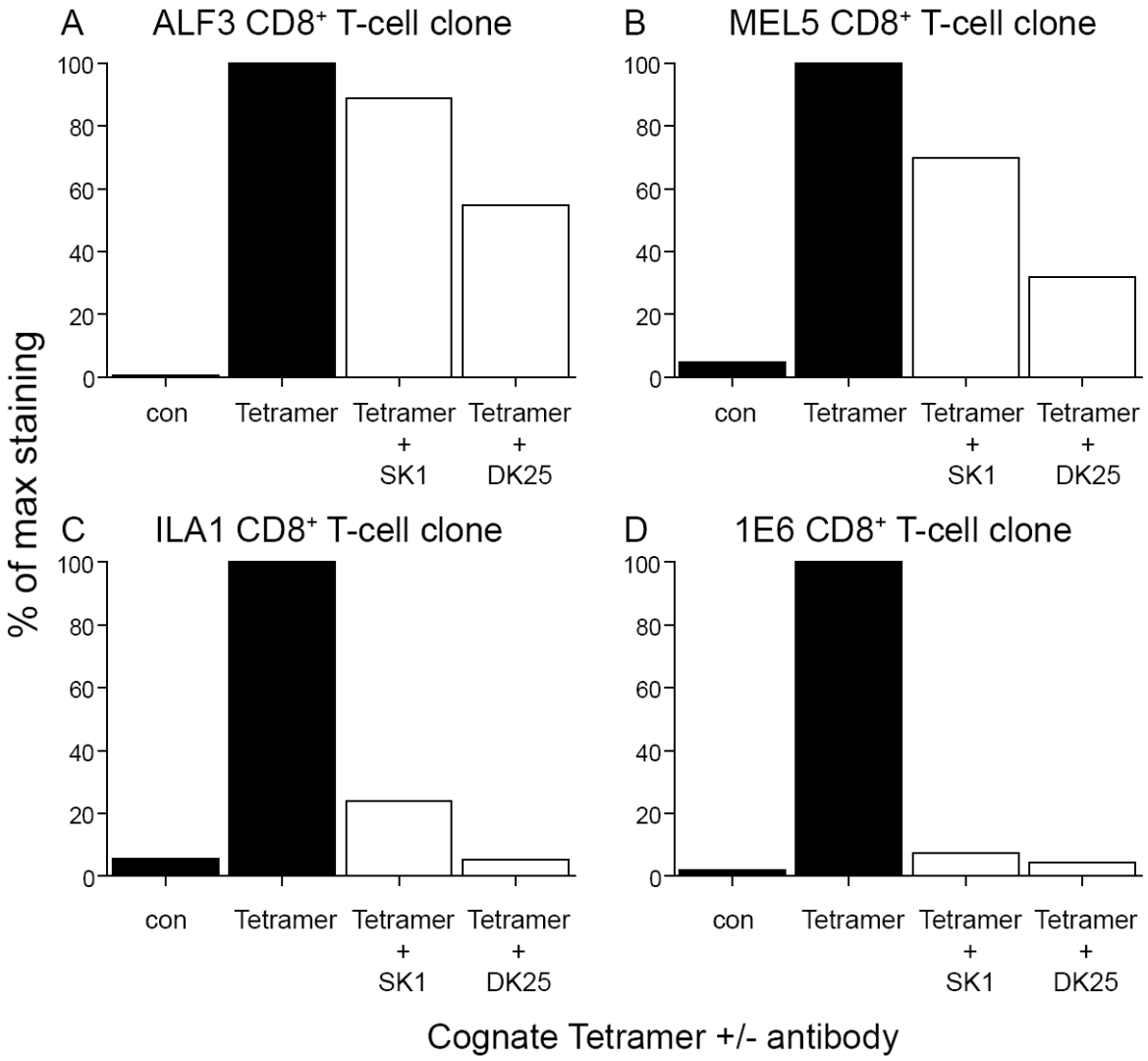

Figure 5.2: Weak TCR/pMHCI interactions are extremely susceptible to blockade with anti-CD8 antibodies. 5 x 10^4 (**A**) ALF3 (K_D 5.4 μM), (**B**) MEL5 (K_D 18 μM), (**C**) ILA1 (K_D 36 μM), and (**D**) 1E6 (K_D 278 μM), $CD8^+$ T-cells were removed from culture, washed twice and resuspended in 40 μl PBS with or without anti-human CD8 antibody at SK1 6.25 μg/ml or DK25 12.5 μg/ml, then incubated at 4°C for 25 minutes. Cognate PE or BV421-conjugated HLA A*0201 tetramer was added in each case at 25 μg/ml at 37°C for 15 minutes. Data were acquired using a FACSCantoII flow cytometer and analyzed with FlowJo software.

most effective blocking antibodies were clones SK1 and DK25. Pre-incubation with SK1 and DK25 resulted in reduced levels of pMHCI tetramer binding to all $CD8^+$ T-cell clones tested (Figure 5.2 A-D) albeit to a differing extent. As TCR/pMHCI interaction strength is reduced then the effect of CD8 blocking antibody on pMHCI tetramer binding becomes more dramatic (Figure 5.2 B-D). In fact, the most dramatic effect was observed (>95% blockade) on pMHCI tetramer staining of 1E6 $CD8^+$ T-cell clones with both blocking antibodies (Figure 5.2 D). Therefore, pMHCI binding at the cell surface is extremely susceptible to anti-CD8 antibody mediated blockade if the TCR/pMHCI interaction is weak.

5.2.3 Titration of antibody reveals concentration for efficient blockade of autoreactive TCR/pMHCI interactions

Next, I wanted to assess whether it is possible to identify a concentration of blocking anti-CD8 antibody that can efficiently block tetramer binding to autoreactive $CD8^+$ T-cells (1E6) in the absence of any significant effect on higher affinity TCR/pMHCI interactions (typical of pathogen specific $CD8^+$ T-cells). I therefore proceeded to titrate the concentration of the most inhibitory antibody DK25 to identify a threshold concentration (Figure 5.3 A-H). The inhibitory effect of the antibody was titrated to a level where a decrease in the concentration resulted in an increase in tetramer binding (Figure 5.3 A-H). Use of DK25 at a concentration of 1 μg/ml resulted in ~80% inhibition of tetramer binding to the autoreactive 1E6 $CD8^+$ T-cell clone (Figure 5.3 H). This concentration had little or no effect on the tetramer binding to MEL5 and ALF8 where the TCR/pMHCI interaction is much stronger (Figure 5.3 A-D) (Table 5.1). Therefore at a concentration of 1 μg/ml, DK25 can be used to block autoreactive TCR/pMHCI interactions at the cell surface whilst not affecting the stronger TCR/pMHCI interactions of anti-viral and some anti-tumour responses.

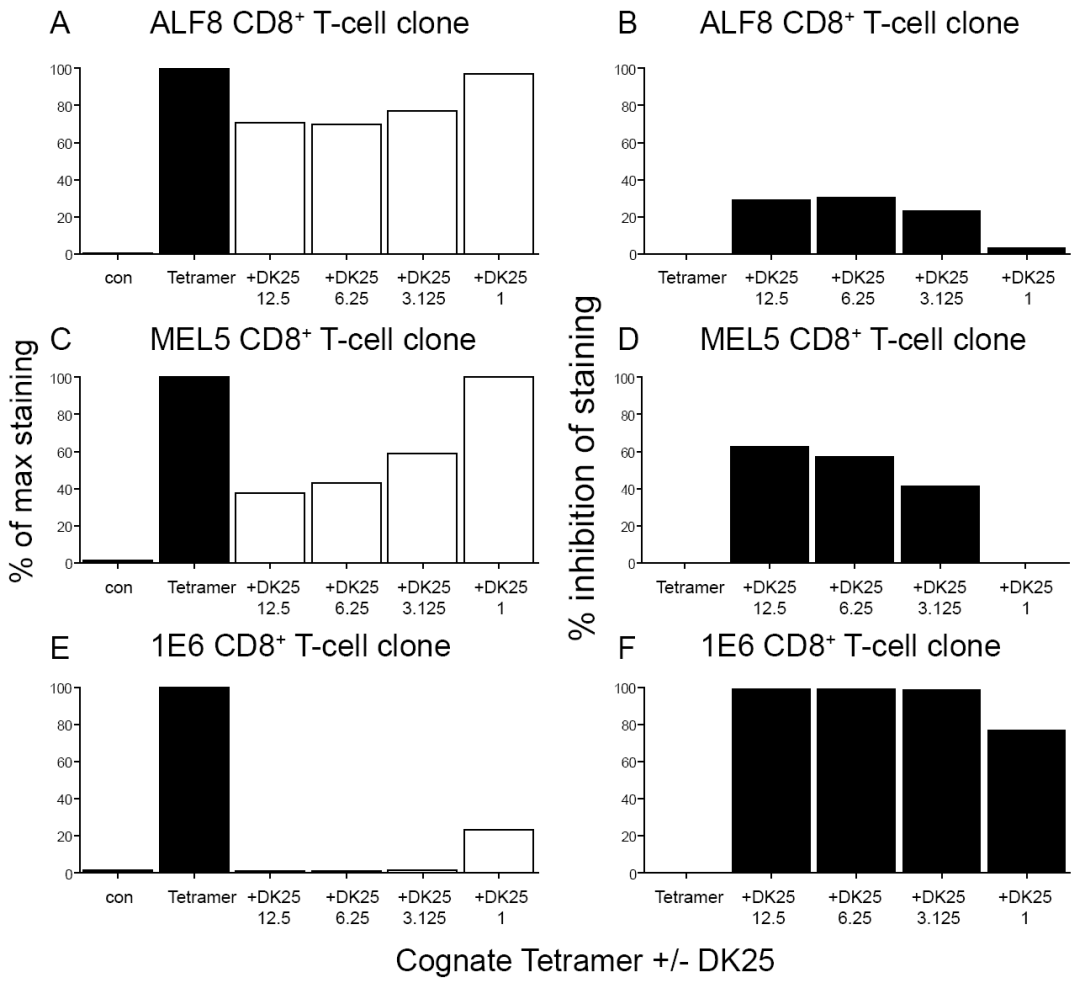

Figure 5.3: Antibody blocking of tetramer binding can be titrated to a low level in the context of weak TCR/pMHCI interactions whilst not affecting stronger TCR/pMHCI interactions. 5 x 10^4 (**A**) ALF8, (**B**) MEL5 and (**C**) 1E6 $CD8^+$ T-cells were removed from culture, washed twice and resuspended in 40 µl PBS with or without anti-human CD8 antibody DK25 at 12.5 µg/ml, 6.25 µg/ml, 3.125 µg/ml or 1 µg/ml then incubated at 4°C for 25 minutes. Cognate PE-conjugated HLA A*0201 tetramer was added in each case at 25 µg/ml at 37°C for 15 minutes. Data were acquired using a FACSCantoII flow cytometer and analyzed with FlowJo software. Data is presented in the left column as percentage of maximal tetramer staining whereas data in the right column represents percentage of inhibition of tetramer staining.

5.2.4 CD8 antibodies efficiently block activation when the TCR/pMHCI affinity is weak

The results from my pMHCI tetramer blocking experiments suggest that blocking anti-CD8 antibodies can be used to preferentially target T-cells with weak affinity TCR/pMHCI interactions (Figure 5.3). This observation is important because it suggests that targeting CD8 could be a desirable strategy for blocking the activation of $CD8^+$ T-cells characterised by low affinity TCR/pMHCI interactions such as the autoreactive $CD8^+$ T-cell clone 1E6 which can directly target and kill islet β-cells. In order to test this hypothesis I decided to test the ability of DK25 to block 1E6 recognition of its cognate ligand **ALW**GPDPAAA (K_D ~278 μM) and an altered peptide ligand **YQF**GPDPAAA, identified in a previous study which is capable of binding to the 1E6 TCR with high affinity (K_D ~9 μM) (Table 5.2) (Wooldridge, Ekeruche-Makinde et al. 2012). This falls within the typical affinity range observed for pathogen specific TCR/pMHCI interactions (Table 5.1 & 5.2 & Appendix 3). This provides a monoclonal T cell system to examine the effect of DK25 on T-cell activation where the only parameter that is varied is the affinity of the TCR/pMHCI interaction.

In the absence of anti-CD8 antibody, the 1E6 $CD8^+$ T-cell clone can be seen to be killing targets presenting **ALW** and **YQF**, the level of killing is directly proportional to the binding affinity of the TCR/pMHCI interaction (Figure 5.4 A). However in the presence of anti-CD8 antibody DK25, at both concentrations tested the killing of targets presenting cognate **ALW** antigen as measured by chromium release is inhibited by 100% (Figure 5.4 B). At the higher concentration of DK25 used (1 μg/ml) some effect on the killing of targets presenting the high affinity ligand **YQF** was observed (Figure 5.4 C). However, no inhibition of **YQF** was observed when this concentration was lowered to 0.5 μg/ml. Therefore targeting CD8 can be

$CD8^+$ T-cell clone	1E6	
Epitope	ALWGPDPAAA	**YQF**GPDPAAA
TCR/pMHCI K_D μM	278	9[1]

Table 5.2: TCR/pMHCI binding affinities of different ligands recognized by the 1E6 $CD8^+$ T-cell clone. Summary of the TCR/pMHCI binding affinities of wild-type and enhanced peptide ligand specific for the 1E6 $CD8^+$ T-cell clones used. [1] See Appendix 3 for SPR Biophysical data.

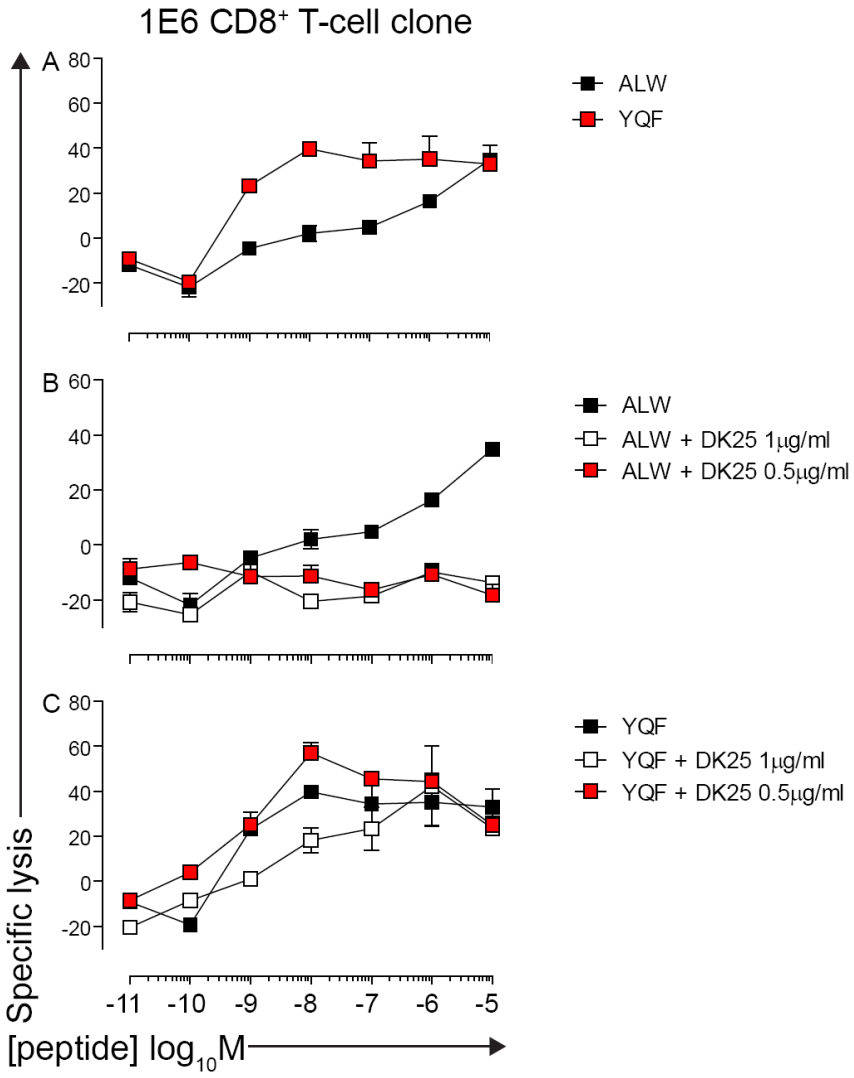

Figure 5.4: Targeting CD8 can be used to block autoreactive CD8$^+$ T-cell killing. 2x10^3 C1R A2 wt target cells were labelled with 30 µCi of ^{51}Cr (Perkin Elmer, Cambridge, UK) per 10^6 cells for 1 hour at 37°C. Targets were also cultured alone (target spontaneous release) and with TritonX-100 (Sigma-Aldrich) at a final concentration of 5% (target total release). Targets were pulsed with either (A&B) ALWGPDPAAA, or (A&C) YQFGPDPAAA for 1 hour at 37˚C. 1x10^4 HLA-A*0201-restricted 1E6 ALWGPDPAAA ($PPI_{15–24}$) CD8$^+$ T-cell clone were then plated out to a final volume of 60 µl R10 at an E:T ratio of 5:1 with or without purified anti-human CD8 antibody (DK25) @ 1 µg/ml and 0.5 µg/ml. Cells were incubated at 37˚C for 4 hours in a 5% CO_2 atmosphere. For each sample, 10 µl supernatant was harvested and mixed with 150 µl OptiPhase Supermix Scintillation Cocktail (Perkin Elmer). Plates were analyzed using a liquid scintillator and luminescence counter (MicroBeta TriLux; Perkin Elmer) with Microbeta Windows Workstation software (Perkin Elmer). Specific lysis was calculated according to the following formula: (experimental release - target spontaneous release/target total release - target spontaneous release) x 100. The mean ± SD of three replicate assays is shown.

used to inhibit 1E6 $CD8^+$ T-cell clone recognition of cognate antigen by 100% whilst retaining the ability to kill antigens characterised by higher affinity TCR/pMHCI interactions.

5.2.5 Blocking CD8 antibodies can be used to achieve complete inhibition of autoreactive $CD8^+$ T-cell activation whilst retaining anti-viral $CD8^+$ T-cell activation

I decided to examine the ability of the blocking anti-CD8 antibody (DK25) to inhibit activation of the autoreactive $CD8^+$ T-cell clone 1E6 compared to its ability to inhibit pathogen specific $CD8^+$ T-cell activation. Using the CD8 independent anti-viral ALF8 $CD8^+$ T-cell clone and the 'highly' CD8 dependent autoreactive 1E6 $CD8^+$ T-cell clone, a similar effect was seen to that of the tetramer binding. I observed 100% blockade of 1E6 T-cell activation when DK25 was used at a concentration of 1 μg/ml (Figure 5.5 A). In stark contrast, the same concentration of DK25 had a very minimal effect on activation of the relatively CD8 independent ALF8 $CD8^+$ T-cell clone (Figure 5.5 B). This highlighted a concentration of blocking anti-CD8 antibody where complete inhibition of autoreactive $CD8^+$ T-cells activation is observed whilst anti-viral $CD8^+$ T-cell activation remains intact.

Next, I decided to test the efficacy of DK25 on more $CD8^+$ T-cell clones including those that are restricted by different HLA class molecules. Here, I used the autoreactive $CD8^+$ T-cell clones 1E6 (HLA A2 restricted), 3F2 (HLA A2 restricted) and 4C6 (HLA A*2402 restricted) which have all been previously shown to kill pancreatic islet β-cells (Knight, Kronenberg et al. 2012; Skowera, Ellis et al. 2008). I also compared these autoreactive clones to the CD8 independent anti-viral $CD8^+$ T-cell clones ALF3 (HLA A2 restricted), NLV2 (HLA A2 restricted) and SBS1 (HLA B*3508 restricted). The result obtained was the same as the effect

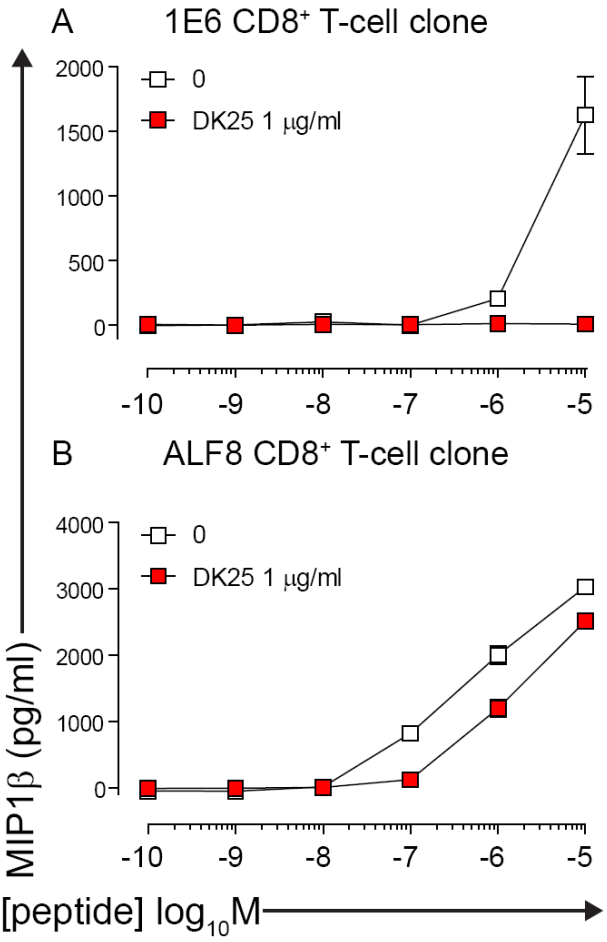

Figure 5.5: Titration of anti-CD8 antibody reveals concentration for optimal inhibition of autoreactive CD8$^+$ T-cell activation. (**A&B**) 6.0 x 10^4 HLA A2*0201 C1R with wild-type pMHCI/CD8 interaction where pre-incubated with titrated cognate peptides @ 10^{-5}M to 10^{-11}M (**A**) ALWGPDPAAA, (**B**) GILGFVFTL for 1 hour @ 37°C. Cells were then washed twice using 100 µl of PSG @ 561 x g for 5 minutes. 3 x 10^4 1E6 ALWGPDPAAA ($PPI_{15–24}$) CD8$^+$ T-cell clone or ALF8 GILGFVFTL ($MP1_{58-66}$) epitope which had been pre-incubated for 60 minutes @ 37°C with purified anti-human CD8 antibody (DK25) @ 1 µg/ml where then added to each sample and incubated for 4 hours @ 37°C. Supernatants were harvested and assayed for MIP-1β production by ELISA (RandD Medsystems) and performed according to the manufacturer's instructions. The mean ± SD of two replicate assays is shown.

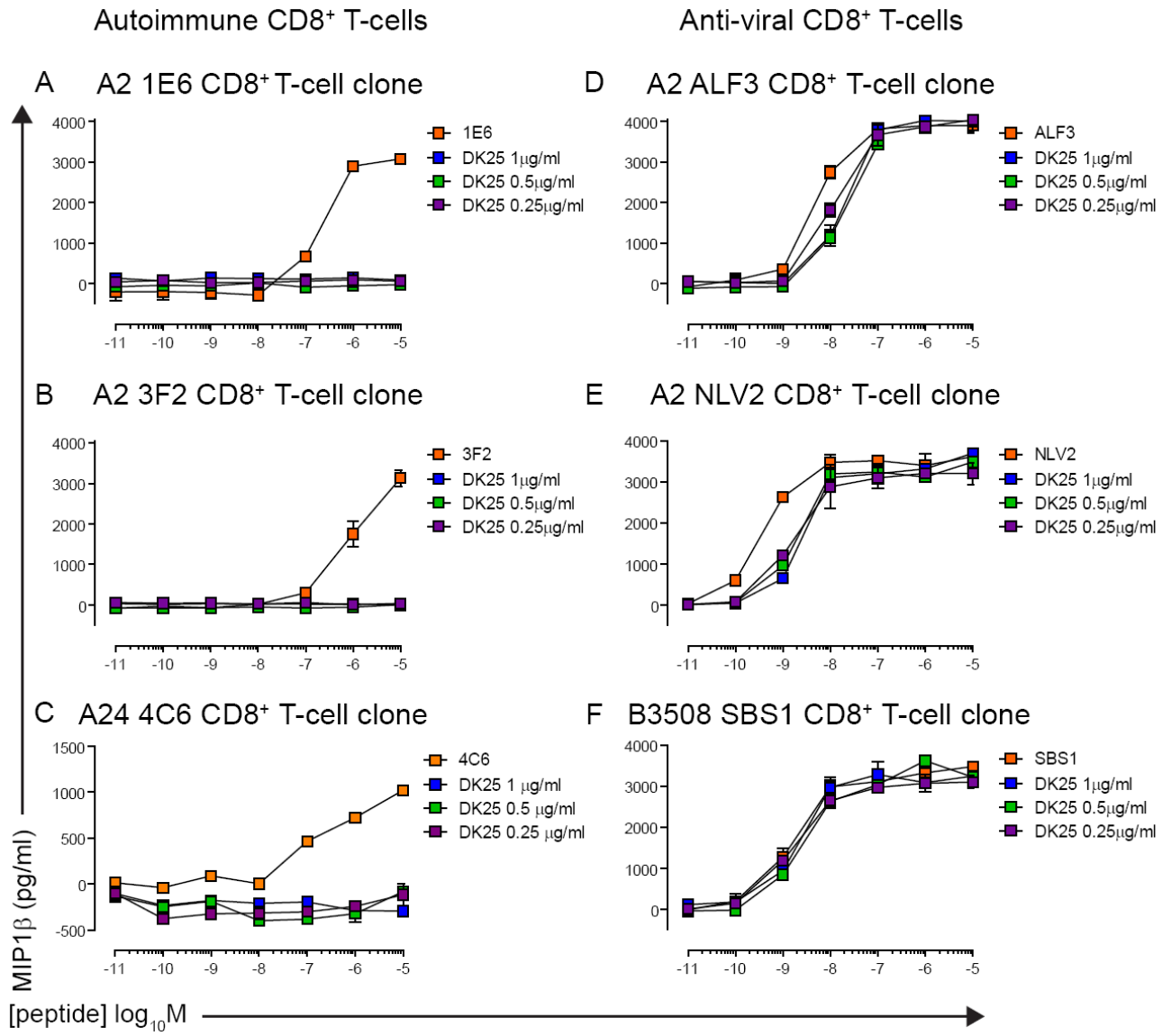

Figure 5.6: Titration of anti-CD8 antibody reveals concentration for optimal inhibition of autoreactive CD8$^+$ T-cell activation. 6.0 x 10^4 HLA A2*0201 C1R were pre-incubated with titrated cognate peptides @ 10^{-5}M to 10^{-11}M (**A**) ALWGPDPAAA, (**B**) ALWGPDPAAA, (**D**) GILGFVFTL, (**E**) NLVPMVATV or (**C**) A*2402 K562 with LWMRLLPLL or (**F**) HLA B*3508 C1R with LPEPLPQGQLTAY for 1 hour @ 37°C. Cells were then washed twice using 100 µl of PSG @ 1500 rpm for 5 minutes. 3 x 10^4 (**A**) 1E6 ($PPI_{15–24}$), (**B**) 3F2 ($PPI_{15–24}$), (**C**) 4C6 (PPI_{3-11}), (**D**) ALF3 ($M1_{58-66}$), (**E**) NLV2 (CMV-$pp65_{495-503}$), or (**F**) SBS1 (EBV-$BZLF1_{52-64}$) CD8$^+$ T-cell clone pre-incubated for 60 minutes @ 37°C with purified anti-human CD8 antibody (DK25) @ 1, 0.5 and 0.25 µg/ml where then added to each sample and incubated for 4 hours @ 37°C. Supernatants were harvested and assayed for MIP-1β production by ELISA (RandD Medsystems) and performed according to the manufacturer's instructions. The mean ± SD of two replicate assays is shown.

described above. Thus, regardless of the MHCI restriction $CD8^+$ T-cell clones with lower affinity TCR/pMHC interactions, as typified by autoimmune T-cells, are more CD8-dependent (Figure 5.6 A-C). In contrast, the DK25 antibody was seen to have minimal effect on the activation of all anti-viral $CD8^+$ T-cell clones tested regardless of the MHCI restriction (Figure 5.6 D-F).

5.3 Discussion

Over the last decade there has been a substantial amount of evidence accumulating in the literature to suggest that $CD8^+$ T-cells play a significant role in the pathogenesis of common autoimmune diseases such as T1D (Roep and Peakman 2011; Coppieters, Dotta et al. 2012), MS (Huseby, Huseby et al. 2012; Friese and Fugger 2009) and Psoriasis (Prinz 2003). Strategies that specifically target this important cell type are therefore highly desirable. However, it would be dangerous to use treatments that mediate a non-specific inhibition of $CD8^+$ T-cell activation because $CD8^+$ T-cells play an essential role in defending our bodies against pathogen attack. Therefore, strategies that specifically target autoreactive T-cells whilst leaving pathogen specific $CD8^+$ T-cells untouched could have a role in treating these diseases. It is emerging that autoreactive TCR/pMHCI interactions are characterised by low affinity compared to typical pathogen specific TCR/pMHCI interactions. Based on previous studies I predicted that this would make self reactive $CD8^+$ T-cells highly dependent on CD8 for activation. If autoreactive $CD8^+$ T-cells are characterized by high levels of CD8-dependency then CD8 would represent a desirable target to block unwanted autoreactive $CD8^+$ T-cell activation. I decided to conduct a study in order to test this hypothesis.

I examined how CD8-dependency is influenced by the strength of the TCR/pMHCI interaction. Previous data supports the theory that CD8-dependency is directly linked to the affinity of the TCR/pMHCI interaction where a weak TCR/pMHCI interaction is highly CD8 dependent and the reverse is also true (Holler, Lim et al. 2001; Holler and Kranz 2003; Laugel, van den Berg et al. 2007). A panel of four $CD8^+$ T-cell clones were shown to be either highly CD8 independent, ALF8 $CD8^+$ T-cell clone (Figure 5.1 A&B), moderately CD8 dependent, MEL5 $CD8^+$ T-cell clone and ILA1 $CD8^+$ T-cell clone (Figure 5.1 C-F), or highly CD8 dependent, 1E6 $CD8^+$ T-cell clone (Figure 5.1 G&H) for $CD8^+$ T-cell activation. The level of CD8 dependency by this panel of $CD8^+$ T-cell clones each with varying TCR/pMHCI affinities (Table 5.1) demonstrated a direct correlation between the TCR/pMHCI binding affinity and the requirement of CD8 for efficient $CD8^+$ T-cell activation.

One approach to target the CD8 co-receptor is the use of anti-CD8 antibodies. In a previous chapter (chapter 4), I characterized a panel of anti-CD8 antibodies which allowed me to select two antibodies with a blocking phenotype for further study. I examined the ability of these antibodies to disrupt TCR/pMHCI interactions at the cell surface. The effect of the blocking antibodies was shown to be most dramatic for the highly CD8-dependent 1E6 $CD8^+$ T-cell clone, a clinically relevant *in-vivo* T1D specific $CD8^+$ T-cell clone, where tetramer staining could be inhibited by >95% (Figure 5.2 D & 5.3 G&H). Overall, targeting CD8 is a very efficient way of blocking pMHCI staining to the cell surface when the TCR/pMHCI interaction is extremely weak, with little or no effect observed with higher affinity TCR/pMHCI interactions typical of pathogen specific $CD8^+$ T-cells.

To examine the effect of the blocking antibody in directly inhibiting epitope specific killing by the 1E6 $CD8^+$ T-cell clone, killing assays were performed using targets bearing the cognate ligand (**ALW**GPDPAAA) and high affinity ligand (**YQF**GPDPAAA) representative of antigens that $CD8^+$ T-cells may be exposed to in the periphery (Figure 5.4 A-C) (Table 5.2). As expected the levels of killing observed correlated with the TCR/pMHCI affinity of the ligand tested (Figure 5.4 A). Killing on recognition of cognate ligand was inhibited in the presence of anti-CD8 antibody, whereas no effect was observed on the recognition of the high affinity ligand (Figure 5.4 B&C). In addition, the same concentration of antibody had a very minimal effect on the inhibition of the anti-viral ALF8 $CD8^+$ T-cell clone rendering these pathogen specific $CD8^+$ T-cells intact (Figure 5.5 B). Further investigation demonstrated that all autoimmune $CD8^+$ T-cells tested within this study, 1E6, 3F2 and 4C6, restricted by different HLA class molecules, can be completely blocked using anti-CD8 antibodies (Figure 5.6 A-C). Simultaneously, a very minimal effect and in one case no blocking effect was seen on all anti-viral $CD8^+$ T-cell clones tested (Figure 5.6 D-F). This data supports the theory that targeting CD8 has the strong potential to inhibit autoreactive $CD8^+$ T-cell activation and killing whilst ensuring that pathogen specific $CD8^+$ T-cells can remain able to identify and kill their targets.

There have been many studies highlighting the potential use of antibodies in autoreactive settings however none have examined the potential of anti-CD8 antibody mediated blockade. There has been extensive data highlighting the use of anti-CD3 antibodies in the study of T1D. Interestingly anti-CD3 antibodies have been shown to reverse diabetes onset in Non-obese diabetic (NOD) mice which was the initial basis for the use of this antibody in human clinical trials (Chatenoud, Thervet et al. 1994; Herold, Hagopian et al. 2002; Keymeulen,

Vandemeulebroucke et al. 2005). Indeed in human studies the use of anti-CD3 antibodies have been shown to preserve islet β cell function by up to two years and can increase insulin production (Herold, Gitelman et al. 2009). The mechanism by which the anti-CD3 antibodies is thought to be having its effect has been shown to be as a result of an induction of regulatory T cells, which may play a key role in maintaining tolerance and has been reported to be TGFβ-dependent (Cobbold, Castejon et al. 2004; You, Leforban et al. 2007). However data does suggest that the anti-CD3 antibody, despite undergoing Fc modification results in side effects relating to cytokine release and a transient EBV viral reactivation (Keymeulen, Vandemeulebroucke et al. 2005; Chatenoud and Bluestone 2007). Interestingly none of the anti-CD8 antibodies tested in chapter 4 induced any cytokine release which may make them desirable.

Previous studies have also examined the use of both anti-CD4 and anti-CD8 antibodies in therapeutic design for T1D. These studies have pointed to the use of these antibodies to induce tolerance and halt diabetes onset (Phillips, Parish et al. 2009; Yi, Diz et al. 2012). Similarly to the use of anti-CD3 antibodies, non-depleting anti-CD4 antibodies have been shown to induce regulatory T-cells. Whereas the tolerance which is induced by the use of non-depleting anti-CD8 antibodies is dependent on IL-10 (Parish, Bowie et al. 1998; Parish and Cooke 2005; Phillips, Parish et al. 2009). In contrast to previous studies which have alluded to a role for anti-CD8 antibodies in the induction of tolerance, it is important to note that the study described in this chapter is aimed at examining the ability of anti-CD8 antibodies to preferentially block autoreactive $CD8^+$ T-cell activation which could be a more targeted means of controlling disease symptoms.

There are currently treatments that are available and approved for the treatment of autoimmune and inflammatory diseases, or those in the later stages of development. These agents usually rely on the induction of profound and/or long-lasting immunosuppression and their effect can be achieved by global depletion of entire cell types or lineages in the periphery. These agents can also induce immunosuppression by preventing peripheral leukocyte trafficking and transport in and out of lymphoid organs and also target the systemic activity of cytokines involved in disease pathogenesis (Dinarello 2010; Rammohan and Shoemaker 2010; Steward-Tharp, Song et al. 2010). These drugs have been shown to possess good efficacy, however the side effects can be quite adverse. Anti-CD3 treatment in T1D is an example where the side effects of the drug could potentially outweigh the benefits of the drug where severe reactivation of latent viral infections would be clinically deleterious.

The data provided here has highlighted that targeting CD8 can preferentially inhibit pathogenic $CD8^+$ T-cell responses directed against clinically relevant autoreactive self-determinants and leave cellular immunity to anti-viral and microbial pathogens largely intact. This could also be explored further using agents that target the CD8 binding site on MHCI such as soluble versions of the inhibitory Immunoglobulin like transcript (ILT2) receptor. High affinity forms of the soluble ILT2 receptor have been manufactured by phage display and have been shown to interact with MHCI with extremely high affinities at nanomolar levels and have been shown to inhibit $CD8^+$ T-cell activation (Moysey, Li et al. 2010). It would be of interest to study the effect that this molecule has in the context of both autoreactive and anti-viral $CD8^+$ T-cells used in this study as this may overcome any issues of having to generate an antibody molecule for use *in-vivo* (Moysey, Li et al. 2010). To fully examine this strategy of using engineered molecules as previously described, the effect these

molecules pose on cancer immune-surveillance, thymic selection and also on naive T-cells in the periphery would have to be fully examined.

It would also be useful to study the effect of anti-CD8 antibodies in the NOD mouse system examining the effect of both blocking and enhancing phenotypes of anti-CD8 antibodies *in-vivo*. Interestingly, the distinct epitope required for binding for anti-CD8 antibodies may potentially underlie future directed therapy targets. Blocking antibodies appear to bind to a site which is distant and distinct from the activatory antibody binding site in both the murine and human systems (Figure 4.15) (Sanders, Fox et al. 1991, Devine, Hodsdon et al. 2004). Further studies of both epitope regions may allow for design of therapies aimed at either enhancing or inhibiting $CD8^+$ T-cell function and may uncover further heterogeneity of these regions, similarly to those seen in the murine system (chapter 4).

In summary, I have shown that: (i) as the TCR/pMHCI affinity increases, the level of CD8 dependency exhibited by the $CD8^+$ T-cell clone decreases; (ii) anti-CD8 antibodies can be used to block the binding of cognate tetramer to $CD8^+$ T-cells and the inhibition is more dramatic when the $CD8^+$ T-cell clone becomes increasingly CD8 dependent; (iii) inhibition of tetramer staining using anti-CD8 antibodies can be titrated to low levels ensuring highly CD8 dependent $CD8^+$ T-cells are inhibited whilst highly CD8 independent $CD8^+$ T-cells are not impaired; and, (iv) an optimal concentration of blocking anti-CD8 antibody can completely inhibit the activation and epitope specific killing of the highly CD8-dependent 1E6 $CD8^+$ T-cell clone, an autoreactive T1D specific $CD8^+$ T-cell. This concentration of antibody was shown to have a no effect on highly CD8-independent pathogen specific $CD8^+$ T-cell clones.

My results show that CD8-blockade can specifically inhibit activation of autoimmune $CD8^+$ T-cells. This approach therefore warrants further investigation as a potential therapeutic tool.

6

CD8 CAN RE-ARRANGE THE RELATIVE POTENCIES OF EACH POTENTIAL TCR AGONIST: IDENTIFICATION OF A NOVEL CD8 FOCUSSING MECHANISM

(Clement et al., manuscript in preparation)

6.1 Introduction

6.1.1 CD8 focussing: a novel role for CD8 in T-cell activation?

Previous results chapters have underlined the potent ability of CD8 to modulate the antigen specific $CD8^+$ T-cell response, especially chapter 3 where a super-enhanced interaction with CD8 was shown to result in non-specific activation. Multiple roles for CD8 in $CD8^+$ T-cell activation have been demonstrated. CD8 has been shown to modify the affinity of the TCR/pMHCI interaction, in addition to modulating the triggering threshold of the TCR (Gakamsky, Luescher et al. 2005). A previous mathematical analysis of these modulatory effects predicted that CD8 could alter the functional avidity of a $CD8^+$ T-cell for its agonists and act to re-arrange the relative potencies of each of its potential agonists (van den Berg, Wooldridge et al. 2007). If true then this would allow $CD8^+$ T-cells to increase their functional sensitivity for one agonist, while decreasing their functional sensitivity for other potential agonists. This potential "focussing mechanism" could be extremely important because it would allow each $CD8^+$ T-cell to centre recognition on a particular subset of potential agonist ligands.

6.1.2 $CD8^+$ T-cells are inherently crossreactive

Early studies suggested that individual TCRs only recognize a single pMHCI. However, studies published in the 1990s demonstrated that T-cells can recognize several peptides (Wraith, Bruun et al. 1992; Bhardwaj, Kumar et al. 1993; Reay, Kantor et al. 1994; Evavold, Sloan-Lancaster et al. 1995; Wucherpfennig and Strominger 1995; Hemmer, Fleckenstein et al. 1997; Kersh, Shaw et al. 1998). Since then, observations of TCR degeneracy have continued to accumulate in the literature (Hausmann, Martin et al. 1999; Kissler, Anderton et

al. 2002; Crawford, Huseby et al. 2004; Lee, Stewart-Jones et al. 2004; Nino-Vasquez, Allicotti et al. 2004; Kan-Mitchell, Bajcz et al. 2006; Dai, Huseby et al. 2008; Ishizuka, Grebe et al. 2009). The majority of previous studies of TCR degeneracy utilized small peptide sets (2-200) or estimates based on peptide library screening where it is necessary to make assumptions about individual peptide concentrations. A recent study examined ~4000 peptides, although this number still only represents an extremely small portion of the entire peptide universe. Despite the caveats of previous studies, two independent studies suggested that individual MHCII-restricted TCRs can recognize ~10^6 peptides (Hiemstra, van Veelen et al. 1999; Maynard, Petersson et al. 2005). Wilson *et al* suggested that MHCI-restricted TCRs might exhibit lower levels of degeneracy (Wilson, Wilson et al. 2004), although, no attempt had been made to quantify this. In an attempt to rectify this, a recent study performed a comprehensive analysis and demonstrated that a single autoimmune TCR (1E6) can recognize over one million different peptide sequences in the context of a single MHCI (Wooldridge, Ekeruche-Makinde et al. 2012). Recent data from the laboratory suggests that not all MHCI-restricted TCRs recognize one million peptides but for most the number is still quite large. This remarkable promiscuity explains how a limited TCR repertoire (~25 million) can recognize the multitude of peptides that can be presented by MHCI (~$8x10^{14}$) and is therefore essential for the provision of effective $CD8^+$ T-cell immunity.

6.1.3 CD8 controls levels of T-cell crossreactivity

Recent data suggests that $CD8^+$ T-cell crossreactivity is controlled by CD8. Data by Wooldridge *et al* showed that CD8 extends the range of pMHCI ligands that can be seen by an individual cell surface bound TCR, thereby ensuring that the peripheral $CD8^+$ T-cell repertoire is optimally poised to negotiate the competing demands of responsiveness in the

face of danger and quiescence in the presence of self (Wooldridge, Laugel et al. 2010). The authors used combinatorial peptide library (CPL) screens to assess the levels of crossreactivity exhibited by a $CD8^+$ T-cell. In the absence of a pMHCI/CD8 interaction, the level of $CD8^+$ T-cell activation by the CPL screens was very minimal. However, on increasing the strength of the pMHCI/CD8 interaction, the range of ligands (i.e. number of peptides) recognized by an individual TCR was increased. In addition, increasing the strength of the pMHCI/CD8 interaction resulted in a change in the pattern of the ligands recognised by an individual TCR (Wooldridge, Laugel et al. 2010). This data suggests that CD8 is exerting a focussing effect and I intend to examine this effect in more detail during this chapter.

6.1.4 Summary and Aims

TCRs are inherently degenerate recognizing a large number of different peptides. Mathematical analysis suggests that CD8 is a key regulator of TCR degeneracy allowing a single T-cell to focus on different ligands by adjusting its fine sensitivity to potential agonists. This would manifest in the ability of CD8 to re-arrange the relative potencies of each of its potential agonists (van den Berg, Wooldridge et al. 2007). I intend to test whether such a mechanism exists, using multiple $CD8^+$ T-cell clones and multiple altered peptide ligands (APLs). I will examine how the strength of the pMHCI/CD8 interaction influences the potency of multiple ligands in three different monoclonal systems.

6.2 Results

6.2.1 MHCI mutations that alter the strength of the pMHCI/CD8 interaction

To study the effect of varying the strength of the pMHCI/CD8 interaction at the cell surface on the potency of multiple ligands for an individual TCR, I used a panel of C1R B-cell lines stably transfected with mutant MHCI. Each C1R had been previously transfected with MHCI molecules that bear mutations in the CD8 binding domain which either abrogate (HLA A2 227/8KA), retain wild-type properties (HLA A2) (Purbhoo, Boulter et al. 2001), increase CD8 binding (HLA A2 Q115E) (Wooldridge, Lissina et al. 2007) or greatly increase CD8 binding (HLA A2 K^b) (Wooldridge, Clement et al. 2010) (Figure 6.1). A previous study used SPR to demonstrate that these mutations do not affect the strength of the TCR/pMHCI interaction (Wooldridge, van den Berg et al. 2005).

6.2.2 Examining the effect that pMHCI/CD8 affinity exerts on functional sensitivity of the TCR/pMHCI interaction

In order to perform a comprehensive study to examine the effect that the strength of the pMHCI/CD8 interaction exerts on the functional sensitivity of the TCR/pMHCI interaction, I decided to examine three different $CD8^+$ T-cell clones: ILA1, MEL5 and 1E6. For each of these TCR clonotypes, I selected a panel of peptide ligands which included superagonists, cognate ligands and weak agonists for all three monoclonal $CD8^+$ T-cell systems (Table 6.1). The majority of these agonists were designed using combinatorial peptide library technology (Ekeruche-Makinde, Clement et al. 2012). TCR/pMHCI biophysical data was already available for some of the peptide ligands and I performed surface plasmon resonance to measure the strength of some of the other TCR/pMHCI interactions. It was not possible to

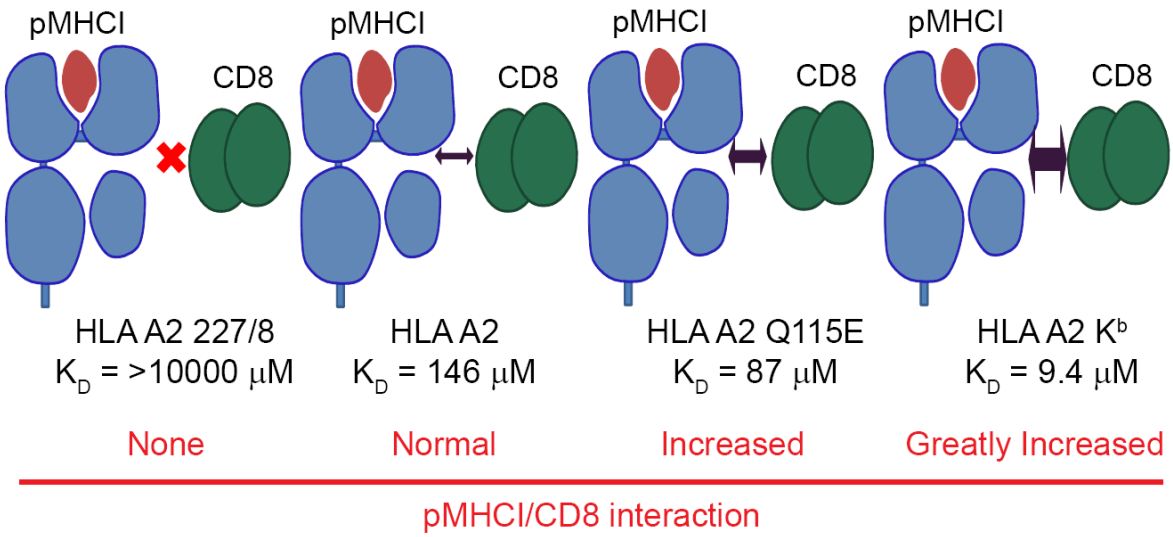

Figure 6.1: Mutant MHCI stably transfected into C1R B-cells can be used to alter the strength of the pMHCI/CD8 interaction without any affect on TCR/pMHCI binding. SPR was used to measure the strength of the pMHCI/CD8 interaction following mutation of the CD8 binding site. MHCI mutants were then stably transfected into C1R-B-cells using a pcDNA3.1 vector

Name	MHCI restriction	Epitope	K_D (μM)
ILA1	HLA*A0201	ILAKFLHWL	36[1]
ILA1	HLA*A0201	ILAK**Y**LHWL	242[1]
ILA1	HLA*A0201	IL**G**KFLH**R**L	16.5 ± 2.5[6]
ILA1	HLA*A0201	IL**G**KFLHWL	3.7[1]
MEL5	HLA*A0201	ELAGIGILTV	17 ± 1[1]
MEL5	HLA*A0201	EL**T**GIGILTV	82 ± 4[2]
MEL5	HLA*A0201	**FAT**GIGI**I**TV	3 ± 1[3]
MEL5	HLA*A0201	**I**LAGIGILTV	nm
1E6	HLA*A0201	ALWGPDPAAA	278[4]
1E6	HLA*A0201	A**Q**WGPD**F**AA**V**	nm[1]
1E6	HLA*A0201	**WQYW**PD**SMS**A	nm[1]
1E6	HLA*A0201	**RQ**WGPDPAA**V**	14[5]
1E6	HLA*A0201	**YQF**GPD**FPI**A	9[6]

Table 6.1: Biophysical measurements of multiple different TCR/pMHCI interactions in three different monoclonal $CD8^+$ T-cell systems. Superagonists are shown in red, cognate ligands in black and weak agonists in green. 1 - (Laugel, van den Berg et al. 2007), 2 - (Clement, Ladell et al. 2011), 3 - (Ekeruche-Makinde, Clement et al. 2012), 4 - (Bulek, Cole et al. 2012), 5 - (Knight, Kronenberg et al. 2012), 6 – see Appendix 4, nm = not measured, nm[1] = non-measurable

obtain biophysical data for the weak agonists in the 1E6 system because their affinity for the TCR is below the level that can be measured by SPR.

I examined the recognition of all peptides in the context of an abrogated, wild type, slightly enhanced and greatly enhanced pMHCI/CD8 interaction by ILA1 (Figure 6.2), MEL5 (Figure 6.3) and 1E6 (Figure 6.4). Activation was measured by both IFN-γ and MIP-1β ELISA. Dose response curves were fitted (with the assistance of Dr Hugo van den Berg, Warwick University) to all peptide titration results and pEC50s calculated. The data was then used to examine the way in which the pMHCI/CD8 interaction modulates the TCR/pMHCI interaction for multiple agonists.

6.2.3 Differential modulation of TCR/pMHCI functional sensitivity by CD8

Using the curves fitted in Figures 6.2, 6.3 and 6.4, it was possible to calculate the $p\mathrm{EC}_{50}$ for all ligands examined. $p\mathrm{EC}_{50}$ is defined as minus 1 x the base 10 logarithm (*p*) of the 50% efficacy concentration (EC50). Therefore a greater functional sensitivity is indicated by a larger *p*EC50 value. Abrogating the pMHCI/CD8 interaction had a significant impact on the recognition of all peptide ligands in all three monoclonal $CD8^+$ T-cell systems (ILA1, MEL5 and 1E6). This is consistent with a previous study which showed that CD8 has a major impact on the number of peptide ligands that can be recognized by the TCR (Wooldridge, Laugel et al. 2010). When the strength of the pMHCI/CD8 interaction is increased then two different effects could be observed. In general, for weak agonists, increasing the strength of the pMHCI/CD8 interaction resulted in a steady improvement in functional sensitivity (monotone) (Figure 6.5).

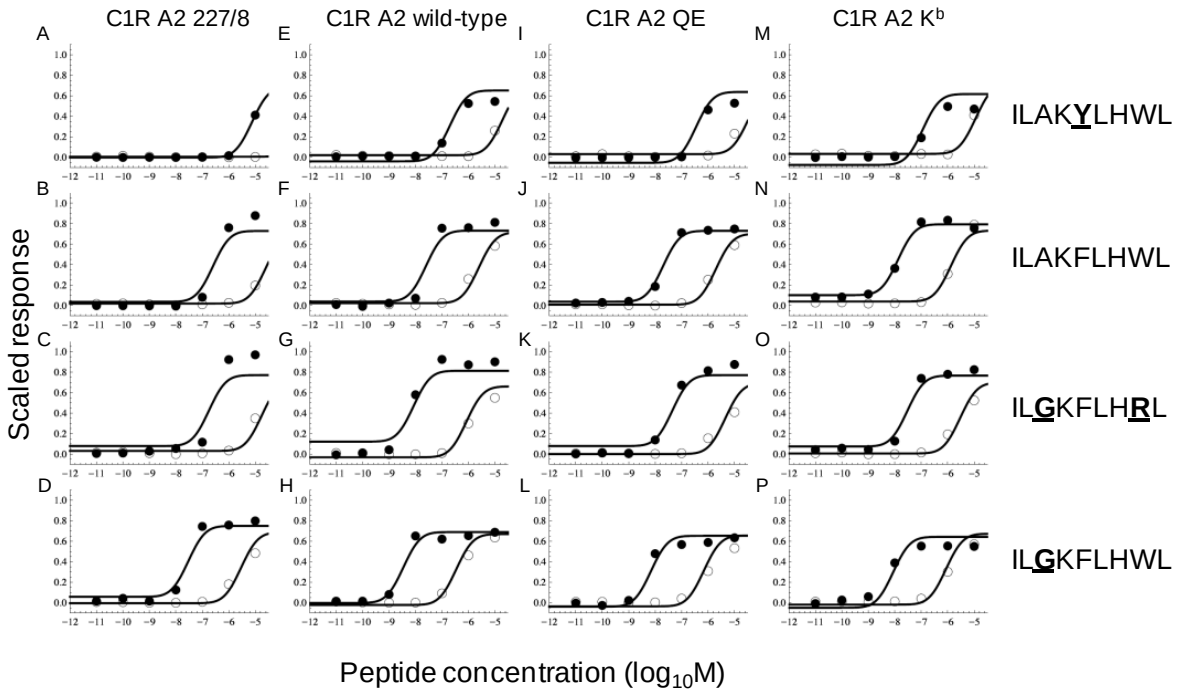

Figure 6.2: The influence that CD8 exerts on recognition of multiple ligands. (**A-P**) 6 x 10^4 HLA A2 C1R with varying pMHCI/CD8 interactions were pre-incubated with titrated APL peptides @ 10^{-5}M to 10^{-12}M ILAKFLWHWL, ILAKY**L**WHWL, IL**G**KLFW**R**WL and IL**G**KFLWHWL for 1 hour @ 37°C. Excess peptide was removed by washing twice with PSG. 3 x 10^4 ILA1 (hTERT) (residues 540-548) $CD8^+$ T-cell clone where then added to each sample and incubated for 4 hours @ 37°C. Supernatants were harvested and assayed for MIP-1β and IFN-γ production by ELISA (RandD Medsystems) and performed according to the manufacturer's instructions. Data is displayed as scaled dose response curves, ●: read-out is MIP-1β; ○: read-out is IFN-γ. Assays were performed in duplicate.

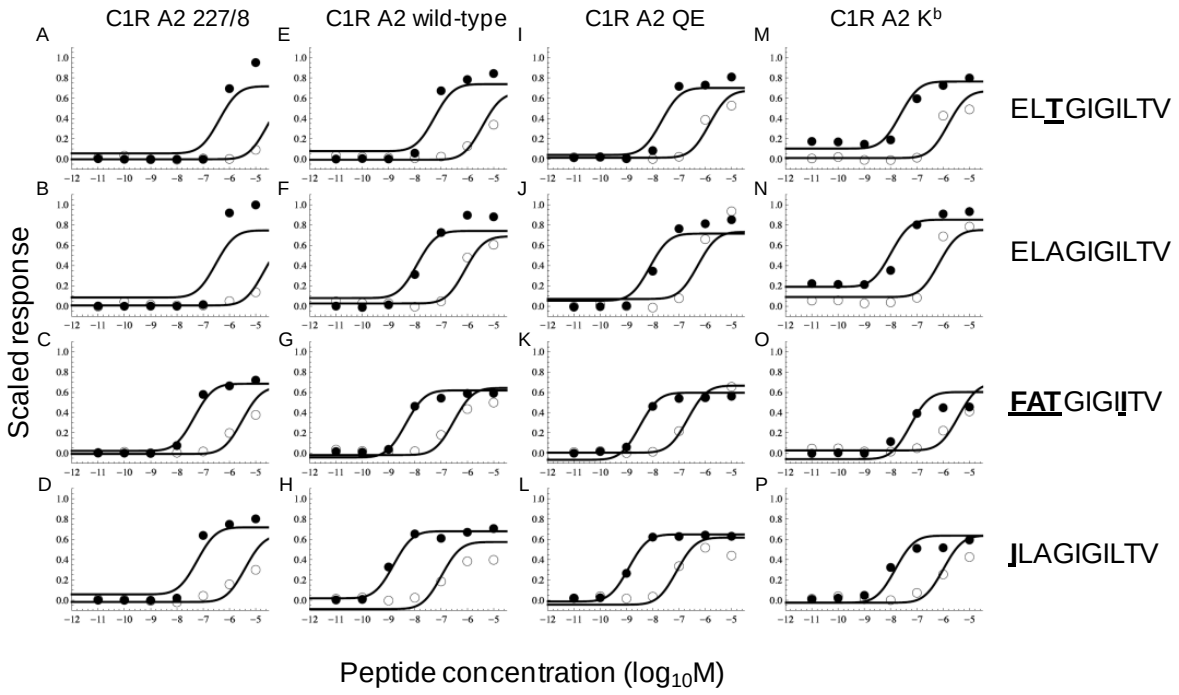

Figure 6.3: The influence that CD8 exerts on recognition of multiple ligands. (**A-P**) 6 x 10^4 HLA A2 C1R with varying pMHCI/CD8 interactions were pre-incubated with titrated APL peptides @ 10^{-5}M to 10^{-12}M ELAGIGILTV, EL**T**GIGILTV, **FAT**GIGI**I**TV and **I**LAGIGILTV for 1 hour @ 37°C. Excess peptide was removed by washing twice with PSG. 3 x 10^4 MEL5 (Melan-A-residues 26-35) $CD8^+$ T-cell clone where then added to each sample and incubated for 4 hours @ 37°C. Supernatants were harvested and assayed for MIP-1β and IFN-γ production by ELISA (RandD Medsystems) and performed according to the manufacturer's instructions. Data is displayed as scaled dose response curves, ●: read-out is MIP-1β; ○: read-out is IFN-γ. Assays were performed in duplicate.

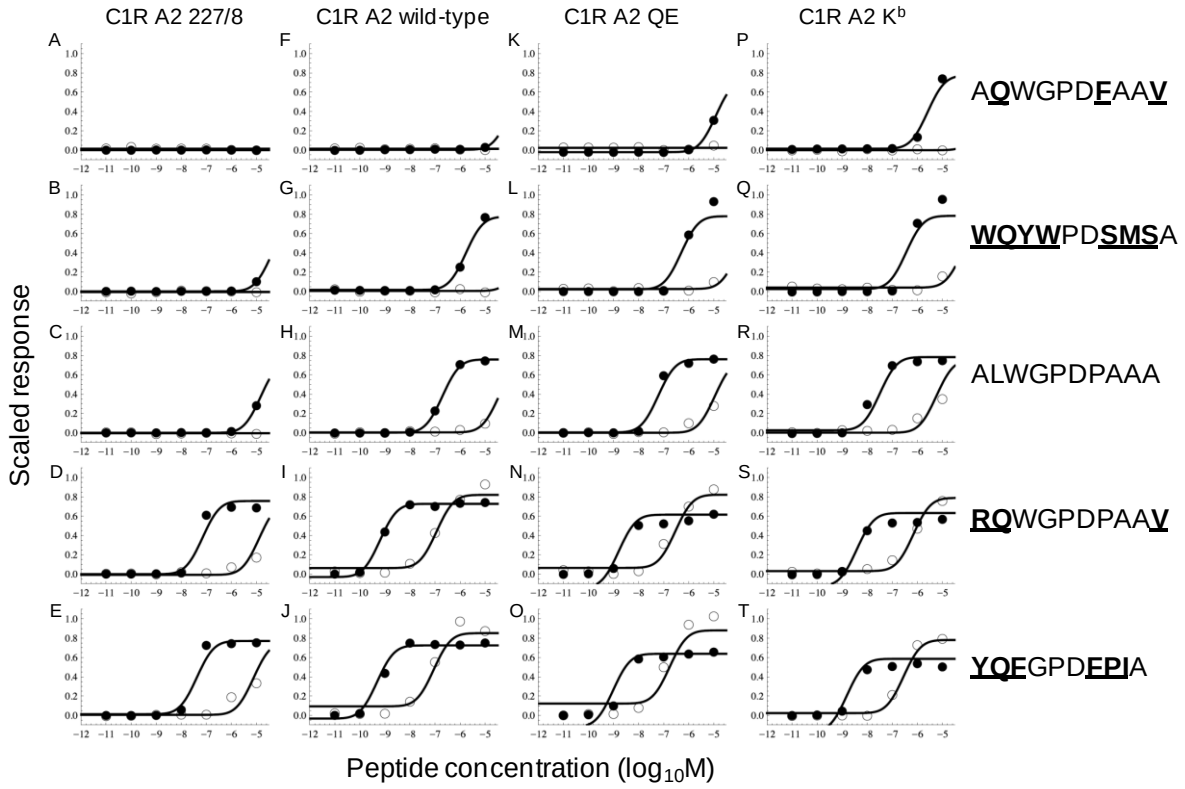

Figure 6.4: The influence that CD8 exerts on recognition of multiple ligands. (**A**-**T**) 6 x 10^4 HLA A2 C1R with varying pMHCI/CD8 interactions were pre-incubated with titrated APL peptides @ 10^{-5}M to 10^{-12}M ALWGPDPAAA, A**Q**WGPD**F**AA**V**, **WQY**WPD**SMS**A, **RQ**WGPDPAA**V**, **YQF**GPD**FPI**A for 1 hour @ 37°C. Excess peptide was removed by washing twice with PSG. 3 x 10^4 1E6 ($PPI_{15–24}$) $CD8^+$ T-cell clone where then added to each sample and incubated for 4 hours @ 37°C. Supernatants were harvested and assayed for MIP-1β and IFN-γ production by ELISA (RandD Medsystems) and performed according to the manufacturer's instructions. Data is displayed as scaled dose response curves, ●: read-out is MIP-1β; ○: read-out is IFN-γ. Assays were performed in duplicate.

In contrast, for superagonists, increasing the strength of the pMHCI/CD8 interaction resulted in an increase followed by a decrease in functional sensitivity (non-monotone) (Figure 6.5). These trends indicate that the relative distances between the pEC_{50} values for the various ligands to a given $CD8^+$ T-cell clone can be modulated through CD8 (Figure 6.6). This was particularly pronounced in the MEL5 system where CD8 was able to mediate a complete change in the order of ligand potency. In the context of a wild-type pMHCI/CD8 interaction, the order of ligand potency was **I**LAGIGILTV > **FAT**GIGI**I**TV > ELAGIGILTV > EL**T**GIGILTV (Figure 6.5). However, in the context of a super-enhanced interaction with CD8 the order of ligand potency was ELAGIGILTV > **I**LAGIGILTV > EL**T**GIGILTV > **FAT**GIGI**I**TV, which is entirely different (Figure 6.5). The data indicate that CD8 has a differential effect on the recognition of peptide ligands and is capable of re-arranging the relative potencies of each potential agonist.

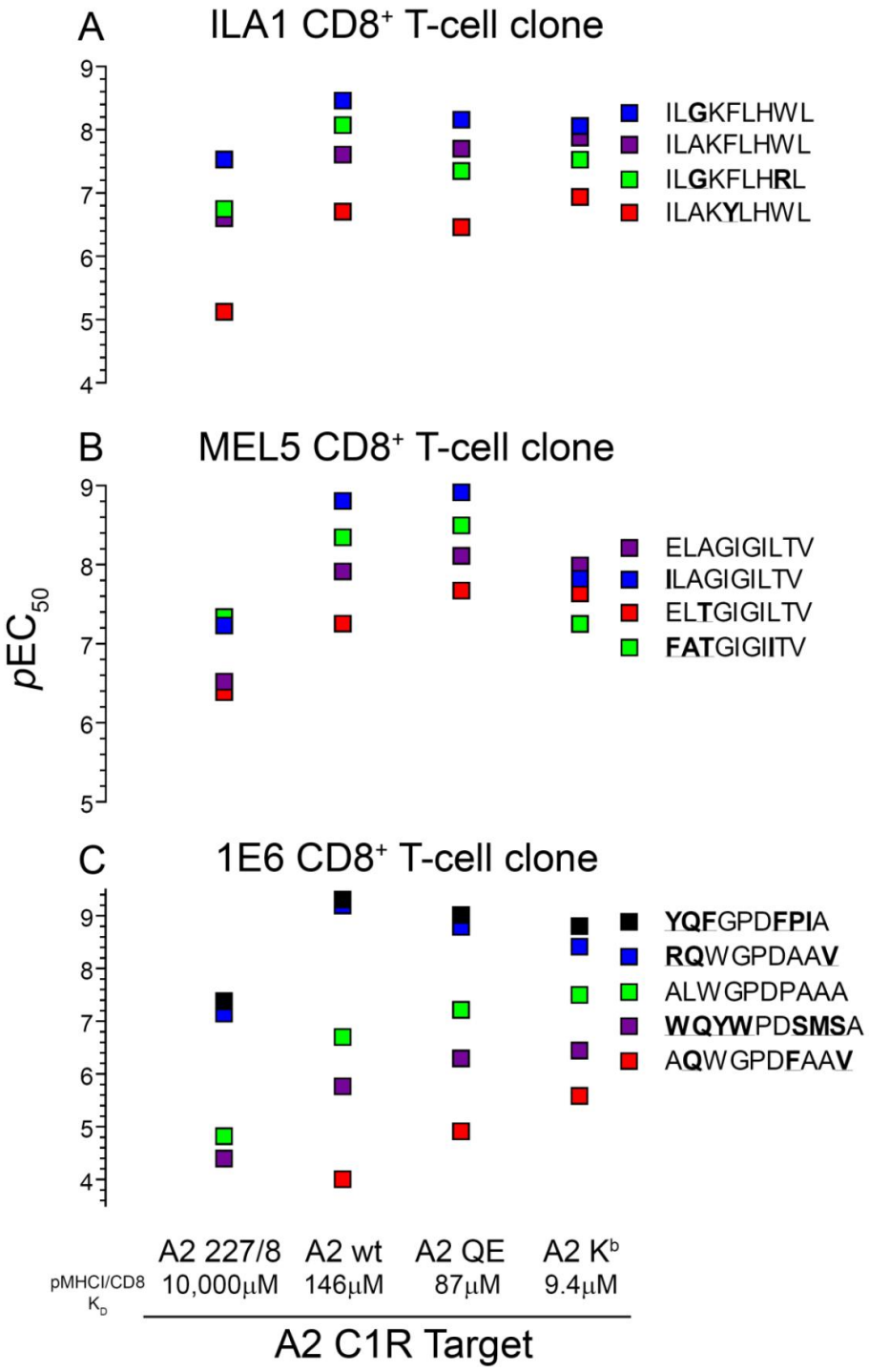

Figure 6.5: Differential modulation of TCR/pMHCI functional sensitivity by CD8. (**A-C**) Using data generated from Figures 6.2, 6.3 & 6.4, pEC50 values of each ligand used in (**A**) ILA1, (**B**) MEL5 and (**C**) 1E6 CD8+ T-cell clone were plotted against each stably transfected C1R A2 B-cells each with varying pMHCI/CD8 affinities.

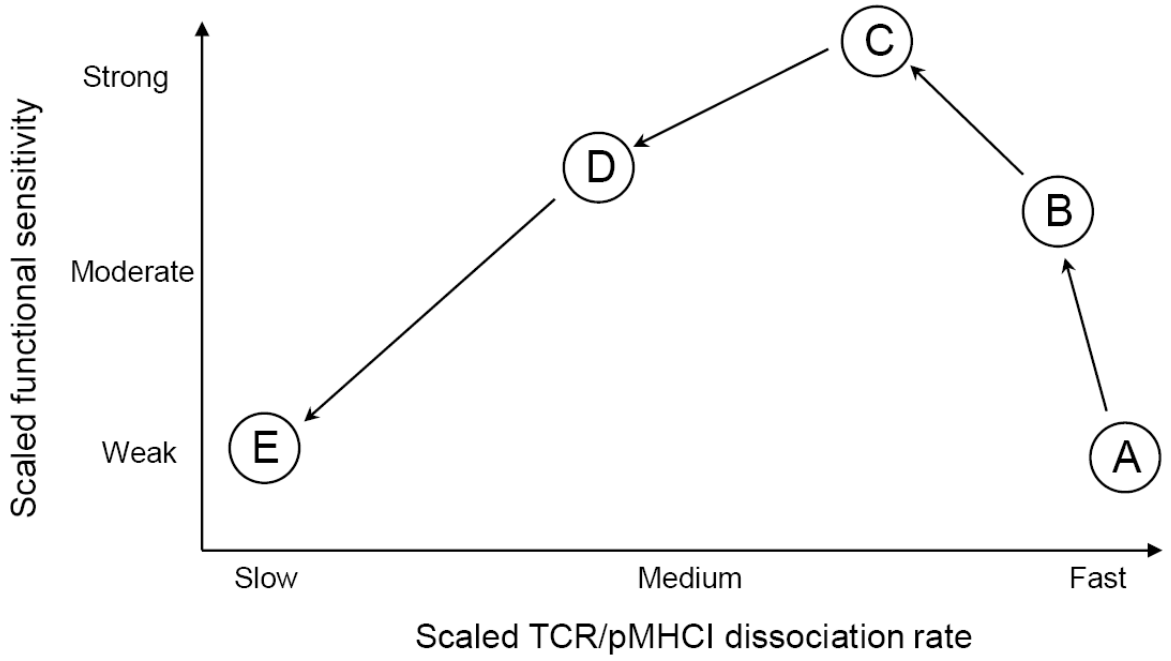

Figure 6.6: Curve representing the dependence of functional sensitivity on the TCR/pMHCI off-rate. The stabilising effect of the pMHCI/CD8 interaction may render a weak agonist (A) into a suboptimal (B) or even optimal agonist (C). A suboptimal agonist (B) may become optimal (C) and subsequently suboptimal again (D) as the strength of the pMHCI/CD8 interaction further increases. A ligand that is already optimal in the absence of the pMHCI/CD8 interaction (C) may become suboptimal (D) or weaker (E).

6.3 Discussion

$CD8^+$ T-cells are inherently crossreactive recognizing a large range of different peptide ligands. It is well established that CD8 can enhance the sensitivity of antigen recognition by a range of different mechanisms and it is assumed that CD8 would enhance the recognition of all potential ligands for an individual TCR to the same extent. However a recent mathematical analysis predicted that CD8 may exert a differential effect on the functional sensitivity of individual ligands. This is expected to manifest as a "focussing effect" whereby CD8 could act to re-arrange the relative potencies of the ligands recognized by an individual TCR. In this chapter I examined the effect that altering the strength of the pMHCI/CD8 interaction exerts on the recognition of multiple ligands in three different monoclonal $CD8^+$ T-cell systems. I demonstrated that in all three systems, CD8 acts to differentially modulate the functional sensitivity of the TCR/pMHCI interaction. The data presented here highlights a novel role for CD8 in T-cell activation.

My findings suggest that although the TCR can recognize multiple different ligands, CD8 acts to focus the TCR onto a range of ligands which might be an important mechanism for avoiding autoreactivity. This focus is likely to be dynamic i.e. CD8 can alter the range of ligands that are seen at high functional sensitivity at any one time. Understanding this could be useful therapeutically in order to refocus the $CD8^+$ T-cell response away from targeting self pMHCI. Here I have only examined the effect of increasing the strength of the pMHCI/CD8 interaction but other mechanisms, such as alterations in the expression level of CD8 at the cell surface, may have a similar effect. This CD8 focussing effect may control and optimize the degree of crossreactivity and antigen sensitivity of $CD8^+$ T-cells at various stages of T-cell development. Mechanisms that regulate CD8, both during thymic education

and in the periphery, include transcriptional inhibition of CD8 expression in double-positive thymocytes (Bosselut, Guinter et al. 2003), selective co-receptor internalization following antigenic stimulation (Maile, Siler et al. 2005), switching to the expression of the CD8aa isoform (reviewed in (Gangadharan and Cheroutre 2004)), changes in the pattern of glycosylation (Daniels, Devine et al. 2001; Moody, Chui et al. 2001; Daniels, Hogquist et al. 2002), and cytokine signals that transcriptionally tailor CD8 co-receptor expression (Park, Adoro et al. 2007). It is likely that these mechanisms work together to fine-tune the degree of functional crossreactivity at particular stages of development, facilitating selection of the TCR repertoire in the thymus while restraining deleterious activation in the periphery.

In addition, I observed that CD8 can limit the functional sensitivity of the TCR/pMHCI interaction, i.e. CD8 can control the kinetic window of TCR/pMHCI activation where optimal ligands can become sub-optimal ligands. When the pMHCI/CD8 interaction is greatly increased in conjunction with strong TCR/pMHCI agonists, $CD8^+$ T-cell activation decreases (Figures 6.2, 6.3 and 6.4). This decrease in $CD8^+$ T-cell activation is only observed when both the pMHCI/CD8 and TCR/pMHCI interactions are increased above wild-type levels. This suggests that CD8 can limit the kinetic window of T-cell activation which may be important in preventing unwanted T-cell activation. This effect was seen in all $CD8^+$ T-cell systems restricted by different epitopes (Figure 6.5).

The precise mechanism to explain how CD8 focussing is controlling $CD8^+$ T-cell sensitivity is unknown. Interestingly, increasing the pMHCI/CD8 interaction by >10 fold has been previously shown to maximally stabilise the TCR/pMHCI interaction (Wooldridge, van den Berg et al. 2005) This >10 fold increase may interfere with the rapid TCR/pMHCI

dissociation required to allow serial engagement of the TCR, which is thought to be critical for $CD8^+$ T-cell activation (Valitutti, Muller et al. 1995). Alternatively, alterations in the kinetics of the pMHCI/CD8 interaction may have significant affects on $CD8^+$ T-cell activation. Data suggests that recruitment of CD8 to the same pMHCI as the TCR can enhance synergistic adhesion which amplifies ligand discrimination (Jiang, Huang et al. 2010). Yachi *et al* used FRET to show that in the presence of CD8, the TCR can specifically distinguish between structurally similar peptides via the kinetics of CD8 recruitment to the TCR (Yachi, Ampudia et al. 2006). The kinetics of the pMHCI/CD8 interaction ($K_{off} \geq 18s^{-1}$) are considerably faster than that measured for agonist TCR/pMHCI interactions (K_{off} = 0.01-$0.63s^{-1}$). As a result there is the potential for many pMHCI/CD8 interactions to take place during a single TCR/pMHCI interaction. This may be critical for optimal $CD8^+$ T-cell activation. Extreme increases in the strength of the pMHCI/CD8 interaction may interfere with the rapid association/dissociation of CD8 with pMHCI engaged by the TCR therefore compromising the serial recruitment of signalling molecules to the TCR/CD3 complex and prevent the TCR from recognising self-reactive peptides.

In summary, I have shown that CD8 can exert a differential effect on TCR/pMHCI functional sensitivity. This can result in a re-arrangement of the relative potencies of the ligands for an individual TCR and can also limit the functional sensitivity of the TCR/pMHCI interaction where optimal ligands can become sub-optimal ligands. This study highlights the significance of CD8 in ensuring that a $CD8^+$ T-cell cannot become hyper-activated by focussing the $CD8^+$ T-cell on ligands that bind within specific kinetic window. The data presented here supports the theory that CD8 is playing a significant role in the TCR triggering event and influences the kinetic parameters of $CD8^+$ T-cell activation, which has important implications and

potential disease relevance. It would be very interesting to study the effect of CD8 focussing in models where natural polymorphisms in the MHCI binding domain exist that may enhance or even abrogate pMHCI/CD8 affinity. The phenomenon described here could also be further studied by altering the levels of both CD8αα and CD8αβ expression at the cell surface and analysing the effect that exerts on the recognition of a range of APL. This is discussed further in chapter 7.

7

DISCUSSION

7 Discussion

In this thesis, I have furthered our knowledge of the role that CD8 plays in T-cell activation and identified CD8 as a potential target for therapy during autoimmune disease. I have also highlighted a novel "focussing" role for CD8 in controlling $CD8^+$ T-cell recognition of pMHCI antigen.

7.1 Increased knowledge of the role that CD8 plays in T-cell activation

7.1.1 The role of the low solution binding affinity of pMHCI/CD8

To date no study has investigated the biological significance of the low solution binding affinity of the pMHCI/CD8 interaction. In Chapter 3 I investigated the effect of increasing the strength of pMHCI/CD8 interaction by 15 fold. The pMHCI/CD8 interaction is characterized by very low solution binding affinities (K_D ~146 μM) and rapid kinetics (Wyer, Willcox et al. 1999; Gao, Willcox et al. 2000). In stark contrast, the TCR/pMHCI interaction can be more than 100-fold stronger than the pMHCI/CD8 interaction (K_D range for agonists from 0.13 μM, the strongest natural TCR/pMHCI interaction measured to date) and exhibits considerably slower kinetics (Davis, Boniface et al. 1998; Cole, Pumphrey et al. 2007; Laugel, van den Berg et al. 2007; Varela-Rohena, Molloy et al. 2008; Stone, Chervin et al. 2009). It seems extremely unlikely that the striking biophysical characteristics of the pMHCI/CD8 interaction have occurred by accident. In Chapter 3 I demonstrated that there is a complete loss of T-cell specificity when the pMHCI/CD8 interaction is increased by 15 fold. This data suggests that CD8 has specifically evolved to operate at very low solution affinities and the low solution binding affinity is essential for the maintenance of $CD8^+$ T-cell antigen specificity and T-cell homeostasis. It has been previously shown that the pMHC/CD8

interaction retained the majority of its ability to augment antigen recognition by $CD8^+$ T-cells even when this interaction was reduced to an extremely low affinity (K_D <500 μM). This result is relevant to the pMHCII/CD4 interaction which still augments antigen recognition despite being extremely weak (K_D <1000 μM) (Hutchinson, Wooldridge et al. 2003). My results suggest that T-cell co-receptors have evolved to function at uniquely low affinities in order to ensure that the TCR/pMHC interaction dominates TCR/pMHCI/CD8 or TCR/pMHCII/CD4 interactions at the cell surface thereby upholding antigen specificity.

7.1.2 The use of anti-CD8 antibodies to activate $CD8^+$ T-cells

Data from Chapter 3 indicated that an increase in pMHCI/CD8 interaction by 15 fold results in a complete loss of T-cell specificity. This result suggested that it might be possible to induce T-cell activation by cross-linking CD8 and the TCR using anti-CD8 antibodies. In Chapter 4 I examined the potential for anti-CD8 antibodies to induce T-cell activation. Anti-CD8 antibodies have been used widely to investigate the role of CD8 in $CD8^+$ T-cell activation. Many studies have concluded that anti-CD8 antibodies can inhibit the TCR/pMHCI interaction (MacDonald, Glasebrook et al. 1982; Janeway 1992), whereas contrasting studies have concluded that anti-CD8 antibodies can enhance TCR/pMHCI interaction and can even activate $CD8^+$ T-cells (Veillette, Zuniga-Pflucker et al. 1989; Tomonari and Spencer 1990). I decided that it was important to address these contradictory findings because of the widespread use of anti-CD8 antibodies in CD8 biology. Therefore, I assembled a panel of seven different monoclonal anti-human CD8 antibodies and four anti-mouse human CD8 antibodies. This is the first time that a comprehensive panel of anti-CD8 antibodies have been compared in the same study. Interestingly, the data showed that multiple functional phenotypes exist within the anti-CD8 antibodies and that it is possible to

induce $CD8^+$ T-cell activation independently of the TCR/pMHCI interaction. This correlated with the ability of one antibody (OKT8) to enhance TCR/pMHCI tetramer binding. Conversely anti-CD8 antibodies can also block TCR/pMHCI binding suggesting that both the enhancing and inhibitory effects of these antibodies are by the same mechanism. Interestingly the enhancing antibody OKT8 induces CD8 mediated ligation with release of chemokines and cytotoxicity in the absence of cytokine release. This may further highlight the importance of the function of CD8 in $CD8^+$ T-cell signalling.

In summary, multiple phenotypes exist across anti-CD8 antibodies. The effects observed using these antibodies may highlight the potential for targeting different binding sites on CD8 to design therapeutic agents that either block or enhance T-cell activation. My study has identified and classified multiple phenotypes across a panel of anti-CD8 antibodies. The differing effects varied according to the antibody clone under investigation and suggest that caution should be taken when interpreting studies using these reagents.

7.1.3 Identification of a novel CD8 "focussing" mechanism

CD8 has been shown to play a major role in controlling the activation threshold of individual T-cells. The data I have shown in Chapter 6 reveals a novel mechanism termed "CD8 focussing" where CD8 controls the levels of activation of individual TCRs by identifying a specific kinetic window which ensures that a $CD8^+$ T-cell cannot become over activated and therefore restricts subsequent non-specific activation. Here I used multiple $CD8^+$ T-cell clones with APLs, each with different binding affinities to the TCR, in conjunction with C1R

B-cell lines which had been stably transfected with mutant MHCI that enhance or abrogate pMHCI/CD8 binding.

I found that CD8 can exert a differential effect on TCR/pMHCI functional sensitivity i.e. CD8 can act to re-arrange the relative potencies of the ligands for an individual TCR. This is the first time this has been presented and also supports mathematical modelling by van den Berg *et al* (van den Berg, Wooldridge et al. 2007) who predicted that a T-cell can alter its functional avidity for its agonists and rearrange the relative potencies of each of its potential agonists. I have demonstrated that this is indeed the case and showed that a T-cell can specifically increase its sensitivity for one agonist while decreasing its sensitivity for other potential ligands. This focussing mechanism means that TCR degeneracy would be inherently dynamic, allowing each TCR to have a wide range of agonists while avoiding autorecognition. The precise mechanism to explain CD8 focussing is still unknown and would require further study. One potential mechanism may be due to an increase in the optimal dwell-time of ligands to serially trigger TCRs. CD8 can increase the dwell-time by approximately 2.2 fold. Thus CD8 may be increasing the dwell-time of a weak ligand and increase it to optimal dwell-time levels. If ligands that are already near optimal, then an increase in dwell-time may inhibit the ability of these ligands to serially trigger TCRs. This study moves to highlight the importance of CD8 in the T-cell triggering event and disease relevance which may lead to improved therapy design.

Taken together, the data provided here highlights the importance of CD8 in homeostatic $CD8^+$ T-cell activation. I have demonstrated that the low solution binding affinity of the

pMHCI/CD8 interaction is essential for the maintenance of T-cell specificity. $CD8^+$ T-cells can become non-specifically activated independently of the TCR/pMHCI interaction by super-enhancing the pMHCI/CD8 and also by the use of anti-CD8 antibodies. In addition, I have identified a novel function termed "CD8 focussing" where CD8 can act to re-arrange the relative potencies of the ligands recognized by an individual TCR.

7.2 The therapeutic potential of targeting CD8

The design of efficient and safe therapies that target T-cell activity faces major challenges. On the one hand, targeting the entire T-cell compartment threatens harmful immunosuppression. On the other hand, specific T-cell targeting approaches require detailed knowledge of the putative self-antigens that drive autoimmune pathogenesis, which is presently an unrealistic goal considering the tremendous diversity of potential T-cell antigens and the vast allelic variability within the human MHC locus.

Recent advances have significantly improved the understanding of the role that CD8 plays during antigen recognition. Previously, it was thought that CD8 involvement was critical in the majority of $CD8^+$ T-cell responses. Because of this, a number of studies have been performed to examine the effect of blocking the pMHCI/CD8 interaction using soluble CD8 variants (Sewell, Gerth et al. 1999; Cole, Rizkallah et al. 2007), antibodies (Wooldridge, Scriba et al. 2006) and other small molecules (Choksi, Jameson et al. 1998; Kern, Hussey et al. 1999), However, it is now appreciated that CD8 does not contribute equally in all $CD8^+$ T-cell responses in that the degree of CD8-dependence is inversely related to the strength of the TCR/pMHCI interaction (Holler, Holman et al. 2000; Holler and Kranz 2003; Laugel, van

den Berg et al. 2007; Wooldridge, Laugel et al. 2010). In fact, detailed biochemical and cellular investigations have established that the CD8 co-receptor is essential for the recognition of weak, low affinity ligands but dispensable for potent, high affinity ligands (Holler, Holman et al. 2000; Holler and Kranz 2003). This knowledge holds translational promise, especially in the setting of autoimmunity where TCR/pMHCI interactions are generally very weak (Bridgeman, Sewell et al. 2011; Bulek, Cole et al. 2012).

I hypothesised that CD8 blockade should enable the selective targeting of weak TCR/pMHCI interactions without affecting high affinity cognate TCRs. In support of this idea, accumulated evidence, suggests that self-reactive (autoimmune) $CD8^+$ T-cells, bear weaker binding TCRs to cognate ligand compared to non-self and alloreactive $CD8^+$ T-cells (van der Merwe and Davis 2003; Laugel, Boulter et al. 2005; Cole, Pumphrey et al. 2007; Macdonald, Chen et al. 2009; Cole, Edwards et al. 2010; Bulek, Cole et al. 2012). Therefore, therapeutic targeting of CD8 may be useful in the setting of autoimmune diseases including type-1 diabetes (Skowera, Ellis et al. 2008; Wong, Siew et al. 2008; Faustman and Davis 2009), multiple sclerosis (Friese and Fugger 2009), vitiligo (van den Boorn, Konijnenberg et al. 2009), neurodegenerative diseases such as certain paraneoplastic syndromes (Darnell and Posner 2003), Hashimotos throiditis, autoimmune myocarditis and autoimmune hepatitis (Walter and Santamaria 2005).

7.3 Blockade of $CD8^+$ T-cell function using anti-CD8 antibodies

The results in Chapter 4 demonstrate that it is possible to use anti-CD8 antibodies to block pMHCI tetramer binding at the cell surface. Importantly it has long been known that anti-

CD8 antibodies could be used to block the activation of multiple $CD8^+$ T-cells (MacDonald, Glasebrook et al. 1982). However no study incorporated the use of these blocking antibodies in a setting where high levels of CD8-dependency are important. Indeed it has been shown that very low TCR/pMHCI binding affinities characterised by K_D values >100-200 μM are entirely CD8-dependent. These K_D values are found to be characteristic of autoreactive TCRs. In this thesis, I demonstrated that anti-CD8 antibodies efficiently block the activation of $CD8^+$ T-cells characterised by low affinity TCR/pMHCI interactions. I then went on to show that anti-CD8 antibodies can be used to inhibit the activation of a diabetogenic $CD8^+$ T-cell clone. The effect of the anti-CD8 antibodies is less profound if TCR/pMHCI binding affinities are <30 μM. This suggests that anti-CD8 antibodies could be used as a direct therapeutic agent in autoimmune disorders without compromising $CD8^+$ T-cells that recognize viral or tumour targets.

In this thesis I have studied a strategy to block autoreactive T-cell activation using antibodies. This is in contrast to the use of antibodies to induce tolerance which has been studied in a type-1 diabetes setting. Diabetes onset has been shown to be halted in the NOD mouse using non-depletive anti-CD4 and anti-CD8 antibodies (Phillips, Parish et al. 2009). There has also been extensive data highlighting the use of anti-CD3 antibodies in the study of type-1 diabetes. Interestingly anti-CD3 antibodies have been shown to reverse diabetes onset in NOD mice and was the initial basis for the use of this antibody in human clinical trials (Chatenoud, Thervet et al. 1994; Herold, Hagopian et al. 2002; Keymeulen, Vandemeulebroucke et al. 2005). Indeed in human studies, the use of anti-CD3 antibodies has been shown to increase islet β cell function by up to two years and can increase insulin production (Herold, Gitelman et al. 2009). It is thought that this is due to the induction of

regulatory T-cells, which may play a key role in maintaining tolerance and have been reported to be TGFβ-dependent (Cobbold, Castejon et al. 2004; You, Leforban et al. 2007). It will be interesting to examine the pros and cons of blocking versus tolerance strategies in future studies.

7.4 Future prospective studies

7.4.1 Identification of a pMHCI/CD8 K_D threshold for non-specific activation

In Chapter 3 I demonstrated that increasing the strength of the pMHCI/CD8 interaction by approximately 15 fold (K_D 9.4 μM) results in the T-cell becoming activated independently of the TCR/pMHCI interaction and subsequently a loss in $CD8^+$ T-cell specificity. Therefore between a K_D of 9.4 and 98 μM there may exist a threshold of pMHCI/CD8 affinity where the increase in this interaction switches from being advantageous to being detrimental in terms of $CD8^+$ T-cell specificity. It would be of great importance to identify this threshold level in further study of CD8 in $CD8^+$ T-cell activation. This may allow for a further understanding of the kinetics of the pMHCI/CD8 interaction and its potential implications in TCR/pMHCI specificity and activation.

7.4.2 Identifying the precise mechanism by which anti-CD8 antibodies elicit $CD8^+$ T-cell effector function

As discussed in Chapter 4, multiple phenotypes exist in anti-CD8 antibodies (both human and mice). The precise mechanism by which each phenotype is exerted is still conjecture. To definitively assess the molecular interaction of the anti-CD8 antibodies at the cell surface, both fluorescence resonance energy transfer FRET and also bioluminescence resonance

energy transfer BRET techniques can be used. FRET can be performed by microscopy to quantify the extent and kinetics of molecular interactions between fluorophore-tagged proteins within sub-cellular regions such as the immunological synapse (Zal, Zal et al. 2002). Therefore FRET can be used to visualise differences in the TCR/pMHCI/CD8 interaction. The introduction of anti-CD8 antibodies into this system would help to understand the mechanism of action for each anti-CD8 antibody tested in this thesis, most notably those that both enhance and inhibit the TCR/pMHCI interaction. Another way to study this interaction is using BRET which works on the similar premise to FRET however uses bioluminescent markers instead of fluorescence, increasing the stability of the interaction which becomes more suitable for protein-protein interactions (Pfleger, Seeber et al. 2006).

7.4.3 Altering CD8 expression levels at the cell surface

Data from Chapter 6 highlighted a potential new role for CD8 in controlling the window of ligands that are available to a TCR. However, these experiments were conducted using MHCI mutations with a varied interaction with CD8. It is more likely that *in-vivo* this focussing effect is achieved by altering the cell surface levels of CD8. It has been shown that CD8 levels at the cell surface are very dynamic and change during the course of an immune response. It will be important to construct a system where levels of CD8 can be altered in order to repeat the study of APL recognition.

7.4.4 Solving the human CD8αβ heterodimer crystal structure

To date, a soluble human CD8αβ heterodimer has yet to be assembled. This is mainly due to the preference of human CD8α to homodimerise during manufacture. If this problem was

addressed and solved then this would allow for biophysical data for the human heterodimer to be determined for the first time. Murine studies concluded that CD8αα and CD8αβ bind murine pMHCI with similar affinity (Sun and Kavathas 1997) (Arcaro, Gregoire et al. 2001; Wang, Natarajan et al. 2009). However observations made by Chang and colleagues after studying the crystal structures of murine CD8αα and CD8αβ highlighted important differences that could lead to subtle binding differences to MHCI (Chang, Tan et al. 2005). Jiang and colleagues confirmed that the murine CD8αα and CD8αβ do bind to MHCI with similar affinity, though indeed subtle differences were noted in the affinity of the interaction (Wang, Natarajan et al. 2009).

It is possible that the binding of CD8αα and CD8αβ to the MHCI may be different in the human system. The average murine pMHCI/CD8 interaction is approximately 5 times as strong as the human pMHCI/CD8 interaction, i.e. murine pMHCI/CD8 K_D ~ 30μM, whereas human pMHCI/CD8 K_D ~ 146μM as measured by SPR (Purbhoo, Boulter et al. 2001). These differences observed in the murine CD8αα and CD8αβ binding affinity to pMHCI may translate into the human system. It would also be of interest to study the differences in binding interactions using the newly developed 2D micropipette adhesion frequency assays (Jiang, Huang et al. 2010).

Another advantage in successfully manufacturing soluble CD8αβ would allow for crystal structures and co-crytsal structures of CD8αβ with varying allelic pMHCI, which would provide an interesting insight as to the exact orientation of binding. This could potentially allow for designed therapies based on structural information. It would also be of interest to

solve the co-crystal structure of both enhancing and inhibitory anti-CD8 antibodies to pMHCI/CD8αα/αβ. This would help to visualise direct molecular interactions between the antibody and CD8; thereby facilitating the design of immune based therapies (Shore, Issafras et al. 2008).

7.4.5 Developing novel therapeutics that inhibit the pMHCI/CD8 interaction

My preliminary experiments suggest that the phenotype of CD8 antibodies might be determined by the binding site of the epitope. Therefore it may be possible to design therapeutics that target specific sites on CD8 in order to achieve either inhibitory or activatory effects. The enhancing effects that are seen by the antibody clone OKT8 may be due to the position that this antibody binds. Indeed Sanders *et al* identified that OKT8 binds to a distinct site compared to anti-CD8 antibodies with an inhibitory phenotype (Figure 4.15) (Sanders, Fox et al. 1991). Further studies may allow for design of therapies aimed at either enhancing or inhibiting $CD8^+$ T-cell function and may uncover further heterogeneity of these regions as seen in the murine system (Chapter 4).

The use of antibodies in therapy is dramatically on the rise, therefore the timing of this study is very significant. By the late 1990s many monoclonal antibodies were in advanced clinical development and as of 2004, there were 15 monoclonal antibodies licensed for clinical use and only one licensed for use in an infectious disease (Rous sarcoma virus (RSV) infection) as reviewed in (Casadevall, Dadachova et al. 2004). However as of 2010 more than 30 mAbs are licensed for therapy covering a large range of pathologies including oncogenic and inflammatory disorders with many more antibodies in clinical trials including 26 at Phase III

as reviewed in (Beck, Wurch et al. 2010) indicating a dramatic increase in the use of antibodies as therapeutic agents.

7.5 Concluding Remarks

To date there are studies that suggest that CD8 is not essential for $CD8^+$ T-cell activation (as reviewed in (van der Merwe and Dushek 2011). Recent studies have suggested that CD8 has important implications in controlling T-cell homeostasis and is essential in controlling TCR/pMHCI stability and T-cell crossreactivity (Wooldridge, van den Berg et al. 2005; Wooldridge, Laugel et al. 2010). This thesis has further demonstrated the need for CD8 in controlling T-cell specificity, identified CD8 as a potential target for immune based therapies and identified a novel potential role for CD8 in controlling the specificity of ligands that a T-cell can recognise. Taking all of these findings together, it is clear that CD8 is playing a critical role in T-cell activation and the findings of this thesis would definitely warrant further study of CD8. This would allow for the potential modulation of CD8 as a therapeutic target in T-cell responses.

REFERENCES

Abidi, S. H., T. Dong, M. T. Vuong, V. B. Sreenu, S. L. Rowland-Jones, E. J. Evans and S. J. Davis (2008). "Differential remodeling of a T-cell transcriptome following CD8- versus CD3-induced signaling." Cell Res **18**(6): 641-8.

Abraham, N. and A. Veillette (1990). "Activation of p56lck through mutation of a regulatory carboxy-terminal tyrosine residue requires intact sites of autophosphorylation and myristylation." Mol Cell Biol **10**(10): 5197-206.

Agrawal, A. and D. G. Schatz (1997). "RAG1 and RAG2 form a stable postcleavage synaptic complex with DNA containing signal ends in V(D)J recombination." Cell **89**(1): 43-53.

Alarcon, B., B. Berkhout, J. Breitmeyer and C. Terhorst (1988). "Assembly of the human T cell receptor-CD3 complex takes place in the endoplasmic reticulum and involves intermediary complexes between the CD3-gamma.delta.epsilon core and single T cell receptor alpha or beta chains." J Biol Chem **263**(6): 2953-61.

Alexander, M. A., C. A. Damico, K. M. Wieties, T. H. Hansen and J. M. Connolly (1991). "Correlation between CD8 dependency and determinant density using peptide-induced, Ld-restricted cytotoxic T lymphocytes." J Exp Med **173**(4): 849-58.

Altman, J. D., P. A. Moss, P. J. Goulder, D. H. Barouch, M. G. McHeyzer-Williams, J. I. Bell, A. J. McMichael and M. M. Davis (1996). "Phenotypic analysis of antigen-specific T lymphocytes." Science **274**(5284): 94-6.

Anikeeva, N., T. Lebedeva, A. R. Clapp, E. R. Goldman, M. L. Dustin, H. Mattoussi and Y. Sykulev (2006). "Quantum dot/peptide-MHC biosensors reveal strong CD8-dependent cooperation between self and viral antigens that augment the T cell response." Proc Natl Acad Sci U S A **103**(45): 16846-51.

Antoniou, A. N., S. J. Powis and T. Elliott (2003). "Assembly and export of MHC class I peptide ligands." Curr Opin Immunol **15**(1): 75-81.

Arcaro, A., C. Gregoire, T. R. Bakker, L. Baldi, M. Jordan, L. Goffin, N. Boucheron, F. Wurm, P. A. van der Merwe, B. Malissen and I. F. Luescher (2001). "CD8beta endows CD8 with efficient coreceptor function by coupling T cell receptor/CD3 to raft-associated CD8/p56(lck) complexes." J Exp Med **194**(10): 1485-95.

Arcaro, A., C. Gregoire, N. Boucheron, S. Stotz, E. Palmer, B. Malissen and I. F. Luescher (2000). "Essential role of CD8 palmitoylation in CD8 coreceptor function." J Immunol **165**(4): 2068-76.

Archbold, J. K., W. A. Macdonald, S. Gras, L. K. Ely, J. J. Miles, M. J. Bell, R. M. Brennan, T. Beddoe, M. C. Wilce, C. S. Clements, A. W. Purcell, J. McCluskey, S. R. Burrows and J. Rossjohn (2009). "Natural micropolymorphism in human leukocyte antigens provides a basis for genetic control of antigen recognition." J Exp Med **206**(1): 209-19.

Ashwell, J. D. and U. D'Oro (1999). "CD45 and Src-family kinases: and now for something completely different." Immunol Today **20**(9): 412-6.

Barber, E. K., J. D. Dasgupta, S. F. Schlossman, J. M. Trevillyan and C. E. Rudd (1989). "The CD4 and CD8 antigens are coupled to a protein-tyrosine kinase (p56lck) that phosphorylates the CD3 complex." Proc Natl Acad Sci U S A **86**(9): 3277-81.

Basson, M. A. and R. Zamoyska (2000). "The CD4/CD8 lineage decision: integration of signalling pathways." Immunol Today **21**(10): 509-14.

Baxter, A. G. and P. D. Hodgkin (2002). "Activation rules: the two-signal theories of immune activation." Nat Rev Immunol **2**(6): 439-46.

Beach, D., R. Gonen, Y. Bogin, I. G. Reischl and D. Yablonski (2007). "Dual role of SLP-76 in mediating T cell receptor-induced activation of phospholipase C-gamma1." J Biol Chem **282**(5): 2937-46.

Beck, A., T. Wurch, C. Bailly and N. Corvaia (2010). "Strategies and challenges for the next generation of therapeutic antibodies." Nat Rev Immunol **10**(5): 345-52.

Bentley, G. A. and R. A. Mariuzza (1996). "The structure of the T cell antigen receptor." Annu Rev Immunol **14**: 563-90.

Bergman, M., T. Mustelin, C. Oetken, J. Partanen, N. A. Flint, K. E. Amrein, M. Autero, P. Burn and K. Alitalo (1992). "The human p50csk tyrosine kinase phosphorylates p56lck at Tyr-505 and down regulates its catalytic activity." Embo J **11**(8): 2919-24.

Betts, M. R., J. M. Brenchley, D. A. Price, S. C. De Rosa, D. C. Douek, M. Roederer and R. A. Koup (2003). "Sensitive and viable identification of antigen-specific CD8+ T cells by a flow cytometric assay for degranulation." J Immunol Methods **281**(1-2): 65-78.

Beyers, A. D., L. L. Spruyt and A. F. Williams (1992). "Molecular associations between the T-lymphocyte antigen receptor complex and the surface antigens CD2, CD4, or CD8 and CD5." Proc Natl Acad Sci U S A **89**(7): 2945-9.

Bhardwaj, V., V. Kumar, H. M. Geysen and E. E. Sercarz (1993). "Degenerate recognition of a dissimilar antigenic peptide by myelin basic protein-reactive T cells. Implications for thymic education and autoimmunity." J Immunol **151**(9): 5000-10.

Biddison, W. E., P. E. Rao, M. A. Talle, C. M. Boselli and G. Goldstein (1984). "Distinct epitopes on the T8 molecule are differentially involved in cytotoxic T cell function." Hum Immunol **9**(2): 117-30.

Bierer, B. E., B. P. Sleckman, S. E. Ratnofsky and S. J. Burakoff (1989). "The biologic roles of CD2, CD4, and CD8 in T-cell activation." Annu Rev Immunol **7**: 579-99.

Bjorkman, P. J., M. A. Saper, B. Samraoui, W. S. Bennett, J. L. Strominger and D. C. Wiley (1987). "Structure of the human class I histocompatibility antigen, HLA-A2." Nature **329**(6139): 506-12.

Block, M. S., A. J. Johnson, Y. Mendez-Fernandez and L. R. Pease (2001). "Monomeric class I molecules mediate TCR/CD3 epsilon/CD8 interaction on the surface of T cells." J Immunol **167**(2): 821-6.

Blumberg, R. S., B. Alarcon, J. Sancho, F. V. McDermott, P. Lopez, J. Breitmeyer and C. Terhorst (1990). "Assembly and function of the T cell antigen receptor. Requirement of either the lysine or arginine residues in the transmembrane region of the alpha chain." J Biol Chem **265**(23): 14036-43.

Bogin, Y., C. Ainey, D. Beach and D. Yablonski (2007). "SLP-76 mediates and maintains activation of the Tec family kinase ITK via the T cell antigen receptor-induced association between SLP-76 and ITK." Proc Natl Acad Sci U S A **104**(16): 6638-43.

Borbulevych, O. Y., K. H. Piepenbrink and B. M. Baker (2011). "Conformational melding permits a conserved binding geometry in TCR recognition of foreign and self molecular mimics." J Immunol **186**(5): 2950-8.

Borbulevych, O. Y., K. H. Piepenbrink, B. E. Gloor, D. R. Scott, R. F. Sommese, D. K. Cole, A. K. Sewell and B. M. Baker (2009). "T cell receptor cross-reactivity directed by antigen-dependent tuning of peptide-MHC molecular flexibility." Immunity **31**(6): 885-96.

Borg, N. A., L. K. Ely, T. Beddoe, W. A. Macdonald, H. H. Reid, C. S. Clements, A. W. Purcell, L. Kjer-Nielsen, J. J. Miles, S. R. Burrows, J. McCluskey and J. Rossjohn (2005). "The CDR3 regions of an immunodominant T cell receptor dictate the 'energetic landscape' of peptide-MHC recognition." Nat Immunol **6**(2): 171-80.

Bosselut, R., T. I. Guinter, S. O. Sharrow and A. Singer (2003). "Unraveling a revealing paradox: Why major histocompatibility complex I-signaled thymocytes "paradoxically" appear as CD4+8lo transitional cells during positive selection of CD8+ T cells." J Exp Med **197**(12): 1709-19.

Bosselut, R., S. Kubo, T. Guinter, J. L. Kopacz, J. D. Altman, L. Feigenbaum and A. Singer (2000). "Role of CD8beta domains in CD8 coreceptor function: importance for MHC I binding, signaling, and positive selection of CD8+ T cells in the thymus." Immunity **12**(4): 409-18.

Bosselut, R., W. Zhang, J. M. Ashe, J. L. Kopacz, L. E. Samelson and A. Singer (1999). "Association of the adaptor molecule LAT with CD4 and CD8 coreceptors identifies a new coreceptor function in T cell receptor signal transduction." J Exp Med **190**(10): 1517-26.

Bossi, G. and G. M. Griffiths (1999). "Degranulation plays an essential part in regulating cell surface expression of Fas ligand in T cells and natural killer cells." Nat Med **5**(1): 90-6.

Brady, R. L. and A. N. Barclay (1996). "The structure of CD4." Curr Top Microbiol Immunol **205**: 1-18.

Bridgeman, J. S., A. K. Sewell, J. J. Miles, D. A. Price and D. K. Cole (2011). "Structural and biophysical determinants of alphabeta T-cell antigen recognition." Immunology **135**(1): 9-18.

Bromley, S. K., W. R. Burack, K. G. Johnson, K. Somersalo, T. N. Sims, C. Sumen, M. M. Davis, A. S. Shaw, P. M. Allen and M. L. Dustin (2001). "The immunological synapse." Annu Rev Immunol **19**: 375-96.

Brown, J. H., T. S. Jardetzky, J. C. Gorga, L. J. Stern, R. G. Urban, J. L. Strominger and D. C. Wiley (1993). "Three-dimensional structure of the human class II histocompatibility antigen HLA-DR1." Nature **364**(6432): 33-9.

Brownlie, R. and R. Zamoyska (2009). "LAT polices T cell activation." Immunity **31**(2): 174-6.

Bulek, A. M., D. K. Cole, A. Skowera, G. Dolton, S. Gras, F. Madura, A. Fuller, J. J. Miles, E. Gostick, D. A. Price, J. W. Drijfhout, R. R. Knight, G. C. Huang, N. Lissin, P. E. Molloy, L. Wooldridge, B. K. Jakobsen, J. Rossjohn, M. Peakman, P. J. Rizkallah and A. K. Sewell (2012). "Structural basis for the killing of human beta cells by CD8(+) T cells in type 1 diabetes." Nat Immunol.

Bulek, A. M., F. Madura, A. Fuller, C. J. Holland, A. J. Schauenburg, A. K. Sewell, P. J. Rizkallah and D. K. Cole (2012) "TCR/pMHC Optimized Protein crystallization Screen." J Immunol Methods **382**(1-2): 203-10.

Bunnell, S. C., D. I. Hong, J. R. Kardon, T. Yamazaki, C. J. McGlade, V. A. Barr and L. E. Samelson (2002). "T cell receptor ligation induces the formation of dynamically regulated signaling assemblies." J Cell Biol **158**(7): 1263-75.

Burkhardt, J. K., E. Carrizosa and M. H. Shaffer (2008). "The actin cytoskeleton in T cell activation." Annu Rev Immunol **26**: 233-59.

Burrows, S. R., N. Kienzle, A. Winterhalter, M. Bharadwaj, J. D. Altman and A. Brooks (2000). "Peptide-MHC class I tetrameric complexes display exquisite ligand specificity." J Immunol **165**(11): 6229-34.

Burrows, S. R., S. L. Silins, D. J. Moss, R. Khanna, I. S. Misko and V. P. Argaet (1995). "T cell receptor repertoire for a viral epitope in humans is diversified by tolerance to a background major histocompatibility complex antigen." J Exp Med **182**(6): 1703-15.

Busch, D. H. and E. G. Pamer (1999). "T cell affinity maturation by selective expansion during infection." J Exp Med **189**(4): 701-10.

Campanelli, R., B. Palermo, S. Garbelli, S. Mantovani, P. Lucchi, A. Necker, E. Lantelme and C. Giachino (2002). "Human CD8 co-receptor is strictly involved in MHC-peptide tetramer-TCR binding and T cell activation." Int Immunol **14**(1): 39-44.

Campi, G., R. Varma and M. L. Dustin (2005). "Actin and agonist MHC-peptide complex-dependent T cell receptor microclusters as scaffolds for signaling." J Exp Med **202**(8): 1031-6.

Capps, G. G. and M. C. Zuniga (1994). "Class I histocompatibility molecule association with phosphorylated calnexin. Implications for rates of intracellular transport." J Biol Chem **269**(15): 11634-9.

Caron, L., N. Abraham, T. Pawson and A. Veillette (1992). "Structural requirements for enhancement of T-cell responsiveness by the lymphocyte-specific tyrosine protein kinase p56lck." Mol Cell Biol **12**(6): 2720-9.

Cary, L. A. and J. A. Cooper (2000). "Molecular switches in lipid rafts." Nature **404**(6781): 945, 947.

Casadevall, A., E. Dadachova and L. A. Pirofski (2004). "Passive antibody therapy for infectious diseases." Nat Rev Microbiol **2**(9): 695-703.

Chan, A. C., M. Dalton, R. Johnson, G. H. Kong, T. Wang, R. Thoma and T. Kurosaki (1995). "Activation of ZAP-70 kinase activity by phosphorylation of tyrosine 493 is required for lymphocyte antigen receptor function." Embo J **14**(11): 2499-508.

Chan, A. C., D. M. Desai and A. Weiss (1994). "The role of protein tyrosine kinases and protein tyrosine phosphatases in T cell antigen receptor signal transduction." Annu Rev Immunol **12**: 555-92.

Chan, A. C., M. Iwashima, C. W. Turck and A. Weiss (1992). "ZAP-70: a 70 kd protein-tyrosine kinase that associates with the TCR zeta chain." Cell **71**(4): 649-62.

Chan, A. C. and A. S. Shaw (1996). "Regulation of antigen receptor signal transduction by protein tyrosine kinases." Curr Opin Immunol **8**(3): 394-401.

Chang, H. C., K. Tan, J. Ouyang, E. Parisini, J. H. Liu, Y. Le, X. Wang, E. L. Reinherz and J. H. Wang (2005). "Structural and mutational analyses of a CD8alphabeta heterodimer and comparison with the CD8alphaalpha homodimer." Immunity **23**(6): 661-71.

Chatenoud, L. and J. A. Bluestone (2007). "CD3-specific antibodies: a portal to the treatment of autoimmunity." Nat Rev Immunol **7**(8): 622-32.

Chatenoud, L., E. Thervet, J. Primo and J. F. Bach (1994). "Anti-CD3 antibody induces long-term remission of overt autoimmunity in nonobese diabetic mice." Proc Natl Acad Sci U S A **91**(1): 123-7.

Chen, J. L., G. Stewart-Jones, G. Bossi, N. M. Lissin, L. Wooldridge, E. M. Choi, G. Held, P. R. Dunbar, R. M. Esnouf, M. Sami, J. M. Boulter, P. Rizkallah, C. Renner, A. Sewell, P. A. van der Merwe, B. K. Jakobsen, G. Griffiths, E. Y. Jones and V. Cerundolo (2005). "Structural and kinetic basis for heightened immunogenicity of T cell vaccines." J Exp Med **201**(8): 1243-55.

Chervin, A. S., J. D. Stone, N. A. Bowerman and D. M. Kranz (2009). "Cutting edge: inhibitory effects of CD4 and CD8 on T cell activation induced by high-affinity noncognate ligands." J Immunol **183**(12): 7639-43.

Chiang, G. G. and B. M. Sefton (2001). "Specific dephosphorylation of the Lck tyrosine protein kinase at Tyr-394 by the SHP-1 protein-tyrosine phosphatase." J Biol Chem **276**(25): 23173-8.

Choi, E. M., J. L. Chen, L. Wooldridge, M. Salio, A. Lissina, N. Lissin, I. F. Hermans, J. D. Silk, F. Mirza, M. J. Palmowski, P. R. Dunbar, B. K. Jakobsen, A. K. Sewell and V. Cerundolo (2003). "High avidity antigen-specific CTL identified by CD8-independent tetramer staining." J Immunol **171**(10): 5116-23.

Choi, E. M., M. Palmowski, J. Chen and V. Cerundolo (2002). "The use of chimeric A2K(b) tetramers to monitor HLA A2 immune responses in HLA A2 transgenic mice." J Immunol Methods **268**(1): 35-41.

Choksi, S., B. A. Jameson and R. Korngold (1998). "A structure-based approach to designing synthetic CD8alpha peptides that can inhibit cytotoxic T-lymphocyte responses." Nat Med **4**(3): 309-14.

Choudhuri, K. and P. A. van der Merwe (2007). "Molecular mechanisms involved in T cell receptor triggering." Semin Immunol **19**(4): 255-61.

Chow, L. M. and A. Veillette (1995). "The Src and Csk families of tyrosine protein kinases in hemopoietic cells." Semin Immunol **7**(4): 207-26.

Ciechanover, A. (1994). "The ubiquitin-proteasome proteolytic pathway." Cell **79**(1): 13-21.

Clark, S. J., D. A. Law, D. J. Paterson, M. Puklavec and A. F. Williams (1988). "Activation of rat T lymphocytes by anti-CD2 monoclonal antibodies." J Exp Med **167**(6): 1861-72.

Clement, M., K. Ladell, J. Ekeruche-Makinde, J. J. Miles, E. S. Edwards, G. Dolton, T. Williams, A. J. Schauenburg, D. K. Cole, S. N. Lauder, A. M. Gallimore, A. J. Godkin, S. R. Burrows, D. A. Price, A. K. Sewell and L. Wooldridge (2011). "Anti-CD8 antibodies can trigger CD8+ T cell effector function in the absence of TCR engagement and improve peptide-MHCI tetramer staining." J Immunol **187**(2): 654-63.

Cobbold, S. P., R. Castejon, E. Adams, D. Zelenika, L. Graca, S. Humm and H. Waldmann (2004). "Induction of foxP3+ regulatory T cells in the periphery of T cell receptor transgenic mice tolerized to transplants." J Immunol **172**(10): 6003-10.

Cole, D. K., S. M. Dunn, M. Sami, J. M. Boulter, B. K. Jakobsen and A. K. Sewell (2008). "T cell receptor engagement of peptide-major histocompatibility complex class I does not modify CD8 binding." Mol Immunol **45**(9): 2700-9.

Cole, D. K., E. S. Edwards, K. K. Wynn, M. Clement, J. J. Miles, K. Ladell, J. Ekeruche, E. Gostick, K. J. Adams, A. Skowera, M. Peakman, L. Wooldridge, D. A. Price and A. K. Sewell (2010). "Modification of MHC anchor residues generates heteroclitic peptides that alter TCR binding and T cell recognition." J Immunol **185**(4): 2600-10.

Cole, D. K. and G. F. Gao (2004). "CD8: adhesion molecule, co-receptor and immuno-modulator." Cell Mol Immunol **1**(2): 81-8.

Cole, D. K., N. J. Pumphrey, J. M. Boulter, M. Sami, J. I. Bell, E. Gostick, D. A. Price, G. F. Gao, A. K. Sewell and B. K. Jakobsen (2007). "Human TCR-Binding Affinity is Governed by MHC Class Restriction." J Immunol **178**(9): 5727-34.

Cole, D. K., P. J. Rizkallah, J. M. Boulter, M. Sami, A. L. Vuidepot, M. Glick, F. Gao, J. I. Bell, B. K. Jakobsen and G. F. Gao (2007). "Computational design and crystal structure of an enhanced affinity mutant human CD8 alphaalpha coreceptor." Proteins **67**(1): 65-74.

Cole, D. K., F. Yuan, P. J. Rizkallah, J. J. Miles, E. Gostick, D. A. Price, G. F. Gao, B. K. Jakobsen and A. K. Sewell (2009). "Germ line-governed recognition of a cancer epitope by an immunodominant human T-cell receptor." J Biol Chem **284**(40): 27281-9.

Connolly, J. M., T. H. Hansen, A. L. Ingold and T. A. Potter (1990). "Recognition by CD8 on cytotoxic T lymphocytes is ablated by several substitutions in the class I alpha 3 domain: CD8 and the T-cell receptor recognize the same class I molecule." Proc Natl Acad Sci U S A **87**(6): 2137-41.

Coppieters, K. T., F. Dotta, N. Amirian, P. D. Campbell, T. W. Kay, M. A. Atkinson, B. O. Roep and M. G. von Herrath (2012). "Demonstration of islet-autoreactive CD8 T cells in insulitic lesions from recent onset and long-term type 1 diabetes patients." J Exp Med **209**(1): 51-60.

Crawford, F., E. Huseby, J. White, P. Marrack and J. W. Kappler (2004). "Mimotopes for alloreactive and conventional T cells in a peptide-MHC display library." PLoS Biol **2**(4): E90.

Curtsinger, J. M., C. S. Schmidt, A. Mondino, D. C. Lins, R. M. Kedl, M. K. Jenkins and M. F. Mescher (1999). "Inflammatory cytokines provide a third signal for activation of naive CD4+ and CD8+ T cells." J Immunol **162**(6): 3256-62.

D'Oro, U. and J. D. Ashwell (1999). "Cutting edge: the CD45 tyrosine phosphatase is an inhibitor of Lck activity in thymocytes." J Immunol **162**(4): 1879-83.

Dai, S., E. S. Huseby, K. Rubtsova, J. Scott-Browne, F. Crawford, W. A. Macdonald, P. Marrack and J. W. Kappler (2008). "Crossreactive T Cells spotlight the germline rules for alphabeta T cell-receptor interactions with MHC molecules." Immunity **28**(3): 324-34.

Daniels, M. A., L. Devine, J. D. Miller, J. M. Moser, A. E. Lukacher, J. D. Altman, P. Kavathas, K. A. Hogquist and S. C. Jameson (2001). "CD8 binding to MHC class I molecules is influenced by T cell maturation and glycosylation." Immunity **15**(6): 1051-61.

Daniels, M. A., K. A. Hogquist and S. C. Jameson (2002). "Sweet 'n' sour: the impact of differential glycosylation on T cell responses." Nat Immunol **3**(10): 903-10.

Daniels, M. A. and S. C. Jameson (2000). "Critical role for CD8 in T cell receptor binding and activation by peptide/major histocompatibility complex multimers." J Exp Med **191**(2): 335-46.

Darnell, R. B. and J. B. Posner (2003). "Paraneoplastic syndromes involving the nervous system." N Engl J Med **349**(16): 1543-54.

Davis-Harrison, R. L., K. M. Armstrong and B. M. Baker (2005). "Two different T cell receptors use different thermodynamic strategies to recognize the same peptide/MHC ligand." J Mol Biol **346**(2): 533-50.

Davis, M. M. (2002). "A new trigger for T cells." Cell **110**(3): 285-7.

Davis, M. M., J. J. Boniface, Z. Reich, D. Lyons, J. Hampl, B. Arden and Y. Chien (1998). "Ligand recognition by alpha beta T cell receptors." Annu Rev Immunol **16**: 523-44.

Davis, S. J. and P. A. van der Merwe (2001). "The immunological synapse: required for T cell receptor signalling or directing T cell effector function?" Curr Biol **11**(8): R289-91.

DeFord-Watts, L. M., D. S. Dougall, S. Belkaya, B. A. Johnson, J. L. Eitson, K. T. Roybal, B. Barylko, J. P. Albanesi, C. Wulfing and N. S. van Oers (2011). "The CD3 zeta subunit contains a phosphoinositide-binding motif that is required for the stable accumulation of TCR-CD3 complex at the immunological synapse." J Immunol **186**(12): 6839-47.

Delon, J. and R. N. Germain (2000). "Information transfer at the immunological synapse." Curr Biol **10**(24): R923-33.

Delves, P. J. and I. M. Roitt (2000). "The immune system. First of two parts." N Engl J Med **343**(1): 37-49.

Delves, P. J. and I. M. Roitt (2000). "The immune system. Second of two parts." N Engl J Med **343**(2): 108-17.

Demotte, N., V. Stroobant, P. J. Courtoy, P. Van Der Smissen, D. Colau, I. F. Luescher, C. Hivroz, J. Nicaise, J. L. Squifflet, M. Mourad, D. Godelaine, T. Boon and P. van der Bruggen (2008). "Restoring the association of the T cell receptor with CD8 reverses anergy in human tumor-infiltrating lymphocytes." Immunity **28**(3): 414-24.

Denkberg, G., C. J. Cohen and Y. Reiter (2001). "Critical role for CD8 in binding of MHC tetramers to TCR: CD8 antibodies block specific binding of human tumor-specific MHC-peptide tetramers to TCR." J Immunol **167**(1): 270-6.

Devine, L., M. E. Hodsdon, M. A. Daniels, S. C. Jameson and P. B. Kavathas (2004). "Location of the epitope for an anti-CD8alpha antibody 53.6.7 which enhances CD8alpha-MHC class I interaction indicates antibody stabilization of a higher affinity CD8 conformation." Immunol Lett **93**(2-3): 123-30.

Devine, L., J. Sun, M. R. Barr and P. B. Kavathas (1999). "Orientation of the Ig domains of CD8 alpha beta relative to MHC class I." J Immunol **162**(2): 846-51.

Dinarello, C. A. (2010). "Anti-inflammatory Agents: Present and Future." Cell **140**(6): 935-50.

Ding, Y. H., B. M. Baker, D. N. Garboczi, W. E. Biddison and D. C. Wiley (1999). "Four A6-TCR/peptide/HLA-A2 structures that generate very different T cell signals are nearly identical." Immunity **11**(1): 45-56.

Doucey, M. A., L. Goffin, D. Naeher, O. Michielin, P. Baumgartner, P. Guillaume, E. Palmer and I. F. Luescher (2003). "CD3 delta establishes a functional link between the T cell receptor and CD8." J Biol Chem **278**(5): 3257-64.

Dustin, M. L., D. E. Golan, D. M. Zhu, J. M. Miller, W. Meier, E. A. Davies and P. A. van der Merwe (1997). "Low affinity interaction of human or rat T cell adhesion molecule CD2 with its ligand aligns adhering membranes to achieve high physiological affinity." J Biol Chem **272**(49): 30889-98.

Ekeruche-Makinde, J., M. Clement, D. K. Cole, E. S. Edwards, K. Ladell, J. J. Miles, K. K. Matthews, A. Fuller, K. A. Lloyd, F. Madura, G. M. Dolton, J. Pentier, A. Lissina, E. Gostick, T. K. Baxter, B. M. Baker, P. J. Rizkallah, D. A. Price, L. Wooldridge and A. K. Sewell (2012). "T-Cell Receptor optimized peptide skewing of the T-cell repertoire can enhance antigen targeting." J Biol Chem.

EMBL-EBI. (2012). "IMGT/HLA database."

Engelhard, V. H. (1994). "Structure of peptides associated with class I and class II MHC molecules." Annu Rev Immunol **12**: 181-207.

Evavold, B. D., J. Sloan-Lancaster, K. J. Wilson, J. B. Rothbard and P. M. Allen (1995). "Specific T cell recognition of minimally homologous peptides: evidence for multiple endogenous ligands." Immunity **2**(6): 655-63.

Fantl, W. J., J. A. Escobedo, G. A. Martin, C. W. Turck, M. del Rosario, F. McCormick and L. T. Williams (1992). "Distinct phosphotyrosines on a growth factor receptor bind to specific molecules that mediate different signaling pathways." Cell **69**(3): 413-23.

Faustman, D. L. and M. Davis (2009). "The primacy of CD8 T lymphocytes in type 1 diabetes and implications for therapies." J Mol Med (Berl) **87**(12): 1173-8.

Fong, T. A. and T. R. Mosmann (1990). "Alloreactive murine CD8+ T cell clones secrete the Th1 pattern of cytokines." J Immunol **144**(5): 1744-52.

Fraser, I. P., H. Koziel and R. A. Ezekowitz (1998). "The serum mannose-binding protein and the macrophage mannose receptor are pattern recognition molecules that link innate and adaptive immunity." Semin Immunol **10**(5): 363-72.

Freiberg, B. A., H. Kupfer, W. Maslanik, J. Delli, J. Kappler, D. M. Zaller and A. Kupfer (2002). "Staging and resetting T cell activation in SMACs." Nat Immunol **3**(10): 911-7.

Friese, M. A. and L. Fugger (2009). "Pathogenic CD8(+) T cells in multiple sclerosis." Ann Neurol **66**(2): 132-41.

Fung-Leung, W. P., M. W. Schilham, A. Rahemtulla, T. M. Kundig, M. Vollenweider, J. Potter, W. van Ewijk and T. W. Mak (1991). "CD8 is needed for development of cytotoxic T cells but not helper T cells." Cell **65**(3): 443-9.

Gabert, J., C. Langlet, R. Zamoyska, J. R. Parnes, A. M. Schmitt-Verhulst and B. Malissen (1987). "Reconstitution of MHC class I specificity by transfer of the T cell receptor and Lyt-2 genes." Cell **50**(4): 545-54.

Gakamsky, D. M., E. Lewitzki, E. Grell, X. Saulquin, B. Malissen, F. Montero-Julian, M. Bonneville and I. Pecht (2007). "Kinetic evidence for a ligand-binding-induced conformational transition in the T cell receptor." Proc Natl Acad Sci U S A **104**(42): 16639-44.

Gakamsky, D. M., I. F. Luescher, A. Pramanik, R. B. Kopito, F. Lemonnier, H. Vogel, R. Rigler and I. Pecht (2005). "CD8 kinetically promotes ligand binding to the T-cell antigen receptor." Biophys J **89**(3): 2121-33.

Gallagher, P. F., B. Fazekas de St Groth and J. F. Miller (1989). "CD4 and CD8 molecules can physically associate with the same T-cell receptor." Proc Natl Acad Sci U S A **86**(24): 10044-8.

Gangadharan, D. and H. Cheroutre (2004). "The CD8 isoform CD8alphaalpha is not a functional homologue of the TCR co-receptor CD8alphabeta." Curr Opin Immunol **16**(3): 264-70.

Gao, G. F. and B. K. Jakobsen (2000). "Molecular interactions of coreceptor CD8 and MHC class I: the molecular basis for functional coordination with the T-cell receptor." Immunol Today **21**(12): 630-6.

Gao, G. F., J. Tormo, U. C. Gerth, J. R. Wyer, A. J. McMichael, D. I. Stuart, J. I. Bell, E. Y. Jones and B. K. Jakobsen (1997). "Crystal structure of the complex between human CD8alpha(alpha) and HLA-A2." Nature **387**(6633): 630-4.

Gao, G. F., B. E. Willcox, J. R. Wyer, J. M. Boulter, C. A. O'Callaghan, K. Maenaka, D. I. Stuart, E. Y. Jones, P. A. Van Der Merwe, J. I. Bell and B. K. Jakobsen (2000). "Classical and nonclassical class I major histocompatibility complex molecules exhibit subtle conformational differences that affect binding to CD8alphaalpha." J Biol Chem **275**(20): 15232-8.

Garboczi, D. N., P. Ghosh, U. Utz, Q. R. Fan, W. E. Biddison and D. C. Wiley (1996). "Structure of the complex between human T-cell receptor, viral peptide and HLA-A2." Nature **384**(6605): 134-41.

Garcia, K. C., C. A. Scott, A. Brunmark, F. R. Carbone, P. A. Peterson, I. A. Wilson and L. Teyton (1996). "CD8 enhances formation of stable T-cell receptor/MHC class I molecule complexes." Nature **384**(6609): 577-81.

Gay, D., C. Coeshott, W. Golde, J. Kappler and P. Marrack (1986). "The major histocompatibility complex-restricted antigen receptor on T cells. IX. Role of accessory molecules in recognition of antigen plus isolated IA." J Immunol **136**(6): 2026-32.

Gibbings, D. and A. D. Befus (2009). "CD4 and CD8: an inside-out coreceptor model for innate immune cells." J Leukoc Biol **86**(2): 251-9.

Gostick, E., D. K. Cole, S. L. Hutchinson, L. Wooldridge, S. Tafuro, B. Laugel, A. Lissina, A. Oxenius, J. M. Boulter, D. A. Price and A. K. Sewell (2007). "Functional and biophysical characterization of an HLA-A*6801-restricted HIV-specific T cell receptor." Eur J Immunol **37**(2): 479-86.

Graham, F. L., J. Smiley, W. C. Russell and R. Nairn (1977). "Characteristics of a human cell line transformed by DNA from human adenovirus type 5." J Gen Virol **36**(1): 59-74.

Grakoui, A., S. K. Bromley, C. Sumen, M. M. Davis, A. S. Shaw, P. M. Allen and M. L. Dustin (1999). "The immunological synapse: a molecular machine controlling T cell activation." Science **285**(5425): 221-7.

Gras, S., S. R. Burrows, L. Kjer-Nielsen, C. S. Clements, Y. C. Liu, L. C. Sullivan, M. J. Bell, A. G. Brooks, A. W. Purcell, J. McCluskey and J. Rossjohn (2009). "The shaping of T cell receptor recognition by self-tolerance." Immunity **30**(2): 193-203.

Gras, S., Z. Chen, J. J. Miles, Y. C. Liu, M. J. Bell, L. C. Sullivan, L. Kjer-Nielsen, R. M. Brennan, J. M. Burrows, M. A. Neller, R. Khanna, A. W. Purcell, A. G. Brooks, J.

McCluskey, J. Rossjohn and S. R. Burrows (2010). "Allelic polymorphism in the T cell receptor and its impact on immune responses." J Exp Med **207**(7): 1555-67.

Gras, S., X. Saulquin, J. B. Reiser, E. Debeaupuis, K. Echasserieau, A. Kissenpfennig, F. Legoux, A. Chouquet, M. Le Gorrec, P. Machillot, B. Neveu, N. Thielens, B. Malissen, M. Bonneville and D. Housset (2009). "Structural bases for the affinity-driven selection of a public TCR against a dominant human cytomegalovirus epitope." J Immunol **183**(1): 430-7.

Grebe, K. M., R. L. Clarke and T. A. Potter (2004). "Ligation of CD8 leads to apoptosis of thymocytes that have not undergone positive selection." Proc Natl Acad Sci U S A **101**(28): 10410-5.

Green, K. J., J. J. Miles, J. Tellam, W. J. van Zuylen, G. Connolly and S. R. Burrows (2004). "Potent T cell response to a class I-binding 13-mer viral epitope and the influence of HLA micropolymorphism in controlling epitope length." Eur J Immunol **34**(9): 2510-9.

Guttinger, M., M. Gassmann, K. E. Amrein and P. Burn (1992). "CD45 phosphotyrosine phosphatase and p56lck protein tyrosine kinase: a functional complex crucial in T cell signal transduction." Int Immunol **4**(11): 1325-30.

Hampl, J., Y. H. Chien and M. M. Davis (1997). "CD4 augments the response of a T cell to agonist but not to antagonist ligands." Immunity **7**(3): 379-85.

Harder, T. and M. Kuhn (2000). "Selective accumulation of raft-associated membrane protein LAT in T cell receptor signaling assemblies." J Cell Biol **151**(2): 199-208.

Harty, J. T., A. R. Tvinnereim and D. W. White (2000). "CD8+ T cell effector mechanisms in resistance to infection." Annu Rev Immunol **18**: 275-308.

Hasegawa, K., F. Martin, G. Huang, D. Tumas, L. Diehl and A. C. Chan (2004). "PEST domain-enriched tyrosine phosphatase (PEP) regulation of effector/memory T cells." Science **303**(5658): 685-9.

Hausmann, S., M. Martin, L. Gauthier and K. W. Wucherpfennig (1999). "Structural features of autoreactive TCR that determine the degree of degeneracy in peptide recognition." J Immunol **162**(1): 338-44.

Hemmer, B., B. T. Fleckenstein, M. Vergelli, G. Jung, H. McFarland, R. Martin and K. H. Wiesmuller (1997). "Identification of high potency microbial and self ligands for a human autoreactive class II-restricted T cell clone." J Exp Med **185**(9): 1651-9.

Hennecke, J. and D. C. Wiley (2001). "T cell receptor-MHC interactions up close." Cell **104**(1): 1-4.

Hermiston, M. L., Z. Xu and A. Weiss (2003). "CD45: a critical regulator of signaling thresholds in immune cells." Annu Rev Immunol **21**: 107-37.

Herold, K. C., J. B. Burton, F. Francois, E. Poumian-Ruiz, M. Glandt and J. A. Bluestone (2003). "Activation of human T cells by FcR nonbinding anti-CD3 mAb, hOKT3gamma1(Ala-Ala)." J Clin Invest **111**(3): 409-18.

Herold, K. C., S. Gitelman, C. Greenbaum, J. Puck, W. Hagopian, P. Gottlieb, P. Sayre, P. Bianchine, E. Wong, V. Seyfert-Margolis, K. Bourcier and J. A. Bluestone (2009). "Treatment of patients with new onset Type 1 diabetes with a single course of anti-CD3 mAb Teplizumab preserves insulin production for up to 5 years." Clin Immunol **132**(2): 166-73.

Herold, K. C., W. Hagopian, J. A. Auger, E. Poumian-Ruiz, L. Taylor, D. Donaldson, S. E. Gitelman, D. M. Harlan, D. Xu, R. A. Zivin and J. A. Bluestone (2002). "Anti-CD3 monoclonal antibody in new-onset type 1 diabetes mellitus." N Engl J Med **346**(22): 1692-8.

Heusel, J. W., R. L. Wesselschmidt, S. Shresta, J. H. Russell and T. J. Ley (1994). "Cytotoxic lymphocytes require granzyme B for the rapid induction of DNA fragmentation and apoptosis in allogeneic target cells." Cell **76**(6): 977-87.

Hiemstra, H. S., P. A. van Veelen, S. J. Willemen, W. E. Benckhuijsen, A. Geluk, R. R. de Vries, B. O. Roep and J. W. Drijfhout (1999). "Quantitative determination of TCR cross-reactivity using peptide libraries and protein databases." Eur J Immunol **29**(8): 2385-91.

Holler, P. D., P. O. Holman, E. V. Shusta, S. O'Herrin, K. D. Wittrup and D. M. Kranz (2000). "In vitro evolution of a T cell receptor with high affinity for peptide/MHC." Proc Natl Acad Sci U S A **97**(10): 5387-92.

Holler, P. D. and D. M. Kranz (2003). "Quantitative analysis of the contribution of TCR/pepMHC affinity and CD8 to T cell activation." Immunity **18**(2): 255-64.

Holler, P. D., A. R. Lim, B. K. Cho, L. A. Rund and D. M. Kranz (2001). "CD8(-) T cell transfectants that express a high affinity T cell receptor exhibit enhanced peptide-dependent activation." J Exp Med **194**(8): 1043-52.

Hoo, W. S. and D. M. Kranz (1993). "Role of CD8 in staphylococcal enterotoxin B-mediated lysis by cytotoxic T lymphocytes." J Immunol **150**(10): 4331-7.

Howard, F. D., P. Moingeon, U. Moebius, D. J. McConkey, B. Yandava, T. E. Gennert and E. L. Reinherz (1992). "The CD3 zeta cytoplasmic domain mediates CD2-induced T cell activation." J Exp Med **176**(1): 139-45.

Howarth, M., A. Williams, A. B. Tolstrup and T. Elliott (2004). "Tapasin enhances MHC class I peptide presentation according to peptide half-life." Proc Natl Acad Sci U S A **101**(32): 11737-42.

Huesmann, M., B. Scott, P. Kisielow and H. von Boehmer (1991). "Kinetics and efficacy of positive selection in the thymus of normal and T cell receptor transgenic mice." Cell **66**(3): 533-40.

Huseby, E. S., P. G. Huseby, S. Shah, R. Smith and B. D. Stadinski (2012). "Pathogenic CD8 T cells in multiple sclerosis and its experimental models." Front Immunol **3**: 64.

Hutchinson, S. L., L. Wooldridge, S. Tafuro, B. Laugel, M. Glick, J. M. Boulter, B. K. Jakobsen, D. A. Price and A. K. Sewell (2003). "The CD8 T cell coreceptor exhibits disproportionate biological activity at extremely low binding affinities." J Biol Chem **278**(27): 24285-93.

Irie, H. Y., K. S. Ravichandran and S. J. Burakoff (1995). "CD8 beta chain influences CD8 alpha chain-associated Lck kinase activity." J Exp Med **181**(4): 1267-73.

Irvine, D. J., M. A. Purbhoo, M. Krogsgaard and M. M. Davis (2002). "Direct observation of ligand recognition by T cells." Nature **419**(6909): 845-9.

Ishizuka, J., K. Grebe, E. Shenderov, B. Peters, Q. Chen, Y. Peng, L. Wang, T. Dong, V. Pasquetto, C. Oseroff, J. Sidney, H. Hickman, V. Cerundolo, A. Sette, J. R. Bennink, A. McMichael and J. W. Yewdell (2009). "Quantitating T cell cross-reactivity for unrelated peptide antigens." J Immunol **183**(7): 4337-45.

Iwashima, M., B. A. Irving, N. S. van Oers, A. C. Chan and A. Weiss (1994). "Sequential interactions of the TCR with two distinct cytoplasmic tyrosine kinases." Science **263**(5150): 1136-9.

Janes, P. W., S. C. Ley, A. I. Magee and P. S. Kabouridis (2000). "The role of lipid rafts in T cell antigen receptor (TCR) signalling." Semin Immunol **12**(1): 23-34.

Janeway, C. A., Jr. (1988). "T-cell development. Accessories or coreceptors?" Nature **335**(6187): 208-10.

Janeway, C. A., Jr. (1989). "The role of CD4 in T-cell activation: accessory molecule or co-receptor?" Immunol Today **10**(7): 234-8.

Janeway, C. A., Jr. (1992). "The T cell receptor as a multicomponent signalling machine: CD4/CD8 coreceptors and CD45 in T cell activation." Annu Rev Immunol **10**: 645-74.

Janeway, C. A., Jr. and R. Medzhitov (2002). "Innate immune recognition." Annu Rev Immunol **20**: 197-216.

Janeway, C. A., Jr., K. Murphy, P. Travers and M. Walport (2008). ImmunoBiology, Garland Science.

Jiang, N., J. Huang, L. J. Edwards, B. Liu, Y. Zhang, C. D. Beal, B. D. Evavold and C. Zhu (2010). "Two-stage cooperative T cell receptor-peptide major histocompatibility complex-CD8 trimolecular interactions amplify antigen discrimination." Immunity **34**(1): 13-23.

Jonsson, J. I., N. W. Boyce and K. Eichmann (1989). "Immunoregulation through CD8 (Ly-2): state of aggregation with the alpha/beta/CD3 T cell receptor controls interleukin 2-dependent T cell growth." Eur J Immunol **19**(2): 253-60.

Kabelitz, D. and O. Janssen (1997). "Antigen-induced death of T-lymphocytes." Front Biosci **2**: d61-77.

Kabelitz, D., D. Wesch and W. He (2007). "Perspectives of gammadelta T cells in tumor immunology." Cancer Res **67**(1): 5-8.

Kabouridis, P. S., A. I. Magee and S. C. Ley (1997). "S-acylation of LCK protein tyrosine kinase is essential for its signalling function in T lymphocytes." Embo J **16**(16): 4983-98.

Kan-Mitchell, J., M. Bajcz, K. L. Schaubert, D. A. Price, J. M. Brenchley, T. E. Asher, D. C. Douek, H. L. Ng, O. O. Yang, C. R. Rinaldo, Jr., J. M. Benito, B. Bisikirska, R.

Hegde, F. M. Marincola, C. Boggiano, D. Wilson, J. Abrams, S. E. Blondelle and D. B. Wilson (2006). "Degeneracy and repertoire of the human HIV-1 Gag p17(77-85) CTL response." J Immunol **176**(11): 6690-701.

Kappler, J. W., N. Roehm and P. Marrack (1987). "T cell tolerance by clonal elimination in the thymus." Cell **49**(2): 273-80.

Karaki, S., M. Tanabe, H. Nakauchi and M. Takiguchi (1992). "Beta-chain broadens range of CD8 recognition for MHC class I molecule." J Immunol **149**(5): 1613-8.

Kelso, A. and A. L. Glasebrook (1984). "Secretion of interleukin 2, macrophage-activating factor, interferon, and colony-stimulating factor by alloreactive T lymphocyte clones." J Immunol **132**(6): 2924-31.

Kern, P., R. E. Hussey, R. Spoerl, E. L. Reinherz and H. C. Chang (1999). "Expression, purification, and functional analysis of murine ectodomain fragments of CD8alphaalpha and CD8alphabeta dimers." J Biol Chem **274**(38): 27237-43.

Kern, P. S., M. K. Teng, A. Smolyar, J. H. Liu, J. Liu, R. E. Hussey, R. Spoerl, H. C. Chang, E. L. Reinherz and J. H. Wang (1998). "Structural basis of CD8 coreceptor function revealed by crystallographic analysis of a murine CD8alphaalpha ectodomain fragment in complex with H-2Kb." Immunity **9**(4): 519-30.

Kersh, E. N., A. S. Shaw and P. M. Allen (1998). "Fidelity of T cell activation through multistep T cell receptor zeta phosphorylation." Science **281**(5376): 572-5.

Kersh, G. J. and P. M. Allen (1996). "Essential flexibility in the T-cell recognition of antigen." Nature **380**(6574): 495-8.

Kersh, G. J., E. N. Kersh, D. H. Fremont and P. M. Allen (1998). "High- and low-potency ligands with similar affinities for the TCR: the importance of kinetics in TCR signaling." Immunity **9**(6): 817-26.

Keymeulen, B., E. Vandemeulebroucke, A. G. Ziegler, C. Mathieu, L. Kaufman, G. Hale, F. Gorus, M. Goldman, M. Walter, S. Candon, L. Schandene, L. Crenier, C. De Block, J. M. Seigneurin, P. De Pauw, D. Pierard, I. Weets, P. Rebello, P. Bird, E. Berrie, M. Frewin, H. Waldmann, J. F. Bach, D. Pipeleers and L. Chatenoud (2005). "Insulin needs after CD3-antibody therapy in new-onset type 1 diabetes." N Engl J Med **352**(25): 2598-608.

Kim, P. W., Z. Y. Sun, S. C. Blacklow, G. Wagner and M. J. Eck (2003). "A zinc clasp structure tethers Lck to T cell coreceptors CD4 and CD8." Science **301**(5640): 1725-8.

Kim, S. T., Y. Shin, K. Brazin, R. J. Mallis, Z. J. Sun, G. Wagner, M. J. Lang and E. Reinherz (2012). "TCR mechanobiology: torques and tunable structures linked to early T cell signaling." Frontiers in Tcell Biology **3**(76).

Kim, T. K., M. J. Billard, E. D. Wieder, B. W. McIntyre and K. V. Komanduri (2010). "Co-engagement of alpha(4)beta(1) integrin (VLA-4) and CD4 or CD8 is necessary to induce maximal Erk1/2 phosphorylation and cytokine production in human T cells." Hum Immunol **71**(1): 23-8.

Kissler, S., S. M. Anderton and D. C. Wraith (2002). "Cross-reactivity and T-cell receptor antagonism of myelin basic protein-reactive T cells is modulated by the activation state of the antigen presenting cell." J Autoimmun **19**(4): 183-93.

Kjer-Nielsen, L., C. S. Clements, A. W. Purcell, A. G. Brooks, J. C. Whisstock, S. R. Burrows, J. McCluskey and J. Rossjohn (2003). "A structural basis for the selection of dominant alphabeta T cell receptors in antiviral immunity." Immunity **18**(1): 53-64.

Knight, R. R., D. Kronenberg, M. Zhao, G. C. Huang, M. Eichmann, A. Bulek, L. Wooldridge, D. K. Cole, A. K. Sewell, M. Peakman and A. Skowera (2012). "Human beta-Cell Killing by Autoreactive Preproinsulin-Specific CD8 T Cells Is Predominantly Granule-Mediated With the Potency Dependent Upon T-Cell Receptor Avidity." Diabetes.

Koyasu, S., D. J. McConkey, L. K. Clayton, S. Abraham, B. Yandava, T. Katagiri, P. Moingeon, T. Yamamoto and E. L. Reinherz (1992). "Phosphorylation of multiple CD3 zeta tyrosine residues leads to formation of pp21 in vitro and in vivo. Structural changes upon T cell receptor stimulation." J Biol Chem **267**(5): 3375-81.

Krogsgaard, M., Q. J. Li, C. Sumen, J. B. Huppa, M. Huse and M. M. Davis (2005). "Agonist/endogenous peptide-MHC heterodimers drive T cell activation and sensitivity." Nature **434**(7030): 238-43.

Krummel, M. F., M. D. Sjaastad, C. Wulfing and M. M. Davis (2000). "Differential clustering of CD4 and CD3zeta during T cell recognition." Science **289**(5483): 1349-52.

Kuhns, M. S. and M. M. Davis (2007). "Disruption of extracellular interactions impairs T cell receptor-CD3 complex stability and signaling." Immunity **26**(3): 357-69.

Kuhns, M. S., M. M. Davis and K. C. Garcia (2006). "Deconstructing the form and function of the TCR/CD3 complex." Immunity **24**(2): 133-9.

Kung, P., G. Goldstein, E. L. Reinherz and S. F. Schlossman (1979). "Monoclonal antibodies defining distinctive human T cell surface antigens." Science **206**(4416): 347-9.

Lange, G., S. J. Lewis, G. N. Murshudov, G. G. Dodson, P. C. Moody, J. P. Turkenburg, A. N. Barclay and R. L. Brady (1994). "Crystal structure of an extracellular fragment of the rat CD4 receptor containing domains 3 and 4." Structure **2**(6): 469-81.

Langlet, C., A. M. Bernard, P. Drevot and H. T. He (2000). "Membrane rafts and signaling by the multichain immune recognition receptors." Curr Opin Immunol **12**(3): 250-5.

Latour, S. and A. Veillette (2001). "Proximal protein tyrosine kinases in immunoreceptor signaling." Curr Opin Immunol **13**(3): 299-306.

Laugel, B., J. M. Boulter, N. Lissin, A. Vuidepot, Y. Li, E. Gostick, L. E. Crotty, D. C. Douek, J. Hemelaar, D. A. Price, B. K. Jakobsen and A. K. Sewell (2005). "Design of soluble recombinant T cell receptors for antigen targeting and T cell inhibition." J Biol Chem **280**(3): 1882-92.

Laugel, B., D. K. Cole, M. Clement, L. Wooldridge, D. A. Price and A. K. Sewell (2011). "The multiple roles of the CD8 coreceptor in T cell biology: opportunities for the selective modulation of self-reactive cytotoxic T cells." J Leukoc Biol **90**(6): 1089-99.

Laugel, B., H. A. van den Berg, E. Gostick, D. K. Cole, L. Wooldridge, J. Boulter, A. Milicic, D. A. Price and A. K. Sewell (2007). "Different T cell receptor affinity thresholds and CD8 coreceptor dependence govern cytotoxic T lymphocyte activation and tetramer binding properties." J Biol Chem **282**(33): 23799-810.

Ledbetter, J. A., W. E. Seaman, T. T. Tsu and L. A. Herzenberg (1981). "Lyt-2 and lyt-3 antigens are on two different polypeptide subunits linked by disulfide bonds. Relationship of subunits to T cell cytolytic activity." J Exp Med **153**(6): 1503-16.

Lee, J. K., G. Stewart-Jones, T. Dong, K. Harlos, K. Di Gleria, L. Dorrell, D. C. Douek, P. A. van der Merwe, E. Y. Jones and A. J. McMichael (2004). "T cell cross-reactivity and conformational changes during TCR engagement." J Exp Med **200**(11): 1455-66.

Lee, K. H., A. D. Holdorf, M. L. Dustin, A. C. Chan, P. M. Allen and A. S. Shaw (2002). "T cell receptor signaling precedes immunological synapse formation." Science **295**(5559): 1539-42.

Lee, P. U. and D. M. Kranz (2003). "Allogeneic and syngeneic class I MHC complexes drive the association of CD8 and TCR on 2C T cells." Mol Immunol **39**(12): 687-95.

Lefranc, M. P. and G. Lefranc (2001). The T cell receptor FactsBook. London, Academic Press.

Leishman, A. J., O. V. Naidenko, A. Attinger, F. Koning, C. J. Lena, Y. Xiong, H. C. Chang, E. Reinherz, M. Kronenberg and H. Cheroutre (2001). "T cell responses modulated through interaction between CD8alphaalpha and the nonclassical MHC class I molecule, TL." Science **294**(5548): 1936-9.

Li, Y. C., B. M. Chen, P. C. Wu, T. L. Cheng, L. S. Kao, M. H. Tao, A. Lieber and S. R. Roffler (2010). "Cutting Edge: mechanical forces acting on T cells immobilized via the TCR complex can trigger TCR signaling." J Immunol **184**(11): 5959-63.

Lissina, A., K. Ladell, A. Skowera, M. Clement, E. Edwards, R. Seggewiss, H. A. van den Berg, E. Gostick, K. Gallagher, E. Jones, J. J. Melenhorst, A. J. Godkin, M. Peakman, D. A. Price, A. K. Sewell and L. Wooldridge (2009). "Protein kinase inhibitors substantially improve the physical detection of T-cells with peptide-MHC tetramers." J Immunol Methods **340**(1): 11-24.

Liu, Y., Y. Xiong, O. V. Naidenko, J. H. Liu, R. Zhang, A. Joachimiak, M. Kronenberg, H. Cheroutre, E. L. Reinherz and J. H. Wang (2003). "The crystal structure of a TL/CD8alphaalpha complex at 2.1 A resolution: implications for modulation of T cell activation and memory." Immunity **18**(2): 205-15.

Locksley, R. M., S. L. Reiner, F. Hatam, D. R. Littman and N. Killeen (1993). "Helper T cells without CD4: control of leishmaniasis in CD4-deficient mice." Science **261**(5127): 1448-51.

Love, P. E., E. W. Shores, E. J. Lee, A. Grinberg, T. I. Munitz, H. Westphal and A. Singer (1994). "Differential effects of zeta and eta transgenes on early alpha/beta T cell development." J Exp Med **179**(5): 1485-94.

Luhder, F., Y. Huang, K. M. Dennehy, C. Guntermann, I. Muller, E. Winkler, T. Kerkau, S. Ikemizu, S. J. Davis, T. Hanke and T. Hunig (2003). "Topological requirements and

signaling properties of T cell-activating, anti-CD28 antibody superagonists." J Exp Med **197**(8): 955-66.

Luo, K. X. and B. M. Sefton (1990). "Cross-linking of T-cell surface molecules CD4 and CD8 stimulates phosphorylation of the lck tyrosine protein kinase at the autophosphorylation site." Mol Cell Biol **10**(10): 5305-13.

Ma, Y., U. Pannicke, K. Schwarz and M. R. Lieber (2002). "Hairpin opening and overhang processing by an Artemis/DNA-dependent protein kinase complex in nonhomologous end joining and V(D)J recombination." Cell **108**(6): 781-94.

MacDonald, H. R., A. L. Glasebrook and J. C. Cerottini (1982). "Clonal heterogeneity in the functional requirement for Lyt-2/3 molecules on cytolytic T lymphocytes: analysis by antibody blocking and selective trypsinization." J Exp Med **156**(6): 1711-22.

Macdonald, W. A., Z. Chen, S. Gras, J. K. Archbold, F. E. Tynan, C. S. Clements, M. Bharadwaj, L. Kjer-Nielsen, P. M. Saunders, M. C. Wilce, F. Crawford, B. Stadinsky, D. Jackson, A. G. Brooks, A. W. Purcell, J. W. Kappler, S. R. Burrows, J. Rossjohn and J. McCluskey (2009). "T cell allorecognition via molecular mimicry." Immunity **31**(6): 897-908.

Madakamutil, L. T., U. Christen, C. J. Lena, Y. Wang-Zhu, A. Attinger, M. Sundarrajan, W. Ellmeier, M. G. von Herrath, P. Jensen, D. R. Littman and H. Cheroutre (2004). "CD8alphaalpha-mediated survival and differentiation of CD8 memory T cell precursors." Science **304**(5670): 590-3.

Madrenas, J., L. A. Chau, J. Smith, J. A. Bluestone and R. N. Germain (1997). "The efficiency of CD4 recruitment to ligand-engaged TCR controls the agonist/partial agonist properties of peptide-MHC molecule ligands." J Exp Med **185**(2): 219-29.

Maile, R., C. A. Siler, S. E. Kerry, K. E. Midkiff, E. J. Collins and J. A. Frelinger (2005). "Peripheral "CD8 tuning" dynamically modulates the size and responsiveness of an antigen-specific T cell pool in vivo." J Immunol **174**(2): 619-27.

Mak, T. W. and M. Saunders (2005). The Immune Response: Basic and Clinical Principles.

Malissen, B., E. Aguado and M. Malissen (2005). "Role of the LAT adaptor in T-cell development and Th2 differentiation." Adv Immunol **87**: 1-25.

Mallaun, M., D. Naeher, M. A. Daniels, P. P. Yachi, B. Hausmann, I. F. Luescher, N. R. Gascoigne and E. Palmer (2008). "The T cell receptor's alpha-chain connecting

peptide motif promotes close approximation of the CD8 coreceptor allowing efficient signal initiation." J Immunol **180**(12): 8211-21.

Mamalaki, C., J. Elliott, T. Norton, N. Yannoutsos, A. R. Townsend, P. Chandler, E. Simpson and D. Kioussis (1993). "Positive and negative selection in transgenic mice expressing a T-cell receptor specific for influenza nucleoprotein and endogenous superantigen." Dev Immunol **3**(3): 159-74.

Manz, B. N., B. L. Jackson, R. S. Petit, M. L. Dustin and J. Groves (2011). "T-cell triggering thresholds are modulated by the number of antigen within individual T-cell receptor clusters." Proc Natl Acad Sci U S A **108**(22): 9089-94.

Marrack, P., R. Endres, R. Shimonkevitz, A. Zlotnik, D. Dialynas, F. Fitch and J. Kappler (1983). "The major histocompatibility complex-restricted antigen receptor on T cells. II. Role of the L3T4 product." J Exp Med **158**(4): 1077-91.

Marsh, S. G. E., Parham, P., Barber, L.D. (2000). The HLA FactsBook. London, Academic Press.

Mason, D. W. and A. F. Williams (1980). "The kinetics of antibody binding to membrane antigens in solution and at the cell surface." Biochem J **187**(1): 1-20.

Maynard, J., K. Petersson, D. H. Wilson, E. J. Adams, S. E. Blondelle, M. J. Boulanger, D. B. Wilson and K. C. Garcia (2005). "Structure of an autoimmune T cell receptor complexed with class II peptide-MHC: insights into MHC bias and antigen specificity." Immunity **22**(1): 81-92.

McKeithan, T. W. (1995). "Kinetic proofreading in T-cell receptor signal transduction." Proc Natl Acad Sci U S A **92**(11): 5042-6.

McNeill, L., R. J. Salmond, J. C. Cooper, C. K. Carret, R. L. Cassady-Cain, M. Roche-Molina, P. Tandon, N. Holmes and D. R. Alexander (2007). "The differential regulation of Lck kinase phosphorylation sites by CD45 is critical for T cell receptor signaling responses." Immunity **27**(3): 425-37.

Medzhitov, R. (2007). "Recognition of microorganisms and activation of the immune response." Nature **449**(7164): 819-26.

Medzhitov, R. and C. Janeway, Jr. (2000). "Innate immunity." N Engl J Med **343**(5): 338-44.

Meuer, S. C., S. F. Schlossman and E. L. Reinherz (1982). "Clonal analysis of human cytotoxic T lymphocytes: T4+ and T8+ effector T cells recognize products of different major histocompatibility complex regions." Proc Natl Acad Sci U S A **79**(14): 4395-9.

Miceli, M. C. and J. R. Parnes (1993). "Role of CD4 and CD8 in T cell activation and differentiation." Adv Immunol **53**: 59-122.

Miles, J. J., A. M. Bulek, D. K. Cole, E. Gostick, A. J. Schauenburg, G. Dolton, V. Venturi, M. P. Davenport, M. P. Tan, S. R. Burrows, L. Wooldridge, D. A. Price, P. J. Rizkallah and A. K. Sewell (2010). "Genetic and structural basis for selection of a ubiquitous T cell receptor deployed in epstein-barr virus infection." PLoS Pathog **6**(11): e1001198.

Monks, C. R., B. A. Freiberg, H. Kupfer, N. Sciaky and A. Kupfer (1998). "Three-dimensional segregation of supramolecular activation clusters in T cells." Nature **395**(6697): 82-6.

Moody, A. M., D. Chui, P. A. Reche, J. J. Priatel, J. D. Marth and E. L. Reinherz (2001). "Developmentally regulated glycosylation of the CD8alphabeta coreceptor stalk modulates ligand binding." Cell **107**(4): 501-12.

Morgan, D. A., F. W. Ruscetti and R. Gallo (1976). "Selective in vitro growth of T lymphocytes from normal human bone marrows." Science **193**(4257): 1007-8.

Mosier, D. E. (1974). "Ontogeny of mouse lymphocyte function. I. Paradoxical elevation of reactivity to allogeneic cells and phytohemagglutinin in BALB-c fetal thymocytes." J Immunol **112**(1): 305-10.

Mosmann, T. R., L. Li and S. Sad (1997). "Functions of CD8 T-cell subsets secreting different cytokine patterns." Semin Immunol **9**(2): 87-92.

Moysey, R. K., Y. Li, S. J. Paston, E. E. Baston, M. S. Sami, B. J. Cameron, J. Gavarret, P. Todorov, A. Vuidepot, S. M. Dunn, N. J. Pumphrey, K. J. Adams, F. Yuan, R. E. Dennis, D. H. Sutton, A. D. Johnson, J. E. Brewer, R. Ashfield, N. M. Lissin and B. K. Jakobsen (2010). "High affinity soluble ILT2 receptor: a potent inhibitor of CD8(+) T cell activation." Protein Cell **1**(12): 1118-27.

Murali-Krishna, K., J. D. Altman, M. Suresh, D. J. Sourdive, A. J. Zajac, J. D. Miller, J. Slansky and R. Ahmed (1998). "Counting antigen-specific CD8 T cells: a reevaluation of bystander activation during viral infection." Immunity **8**(2): 177-87.

Mustelin, T. and K. Tasken (2003). "Positive and negative regulation of T-cell activation through kinases and phosphatases." Biochem J **371**(Pt 1): 15-27.

Naeher, D., I. F. Luescher and E. Palmer (2002). "A role for the alpha-chain connecting peptide motif in mediating TCR-CD8 cooperation." J Immunol **169**(6): 2964-70.

Nakayama, E., H. Shiku, E. Stockert, H. F. Oettgen and L. J. Old (1979). "Cytotoxic T cells: Lyt phenotype and blocking of killing activity by Lyt antisera." Proc Natl Acad Sci U S A **76**(4): 1977-81.

Nielsen, M., C. Lundegaard, P. Worning, C. S. Hvid, K. Lamberth, S. Buus, S. Brunak and O. Lund (2004). "Improved prediction of MHC class I and class II epitopes using a novel Gibbs sampling approach." Bioinformatics **20**(9): 1388-97.

Nino-Vasquez, J. J., G. Allicotti, E. Borras, D. B. Wilson, D. Valmori, R. Simon, R. Martin and C. Pinilla (2004). "A powerful combination: the use of positional scanning libraries and biometrical analysis to identify cross-reactive T cell epitopes." Mol Immunol **40**(14-15): 1063-74.

Norment, A. M. and D. R. Littman (1988). "A second subunit of CD8 is expressed in human T cells." Embo J **7**(11): 3433-9.

Norment, A. M., R. D. Salter, P. Parham, V. H. Engelhard and D. R. Littman (1988). "Cell-cell adhesion mediated by CD8 and MHC class I molecules." Nature **336**(6194): 79-81.

Ostergaard, H. L., D. A. Shackelford, T. R. Hurley, P. Johnson, R. Hyman, B. M. Sefton and I. S. Trowbridge (1989). "Expression of CD45 alters phosphorylation of the lck-encoded tyrosine protein kinase in murine lymphoma T-cell lines." Proc Natl Acad Sci U S A **86**(22): 8959-63.

Ostergaard, H. L. and I. S. Trowbridge (1990). "Coclustering CD45 with CD4 or CD8 alters the phosphorylation and kinase activity of p56lck." J Exp Med **172**(1): 347-50.

Palacios, E. H. and A. Weiss (2004). "Function of the Src-family kinases, Lck and Fyn, in T-cell development and activation." Oncogene **23**(48): 7990-8000.

Pamer, E. and P. Cresswell (1998). "Mechanisms of MHC class I--restricted antigen processing." Annu Rev Immunol **16**: 323-58.

Pancer, Z. and M. D. Cooper (2006). "The evolution of adaptive immunity." Annu Rev Immunol **24**: 497-518.

Parish, N. and A. Cooke (2005). "Characterisation of CD8 monoclonal antibody-induced protection from diabetes in NOD mice." Autoimmunity **38**(8): 597-604.

Parish, N. M., L. Bowie, S. Zusman Harach, J. M. Phillips and A. Cooke (1998). "Thymus-dependent monoclonal antibody-induced protection from transferred diabetes." Eur J Immunol **28**(12): 4362-73.

Park, J. H., S. Adoro, T. Guinter, B. Erman, A. S. Alag, M. Catalfamo, M. Y. Kimura, Y. Cui, P. J. Lucas, R. E. Gress, M. Kubo, L. Hennighausen, L. Feigenbaum and A. Singer (2007). "Signaling by intrathymic cytokines, not T cell antigen receptors, specifies CD8 lineage choice and promotes the differentiation of cytotoxic-lineage T cells." Nat Immunol **11**(3): 257-64.

Park, J. H., S. Adoro, P. J. Lucas, S. D. Sarafova, A. S. Alag, L. L. Doan, B. Erman, X. Liu, W. Ellmeier, R. Bosselut, L. Feigenbaum and A. Singer (2007). "'Coreceptor tuning': cytokine signals transcriptionally tailor CD8 coreceptor expression to the self-specificity of the TCR." Nat Immunol **8**(10): 1049-59.

Parkin, J. and B. Cohen (2001). "An overview of the immune system." Lancet **357**(9270): 1777-89.

Parnes, J. R. (1989). "Molecular biology and function of CD4 and CD8." Adv Immunol **44**: 265-311.

Peaper, D. R. and P. Cresswell (2008). "Regulation of MHC class I assembly and peptide binding." Annu Rev Cell Dev Biol **24**: 343-68.

Pfleger, K. D., R. M. Seeber and K. A. Eidne (2006). "Bioluminescence resonance energy transfer (BRET) for the real-time detection of protein-protein interactions." Nat Protoc **1**(1): 337-45.

Phillips, J. M., N. M. Parish, T. Raine, C. Bland, Y. Sawyer, H. De La Pena and A. Cooke (2009). "Type 1 diabetes development requires both CD4+ and CD8+ T cells and can be reversed by non-depleting antibodies targeting both T cell populations." Rev Diabet Stud **6**(2): 97-103.

Pipkin, M. E. and J. Lieberman (2007). "Delivering the kiss of death: progress on understanding how perforin works." Curr Opin Immunol **19**(3): 301-8.

Podack, E. R., P. J. Konigsberg, H. Acha-Orbea, H. Pircher and H. Hengartner (1985). "Cytolytic T-cell granules: biochemical properties and functional specificity." Adv Exp Med Biol **184**: 99-119.

Potter, T. A., T. V. Rajan, R. F. Dick, 2nd and J. A. Bluestone (1989). "Substitution at residue 227 of H-2 class I molecules abrogates recognition by CD8-dependent, but not CD8-independent, cytotoxic T lymphocytes." Nature **337**(6202): 73-5.

Price, D. A., J. M. Brenchley, L. E. Ruff, M. R. Betts, B. J. Hill, M. Roederer, R. A. Koup, S. A. Migueles, E. Gostick, L. Wooldridge, A. K. Sewell, M. Connors and D. C. Douek (2005). "Avidity for antigen shapes clonal dominance in CD8+ T cell populations specific for persistent DNA viruses." J Exp Med **202**(10): 1349-61.

Price, D. A., A. K. Sewell, T. Dong, R. Tan, P. J. Goulder, S. L. Rowland-Jones and R. E. Phillips (1998). "Antigen-specific release of beta-chemokines by anti-HIV-1 cytotoxic T lymphocytes." Curr Biol **8**(6): 355-8.

Prinz, J. C. (2003). "The role of T cells in psoriasis." J Eur Acad Dermatol Venereol **17**(3): 257-70.

Purbhoo, M. A., J. M. Boulter, D. A. Price, A. L. Vuidepot, C. S. Hourigan, P. R. Dunbar, K. Olson, S. J. Dawson, R. E. Phillips, B. K. Jakobsen, J. I. Bell and A. K. Sewell (2001). "The human CD8 coreceptor effects cytotoxic T cell activation and antigen sensitivity primarily by mediating complete phosphorylation of the T cell receptor zeta chain." J Biol Chem **276**(35): 32786-92.

Purbhoo, M. A., D. J. Irvine, J. B. Huppa and M. M. Davis (2004). "T cell killing does not require the formation of a stable mature immunological synapse." Nat Immunol **5**(5): 524-30.

Purbhoo, M. A., Y. Li, D. H. Sutton, J. E. Brewer, E. Gostick, G. Bossi, B. Laugel, R. Moysey, E. Baston, N. Liddy, B. Cameron, A. D. Bennett, R. Ashfield, A. Milicic, D. A. Price, B. J. Classon, A. K. Sewell and B. K. Jakobsen (2007). "The HLA A*0201-restricted hTERT(540-548) peptide is not detected on tumor cells by a CTL clone or a high-affinity T-cell receptor." Mol Cancer Ther **6**(7): 2081-91.

Purcell, A. W. and T. Elliott (2008). "Molecular machinations of the MHC-I peptide loading complex." Curr Opin Immunol **20**(1): 75-81.

Rabinowitz, J. D., C. Beeson, D. S. Lyons, M. M. Davis and H. M. McConnell (1996). "Kinetic discrimination in T-cell activation." Proc Natl Acad Sci U S A **93**(4): 1401-5.

Rahemtulla, A., W. P. Fung-Leung, M. W. Schilham, T. M. Kundig, S. R. Sambhara, A. Narendran, A. Arabian, A. Wakeham, C. J. Paige, R. M. Zinkernagel and et al. (1991). "Normal development and function of CD8+ cells but markedly decreased helper cell activity in mice lacking CD4." Nature **353**(6340): 180-4.

Rammensee, H., J. Bachmann, N. P. Emmerich, O. A. Bachor and S. Stevanovic (1999). "SYFPEITHI: database for MHC ligands and peptide motifs." Immunogenetics **50**(3-4): 213-9.

Rammensee, H. G. (1995). "Chemistry of peptides associated with MHC class I and class II molecules." Curr Opin Immunol **7**(1): 85-96.

Rammohan, K. W. and J. Shoemaker (2010). "Emerging multiple sclerosis oral therapies." Neurology **74 Suppl 1**: S47-53.

Reay, P. A., R. M. Kantor and M. M. Davis (1994). "Use of global amino acid replacements to define the requirements for MHC binding and T cell recognition of moth cytochrome c (93-103)." J Immunol **152**(8): 3946-57.

Renard, V., J. Delon, I. F. Luescher, B. Malissen, E. Vivier and A. Trautmann (1996). "The CD8 beta polypeptide is required for the recognition of an altered peptide ligand as an agonist." Eur J Immunol **26**(12): 2999-3007.

Renard, V., P. Romero, E. Vivier, B. Malissen and I. F. Luescher (1996). "CD8 beta increases CD8 coreceptor function and participation in TCR-ligand binding." J Exp Med **184**(6): 2439-44.

Resh, M. D. (1994). "Myristylation and palmitylation of Src family members: the fats of the matter." Cell **76**(3): 411-3.

Resh, M. D. and H. P. Ling (1990). "Identification of a 32K plasma membrane protein that binds to the myristylated amino-terminal sequence of p60v-src." Nature **346**(6279): 84-6.

Reth, M. (1989). "Antigen receptor tail clue." Nature **338**(6214): 383-4.

Rock, K. L., C. Gramm, L. Rothstein, K. Clark, R. Stein, L. Dick, D. Hwang and A. L. Goldberg (1994). "Inhibitors of the proteasome block the degradation of most cell proteins and the generation of peptides presented on MHC class I molecules." Cell **78**(5): 761-71.

Roep, B. O. and M. Peakman (2011). "Diabetogenic T lymphocytes in human Type 1 diabetes." Curr Opin Immunol **23**(6): 746-53.

Rudd, C. E., J. M. Trevillyan, J. D. Dasgupta, L. L. Wong and S. F. Schlossman (1988). "The CD4 receptor is complexed in detergent lysates to a protein-tyrosine kinase (pp58) from human T lymphocytes." Proc Natl Acad Sci U S A **85**(14): 5190-4.

Rudensky, A., P. Preston-Hurlburt, S. C. Hong, A. Barlow and C. A. Janeway, Jr. (1991). "Sequence analysis of peptides bound to MHC class II molecules." Nature **353**(6345): 622-7.

Rudolph, M. G., R. L. Stanfield and I. A. Wilson (2006). "How TCRs bind MHCs, peptides, and coreceptors." Annu Rev Immunol **24**: 419-66.

Rudolph, M. G. and I. A. Wilson (2002). "The specificity of TCR/pMHC interaction." Curr Opin Immunol **14**(1): 52-65.

Sadasivan, B., P. J. Lehner, B. Ortmann, T. Spies and P. Cresswell (1996). "Roles for calreticulin and a novel glycoprotein, tapasin, in the interaction of MHC class I molecules with TAP." Immunity **5**(2): 103-14.

Sadegh-Nasseri, S., M. Chen, K. Narayan and M. Bouvier (2008). "The convergent roles of tapasin and HLA-DM in antigen presentation." Trends Immunol **29**(3): 141-7.

Sakaguchi, N., T. Takahashi, H. Hata, T. Nomura, T. Tagami, S. Yamazaki, T. Sakihama, T. Matsutani, I. Negishi, S. Nakatsuru and S. Sakaguchi (2003). "Altered thymic T-cell selection due to a mutation of the ZAP-70 gene causes autoimmune arthritis in mice." Nature **426**(6965): 454-60.

Salgame, P., J. S. Abrams, C. Clayberger, H. Goldstein, J. Convit, R. L. Modlin and B. R. Bloom (1991). "Differing lymphokine profiles of functional subsets of human CD4 and CD8 T cell clones." Science **254**(5029): 279-82.

Salio, M., M. J. Palmowski, A. Atzberger, I. F. Hermans and V. Cerundolo (2004). "CpG-matured murine plasmacytoid dendritic cells are capable of in vivo priming of

functional CD8 T cell responses to endogenous but not exogenous antigens." J Exp Med **199**(4): 567-79.

Salmond, R. J., A. Filby, I. Qureshi, S. Caserta and R. Zamoyska (2009). "T-cell receptor proximal signaling via the Src-family kinases, Lck and Fyn, influences T-cell activation, differentiation, and tolerance." Immunol Rev **228**(1): 9-22.

Salojin, K. V., J. Zhang, C. Meagher and T. L. Delovitch (2000). "ZAP-70 is essential for the T cell antigen receptor-induced plasma membrane targeting of SOS and Vav in T cells." J Biol Chem **275**(8): 5966-75.

Salter, R. D., R. J. Benjamin, P. K. Wesley, S. E. Buxton, T. P. Garrett, C. Clayberger, A. M. Krensky, A. M. Norment, D. R. Littman and P. Parham (1990). "A binding site for the T-cell co-receptor CD8 on the alpha 3 domain of HLA-A2." Nature **345**(6270): 41-6.

Salter, R. D., A. M. Norment, B. P. Chen, C. Clayberger, A. M. Krensky, D. R. Littman and P. Parham (1989). "Polymorphism in the alpha 3 domain of HLA-A molecules affects binding to CD8." Nature **338**(6213): 345-7.

Samelson, L. E., J. B. Harford and R. D. Klausner (1985). "Identification of the components of the murine T cell antigen receptor complex." Cell **43**(1): 223-31.

Samelson, L. E., M. D. Patel, A. M. Weissman, J. B. Harford and R. D. Klausner (1986). "Antigen activation of murine T cells induces tyrosine phosphorylation of a polypeptide associated with the T cell antigen receptor." Cell **46**(7): 1083-90.

Sanders, S. K., R. O. Fox and P. Kavathas (1991). "Mutations in CD8 that affect interactions with HLA class I and monoclonal anti-CD8 antibodies." J Exp Med **174**(2): 371-9.

Schatz, D. G., M. A. Oettinger and M. S. Schlissel (1992). "V(D)J recombination: molecular biology and regulation." Annu Rev Immunol **10**: 359-83.

Schilham, M. W., W. P. Fung-Leung, A. Rahemtulla, T. Kuendig, L. Zhang, J. Potter, R. G. Miller, H. Hengartner and T. W. Mak (1993). "Alloreactive cytotoxic T cells can develop and function in mice lacking both CD4 and CD8." Eur J Immunol **23**(6): 1299-304.

Schott, E. and H. L. Ploegh (2002). "Mouse MHC class I tetramers that are unable to bind reveal the need for CD8 engagement in order to activate naive CD8 T cells." Eur J Immunol **32**: 3425-3434.

Seet, B. T., D. M. Berry, J. S. Maltzman, J. Shabason, M. Raina, G. A. Koretzky, C. J. McGlade and T. Pawson (2007). "Efficient T-cell receptor signaling requires a high-affinity interaction between the Gads C-SH3 domain and the SLP-76 RxxK motif." Embo J **26**(3): 678-89.

Sewell, A. K., U. C. Gerth, D. A. Price, M. A. Purbhoo, J. M. Boulter, G. F. Gao, J. I. Bell, R. E. Phillips and B. K. Jakobsen (1999). "Antagonism of cytotoxic T-lymphocyte activation by soluble CD8." Nat Med **5**(4): 399-404.

Sewell, A. K., G. C. Harcourt, P. J. Goulder, D. A. Price and R. E. Phillips (1997). "Antagonism of cytotoxic T lymphocyte-mediated lysis by natural HIV-1 altered peptide ligands requires simultaneous presentation of agonist and antagonist peptides." Eur J Immunol **27**(9): 2323-9.

Shinohara, N. and D. H. Sachs (1979). "Mouse alloantibodies capable of blocking cytotoxic T-cell function. I. Relationship between the antigen reactive with blocking antibodies and the Lyt-2 locus." J Exp Med **150**(3): 432-44.

Shore, D. A., H. Issafras, E. Landais, L. Teyton and I. A. Wilson (2008). "The crystal structure of CD8 in complex with YTS156.7.7 Fab and interaction with other CD8 antibodies define the binding mode of CD8 alphabeta to MHC class I." J Mol Biol **384**(5): 1190-202.

Sicheri, F. and J. Kuriyan (1997). "Structures of Src-family tyrosine kinases." Curr Opin Struct Biol **7**(6): 777-85.

Siggs, O. M., L. A. Miosge, A. L. Yates, E. M. Kucharska, D. Sheahan, T. Brdicka, A. Weiss, A. Liston and C. C. Goodnow (2007). "Opposing functions of the T cell receptor kinase ZAP-70 in immunity and tolerance differentially titrate in response to nucleotide substitutions." Immunity **27**(6): 912-26.

Simons, K. and D. Toomre (2000). "Lipid rafts and signal transduction." Nat Rev Mol Cell Biol **1**(1): 31-9.

Singer, A., S. Adoro and J. H. Park (2008). "Lineage fate and intense debate: myths, models and mechanisms of CD4- versus CD8-lineage choice." Nat Rev Immunol **8**(10): 788-801.

Skowera, A., R. J. Ellis, R. Varela-Calvino, S. Arif, G. C. Huang, C. Van-Krinks, A. Zaremba, C. Rackham, J. S. Allen, T. I. Tree, M. Zhao, C. M. Dayan, A. K. Sewell, W. W. Unger, J. W. Drijfhout, F. Ossendorp, B. O. Roep and M. Peakman (2008).

"CTLs are targeted to kill beta cells in patients with type 1 diabetes through recognition of a glucose-regulated preproinsulin epitope." J Clin Invest **118**(10): 3390-402.

Sloan-Lancaster, J. and P. M. Allen (1996). "Altered peptide ligand-induced partial T cell activation: molecular mechanisms and role in T cell biology." Annu Rev Immunol **14**: 1-27.

Smyth, M. J., E. Cretney, J. M. Kelly, J. A. Westwood, S. E. Street, H. Yagita, K. Takeda, S. L. van Dommelen, M. A. Degli-Esposti and Y. Hayakawa (2005). "Activation of NK cell cytotoxicity." Mol Immunol **42**(4): 501-10.

Stefanova, I., B. Hemmer, M. Vergelli, R. Martin, W. E. Biddison and R. N. Germain (2003). "TCR ligand discrimination is enforced by competing ERK positive and SHP-1 negative feedback pathways." Nat Immunol **4**(3): 248-54.

Steward-Tharp, S. M., Y. J. Song, R. M. Siegel and J. J. O'Shea (2010). "New insights into T cell biology and T cell-directed therapy for autoimmunity, inflammation, and immunosuppression." Ann N Y Acad Sci **1183**: 123-48.

Stone, J. D., A. S. Chervin and D. M. Kranz (2009). "T-cell receptor binding affinities and kinetics: impact on T-cell activity and specificity." Immunology **126**(2): 165-76.

Storkus, W. J., D. N. Howell, R. D. Salter, J. R. Dawson and P. Cresswell (1987). "NK susceptibility varies inversely with target cell class I HLA antigen expression." J Immunol **138**(6): 1657-9.

Sun, J. and P. B. Kavathas (1997). "Comparison of the roles of CD8 alpha alpha and CD8 alpha beta in interaction with MHC class I." J Immunol **159**(12): 6077-82.

Sun, Z. J., K. S. Kim, G. Wagner and E. L. Reinherz (2001). "Mechanisms contributing to T cell receptor signaling and assembly revealed by the solution structure of an ectodomain fragment of the CD3 epsilon gamma heterodimer." Cell **105**(7): 913-23.

Surh, C. D. and J. Sprent (2008). "Homeostasis of naive and memory T cells." Immunity **29**(6): 848-62.

Suzuki, H., Y. Kurihara, M. Takeya, N. Kamada, M. Kataoka, K. Jishage, O. Ueda, H. Sakaguchi, T. Higashi, T. Suzuki, Y. Takashima, Y. Kawabe, O. Cynshi, Y. Wada, M. Honda, H. Kurihara, H. Aburatani, T. Doi, A. Matsumoto, S. Azuma, T. Noda, Y. Toyoda, H. Itakura, Y. Yazaki, T. Kodama and et al. (1997). "A role for macrophage

scavenger receptors in atherosclerosis and susceptibility to infection." Nature **386**(6622): 292-6.

Suzuki, S., J. Kupsch, K. Eichmann and M. K. Saizawa (1992). "Biochemical evidence of the physical association of the majority of CD3 delta chains with the accessory/co-receptor molecules CD4 and CD8 on nonactivated T lymphocytes." Eur J Immunol **22**(10): 2475-9.

Sykulev, Y., M. Joo, I. Vturina, T. J. Tsomides and H. N. Eisen (1996). "Evidence that a single peptide-MHC complex on a target cell can elicit a cytolytic T cell response." Immunity **4**(6): 565-71.

Takada, S. and E. G. Engleman (1987). "Evidence for an association between CD8 molecules and the T cell receptor complex on cytotoxic T cells." J Immunol **139**(10): 3231-5.

Tangye, S. G., A. Ferguson, D. T. Avery, C. S. Ma and P. D. Hodgkin (2002). "Isotype switching by human B cells is division-associated and regulated by cytokines." J Immunol **169**(8): 4298-306.

Taylor, P. R., L. Martinez-Pomares, M. Stacey, H. H. Lin, G. D. Brown and S. Gordon (2005). "Macrophage receptors and immune recognition." Annu Rev Immunol **23**: 901-44.

Terry, L. A., J. P. DiSanto, T. N. Small and N. Flomenberg (1990). "Differential expression and regulation of the human CD8 alpha and CD8 beta chains." Tissue Antigens **35**(2): 82-91.

Thirdborough, S. M., J. S. Roddick, J. N. Radcliffe, M. Howarth, F. K. Stevenson and T. Elliott (2008). "Tapasin shapes immunodominance hierarchies according to the kinetic stability of peptide-MHC class I complexes." Eur J Immunol **38**(2): 364-9.

Thomas, C. A., Y. Li, T. Kodama, H. Suzuki, S. C. Silverstein and J. El Khoury (2000). "Protection from lethal gram-positive infection by macrophage scavenger receptor-dependent phagocytosis." J Exp Med **191**(1): 147-56.

Thomas, M. L. (1989). "The leukocyte common antigen family." Annu Rev Immunol **7**: 339-69.

Thomas, S., R. S. Kumar and T. D. Brumeanu (2004). "Role of lipid rafts in T cells." Arch Immunol Ther Exp (Warsz) **52**(4): 215-24.

Thompson, C. B., T. Lindsten, J. A. Ledbetter, S. L. Kunkel, H. A. Young, S. G. Emerson, J. M. Leiden and C. H. June (1989). "CD28 activation pathway regulates the production of multiple T-cell-derived lymphokines/cytokines." Proc Natl Acad Sci U S A **86**(4): 1333-7.

Thorburn, A. (2004). "Death receptor-induced cell killing." Cell Signal **16**(2): 139-44.

Tomonari, K. and S. Spencer (1990). "Epitope-specific binding of CD8 regulates activation of T cells and induction of cytotoxicity." Int Immunol **2**(12): 1189-94.

Tosi, M. F. (2005). "Innate immune responses to infection." J Allergy Clin Immunol **116**(2): 241-9; quiz 250.

Townsend, A. and H. Bodmer (1989). "Antigen recognition by class I-restricted T lymphocytes." Annu Rev Immunol **7**: 601-24.

Trautmann, A. and C. Randriamampita (2003). "Initiation of TCR signalling revisited." Trends Immunol **24**(8): 425-8.

Tsujimura, K., Y. Obata, E. Kondo, K. Nishida, Y. Matsudaira, Y. Akatsuka, K. Kuzushima and T. Takahashi (2003). "Thymus leukemia antigen (TL)-specific cytotoxic T lymphocytes recognize the alpha1/alpha2 domain of TL free from antigenic peptides." Int Immunol **15**(11): 1319-26.

Turner, J. M., M. H. Brodsky, B. A. Irving, S. D. Levin, R. M. Perlmutter and D. R. Littman (1990). "Interaction of the unique N-terminal region of tyrosine kinase p56lck with cytoplasmic domains of CD4 and CD8 is mediated by cysteine motifs." Cell **60**(5): 755-65.

Tynan, F. E., N. A. Borg, J. J. Miles, T. Beddoe, D. El-Hassen, S. L. Silins, W. J. van Zuylen, A. W. Purcell, L. Kjer-Nielsen, J. McCluskey, S. R. Burrows and J. Rossjohn (2005). "High resolution structures of highly bulged viral epitopes bound to major histocompatibility complex class I. Implications for T-cell receptor engagement and T-cell immunodominance." J Biol Chem **280**(25): 23900-9.

Tynan, F. E., S. R. Burrows, A. M. Buckle, C. S. Clements, N. A. Borg, J. J. Miles, T. Beddoe, J. C. Whisstock, M. C. Wilce, S. L. Silins, J. M. Burrows, L. Kjer-Nielsen, L. Kostenko, A. W. Purcell, J. McCluskey and J. Rossjohn (2005). "T cell receptor recognition of a 'super-bulged' major histocompatibility complex class I-bound peptide." Nat Immunol **6**(11): 1114-22.

Unanue, E. R. (1984). "Antigen-presenting function of the macrophage." Annu Rev Immunol **2**: 395-428.

Valitutti, S., S. Muller, M. Cella, E. Padovan and A. Lanzavecchia (1995). "Serial triggering of many T-cell receptors by a few peptide-MHC complexes." Nature **375**(6527): 148-51.

Valitutti, S., S. Muller, M. Dessing and A. Lanzavecchia (1996). "Different responses are elicited in cytotoxic T lymphocytes by different levels of T cell receptor occupancy." J Exp Med **183**(4): 1917-21.

van den Berg, H. A. and D. A. Rand (2007). "Quantitative theories of T-cell responsiveness." Immunol Rev **216**: 81-92.

van den Berg, H. A., L. Wooldridge, B. Laugel and A. K. Sewell (2007). "Coreceptor CD8-driven modulation of T cell antigen receptor specificity." J Theor Biol **249**(2): 395-408.

van den Boorn, J. G., D. Konijnenberg, T. A. Dellemijn, J. P. van der Veen, J. D. Bos, C. J. Melief, F. A. Vyth-Dreese and R. M. Luiten (2009). "Autoimmune destruction of skin melanocytes by perilesional T cells from vitiligo patients." J Invest Dermatol **129**(9): 2220-32.

van der Merwe, P. A. (2001). "The TCR triggering puzzle." Immunity **14**(6): 665-8.

van der Merwe, P. A. and S. J. Davis (2003). "Molecular interactions mediating T cell antigen recognition." Annu Rev Immunol **21**: 659-84.

van der Merwe, P. A. and O. Dushek (2011). "Mechanisms for T cell receptor triggering." Nat Rev Immunol **11**(1): 47-55.

Van Laethem, F., S. D. Sarafova, J. H. Park, X. Tai, L. Pobezinsky, T. I. Guinter, S. Adoro, A. Adams, S. O. Sharrow, L. Feigenbaum and A. Singer (2007). "Deletion of CD4 and CD8 coreceptors permits generation of alphabetaT cells that recognize antigens independently of the MHC." Immunity **27**(5): 735-50.

van Oers, N. S., N. Killeen and A. Weiss (1994). "ZAP-70 is constitutively associated with tyrosine-phosphorylated TCR zeta in murine thymocytes and lymph node T cells." Immunity **1**(8): 675-85.

van Oers, N. S., N. Killeen and A. Weiss (1996). "Lck regulates the tyrosine phosphorylation of the T cell receptor subunits and ZAP-70 in murine thymocytes." J Exp Med **183**(3): 1053-62.

Van Seventer, G. A., R. A. Van Lier, H. Spits, P. Ivanyi and C. J. Melief (1986). "Evidence for a regulatory role of the T8 (CD8) antigen in antigen-specific and anti-T3-(CD3)-induced lytic activity of allospecific cytotoxic T lymphocyte clones." Eur J Immunol **16**(11): 1363-71.

Varela-Rohena, A., P. E. Molloy, S. M. Dunn, Y. Li, M. M. Suhoski, R. G. Carroll, A. Milicic, T. Mahon, D. H. Sutton, B. Laugel, R. Moysey, B. J. Cameron, A. Vuidepot, M. A. Purbhoo, D. K. Cole, R. E. Phillips, C. H. June, B. K. Jakobsen, A. K. Sewell and J. L. Riley (2008). "Control of HIV-1 immune escape by CD8 T cells expressing enhanced T-cell receptor." Nat Med **14**(12): 1390-5.

Varma, R., G. Campi, T. Yokosuka, T. Saito and M. L. Dustin (2006). "T cell receptor-proximal signals are sustained in peripheral microclusters and terminated in the central supramolecular activation cluster." Immunity **25**(1): 117-27.

Veillette, A., J. B. Bolen and M. A. Bookman (1989). "Alterations in tyrosine protein phosphorylation induced by antibody-mediated cross-linking of the CD4 receptor of T lymphocytes." Mol Cell Biol **9**(10): 4441-6.

Veillette, A., M. A. Bookman, E. M. Horak and J. B. Bolen (1988). "The CD4 and CD8 T cell surface antigens are associated with the internal membrane tyrosine-protein kinase p56lck." Cell **55**(2): 301-8.

Veillette, A. and M. Fournel (1990). "The CD4 associated tyrosine protein kinase p56lck is positively regulated through its site of autophosphorylation." Oncogene **5**(10): 1455-62.

Veillette, A., J. C. Zuniga-Pflucker, J. B. Bolen and A. M. Kruisbeek (1989). "Engagement of CD4 and CD8 expressed on immature thymocytes induces activation of intracellular tyrosine phosphorylation pathways." J Exp Med **170**(5): 1671-80.

Veldhoen, M. and B. Seddon (2010). "Empowering T helper 17 cells in autoimmunity." Nat Med **16**(2): 166-8.

Viola, A. (2001). "The amplification of TCR signaling by dynamic membrane microdomains." Trends Immunol **22**(6): 322-7.

Viola, A., M. Salio, L. Tuosto, S. Linkert, O. Acuto and A. Lanzavecchia (1997). "Quantitative contribution of CD4 and CD8 to T cell antigen receptor serial triggering." J Exp Med **186**(10): 1775-9.

Walter, U. and P. Santamaria (2005). "CD8+ T cells in autoimmunity." Curr Opin Immunol **17**(6): 624-31.

Wang, J. H., Y. W. Yan, T. P. Garrett, J. H. Liu, D. W. Rodgers, R. L. Garlick, G. E. Tarr, Y. Husain, E. L. Reinherz and S. C. Harrison (1990). "Atomic structure of a fragment of human CD4 containing two immunoglobulin-like domains." Nature **348**(6300): 411-8.

Wang, R., K. Natarajan and D. H. Margulies (2009). "Structural basis of the CD8 alpha beta/MHC class I interaction: focused recognition orients CD8 beta to a T cell proximal position." J Immunol **183**(4): 2554-64.

Wange, R. L. and L. E. Samelson (1996). "Complex complexes: signaling at the TCR." Immunity **5**(3): 197-205.

Watts, T. H. and M. A. DeBenedette (1999). "T cell co-stimulatory molecules other than CD28." Curr Opin Immunol **11**(3): 286-93.

Weaver, C. T., L. E. Harrington, P. R. Mangan, M. Gavrieli and K. M. Murphy (2006). "Th17: an effector CD4 T cell lineage with regulatory T cell ties." Immunity **24**(6): 677-88.

Weiss, A. and D. R. Littman (1994). "Signal transduction by lymphocyte antigen receptors." Cell **76**(2): 263-74.

Werlen, G., B. Hausmann, D. Naeher and E. Palmer (2003). "Signaling life and death in the thymus: timing is everything." Science **299**(5614): 1859-63.

Werlen, G. and E. Palmer (2002). "The T-cell receptor signalosome: a dynamic structure with expanding complexity." Curr Opin Immunol **14**(3): 299-305.

Wheeler, C. J., P. von Hoegen and J. R. Parnes (1992). "An immunological role for the CD8 beta-chain." Nature **357**(6375): 247-9.

Willcox, B. E., G. F. Gao, J. R. Wyer, J. E. Ladbury, J. I. Bell, B. K. Jakobsen and P. A. van der Merwe (1999). "TCR binding to peptide-MHC stabilizes a flexible recognition interface." Immunity **10**(3): 357-65.

Willemsen, R., C. Ronteltap, M. Heuveling, R. Debets and R. Bolhuis (2005). "Redirecting human CD4+ T lymphocytes to the MHC class I-restricted melanoma antigen MAGE-A1 by TCR alphabeta gene transfer requires CD8alpha." Gene Ther **12**(2): 140-6.

Willemsen, R. A., Z. Sebestyen, C. Ronteltap, C. Berrevoets, J. Drexhage and R. Debets (2006). "CD8 alpha coreceptor to improve TCR gene transfer to treat melanoma: down-regulation of tumor-specific production of IL-4, IL-5, and IL-10." J Immunol **177**(2): 991-8.

Wilson, D. B., D. H. Wilson, K. Schroder, C. Pinilla, S. Blondelle, R. A. Houghten and K. C. Garcia (2004). "Specificity and degeneracy of T cells." Mol Immunol **40**(14-15): 1047-55.

Wolf, P. R. and H. L. Ploegh (1995). "How MHC class II molecules acquire peptide cargo: biosynthesis and trafficking through the endocytic pathway." Annu Rev Cell Dev Biol **11**: 267-306.

Wong, F. S., L. K. Siew and L. Wen (2008). "CD8+ T-cells and their interaction with other cells in damage to islet beta-cells." Biochem Soc Trans **36**(Pt 3): 316-20.

Woodle, E. S., J. R. Thistlethwaite, I. A. Ghobrial, L. K. Jolliffe, F. P. Stuart and J. A. Bluestone (1991). "OKT3 F(ab')2 fragments--retention of the immunosuppressive properties of whole antibody with marked reduction in T cell activation and lymphokine release." Transplantation **52**(2): 354-60.

Wooldridge, L., M. Clement, A. Lissina, E. S. Edwards, K. Ladell, J. Ekeruche, R. E. Hewitt, B. Laugel, E. Gostick, D. K. Cole, R. Debets, C. Berrevoets, J. J. Miles, S. R. Burrows, D. A. Price and A. K. Sewell (2010). "MHC class I molecules with Superenhanced CD8 binding properties bypass the requirement for cognate TCR recognition and nonspecifically activate CTLs." J Immunol **184**(7): 3357-66.

Wooldridge, L., J. Ekeruche-Makinde, H. A. van den Berg, A. Skowera, J. J. Miles, M. P. Tan, G. Dolton, M. Clement, S. Llewellyn-Lacey, D. A. Price, M. Peakman and A. K. Sewell (2012). "A single autoimmune T cell receptor recognizes more than a million different peptides." J Biol Chem **287**(2): 1168-77.

Wooldridge, L., S. L. Hutchinson, E. M. Choi, A. Lissina, E. Jones, F. Mirza, P. R. Dunbar, D. A. Price, V. Cerundolo and A. K. Sewell (2003). "Anti-CD8 antibodies can inhibit or enhance peptide-MHC class I (pMHCI) multimer binding: this is paralleled by their effects on CTL activation and occurs in the absence of an interaction between pMHCI and CD8 on the cell surface." J Immunol **171**(12): 6650-60.

Wooldridge, L., B. Laugel, J. Ekeruche, M. Clement, H. A. van den Berg, D. A. Price and A. K. Sewell (2010). "CD8 controls T cell cross-reactivity." J Immunol **185**(8): 4625-32.

Wooldridge, L., A. Lissina, D. K. Cole, H. A. van den Berg, D. A. Price and A. K. Sewell (2009). "Tricks with tetramers: how to get the most from multimeric peptide-MHC." Immunology **126**(2): 147-64.

Wooldridge, L., A. Lissina, J. Vernazza, E. Gostick, B. Laugel, S. L. Hutchinson, F. Mirza, P. R. Dunbar, J. M. Boulter, M. Glick, V. Cerundolo, H. A. van den Berg, D. A. Price and A. K. Sewell (2007). "Enhanced immunogenicity of CTL antigens through mutation of the CD8 binding MHC class I invariant region." Eur J Immunol **37**(5): 1323-33.

Wooldridge, L., T. J. Scriba, A. Milicic, B. Laugel, E. Gostick, D. A. Price, R. E. Phillips and A. K. Sewell (2006). "Anti-coreceptor antibodies profoundly affect staining with peptide-MHC class I and class II tetramers." Eur J Immunol **36**(7): 1847-55.

Wooldridge, L., H. A. van den Berg, M. Glick, E. Gostick, B. Laugel, S. L. Hutchinson, A. Milicic, J. M. Brenchley, D. C. Douek, D. A. Price and A. K. Sewell (2005). "Interaction between the CD8 coreceptor and major histocompatibility complex class I stabilizes T cell receptor-antigen complexes at the cell surface." J Biol Chem **280**(30): 27491-501.

Wraith, D. C., B. Bruun and P. J. Fairchild (1992). "Cross-reactive antigen recognition by an encephalitogenic T cell receptor. Implications for T cell biology and autoimmunity." J Immunol **149**(11): 3765-70.

Wu, H., P. D. Kwong and W. A. Hendrickson (1997). "Dimeric association and segmental variability in the structure of human CD4." Nature **387**(6632): 527-30.

Wucherpfennig, K. W. and J. L. Strominger (1995). "Molecular mimicry in T cell-mediated autoimmunity: viral peptides activate human T cell clones specific for myelin basic protein." Cell **80**(5): 695-705.

Wyer, J. R., B. E. Willcox, G. F. Gao, U. C. Gerth, S. J. Davis, J. I. Bell, P. A. van der Merwe and B. K. Jakobsen (1999). "T cell receptor and coreceptor CD8 alphaalpha bind peptide-MHC independently and with distinct kinetics." Immunity **10**(2): 219-25.

Wynn, K. K., Z. Fulton, L. Cooper, S. L. Silins, S. Gras, J. K. Archbold, F. E. Tynan, J. J. Miles, J. McCluskey, S. R. Burrows, J. Rossjohn and R. Khanna (2008). "Impact of clonal competition for peptide-MHC complexes on the CD8+ T-cell repertoire selection in a persistent viral infection." Blood **111**(8): 4283-92.

Xavier, R., T. Brennan, Q. Li, C. McCormack and B. Seed (1998). "Membrane compartmentation is required for efficient T cell activation." Immunity **8**(6): 723-32.

Xu, W., A. Doshi, M. Lei, M. J. Eck and S. C. Harrison (1999). "Crystal structures of c-Src reveal features of its autoinhibitory mechanism." Mol Cell **3**(5): 629-38.

Yachi, P. P., J. Ampudia, N. R. Gascoigne and T. Zal (2005). "Nonstimulatory peptides contribute to antigen-induced CD8-T cell receptor interaction at the immunological synapse." Nat Immunol **6**(8): 785-92.

Yachi, P. P., J. Ampudia, T. Zal and N. R. Gascoigne (2006). "Altered peptide ligands induce delayed CD8-T cell receptor interaction--a role for CD8 in distinguishing antigen quality." Immunity **25**(2): 203-11.

Yamamoto, R., T. Isobe, T. Eguchi, W. R. Tang, N. Kiyokawa, H. Amemiya, J. Fujimoto, E. Sato, Y. Takagaki and H. Yasue (2005). "Porcine TCR CD3zeta-chain and eta-chain." Mol Immunol **42**(12): 1485-93.

Yi, Z., R. Diz, A. J. Martin, Y. M. Morillon, D. E. Kline, L. Li, B. Wang and R. Tisch (2012). "Long-Term Remission of Diabetes in NOD Mice Is Induced by Nondepleting Anti-CD4 and Anti-CD8 Antibodies." Diabetes.

Yin, Y., Y. Li and R. A. Mariuzza (2012) "Structural basis for self-recognition by autoimmune T-cell receptors." Immunol Rev **250**(1): 32-48.

Yokosuka, T., W. Kobayashi, K. Sakata-Sogawa, M. Takamatsu, A. Hashimoto-Tane, M. L. Dustin, M. Tokunaga and T. Saito (2008). "Spatiotemporal regulation of T cell costimulation by TCR-CD28 microclusters and protein kinase C theta translocation." Immunity **29**(4): 589-601.

You, S., B. Leforban, C. Garcia, J. F. Bach, J. A. Bluestone and L. Chatenoud (2007). "Adaptive TGF-beta-dependent regulatory T cells control autoimmune diabetes and are a privileged target of anti-CD3 antibody treatment." Proc Natl Acad Sci U S A **104**(15): 6335-40.

Zal, T., M. A. Zal and N. R. Gascoigne (2002). "Inhibition of T cell receptor-coreceptor interactions by antagonist ligands visualized by live FRET imaging of the T-hybridoma immunological synapse." Immunity **16**(4): 521-34.

Zamoyska, R. (1994). "The CD8 coreceptor revisited: one chain good, two chains better." Immunity **1**(4): 243-6.

Zamoyska, R. (1998). "CD4 and CD8: modulators of T-cell receptor recognition of antigen and of immune responses?" Curr Opin Immunol **10**(1): 82-7.

Zamoyska, R. (2007). "Why is there so much CD45 on T cells?" Immunity **27**(3): 421-3.

Zamoyska, R., A. Basson, A. Filby, G. Legname, M. Lovatt and B. Seddon (2003). "The influence of the src-family kinases, Lck and Fyn, on T cell differentiation, survival and activation." Immunol Rev **191**: 107-18.

Zhang, W., J. Sloan-Lancaster, J. Kitchen, R. P. Trible and L. E. Samelson (1998). "LAT: the ZAP-70 tyrosine kinase substrate that links T cell receptor to cellular activation." Cell **92**(1): 83-92.

Zhang, W., R. P. Trible and L. E. Samelson (1998). "LAT palmitoylation: its essential role in membrane microdomain targeting and tyrosine phosphorylation during T cell activation." Immunity **9**(2): 239-46.

Zhao, R., F. T. Yang and D. R. Alexander (2004). "An oncogenic tyrosine kinase inhibits DNA repair and DNA-damage-induced Bcl-xL deamidation in T cell transformation." Cancer Cell **5**(1): 37-49.

Zipfel, P. F. and C. Skerka (2009). "Complement regulators and inhibitory proteins." Nat Rev Immunol **9**(10): 729-40.

Zippelius, A., M. J. Pittet, P. Batard, N. Rufer, M. de Smedt, P. Guillaume, K. Ellefsen, D. Valmori, D. Lienard, J. Plum, H. R. MacDonald, D. E. Speiser, J. C. Cerottini and P. Romero (2002). "Thymic selection generates a large T cell pool recognizing a self-peptide in humans." J Exp Med **195**(4): 485-94.

APPENDICES

Appendix 1 – MHC Class I Molecules with Superenhanced CD8 Binding Properties Bypass the Requirement for Cognate TCR Recognition and Nonspecifically Activate CTLs (Clement et al 2010)

Appendix 2 – Anti-CD8 Antibodies Can Trigger CD8+ T Cell effector Function in the Absence of TCR Engagement and Improve Peptide–MHCI Tetramer Staining (Clement et al 2011)

Appendix 3 – Surface plasmon resonance measurements of 1E6, ALF8, and 1LA TCR binding to peptide variants complexed with HLA A*0201.

The Journal of Immunology

MHC Class I Molecules with Superenhanced CD8 Binding Properties Bypass the Requirement for Cognate TCR Recognition and Nonspecifically Activate CTLs

Linda Wooldridge, Mathew Clement, Anna Lissina, Emily S. J. Edwards, Kristin Ladell, Julia Ekeruche, Rachel E. Hewitt, Bruno Laugel, Emma Gostick, David K. Cole, Reno Debets, Cor Berrevoets, John J. Miles, Scott R. Burrows, David A. Price and Andrew K. Sewell

J. Immunol. published online Feb 26, 2010;
doi:10.4049/jimmunol.0902398

The Journal of Immunology is published twice each month by The American Association of Immunologists, Inc., 9650 Rockville Pike, Bethesda, MD 20814-3994.

Print ISSN: 0022-1767 Online ISSN: 1550-6606.

Published February 26, 2010, doi:10.4049/jimmunol.0902398

MHC Class I Molecules with Superenhanced CD8 Binding Properties Bypass the Requirement for Cognate TCR Recognition and Nonspecifically Activate CTLs

Linda Wooldridge,*,[1] Mathew Clement,*,[1] Anna Lissina,* Emily S. J. Edwards,* Kristin Ladell,* Julia Ekeruche,* Rachel E. Hewitt,[†] Bruno Laugel,* Emma Gostick,* David K. Cole,* Reno Debets,[‡] Cor Berrevoets,[‡] John J. Miles,*,[§] Scott R. Burrows,[§] David A. Price,* and Andrew K. Sewell*

CD8$^+$ CTLs are essential for effective immune defense against intracellular microbes and neoplasia. CTLs recognize short peptide fragments presented in association with MHC class I (MHCI) molecules on the surface of infected or dysregulated cells. Ag recognition involves the binding of both TCR and CD8 coreceptor to a single ligand (peptide MHCI [pMHCI]). The TCR/pMHCI interaction confers Ag specificity, whereas the pMHCI/CD8 interaction mediates enhanced sensitivity to Ag. Striking biophysical differences exist between the TCR/pMHCI and pMHCI/CD8 interactions; indeed, the pMHCI/CD8 interaction can be >100-fold weaker than the cognate TCR/pMHCI interaction. In this study, we show that increasing the strength of the pMHCI/CD8 interaction by ~15-fold results in nonspecific, cognate Ag-independent pMHCI tetramer binding at the cell surface. Furthermore, pMHCI molecules with superenhanced affinity for CD8 activate CTLs in the absence of a specific TCR/pMHCI interaction to elicit a full range of effector functions, including cytokine/chemokine release, degranulation and proliferation. Thus, the low solution binding affinity of the pMHCI/CD8 interaction is essential for the maintenance of CTL Ag specificity. ***The Journal of Immunology*****, 2010, 184: 000–000.**

CD8$^+$ CTLs recognize antigenic determinants in the form of short peptides derived from endogenous proteins bound to MHC class I (MHCI) molecules on the surface of target cells and play a critical role in immune defense against intracellular pathogens and tumors. Ag specificity is conferred by the TCR, which interacts with the peptide-binding platform formed by the α1 and α2 domains of MHCI (1, 2). In contrast, the surface gp CD8 binds to invariant regions of MHCI and is capable of enhancing cellular sensitivity to Ag by up to six orders of magnitude (3, 4). CD8 mediates this profound enhancement of Ag sensitivity through a number of distinct mechanisms: 1) enhancement of the TCR/peptide MHCI (pMHCI) association rate (5–7); 2) stabilization of the TCR/pMHCI interaction (8, 9); 3) recruitment of essential kinases to the intracellular side of the TCR/CD3/ζ complex (10, 11); and 4) localization of TCR/pMHCI complexes within specialized membrane microdomains that are enriched for early intracellular signal transduction molecules and are thought to act as privileged sites for TCR-mediated cascade initiation (12, 13).

The MHCI binding site for CD8 is separate from the peptide-binding domains that are recognized by the TCR (2) and this spatial segregation allows both TCR and CD8 to bind a single MHCI molecule simultaneously (14). Thus, CTL recognition of Ag involves the binding of two receptors (TCR and CD8) to a single ligand (pMHCI), a modus operandi that is unique to αβ T cell biology. The pMHCI/CD8 interaction is characterized by very low solution affinities (K_D ~150 μM) and rapid kinetics (K_{off} ~18 s^{-1}) (15, 16). Indeed, the affinity of the pMHCI/CD8 interaction is even lower than the corresponding values measured for conventional molecular binding events involved in cell-cell recognition, such as the CD2/CD48 interaction (K_D = 60–90 μM) (15, 17). In stark contrast, the TCR/pMHCI interaction can be more than 100-fold stronger than the pMHCI/CD8 interaction (K_D range for agonists from 0.14 μM, the strongest natural TCR/pMHCI interaction measured to date) and exhibits considerably slower kinetics (K_{off} range for agonists 0.01–1 s^{-1}) (1, 6, 18–20). It seems extremely unlikely that the striking biophysical characteristics of the pMHCI/CD8 interaction have occurred by accident. Indeed, this conclusion is strengthened by the finding that the pMHCI/CD8 interaction is capable of exerting the vast majority of its biological function when weakened even further (21), which suggests that CD8 has specifically evolved to operate at very low solution affinities.

In this study, we probe the functional significance of the low solution affinity pMHCI/CD8 interaction using pMHCI molecules with superenhanced CD8 binding properties. Notably, we find that pMHCI molecules with affinities for CD8 that lie within the typical range for agonist TCR/pMHCI interactions (K_D ~10 μM) are able to activate CTL in the absence of a specific TCR/pMHCI interaction. Thus, the biophysical

*Department of Infection, Immunity, and Biochemisty, Cardiff University, Cardiff; [†]Micronutrient Status Research Section, Medical Research Council Human Nutrition Research, Cambridge, United Kingdom; [‡]Laboratory of Experimental Tumor Immunology, Department of Medical Oncology, Erasmus Medical Center-Daniel den Hoed Cancer Center, Rotterdam, The Netherlands; and [§]Division of Immunology, Queensland Institute of Medical Research, Brisbane, Australia

[1]L.W. and M.C. contributed equally to this manuscript.

Received for publication July 23, 2009. Accepted for publication January 20, 2010.

L.W. is a Wellcome Trust Clinical Intermediate Fellow; M.C. is funded by the Wellcome Trust. A.K.S. and A.L. are funded by the Cardiff University Link Chair scheme. D.A.P. is a Medical Research Council Senior Clinical Fellow; E.S.J.E., K. L., and E.G. are also funded by the Medical Research Council. D.K.C. is a Leverhulme Early Career Fellow. J.J.M. is a National Health and Medical Research Council Biomedical Fellow.

Address correspondence and reprint requests to Dr. Linda Wooldridge, Henry Wellcome Building, Heath Park, Cardiff University, Cardiff, CF144XN, U.K. E-mail address: wooldridgel@cardiff.ac.uk

Abbreviations used in this paper: 7-AAD, 7-amino-actinomycin D; C1R, Hmy.2 C1R B; hTERT, human telomerase reverse transcriptase; MHCI, MHC class I; pMHCI, peptide MHCI.

characteristics of the pMHCI/CD8 interaction are essential for the maintenance of CTL Ag specificity.

Materials and Methods

Cells

The CTL clones 003 and NT1 and the CTL line 868 are all specific for the HIV-1 p17 Gag-derived epitope SLYNTVATL (residues 77–85) restricted by HLA A*0201 (A2 from this point forward) (22, 23). The following A2-restricted CTL clones were also used in this study: 1) Mel13, specific for the Melan-A–derived epitope ELAGIGILTV (residues 26–35); and 2) ILA1, specific for the human telomerase reverse transcriptase (hTERT)-derived epitope ILAKFLHWL (residues 540–548) (6, 24). In addition, the following non-A2–restricted CTL clones were used: 1) the HLA A*6801-restricted CTL clone c23, specific for the HIV-1 Tat-derived epitope ITKGLGISYGR (residues 38–48) (25); 2) the HLA B*0702-restricted CTL clone KD4, specific for the EBV EBNA3A-derived epitope RPPIFIRRL (residues 379–387); 3) the HLA B*0801-restricted CTL clone LC13, specific for the EBV EBNA3A-derived epitope FLRGRAYGL (residues 339–347) (26, 27); and 4) the HLA B*3508-restricted CTL clone SB27, specific for the EBV BZLF1-derived epitope LPEPLPQGQLTAY (residues 52–64) (28, 29). All CTLs were maintained in RPMI 1640 (Life Technologies, Rockville, MD) containing 100 U/ml penicillin (Life Technologies), 100 μg/ml streptomycin (Life Technologies), 2 mM L-glutamine (Life Technologies), and 10% heat inactivated FCS (Life Technologies) (R10) supplemented with 2.5% Cellkines (Helvetica Healthcare, Geneva, Switzerland), 200 IU/ml IL-2 (PeproTech, Rocky Hill, NJ) and 25 ng/ml IL-15 (PeproTech). PBMCs were isolated by standard Ficoll-Hypaque density gradient centrifugation from healthy donor blood. The 293T-CD8α cells were manufactured by introducing pBullet-human CD8α (30, 31) into 293T cells using vesicular stomatitis virus-pseudotyped Moloney murine leukemia virus particles. The 293T-CD8α cells were cultured in DMEM (Life Technologies) supplemented with 20% FCS (Life Technologies), 1 mM sodium pyruvate (Life Technologies), 100 U/ml penicillin (Life Technologies), 100 μg/ml streptomycin (Life Technologies), and 2 mM L-glutamine (Life Technologies). Hmy.2 C1R B (C1R) cells expressing full-length A2 and variants thereof were generated as described previously (21).

pMHCI tetramers

Tetrameric complexes of wild-type pMHCI molecules and mutants thereof were produced, stored and used as described previously (9, 21). The following A2-restricted peptide epitopes were used to refold the pMHCI molecules used in this study: SLYNTVATL (HIV-1 p17 Gag, residues 77–85), LLFGYPVYV (HTLV-1 Tax, residues 11–19), GLCTLVAML (EBV BMLF1, residues 259–267), NLVPMVATV (CMV pp65, residues 495–503), ELAGIGILTV (Melan-A, residues 26–35), and ILAKFLHWL (hTERT, residues 540–548). Tetrameric or multimeric pMHCI reagents were constructed by the addition of streptavidin conjugated to PE, quantum dot 605 or quantum dot 800 (Life Technologies) at the appropriate molar ratios.

Abs

The following mAbs were used in this study: purified anti-human CD8 (clone DK-25; Dako, Carpinteria, CA), allophycocyanin-conjugated anti-human CD8 (clone RPA-T8; BD Biosciences, San Jose, CA), FITC-conjugated anti-human CD8 (clone SK1; BD Biosciences), PerCP-conjugated anti-human CD8 (clone SK1; BD Biosciences), PE-conjugated anti-human CD8β (clone 2ST8.5H7; Beckman Coulter, Fullerton, CA), PerCP-conjugated anti-human CD3 (clone SK7; BD Biosciences), FITC-conjugated anti-human αβ-TCR (clone BMA 031; Serotec, Oxford, U.K.), FITC-conjugated or PE-conjugated anti-human γδ-TCR (clone YB5.B8; BD Pharmingen, San Diego, CA), allophycocyanin-conjugated anti-human CD56 (clone AF12-7H3; Miltenyi Biotec, Auburn, CA), FITC-conjugated anti-human CD56 (clone MEM188; Caltag Laboratories, Burlingame, CA), FITC-conjugated anti-A2 (clone BB7.2; Serotec), and FITC-conjugated anti-human CD107a (clone H4A3; BD Biosciences). Unless specified, the anti-human CD8 mAbs used in this study target the α-chain of the coreceptor dimer. Dead cells were excluded from flow cytometric analyses with 7-amino-actinomycin D (7-AAD; BD Biosciences).

Flow cytometry

For pMHCI tetramer staining, 2.5×10^6 PBMC, 5×10^4 CTLs or 2×10^5 293T cells (untransfected or CD8α-transfected) were resuspended in PBS or FACS buffer (2% FCS/PBS) and stained with pMHCI tetramer at the concentrations indicated for 20–30 min at 37°C. Cells were subsequently stained with combinations of the mAbs described previously for 30 min on ice. Prior to staining, 293T cells were treated with Versene (Life Technologies) for 10 min at 37°C. For anti-CD8 mAb blocking experiments: 2.5×10^6 PBMCs were pretreated with 10 μg/ml unconjugated anti-CD8 mAb (clone DK-25; Dako) for 20 min on ice prior to staining with 10 μg/ml pMHCI tetramer for 45 min on ice. For A2 typing: 2.5×10^6 PBMCs were stained with 5 μl FITC-conjugated anti-A2 mAb (clone BB7.2; Serotec) for 30 min on ice. Samples were then washed twice and resuspended in PBS. Data were acquired using a FACSCalibur or FACSAria II flow cytometer (BD Biosciences) and analyzed with either CellQuest (BD Biosciences) or FlowJo (Tree Star, Ashland, OR) software.

TCR downregulation assay

The 10^5 003 CTLs per well were resuspended in a 96-well round-bottomed plate with various concentrations of the indicated PE-conjugated tetramers (A2 SLYNTVATL, A2/K^b SLYNTVATL, A2 LLFGYPVYV, or A2/K^b LLFGYPVYV) diluted in 40 μl RPMI 1640 containing 2% FCS plus penicillin, streptomycin, and glutamine as described previously (R2) for 30 min at 37°C. Cells were then washed, resuspended in ice-cold azide buffer (0.1% azide/2% FCS/PBS), and subsequently stained with FITC-conjugated anti–αβ-TCR (clone BMA 031; Serotec), 7-AAD (BD Biosciences), and allophycocyanin-conjugated anti-CD8 (clone RPA-T8; BD Biosciences) for 30 min on ice. After two additional washes, cells were resuspended in ice-cold azide buffer. Data were acquired using a FACSCalibur flow cytometer and analyzed with CellQuest software (BD Biosciences).

Cytokine/chemokine assays: ELISA, cytometric bead array, and ELISPOT

CTLs were incubated with C1R A2 cells, C1R A2/K^b cells, or medium alone at different E:T ratios overnight at 37°C. Subsequent to incubation, the supernatant was harvested and assayed for MIP-1β, IFN-γ, or RANTES by ELISA (R&D Systems, Minneapolis, MN). Remaining supernatant was assayed with the human Th1/Th2 cytokine kit (BD Biosciences) according to the manufacturer's instructions; data were acquired using a FACSCalibur flow cytometer and analyzed with CBA software (BD Biosciences). For tetramer-based ELISPOT assays, 2×10^3 CTL ± pMHCI tetramer at 1 μg/ml were applied to duplicate wells of PVDF-backed plates (Millipore, Bedford, MA) precoated with IFN-γ capture Ab 1-DIK (Mabtech, Nacka, Sweden) in a total volume of 200 μl R2 and incubated for 4 h at 37°C. To exclude activation by cognate peptide representation or fluorochrome-mediated aggregation, cognate A2 D227K/T228A tetramers were included as controls; these tetramers do not bind CD8 and did not activate 003 or 868 CTLs, despite efficient staining in both cases (data not shown). Plates were developed according to the manufacturer's instructions (Mabtech) and spots were counted using an automated ELISpot Reader System ELR02 (Autoimmun Diagnostika GmbH, Strassberg, Germany).

Degranulation assay

Surface CD107a mobilization was used to assess degranulation as described previously (32). Briefly, CTLs were incubated for 4 h at 37°C with either C1R A2 cells, C1R A2/K^b cells or medium alone at different E:T ratios; alternatively, CTLs were incubated with various pMHCI tetramers. Both FITC-conjugated anti-CD107a (clone H4A3; BD Biosciences) and 0.7 μl/ml monensin (GolgiStop; BD Biosciences) were added prior to incubation. Subsequent to incubation, the cells were washed twice and resuspended in PBS. Data were acquired using a FACSCalibur flow cytometer and analyzed with FlowJo software (Tree Star).

CTL priming assay

Transfected C1R cells were pulsed with 1 μM ELAGIGILTV (Melan-$A_{26–35}$) peptide for 90 min, irradiated, and washed once in RPMI 1640 medium. Pulsed, irradiated C1R cells (2×10^5) were incubated with 10^6 fresh $A2^+$ human PBMCs in R10; 200 IU/ml IL-2 was added on day 3. $CD8^+$ cells specific for Melan-$A_{26–35}$ were quantified on day 10 with wild-type A2 ELAGIGILTV tetramer.

Results

Generation of MHCI molecules with superenhanced CD8 binding affinity

Tetrameric fusion molecules comprising the α1/α2 peptide binding platform of A2 and the α3 domain of H2-K^b (A2/K^b from this point forward) enable the monitoring of $CD8^+$ T cell responses in A2 transgenic mice (33). This reflects a requirement for the murine MHCI α3 domain to engage murine CD8 (11), thus enabling A2/K^b reagents to stain murine CTL with lower affinity TCR/pMHCI interactions (so-called "low avidity" CTLs) (22). The A2/K^b H chain folded with human β2m interacts strongly with human CD8 (K_D ~10 μM, compared with A2 that binds to CD8 with a K_D ~150 μM) but exhibits unaltered A2-restricted TCR binding properties (9, 22). Thus, fusing the murine α3 domain with A2 α1/α2 domains increases

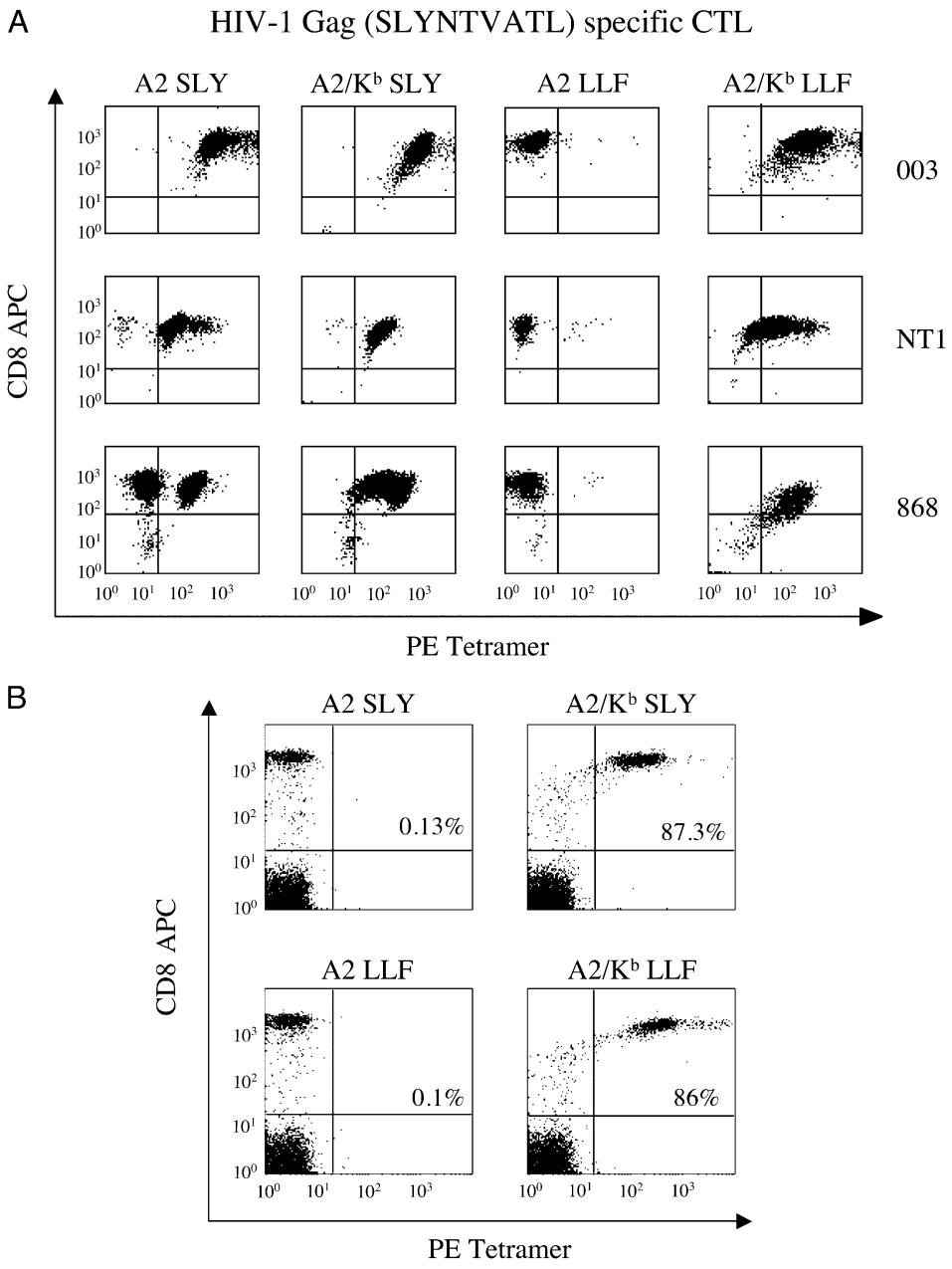

FIGURE 1. The exquisite specificity of pMHCI tetramer staining is lost when the strength of the pMHCI/CD8 interaction is increased by ~15-fold. *A*, The 003 or NT1 CTL clones (10^5 cells) or the 868 CTL line (2.5×10^5 cells), all specific for HIV-1 p17 $Gag_{77–85}$, were stained with 1 μg of the PE-conjugated tetramers A2 SLYNTVATL, A2/K^b SLYNTVATL, A2 LLFGYPVYV, or A2/K^b LLFGYPVYV in 20 μl PBS for 20 min at 37°C. Cells were then stained with allophycocyanin-conjugated anti-CD8 and 7-AAD for 30 min on ice, washed twice, and resuspended in PBS. Data were acquired using a FACSCalibur flow cytometer and analyzed with CellQuest software. *B*, 2.5×10^5 PBMCs were suspended in 250 μl FACS buffer (2% FCS/PBS), then stained with 1 μg of the PE-conjugated tetramers A2 SLYNTVATL, A2/K^b SLYNTVATL, A2 LLFGYPVYV, or A2/K^b LLFGYPVYV for 20 min at 37°C. Each sample was subsequently stained with allophycocyanin-conjugated anti-CD8, PerCP-conjugated anti-CD3, and 7-AAD for 30 min on ice, washed twice, and resuspended in FACS buffer. Data were acquired using a FACSCalibur flow cytometer and analyzed with CellQuest software by gating on the live $CD3^+$ population. The values shown represent the percent of $CD3^+$ $CD8^+$ cells that stain with the indicated tetramer.

the strength of the pMHCI/CD8 interaction by ~15-fold without affecting the TCR/pMHCI interaction.

Superenhanced CD8 binding results in nonspecific pMHCI ligand interactions

Monomeric pMHCI complexes cannot be used to examine TCR/pMHCI binding at the cell surface because of the extremely short half-life of such interactions. Increasing the valency of these molecules by avidin/biotin-based tetramerization overcomes this limitation and produces reagents that are invaluable for the identification and characterization of Ag-specific CTLs (34, 35). Indeed, it is well established that wild-type tetrameric pMHCI reagents bind to cell surface TCR with exquisite specificity (34, 36). Thus, A2/K^b tetrameric reagents were generated to study the effect of superenhanced CD8 binding on the specificity of pMHCI ligand interactions at the cell surface.

Wild-type pMHCI tetrameric reagents bearing cognate peptide stained three distinct A2-restricted CTLs specific for SLYNTVATL (HIV-1 p17 $Gag_{77–85}$), each expressing a different TCR (19, 22, 23) (Fig. 1*A*). Noncognate A2 LLFGYPVYV (HILV-1 $Tax_{11–19}$) tetramers failed to stain any of these in vitro expanded CTL populations to any notable extent. However, A2/K^b LLFGYPVYV tetramers stained all SLYNTVATL-specific CTLs; in addition, both the A2/K^b SLYNTVATL and A2/K^b LLFGYPVYV tetramers stained the noncognate $CD8^+$ cell population in the 868 CTL line (Fig. 1*A*). To examine this effect in more detail, we used A2 and A2/K^b tetramers to stain fresh human PBMCs. Ag-specific $CD8^+$ cell populations were not identified in PBMCs from healthy donors with either the A2 SLYNTVATL or A2 LLFGYPVYV tetramers (Fig. 1*B*). In contrast, both the A2/K^b SLYNTVATL and A2/K^b LLFGYPVYV tetramers stained >85% of $CD8^+$ cells in PBMCs (Fig. 1*B*); similar data were obtained with A2/K^b GLCTLVAML (EBV $BMLF1_{259–267}$) and A2/K^b NLVPMVATV (CMV $pp65_{495–503}$) tetramers (data not shown). Taken together, these data indicate that the exquisite specificity of tetrameric pMHCI reagents is lost when the strength of the pMHCI/CD8

interaction is increased by ~15-fold. Thus, the low solution affinities of the wild-type pMHCI/CD8 interaction are required to maintain pMHCI binding specificity at the cell surface.

A2/K^b tetramers bind the majority of CTLs in peripheral blood

Noncognate A2/K^b tetramers were observed to bind ~80% of the CD8α$^+$ population in peripheral blood (Fig.1*B*). Although CD8α is predominantly found on the surface of αβ-TCR$^+$ CTLs, it is also found on the surface of other lymphocytes, most notably some γδ T cells and NK cells. We therefore sought to determine the identity of the CD8α$^+$ cells that stain with A2/K^b tetramers. Staining of fresh ex vivo PBMCs isolated from healthy A2$^+$ donors revealed that CD8α was expressed on ~39%, 54%, and 32% of the αβ-TCR$^+$, NK cells, and γδ-TCR$^+$ populations, respectively, with some variation between donors (Fig. 2*A*). The majority of γδ-TCR$^+$ (~93.6%) and NK cells (~77%) failed to stain with the A2/K^b ILAKFLHWL (hTERT$_{540–548}$) tetramer and no significant binding was observed with the corresponding A2 tetramer (Fig. 2*B*). However, the vast majority of αβ-TCR$^+$/CD8$^+$ cells within the lymphocyte population stained nonspecifically with the A2/K^b ILAKFLHWL tetramer (Fig. 2*C*).

We hypothesized that most γδ-TCR$^+$ cells and NK cells might fail to bind A2/K^b tetramers because they express the CD8αα homodimer rather than the CD8αβ heterodimer, which is expressed on the surface of CTLs. Thus, we generated a 293T cell line that expressed CD8αα (Fig. 3*A*) to examine the ability of A2/K^b tetramers to bind this homodimeric form of the CD8 coreceptor on the cell surface. In contrast to both A2 and A2 D227K/T228A tetramers, which exhibit normal and abrogated interactions with CD8, respectively, A2/K^b tetramers bound to most (74.3%) of the CD8αα$^+$ 293 T cell transfectants (Fig. 3*A*, 3*B*); no binding was observed in the absence of CD8αα surface expression (Fig. 3*A*). Thus, A2/K^b tetramers are capable of binding to cell surface CD8αα.

Why do A2/K^b tetramers bind predominantly to the CTL population in peripheral blood and not to other cells that express CD8? Fig. 3*B* shows that A2/K^b tetramer staining is directly proportional to the level of CD8αα expression, such that only cells with a higher level

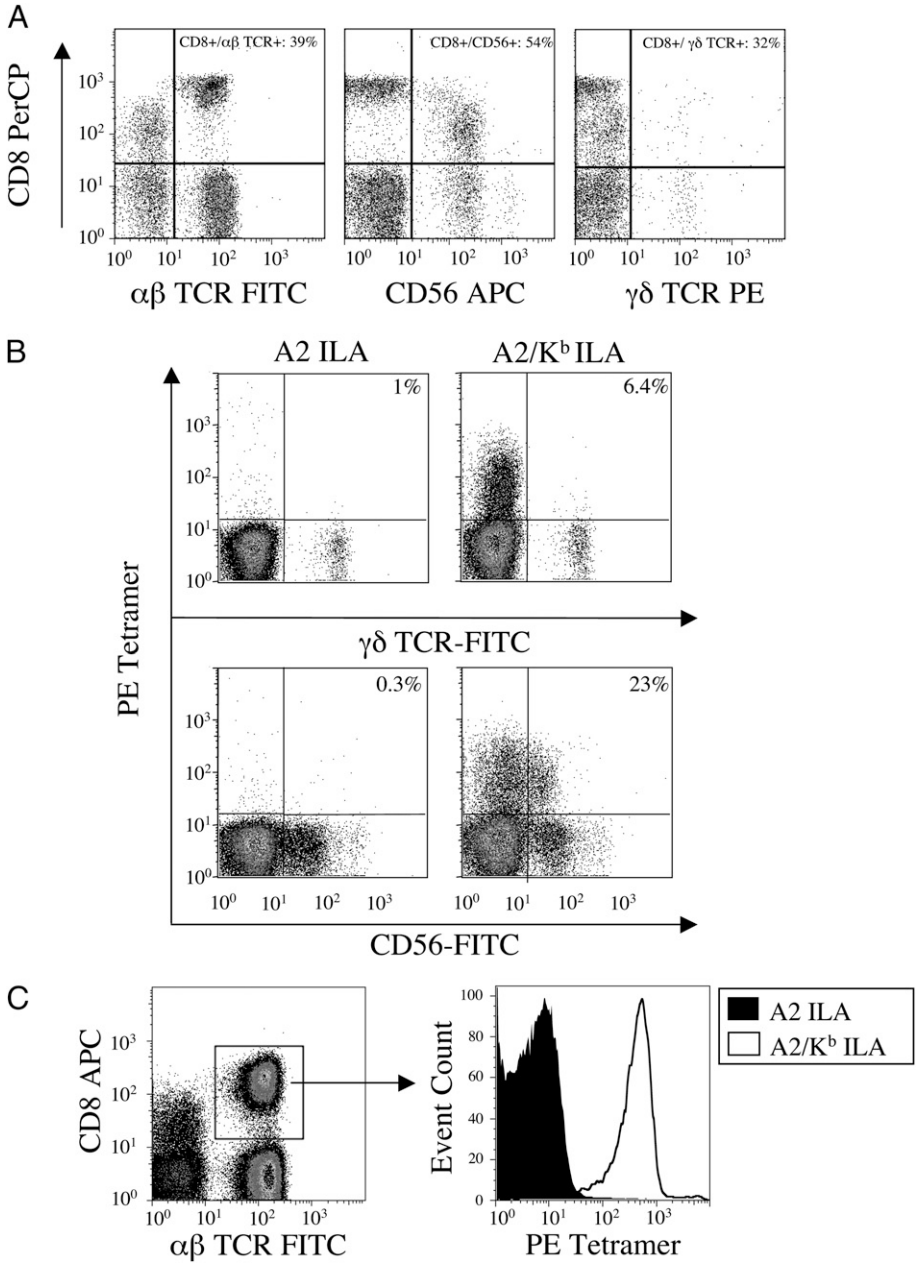

FIGURE 2. A2/K^b tetramers bind the majority of CTLs in peripheral blood. *A*, 2.5 × 10^5 PBMCs from an A2$^+$ donor were stained with PerCP-conjugated anti-CD8, 7-AAD, and either FITC-conjugated anti–αβ-TCR, allophycocyanin-conjugated anti-CD56 or PE-conjugated anti–γδ-TCR for 30 min on ice, washed twice, and resuspended in PBS. *B*, 2.5 × 10^5 A2$^+$ PBMCs were stained with 10 μg/ml of the PE-conjugated tetramers A2 ILAKFLHWL or A2/K^b ILAKFLHWL for 20 min at 37°C. After washing, cells were subsequently stained with 7-AAD and either FITC-conjugated anti–γδ-TCR or FITC-conjugated anti-CD56 for 30 min on ice, washed twice, and resuspended in PBS. *C*, 2.5 × 10^5 A2$^+$ PBMCs were stained with 10 μg/ml of the PE-conjugated tetramers A2 ILAKFLHWL or A2/K^b ILAKFLHWL for 20 min at 37°C. After washing, cells were stained with allophycocyanin-conjugated anti-CD8, FITC-conjugated anti–αβ-TCR and 7-AAD for 30 min on ice, washed twice, and resuspended in PBS. In *A*, *B*, and *C*, data were acquired using a FACSCalibur flow cytometer and analyzed with FlowJo software.

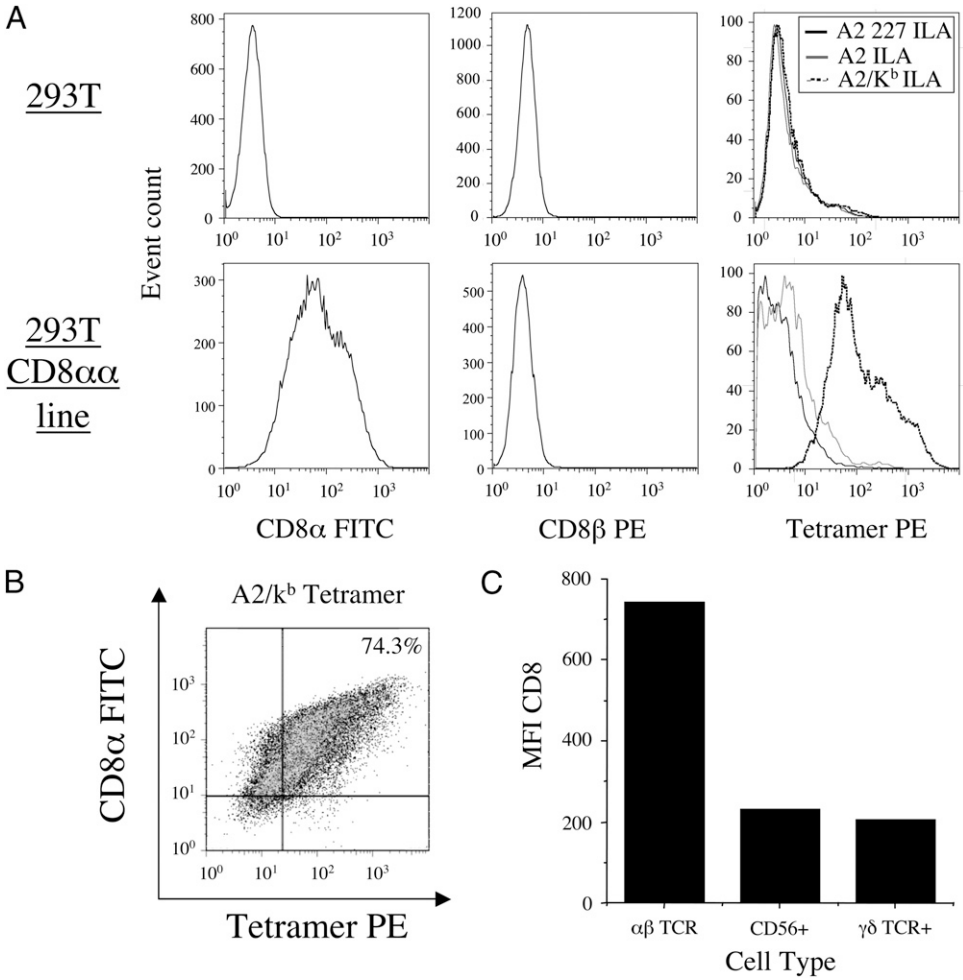

FIGURE 3. Nonspecific A2/K^b tetramer binding is influenced by CD8 cell surface density. *A* and *B*, 2×10^5 293T cells were incubated ± 10 μg/ml of the PE-conjugated tetramers A2 D227K/T228A ILAKFLHWL, A2 ILAKFLHWL, or A2/K^b ILAKFLHWL for 20 min at 37°C, then stained with 7-AAD and either FITC-conjugated anti-CD8 or PE-conjugated anti-CD8β for 30 min on ice, washed twice, and resuspended in PBS. *C*, 2.5×10^5 PBMCs were stained with PerCP-conjugated anti-CD8, 7-AAD, and either FITC-conjugated anti–αβ-TCR, allophycocyanin-conjugated anti-CD56, or PE-conjugated anti–γδ-TCR for 30 min on ice, washed twice, and resuspended in PBS. In *A*, *B*, and *C*, data were acquired using a FACSCalibur flow cytometer and analyzed with FlowJo software.

of CD8αα expression stain with this reagent. Examination of PBMCs from healthy donors revealed that CD8$^+$αβ-TCR$^+$ cells express high levels of CD8, whereas NK and γδ-TCR$^+$ cells express substantially lower levels (Fig. 3*C*). Therefore, increasing the strength of the pMHCI/CD8 interaction allows pMHCI ligand binding at the cell surface that can be mediated through the engagement of either CD8αα or CD8αβ. However, our results suggest that binding is only observed when cells express CD8 at levels above a certain threshold. Importantly, these data demonstrate that TCR expression is not required for cell surface binding of A2/K^b tetramers.

A2/K^b tetramers activate CTLs irrespective of TCR specificity

It is well established that pMHCI tetramers can activate CTLs bearing cognate TCR [reviewed in (35)]. However, previous studies have shown that pMHCI tetrameric binding at the cell surface does not necessarily equate with activation (11, 37). Thus, we next examined whether nonspecific A2/K^b tetramer binding at the cell surface (Figs. 1–3) could activate human CTLs. Initially, we studied the A2-restricted SLYNTVATL-specific CTL clone 003 (23). Consistent with our findings previously stated, both A2 SLYNTVATL and A2/K^b SLYNTVATL tetramers stained 003 CTLs efficiently, as did the noncognate A2/K^b LLFGYPVYV tetramer; no staining was observed with the A2 LLFGYPVYV tetramer (Fig. 4*A*). On ligation, it is known that TCRs are downregulated from the cell surface (38). The cognate A2 tetramer was able to induce significant TCR downregulation, even at tetramer concentrations well below the limits of detection by flow cytometry; no TCR downregulation was observed with the noncognate A2 LLFGYPVYV tetramer (Fig. 4*B*). In contrast, however, both the A2/K^b SLYNTVATL and A2/K^b LLFGYPVYV tetramers induced TCR downregulation, although this occurred to a lesser extent with the noncognate form compared with either of the cognate tetramers (Fig. 4*B*). This TCR downregulation correlated with various functional readouts typical of CTL effector activity, including the production of RANTES (Fig. 4*C*), IFN-γ, and MIP-1β (data not shown). Similar results were observed with SLYNTVATL-specific CTLs bearing an alternative cognate TCR (Fig. 4*D*, 4*E*). Consistent with the staining patterns (Fig. 4*A*), the activation of CTLs by noncognate A2/K^b tetramers was less efficient than that induced by tetramers bearing the agonist peptide (Fig. 4*C–E*).

To dissect this effect further at the single-cell level within a clonal CTL population, we used a flow cytometric assay for degranulation based on the detection of CD107a mobilized on to the cell surface (32). The noncognate A2/K^b tetramer, in this case folded around the GLCTLVAML peptide, induced degranulation in 15% of 003 CTLs at a concentration of 5 μg/ml (Fig. 4*F*); the cognate A2 SLYNTVATL and A2/K^b SLYNTVATL tetramers induced almost 40% degranulation (data not shown). Notably, the cells that degranulated in response to the A2/K^b GLCTLVAML tetramer were contained

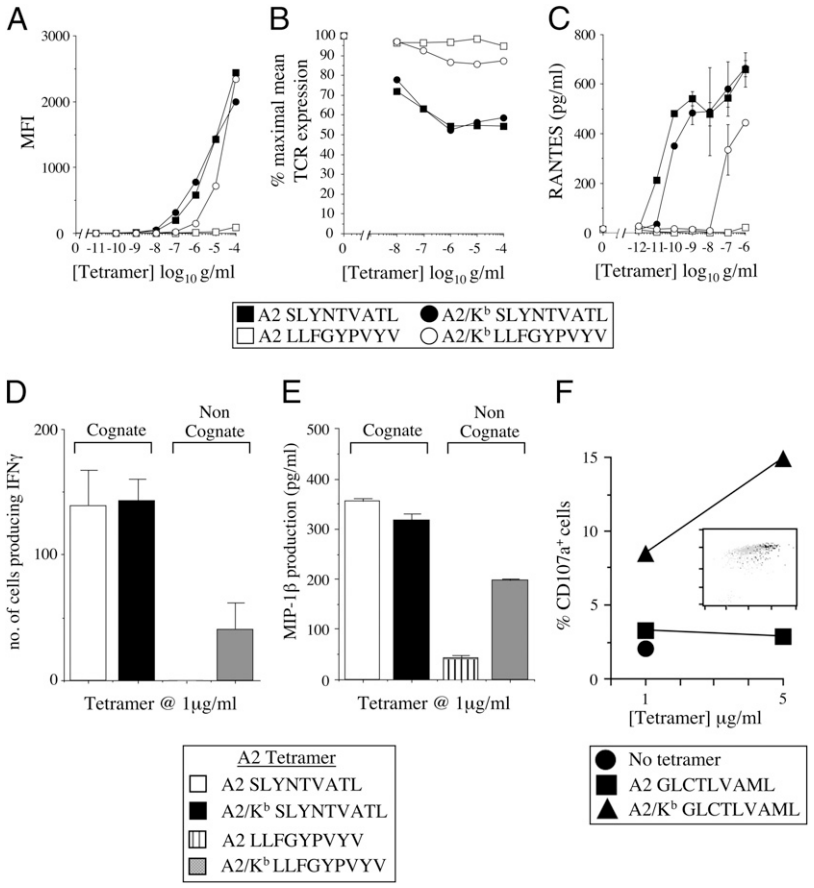

FIGURE 4. A2/K^b tetramers can activate CTLs in the absence of a specific TCR/pMHCI interaction. *A*, 10^5 003 CTLs were suspended in 20 μl PBS and stained with the PE-conjugated tetramers A2 SLYNTVATL, A2/K^b SLYNTVATL, A2 LLFGYPVYV, or A2/K^b LLFGYPVYV at the indicated concentrations and 7-AAD for 20 min at 37°C. Cells were then washed twice and resuspended in PBS. Data were acquired using a FACSCalibur flow cytometer and analyzed with CellQuest software. *B*, 10^5 003 CTLs were suspended in 40 μl R2 with the PE-conjugated tetramers A2 SLYNTVATL, A2/K^b SLYNTVATL, A2 LLFGYPVYV, or A2/K^b LLFGYPVYV at the indicated concentrations for 30 min at 37°C. Cells were subsequently stained with FITC-conjugated anti–αβ-TCR, 7-AAD, and allophycocyanin-conjugated anti-CD8 for 30 min on ice in azide buffer (0.1% azide/2% FCS/PBS). After two washes, data were acquired using a FACSCalibur flow cytometer and analyzed with CellQuest software. *C*, 5×10^5 003 CTLs were incubated with the PE-conjugated tetramers A2 SLYNTVATL, A2/K^b SLYNTVATL, A2 LLFGYPVYV, or A2/K^b LLFGYPVYV at the indicated concentrations. After 4 h at 37°C, supernatants were harvested and assayed for RANTES, IFN-γ and MIP-1β content by ELISA (only RANTES shown). *D*, 2×10^3 868 CTLs were incubated for 4 h at 37°C with 1 μg/ml of the PE-conjugated tetramers A2 SLYNTVATL, A2/K^b SLYNTVATL, A2 LLFGYPVYV, or A2/K^b LLFGYPVYV in an IFN-γ ELISpot assay. *E*, 1.25×10^5 868 CTLs were incubated with 1 μg/ml of the PE-conjugated tetramers A2 SLYNTVATL, A2/K^b SLYNTVATL, A2 LLFGYPVYV, or A2/K^b LLFGYPVYV for 4 h at 37°C. The supernatant was subsequently assayed for MIP-1β content by ELISA. Panels (*C–E)* show the mean ± SD of two replicate assays. Results similar to (*A–E*) were also obtained with tetramers conjugated to fluorochromes other than PE (data not shown). *F*, 003 CTLs were incubated with the PE-conjugated tetramers A2 SLYNTVATL, A2/K^b SLYNTVATL, A2 GLCTLVAML, or A2/K^b GLCTLVAML at the indicated concentrations for 4 h at 37°C, then stained with allophycocyanin-conjugated anti-CD8 for 20 min on ice and assayed for CD107a mobilization as described in *Materials and Methods*. The inset plot shows staining for allophycocyanin-conjugated anti-CD8 on the *x*-axis and PE-conjugated A2/K^b GLCTLVAML tetramer (5 μg/ml) on the *y*-axis. Backgated tetramer$^+$CD107a$^+$ cells are shown in black and tetramer$^+$ CD107a$^-$ cells are shown in gray. Tetramer^{high}CD8^{high} cells are preferentially activated by the A2/K^b tetramer.

almost exclusively within the tetramer^{high}CD8^{high} population (Fig. 4*F*). Thus, at least to some extent, the strong interaction between A2/K^b and CD8 can bypass the requirement for a specific TCR/pMHCI interaction and nonspecifically activate human CTLs.

Cell surface-expressed A2/K^b activates CTLs in the absence of cognate Ag

To extend our investigation to the effects of cell surface pMHCI presentation, C1R cells were transfected with either A2 or A2/K^b; stable transfectants expressing similar cell surface MHCI densities were selected as targets for further experiments. Target cells expressing either A2 or A2/K^b were incubated overnight with three A2-restricted CTL clones with different peptide specificities (Mel13, 003, and ILA1). Targets that expressed A2 failed to activate any of the CTL clones significantly above background (Fig. 5*A*). Remarkably, however, the A2/K^b targets stimulated Mel13, 003, and ILA1 CTLs to produce significant amounts of MIP-1β in the absence of specific peptide (Fig. 5*A*). A2/K^b targets also elicited substantial levels of TNFα and IFN-γ at titratable E:T ratios (Fig. 5*B*), induced degranulation (Fig. 5*C*), and induced significant levels of killing (data not shown) in the absence of specific TCR/pMHCI interactions.

Cell surface-expressed A2/K^b primes noncognate CTL expansions

Thymic output in healthy A2$^+$ individuals is known to generate a high frequency of naïve CD8$^+$ T cells that can recognize the self-Ag Melan-A$_{26–35}$ (39); this system can be used to examine the priming of CTLs directly ex vivo (40). We exploited these observations to investigate the effect of superenhanced pMHCI/CD8 binding on CTL priming. In priming experiments conducted with C1R target cells, the percentages of CTLs specific for Melan-A$_{26–35}$ that were present after 10 d in culture were related to the context of the pMHCI/CD8 interaction in which the cognate ELAGIGILTV peptide was presented.

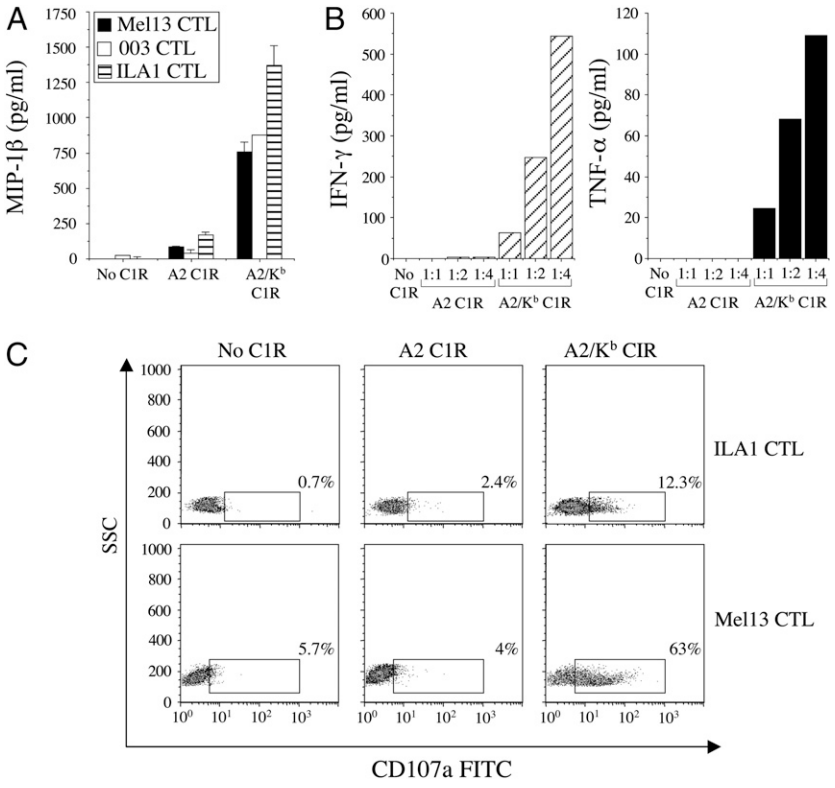

FIGURE 5. Cell surface-expressed A2/K^b activates CTLs in the absence of cognate Ag. *A*, 2.5 × 10^4 Mel13, 003, or ILA1 CTLs were incubated for 12 h at 37°C with 10^5 C1R cells stably transfected to express equal levels of either A2 or A2/K^b at the cell surface. Supernatant was subsequently assayed for MIP-1β content by ELISA. The mean ± SD of two replicate assays is shown. *B*, 2.5 × 10^4 Mel13 CTLs were incubated for 12 h at 37°C with 10^5 C1R cells stably transfected to express either A2 or A2/K^b at the cell surface. Supernatant was assayed for IFN-γ and TNFα content by cytokine bead array. *C*, CD107a expression by ILA1 and Mel13 CTLs after a 12-h incubation at 37°C with C1R cells stably transfected to express either A2 or A2/K^b on the cell surface. For (*A–C*), C1R cells were not previously pulsed with peptide.

Thus, in the absence of a pMHCI/CD8 interaction (A2 D227K/T228A C1R targets), only 1.5% of the CD8$^+$ cell population was specific for Melan-A$_{26–35}$; in contrast, 5.6% and 5.7% of the CD8$^+$ population bound the A2 ELAGIGILTV tetramer in the same experiment when priming was conducted with A2 and A2/K^b C1R targets, respectively (Fig. 6). Exposure to A2/K^b C1R targets also resulted in substantial expansions of the total CD8$^+$ population (Fig. 6). Similar results were obtained with multiple donors (data not shown). Thus, target cells that express MHCI molecules with superenhanced CD8-binding properties can induce nonspecific expansions of CD8$^+$ cells in the absence of cognate Ag.

Nonspecific A2/K^b-mediated CTL activation and tetramer staining are not dependent on TCR expression

In earlier experiments, we observed that A2/K^b tetramers bound to the majority of αβ-TCR$^+$CD8$^+$ cells in PBMCs derived from A2$^+$ donors (Fig. 2). To exclude the possibility that this phenomenon was dependent on the presence of A2-restricted TCRs, we conducted staining experiments with A2$^-$ PBMCs. As previously, the A2/K^b ILAKFLHWL tetramer bound nonspecifically to the majority of CD8$^+$ cells (Fig. 7*A*). Furthermore, A2/K^b tetramer binding favored CD8^{high} cells and was abrogated by pretreatment with the anti-CD8 mAb DK25 (Fig. 7*A*). Thus, consistent with the data shown in Fig. 3, nonspecific A2/K^b tetramer binding is a CD8-mediated effect that is not dependent on the presence of A2-restricted TCRs. In addition, we demonstrated in earlier experiments that A2/K^b, both in soluble and cell-associated form, nonspecifically activated A2-restricted CTL (Figs. 4, 5). To confirm that these functional correlates of nonspecific binding were similarly independent of A2-restricted TCR expression, we extended our studies to CTL clones restricted by non-A2 MHCI molecules. In all cases, cell surface-expressed A2/K^b activated CTL clones regardless of restriction element (Fig. 7*B*).

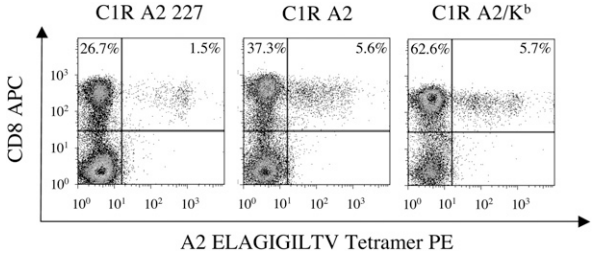

FIGURE 6. Cell surface-expressed A2/K^b primes nonspecific expansion of CD8$^+$ cells. 10^6 A2$^+$ PBMCs were incubated with 2 × 10^5 irradiated A2 D227K/T228A, A2, or A2/K^b C1R cells that had previously been pulsed with 1 μM ELAGIGILTV (Melan-A$_{26–35}$) peptide in R10. From day 3, IL-2 was added in increments to reach a maximum concentration of 200 IU/ml by day 10. Lines were subsequently stained with PE-conjugated A2 ELAGIGILTV tetramer, followed by allophycocyanin-conjugated anti-CD8 and 7-AAD. Data were acquired using a FACSCalibur flow cytometer and analyzed with FlowJo software.

Discussion

CD8 has the potential to engage all pMHCI complexes, both self and foreign, because it binds to largely nonpolymorphic regions of the MHCI molecule. Indeed, recent publications suggest that the ability of CD8 to interact with nonstimulatory pMHCI complexes lowers T cell activation thresholds and enables CTLs to respond to low copy numbers of specific pMHCI (41, 42). It therefore remains unclear how the specificity of TCR recognition is maintained, despite the potential for multiple pMHCI/CD8 interactions at the cell surface. One possibility resides in the fact that the binding of CD8 to MHCI is characterized by very low affinities and extremely rapid kinetics. In this study, we have generated chimeric A2/K^b MHCI molecules that increase the strength of the pMHCI/CD8 interaction by ~15-fold to probe the biophysical and functional significance of the low solution binding affinities observed for the pMHCI/CD8 interaction.

Initially, we examined the effect of superenhanced CD8 binding on pMHCI tetramer binding at the cell surface. Increasing the strength of the pMHCI/CD8 interaction by ~15-fold resulted in the total loss of pMHCI

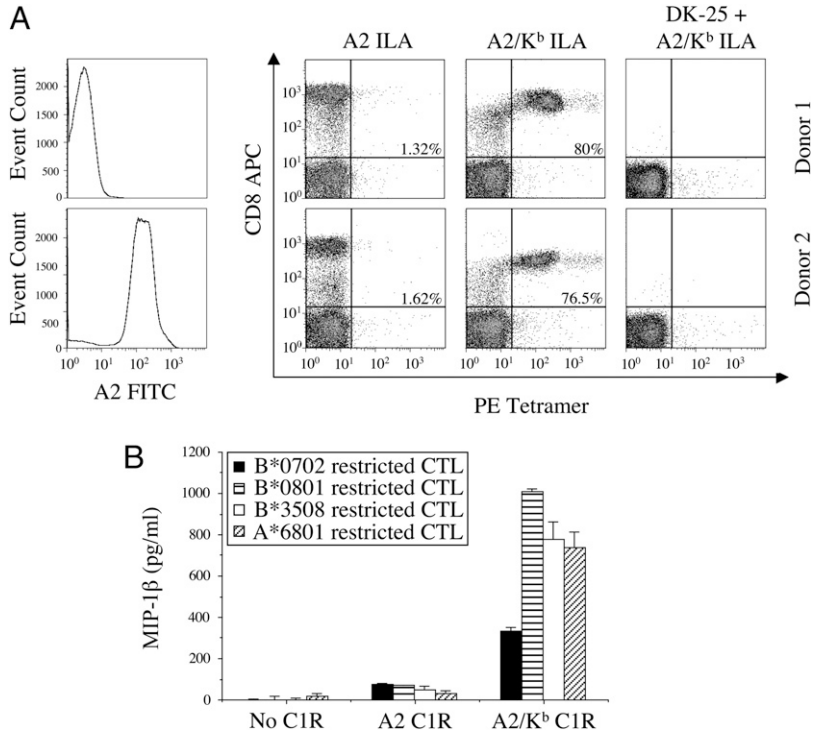

FIGURE 7. Noncognate A2/K^b-mediated CTL activation and tetramer binding is not influenced by MHCI restriction. *A*, 2.5×10^5 PBMCs were suspended in 250 μl FACS buffer (2% FCS/PBS) and stained with FITC-conjugated anti-A2 and 7-AAD for 30 min on ice, then washed twice, and resuspended in PBS. For pMHCI tetramer staining experiments, 2.5×10^5 PBMCs were suspended in 50 μl FACS buffer (2% FCS/PBS) and incubated ± 10 μg/ml unconjugated anti-CD8 for 20 min on ice, then stained with 10 μg/ml of the PE-conjugated tetramers A2 ILAKFLHWL or A2/K^b ILAKFLHWL for 45 min on ice. After washing, cells were subsequently stained with allophycocyanin-conjugated anti-CD8 and 7-AAD, washed again, and resuspended in PBS. Data were acquired using a FACSCalibur flow cytometer and analyzed with FlowJo software. *B*, 2.5×10^4 CTLs were incubated for 12 h at 37°C with 10^5 unpulsed C1R cells expressing either A2 or A2/K^b on the cell surface. The following CTL clones were used: 1) the HLA A*6801-restricted CTL clone c23, specific for the HIV-1 Tat-derived epitope ITKGLGISYGR (residues 38–48); 2) the HLA B*0702-restricted CTL clone KD4, specific for the EBV EBNA3A-derived epitope RPPIFIRRL (residues 379–387); 3) the HLA B*0801-restricted CTL clone LC13, specific for the EBV EBNA3A-derived epitope FLRGRAYGL (residues 339–347); and 4) the HLA B*3508-restricted CTL clone SB27, specific for the EBV BZLF1-derived epitope LPEPLPQGQLTAY (residues 52–64). Supernatant was subsequently assayed for MIP-1β content by ELISA. The mean ± SD of two replicate assays is shown.

tetramer binding specificity. Thus, irrespective of restriction element and the presented peptide, A2/K^b tetramers bound to the surface of all CTL clones examined in this study and to the majority of CTLs present within PBMCs (Figs. 1, 2, 7*A*). In addition, A2/K^b tetramers bound to the cell surface in the absence of TCR expression (Fig. 3) and nonspecific binding was abrogated by pretreatment with an anti-CD8 Ab (Fig. 7*A*), thereby demonstrating that the observed loss of pMHCI tetramer binding specificity was CD8 mediated and TCR independent. These findings indicate that the low solution binding affinities observed for the pMHCI/CD8 interaction are essential for the preservation of pMHCI ligand binding specificity at the cell surface.

It has previously been documented that pMHCI tetramers are efficient activators of cognate CTLs [reviewed in (35)]. However, pMHCI tetramer staining does not necessarily equate with cellular activation. Therefore, we proceeded to examine the ability of A2/K^b tetramers to activate CTL clones. Notably, we found that A2/K^b tetramers activated CTL clones in a nonspecific manner (Fig. 4). Activation resulted in a full range of effector functions, including cytokine/chemokine release, degranulation, and killing. Flow cytometric assessment of degranulation by analysis of CD107a mobilization revealed that CTLs with higher surface expression of CD8 were the cells most likely to activate in response to A2/K^b molecules. This finding led us to examine the effects of cell-surface presented Ag. Strikingly, exposure of PBMCs to C1R target cells bearing A2/K^b molecules caused a general nonspecific expansion of CD8$^+$ cells during the course of the experiment (Fig. 6). Furthermore, A2/K^b C1R cells, unlike their wild-type A2 counterparts, were capable of stimulating effector function in all CTL clones tested regardless of specificity and MHCI restriction (Figs. 5, 7*B*). Although we cannot exclude the possibility that inclusion of the murine α3 domain induces conformational changes at the T cell surface on binding to CD8 that favor noncognate activation, this seems unlikely given that: 1) the TCR binding site remains unaltered (9, 22); 2) a degree of noncognate activation can be observed in long-term assays with nonchimeric human MHCI molecules that exhibit incrementally enhanced CD8 binding (data not shown); and 3) murine and human pMHCI/CD8αα cocrystals exhibit similar binding orientations (14, 43). Furthermore, these results are consistent with the observation that thymus leukemia Ag, which interacts strongly ($K_D \sim 12$ μM) with cell surface CD8αα expressed by intraepithelial lymphocytes, can modulate T cell responses independently of the TCR (44–46).

How does a superenhanced pMHCI/CD8 interaction result in nonspecific CTL activation? We have previously demonstrated that an incremental increase in the pMHCI/CD8 interaction (A2 Q115E) results in enhanced immunogenicity of cognate Ags and that this effect is mediated by enhanced early intracellular signal transduction (9, 47). In contrast, the stimulatory properties of A2/K^b molecules exhibited no peptide specificity requirements whatsoever; indeed, cell surface-expressed A2/K^b was shown to activate even non-A2–restricted CTL clones (Fig. 7*B*), thereby confirming that cognate TCR/pMHCI interactions are not required. Combined with the ability of A2/K^b to engage multiple CD8 molecules at the cell surface, these results suggest that A2/K^b cross-links CD8 and induces activation in an "Ab-like" manner. Indeed, this is consistent with previous studies demonstrating that Ab-induced CD8

cross-linking can induce T cell signaling (48, 49) and elicit downstream effector functions, such as chemokine release (50); such effects are predictable given that the CD8α tail is coupled to p56lck, an essential component of the early intracellular signaling pathway (10). It is interesting to note that the murine pMHCI/CD8 interaction is significantly stronger (K_D ~30 μM) than the equivalent human interaction (K_D ~150 μM) (11), but does not result in noncognate CTL activation. It is therefore likely that a pMHCI/CD8 interaction affinity threshold exists for the maintenance of CTL activation specificity. The strength of the murine pMHCI/CD8 interaction is 3-fold weaker than the strength of the interaction measured between A2/K^b and human CD8, thereby still operating at a level below this threshold.

In summary, we used chimeric MHCI molecules that exhibit a superenhanced interaction with CD8 to probe the physical and functional significance of the low solution binding affinities previously described for the pMHCI/CD8 interaction. We found that increasing the strength of the pMHCI/CD8 interaction by ~15-fold resulted in: 1) total loss of pMHCI binding specificity at the cell surface; 2) noncognate pMHCI tetramer-mediated activation; and 3) nonspecific activation and proliferation triggered by cell surface-expressed pMHCI molecules. Thus, the low solution binding affinity of the pMHCI/CD8 interaction is essential for the preservation of pMHCI ligand binding specificity at the cell surface and its attendant functional repercussions.

Acknowledgments

We thank E. Wang for provision of the allophycocyanin-conjugated mAb specific for human CD56.

Disclosures

The authors have no financial conflicts of interest.

References

1. Davis, M. M., J. J. Boniface, Z. Reich, D. Lyons, J. Hampl, B. Arden, and Y. Chien. 1998. Ligand recognition by alpha beta T cell receptors. *Annu. Rev. Immunol.* 16: 523–544.
2. Rudolph, M. G., and I. A. Wilson. 2002. The specificity of TCR/pMHC interaction. *Curr. Opin. Immunol.* 14: 52–65.
3. Zamoyska, R. 1998. CD4 and CD8: modulators of T-cell receptor recognition of antigen and of immune responses? *Curr. Opin. Immunol.* 10: 82–87.
4. Holler, P. D., and D. M. Kranz. 2003. Quantitative analysis of the contribution of TCR/pepMHC affinity and CD8 to T cell activation. *Immunity* 18: 255–264.
5. Gakamsky, D. M., I. F. Luescher, A. Pramanik, R. B. Kopito, F. Lemonnier, H. Vogel, R. Rigler, and I. Pecht. 2005. CD8 kinetically promotes ligand binding to the T-cell antigen receptor. *Biophys. J.* 89: 2121–2133.
6. Laugel, B., H. A. van den Berg, E. Gostick, D. K. Cole, L. Wooldridge, J. Boulter, A. Milicic, D. A. Price, and A. K. Sewell. 2007. Different T cell receptor affinity thresholds and CD8 coreceptor dependence govern cytotoxic T lymphocyte activation and tetramer binding properties. *J. Biol. Chem.* 282: 23799–23810.
7. van den Berg, H. A., L. Wooldridge, B. Laugel, and A. K. Sewell. 2007. Coreceptor CD8-driven modulation of T cell antigen receptor specificity. *J Theor Biol* 249: 395-408.
8. Luescher, I. F., E. Vivier, A. Layer, J. Mahiou, F. Godeau, B. Malissen, and P. Romero. 1995. CD8 modulation of T-cell antigen receptor-ligand interactions on living cytotoxic T lymphocytes. *Nature* 373: 353–356.
9. Wooldridge, L., H. A. van den Berg, M. Glick, E. Gostick, B. Laugel, S. L. Hutchinson, A. Milicic, J. M. Brenchley, D. C. Douek, D. A. Price, and A. K. Sewell. 2005. Interaction between the CD8 coreceptor and major histocompatibility complex class I stabilizes T cell receptor-antigen complexes at the cell surface. *J. Biol. Chem.* 280: 27491–27501.
10. Veillette, A., M. A. Bookman, E. M. Horak, and J. B. Bolen. 1988. The CD4 and CD8 T cell surface antigens are associated with the internal membrane tyrosine-protein kinase p56lck. *Cell* 55: 301–308.
11. Purbhoo, M. A., J. M. Boulter, D. A. Price, A. L. Vuidepot, C. S. Hourigan, P. R. Dunbar, K. Olson, S. J. Dawson, R. E. Phillips, B. K. Jakobsen, et al. 2001. The human CD8 coreceptor effects cytotoxic T cell activation and antigen sensitivity primarily by mediating complete phosphorylation of the T cell receptor zeta chain. *J. Biol. Chem.* 276: 32786–32792.
12. Arcaro, A., C. Grégoire, T. R. Bakker, L. Baldi, M. Jordan, L. Goffin, N. Boucheron, F. Wurm, P. A. van der Merwe, B. Malissen, and I. F. Luescher. 2001. CD8beta endows CD8 with efficient coreceptor function by coupling T cell receptor/CD3 to raft-associated CD8/p56(lck) complexes. *J. Exp. Med.* 194: 1485–1495.
13. Arcaro, A., C. Grégoire, N. Boucheron, S. Stotz, E. Palmer, B. Malissen, and I. F. Luescher. 2000. Essential role of CD8 palmitoylation in CD8 coreceptor function. *J. Immunol.* 165: 2068–2076.
14. Gao, G. F., J. Tormo, U. C. Gerth, J. R. Wyer, A. J. McMichael, D. I. Stuart, J. I. Bell, E. Y. Jones, and B. K. Jakobsen. 1997. Crystal structure of the complex between human CD8alpha(alpha) and HLA-A2. *Nature* 387: 630–634.
15. Wyer, J. R., B. E. Willcox, G. F. Gao, U. C. Gerth, S. J. Davis, J. I. Bell, P. A. van der Merwe, and B. K. Jakobsen. 1999. T cell receptor and coreceptor CD8 alphaalpha bind peptide-MHC independently and with distinct kinetics. *Immunity* 10: 219–225.
16. Gao, G. F., B. E. Willcox, J. R. Wyer, J. M. Boulter, C. A. O'Callaghan, K. Maenaka, D. I. Stuart, E. Y. Jones, P. A. Van Der Merwe, J. I. Bell, and B. K. Jakobsen. 2000. Classical and nonclassical class I major histocompatibility complex molecules exhibit subtle conformational differences that affect binding to CD8alphaalpha. *J. Biol. Chem.* 275: 15232–15238.
17. Dustin, M. L., D. E. Golan, D. M. Zhu, J. M. Miller, W. Meier, E. A. Davies, and P. A. van der Merwe. 1997. Low affinity interaction of human or rat T cell adhesion molecule CD2 with its ligand aligns adhering membranes to achieve high physiological affinity. *J. Biol. Chem.* 272: 30889–30898.
18. Cole, D. K., N. J. Pumphrey, J. M. Boulter, M. Sami, J. I. Bell, E. Gostick, D. A. Price, G. F. Gao, A. K. Sewell, and B. K. Jakobsen. 2007. Human TCR-binding affinity is governed by MHC class restriction. *J. Immunol.* 178: 5727–5734.
19. Varela-Rohena, A., P. E. Molloy, S. M. Dunn, Y. Li, M. M. Suhoski, R. G. Carroll, A. Milicic, T. Mahon, D. H. Sutton, B. Laugel, et al. 2008. Control of HIV-1 immune escape by CD8 T cells expressing enhanced T-cell receptor. *Nat. Med.* 14: 1390–1395.
20. Stone, J. D., A. S. Chervin, and D. M. Kranz. 2009. T-cell receptor binding affinities and kinetics: impact on T-cell activity and specificity. *Immunology* 126: 165–176.
21. Hutchinson, S. L., L. Wooldridge, S. Tafuro, B. Laugel, M. Glick, J. M. Boulter, B. K. Jakobsen, D. A. Price, and A. K. Sewell. 2003. The CD8 T cell coreceptor exhibits disproportionate biological activity at extremely low binding affinities. *J. Biol. Chem.* 278: 24285–24293.
22. Choi, E. M., J. L. Chen, L. Wooldridge, M. Salio, A. Lissina, N. Lissin, I. F. Hermans, J. D. Silk, F. Mirza, M. J. Palmowski, et al. 2003. High avidity antigen-specific CTL identified by CD8-independent tetramer staining. *J. Immunol.* 171: 5116–5123.
23. Sewell, A. K., G. C. Harcourt, P. J. Goulder, D. A. Price, and R. E. Phillips. 1997. Antagonism of cytotoxic T lymphocyte-mediated lysis by natural HIV-1 altered peptide ligands requires simultaneous presentation of agonist and antagonist peptides. *Eur. J. Immunol.* 27: 2323–2329.
24. Purbhoo, M. A., Y. Li, D. H. Sutton, J. E. Brewer, E. Gostick, G. Bossi, B. Laugel, R. Moysey, E. Baston, N. Liddy, et al. 2007. The HLA A*0201-restricted hTERT(540-548) peptide is not detected on tumor cells by a CTL clone or a high-affinity T-cell receptor. *Mol. Cancer Ther.* 6: 2081–2091.
25. Gostick, E., D. K. Cole, S. L. Hutchinson, L. Wooldridge, S. Tafuro, B. Laugel, A. Lissina, A. Oxenius, J. M. Boulter, D. A. Price, and A. K. Sewell. 2007. Functional and biophysical characterization of an HLA-A*6801-restricted HIV-specific T cell receptor. *Eur. J. Immunol.* 37: 479–486.
26. Burrows, S. R., S. L. Silins, D. J. Moss, R. Khanna, I. S. Misko, and V. P. Argaet. 1995. T cell receptor repertoire for a viral epitope in humans is diversified by tolerance to a background major histocompatibility complex antigen. *J. Exp. Med.* 182: 1703–1715.
27. Kjer-Nielsen, L., C. S. Clements, A. W. Purcell, A. G. Brooks, J. C. Whisstock, S. R. Burrows, J. McCluskey, and J. Rossjohn. 2003. A structural basis for the selection of dominant alphabeta T cell receptors in antiviral immunity. *Immunity* 18: 53–64.
28. Tynan, F. E., S. R. Burrows, A. M. Buckle, C. S. Clements, N. A. Borg, J. J. Miles, T. Beddoe, J. C. Whisstock, M. C. Wilce, S. L. Silins, et al. 2005. T cell receptor recognition of a 'super-bulged' major histocompatibility complex class I-bound peptide. *Nat. Immunol.* 6: 1114–1122.
29. Tynan, F. E., N. A. Borg, J. J. Miles, T. Beddoe, D. El-Hassen, S. L. Silins, W. J. van Zuylen, A. W. Purcell, L. Kjer-Nielsen, J. McCluskey, et al. 2005. High resolution structures of highly bulged viral epitopes bound to major histocompatibility complex class I. Implications for T-cell receptor engagement and T-cell immunodominance. *J. Biol. Chem.* 280: 23900–23909.
30. Willemsen, R., C. Ronteltap, M. Heuveling, R. Debets, and R. Bolhuis. 2005. Redirecting human CD4+ T lymphocytes to the MHC class I-restricted melanoma antigen MAGE-A1 by TCR alphabeta gene transfer requires CD8alpha. *Gene Ther.* 12: 140–146.
31. Willemsen, R. A., Z. Sebestyén, C. Ronteltap, C. Berrevoets, J. Drexhage, and R. Debets. 2006. CD8 alpha coreceptor to improve TCR gene transfer to treat melanoma: down-regulation of tumor-specific production of IL-4, IL-5, and IL-10. *J. Immunol.* 177: 991–998.
32. Betts, M. R., J. M. Brenchley, D. A. Price, S. C. De Rosa, D. C. Douek, M. Roederer, and R. A. Koup. 2003. Sensitive and viable identification of antigen-specific CD8+ T cells by a flow cytometric assay for degranulation. *J. Immunol. Methods* 281: 65–78.
33. Choi, E. M., M. Palmowski, J. Chen, and V. Cerundolo. 2002. The use of chimeric A2K(b) tetramers to monitor HLA A2 immune responses in HLA A2 transgenic mice. *J. Immunol. Methods* 268: 35–41.
34. Altman, J. D., P. A. Moss, P. J. Goulder, D. H. Barouch, M. G. McHeyzer-Williams, J. I. Bell, A. J. McMichael, and M. M. Davis. 1996. Phenotypic analysis of antigen-specific T lymphocytes. *Science* 274: 94–96.
35. Wooldridge, L., A. Lissina, D. K. Cole, H. A. van den Berg, D. A. Price, and A. K. Sewell. 2009. Tricks with tetramers: how to get the most from multimeric peptide-MHC. *Immunology* 126: 147–164.

36. Burrows, S. R., N. Kienzle, A. Winterhalter, M. Bharadwaj, J. D. Altman, and A. Brooks. 2000. Peptide-MHC class I tetrameric complexes display exquisite ligand specificity. *J. Immunol.* 165: 6229–6234.
37. Schott, E., and H. L. Ploegh. 2002. Mouse MHC class I tetramers that are unable to bind to CD8 reveal the need for CD8 engagement in order to activate naive CD8 T cells. *Eur. J. Immunol.* 32: 3425–3434.
38. Valitutti, S., S. Müller, M. Cella, E. Padovan, and A. Lanzavecchia. 1995. Serial triggering of many T-cell receptors by a few peptide-MHC complexes. *Nature* 375: 148–151.
39. Zippelius, A., M. J. Pittet, P. Batard, N. Rufer, M. de Smedt, P. Guillaume, K. Ellefsen, D. Valmori, D. Liénard, J. Plum, et al. 2002. Thymic selection generates a large T cell pool recognizing a self-peptide in humans. *J. Exp. Med.* 195: 485–494.
40. Salio, M., M. J. Palmowski, A. Atzberger, I. F. Hermans, and V. Cerundolo. 2004. CpG-matured murine plasmacytoid dendritic cells are capable of in vivo priming of functional CD8 T cell responses to endogenous but not exogenous antigens. *J. Exp. Med.* 199: 567–579.
41. Yachi, P. P., J. Ampudia, N. R. Gascoigne, and T. Zal. 2005. Nonstimulatory peptides contribute to antigen-induced CD8-T cell receptor interaction at the immunological synapse. *Nat. Immunol.* 6: 785–792.
42. Anikeeva, N., T. Lebedeva, A. R. Clapp, E. R. Goldman, M. L. Dustin, H. Mattoussi, and Y. Sykulev. 2006. Quantum dot/peptide-MHC biosensors reveal strong CD8-dependent cooperation between self and viral antigens that augment the T cell response. *Proc. Natl. Acad. Sci. USA* 103: 16846–16851.
43. Kern, P. S., M. K. Teng, A. Smolyar, J. H. Liu, J. Liu, R. E. Hussey, R. Spoerl, H. C. Chang, E. L. Reinherz, and J. H. Wang. 1998. Structural basis of CD8 coreceptor function revealed by crystallographic analysis of a murine CD8alphaalpha ectodomain fragment in complex with H-2Kb. *Immunity* 9: 519–530.
44. Leishman, A. J., O. V. Naidenko, A. Attinger, F. Koning, C. J. Lena, Y. Xiong, H. C. Chang, E. Reinherz, M. Kronenberg, and H. Cheroutre. 2001. T cell responses modulated through interaction between CD8alphaalpha and the nonclassical MHC class I molecule, TL. *Science* 294: 1936–1939.
45. Tsujimura, K., Y. Obata, E. Kondo, K. Nishida, Y. Matsudaira, Y. Akatsuka, K. Kuzushima, and T. Takahashi. 2003. Thymus leukemia antigen (TL)-specific cytotoxic T lymphocytes recognize the alpha1/alpha2 domain of TL free from antigenic peptides. *Int. Immunol.* 15: 1319–1326.
46. Cole, D. K., and G. F. Gao. 2004. CD8: adhesion molecule, co-receptor and immunomodulator. *Cell. Mol. Immunol.* 1: 81–88.
47. Wooldridge, L., A. Lissina, J. Vernazza, E. Gostick, B. Laugel, S. L. Hutchinson, F. Mirza, P. R. Dunbar, J. M. Boulter, M. Glick, et al. 2007. Enhanced immunogenicity of CTL antigens through mutation of the CD8 binding MHC class I invariant region. *Eur. J. Immunol.* 37: 1323–1333.
48. Grebe, K. M., R. L. Clarke, and T. A. Potter. 2004. Ligation of CD8 leads to apoptosis of thymocytes that have not undergone positive selection. *Proc. Natl. Acad. Sci. USA* 101: 10410–10415.
49. Clarke, R. L., S. Thiemann, Y. Refaeli, G. Werlen, and T. A. Potter. 2009. A new function for LAT and CD8 during CD8-mediated apoptosis that is independent of TCR signal transduction. *Eur. J. Immunol.* 39: 1619–1631.
50. Wooldridge, L., S. L. Hutchinson, E. M. Choi, A. Lissina, E. Jones, F. Mirza, P. R. Dunbar, D. A. Price, V. Cerundolo, and A. K. Sewell. 2003. Anti-CD8 antibodies can inhibit or enhance peptide-MHC class I (pMHCI) multimer binding: this is paralleled by their effects on CTL activation and occurs in the absence of an interaction between pMHCI and CD8 on the cell surface. *J. Immunol.* 171: 6650–6660.

THE JOURNAL OF IMMUNOLOGY

Anti-CD8 Antibodies Can Trigger CD8$^+$ T Cell Effector Function in the Absence of TCR Engagement and Improve Peptide–MHCI Tetramer Staining

Mathew Clement, Kristin Ladell, Julia Ekeruche-Makinde, John J. Miles, Emily S. J. Edwards, Garry Dolton, Tamsin Williams, Andrea J. A. Schauenburg, David K. Cole, Sarah N. Lauder, Awen M. Gallimore, Andrew J. Godkin, Scott R. Burrows, David A. Price, Andrew K. Sewell and Linda Wooldridge

J Immunol; Prepublished online 15 June 2011;
doi:10.4049/jimmunol.1003941
http://www.jimmunol.org/content/early/2011/06/15/jimmunol.1003941

The Journal of Immunology is published twice each month by
The American Association of Immunologists, Inc.,
9650 Rockville Pike, Bethesda, MD 20814-3994.

Print ISSN: 0022-1767 Online ISSN: 1550-6606.

Published June 15, 2011, doi:10.4049/jimmunol.1003941

Anti-CD8 Antibodies Can Trigger CD8$^+$ T Cell Effector Function in the Absence of TCR Engagement and Improve Peptide–MHCI Tetramer Staining

Mathew Clement,* Kristin Ladell,* Julia Ekeruche-Makinde,* John J. Miles,* Emily S. J. Edwards,* Garry Dolton,* Tamsin Williams,* Andrea J. A. Schauenburg,* David K. Cole,* Sarah N. Lauder,* Awen M. Gallimore,* Andrew J. Godkin,* Scott R. Burrows,† David A. Price,* Andrew K. Sewell,*,[1] and Linda Wooldridge*,[1]

CD8$^+$ T cells recognize immunogenic peptides presented at the cell surface bound to MHCI molecules. Ag recognition involves the binding of both TCR and CD8 coreceptor to the same peptide–MHCI (pMHCI) ligand. Specificity is determined by the TCR, whereas CD8 mediates effects on Ag sensitivity. Anti-CD8 Abs have been used extensively to examine the role of CD8 in CD8$^+$ T cell activation. However, as previous studies have yielded conflicting results, it is unclear from the literature whether anti-CD8 Abs per se are capable of inducing effector function. In this article, we report on the ability of seven monoclonal anti-human CD8 Abs to activate six human CD8$^+$ T cell clones with a total of five different specificities. Six of seven anti-human CD8 Abs tested did not activate CD8$^+$ T cells. In contrast, one anti-human CD8 Ab, OKT8, induced effector function in all CD8$^+$ T cells examined. Moreover, OKT8 was found to enhance TCR/pMHCI on-rates and, as a consequence, could be used to improve pMHCI tetramer staining and the visualization of Ag-specific CD8$^+$ T cells. The anti-mouse CD8 Abs, CT-CD8a and CT-CD8b, also activated CD8$^+$ T cells despite opposing effects on pMHCI tetramer staining. The observed heterogeneity in the ability of anti-CD8 Abs to trigger T cell effector function provides an explanation for the apparent incongruity observed in previous studies and should be taken into consideration when interpreting results generated with these reagents. Furthermore, the ability of Ab-mediated CD8 engagement to deliver an activation signal underscores the importance of CD8 in CD8$^+$ T cell signaling. *The Journal of Immunology*, 2011, 187: 000–000.

CD8$^+$ T cells are essential for the control of viral infection and the natural eradication of cancer. CD8$^+$ T cells recognize short peptides, 8–13 aa in length, presented at the target cell surface bound to MHCI molecules. T cell Ag recognition is unique in nature because it involves the binding of a single ligand (peptide–MHC [pMHC]) by two receptors (TCR and coreceptor) (1, 2). The CD8 glycoprotein, which serves as the coreceptor on MHCI-restricted T cells, acts to enhance the Ag sensitivity of CD8$^+$ T cells by binding to a largely invariant region of MHCI at a site distinct from the TCR docking platform. CD8 has multiple enhancing effects on early T cell activation events, which include the following: 1) promotion and stabilization of TCR/pMHCI binding at the cell surface (3–5); 2) recruitment of essential signaling molecules to the intracellular side of the TCR/CD3/ζ complex (6–11); and 3) localization of TCR/pMHCI complexes within specialized membrane microdomains that act as potentially privileged sites for initiation of the TCR-mediated signaling cascade (12, 13). CD8 binding also controls the level of T cell cross-reactivity (14) and can differentially affect the deployment of CD8$^+$ T cell effector functions (15).

Anti-CD8 Abs have been used widely to investigate the role of CD8 in CD8$^+$ T cell activation. Early studies showed that preincubation with anti-CD8 Abs can block conjugate formation between effector and target cells (16) and inhibit CD8$^+$ T cell activation in response to cognate pMHCI presented on the target cell surface (17–20). These findings provided key evidence that CD8 was important in the process of CD8$^+$ T cell activation. However, considerable heterogeneity between different CD8$^+$ T cells was apparent in terms of their ability to activate in the presence of anti-CD8 Abs, and as a result, these reagents were used as tools to classify CD8$^+$ T cells as either CD8 dependent or CD8 independent (21, 22). Ab-mediated ligation of T cell surface molecules, such as CD2, CD3, and CD28 (23, 24), can result in effector function. In contrast, studies of Ab-mediated CD8 ligation in the absence of TCR engagement have yielded conflicting results. Early studies demonstrated that induction of CD8 cross-linking at the cell surface can result in p56^{lck} phosphorylation similar to that seen with anti-CD3 Abs (25) and elicit downstream effector functions, such as chemokine release (26) and potent cytotoxicity (27). However, in conflict with these data, more re-

*Cardiff University School of Medicine, University Hospital, Cardiff CF14 4XN, United Kingdom; and †Cellular Immunology Laboratory, Department of Infectious Disease and Immunology, Queensland Institute of Medical Research, Brisbane, Queensland 4029, Australia

[1]L.W. and A.K.S. contributed equally to this manuscript.

Received for publication December 2, 2010. Accepted for publication May 9, 2011.

This work was supported by a Wellcome Trust Clinical Intermediate fellowship (to L.W.); M.C. and .J.E.-M. are also funded by the Wellcome Trust. A.K.S. is funded by the Cardiff University Link Chair scheme. D.A.P. is a Medical Research Council (U.K.) senior clinical fellow; K.L. is also funded by the Medical Research Council (U.K.). D.K.C. is a Leverhulme Trust Early Career Fellow. J.J.M. is supported by a Welsh Office of Research and Development translational fellowship and a National Health and Medical Research Council Biomedical fellowship. S.R.B. is a National Health and Medical Research Council senior fellow.

Address correspondence and reprint requests to Dr. Linda Wooldridge, Cardiff University School of Medicine, Henry Wellcome Building, University Hospital, Cardiff CF14 4XN, United Kingdom. E-mail address: wooldridgel@cardiff.ac.uk

The online version of this article contains supplemental material.

Abbreviations used in this article: CBA, cytometric bead array; pMHC, peptide–MHC.

cent studies suggest that CD8 ligation alone may actually deliver a negative signal (28, 29).

To date, a cohesive explanation for these widely disparate findings with anti-CD8 Abs has remained elusive. Furthermore, there has been no systematic study of the effects of multiple different anti-human CD8 Abs on CD8$^+$ T cells with different specificities. In this article, we report on the ability of a panel of seven monoclonal anti-human CD8 Abs to induce chemokine/cytokine release and cytotoxicity by six different human CD8$^+$ T cell clones specific for a total of five different pMHCI Ags. The data, supported by parallel observations in a mouse system, reveal that considerable heterogeneity exists in the ability of anti-CD8 Abs to activate CD8$^+$ T cells. These results elucidate the apparent incongruity that has been observed in previous studies and mandate that the disparate effects of anti-CD8 Abs are considered in the interpretation of results generated with these reagents.

Materials and Methods

Cells

The following HLA A*0201-restricted CD8$^+$ T cell clones were used in this study: 1) ILA1, specific for the human telomerase reverse transcriptase-derived epitope ILAKFLHWL (residues 540–548) (30, 31); 2) ALF3, specific for the influenza A matrix protein (M1)-derived epitope GILGFVFTL (residues 58–66); and 3) MEL5 and MEL187.c5, specific for the Melan-A–derived epitope ELAGIGILTV (residues 26–35) (32). The HLA B*0801-restricted CD8$^+$ T cell clone LC13 is specific for the EBV EBNA3A-derived epitope FLRGRAYGL (residues 339–347) (33), and the HLA B*3508-restricted CD8$^+$ T cell clone SB10 is specific for the EBV BZLF1-derived epitope LPEPLPQGQLTAY (residues 52–64) (34). The HLA DR*0101-restricted CD4$^+$ T cell clone C6 recognizes the influenza A hemagglutinin-derived epitope PKYVKQNTLKLAT (residues 307–319). CD8$^+$ T cell lines specific for the EBV BMLF1-derived epitope GLCTLVAML (residues 280–288), restricted by HLA A*0201, were generated as described previously (35). Naive mouse CD8$^+$ T cells were obtained by harvesting splenocytes from transgenic F5 mice. A significant percentage of CD8$^+$ T cells within the splenic population of these mice express the F5 TCR, which recognizes the H-2D^b–restricted influenza H17 nucleoprotein-derived epitope ASNENMDAM (36). C1R-A*0201 target cells were generated as described previously (37).

Anti-CD8 Abs

The following anti-human CD8α Ab clones were used in this study: 1) unconjugated or allophycocyanin-conjugated OKT8 (eBioscience, Hatfield, U.K.); 2) unconjugated, FITC-conjugated, or R-PE–conjugated SK1 (BD Biosciences, Oxford, U.K.); 3) unconjugated MCD8 (IqProducts, Groningen, The Netherlands); 4) unconjugated 32/M4 (Santa Cruz Biotechnology, Heidelberg, Germany); 5) unconjugated C8/144B (Santa Cruz Biotechnology); and 6) allophycocyanin-conjugated DK25 (DakoCytomation, Stockport, U.K.). The anti-human CD8β Ab clone 2ST8.5H7 was also used, either in unconjugated or in PE-conjugated form (Abcam, Cambridge, U.K.). In functional assays, the maximum possible Ab concentrations were used, determined by the concentration of the commercially available preparation in each case. For experiments with mouse cells, the following unconjugated anti-mouse CD8 Abs were used: 1) anti-CD8α clone CT-CD8a (Caltag-Medsystems, Buckingham, U.K.); 2) anti-CD8α clone 53.6.7 (BioLegend, Cambridge, U.K.); 3) anti-CD8β clone KT112 (hybridoma provided by Prof. R. Zamoyska, School of Biological Sciences, University of Edinburgh); and 4) anti-CD8β clone CT-CD8b (Caltag-Medsystems).

Generation of OKT8 Fab, F(ab′)$_2$ and Fc′ fragments

A total of 250 μg of the anti-human CD8 Ab OKT8 or the anti-human CD3 Ab OKT3 were digested to yield Fab and Fc′ fragments using a Pierce Fab micropreparation kit (ThermoScientific, Rockford, IL); F(ab′)$_2$ fragments were produced similarly using a Pierce F(ab′)$_2$ micropreparation kit (ThermoScientific). IgG fragmentation was performed according to the manufacturer's instructions.

CD8$^+$ T cell effector function assays

T cells (3×10^4) were mixed with anti-CD8 Abs at the indicated concentrations, either with or without secondary cross-linking by the addition of 5 μl anti-mouse IgG Ab (Beckman Coulter, High Wycombe, U.K.), and incubated overnight at 37°C in a 5% CO_2 atmosphere. Positive controls included the following: 1) target cells pulsed with 10^{-7} M cognate peptide; 2) 10 μg/ml anti-human CD3 Ab (UCHT1; BD Biosciences); or 3) 50 ng/ml PMA and 1 μg/ml ionomycin (Sigma-Aldrich, Dorset, U.K.). Supernatants were harvested and assayed for MIP1α, MIP1β, and RANTES by ELISA (R&D Systems, Abingdon, U.K.) and for IFN-γ, TNF-α, and IL-2 by cytometric bead array (Th1/Th2 kit; BD Biosciences), according to the manufacturer's instructions in each case; mouse MIP1β and IL-2 assays were performed by ELISA (R&D Systems). Cytometric bead array (CBA) data were acquired using a FACSCalibur flow cytometer and analyzed with CBA 6 Bead analysis software (BD Biosciences). CD107a mobilization was used to measure T cell degranulation by flow cytometry as described previously (38). For chromium release assays, 2×10^3 T cells were treated with anti-CD8 Abs at the indicated concentrations in 100 μl RPMI 1640 medium (Life Technologies, Paisley, U.K.) supplemented with 100 U/ml penicillin (Life Technologies), 100 μg/ml streptomycin (Life Technologies), 2 mM L-glutamine (Life Technologies), and 2% heat-inactivated FCS (Life Technologies) (R2 medium). C1R-A*0201 target cells (2×10^3), labeled with 30 μCi ^{51}Cr (Perkin Elmer, Cambridge, U.K.) per 10^6 cells for 1 h previously, were subsequently added. Targets were also cultured alone (target spontaneous release) and with Triton X-100 (Sigma-Aldrich) at a final concentration of 5% (target total release). Cells were incubated at 37°C for 18 h in a 5% CO_2 atmosphere. For each sample, 20 μl supernatant was harvested and mixed with 150 μl OptiPhase Supermix Scintillation Cocktail (Perkin Elmer). Plates were analyzed using a liquid scintillator and luminescence counter (MicroBeta TriLux; Perkin Elmer) with Microbeta Windows Workstation software (Perkin Elmer). Specific lysis was calculated according to the following formula: (experimental release − target spontaneous release/target total release − target spontaneous release) × 100.

pMHCI tetramer staining and flow cytometry

Soluble biotinylated pMHCI monomers were produced as described previously (3). Tetrameric pMHCI reagents (tetramers) were constructed by the addition of either PE-conjugated streptavidin (Life Technologies) or allophycocyanin-conjugated streptavidin (Prozyme, Hayward, CA) at a pMHCI:streptavidin molar ratio of 4:1. For human CD8$^+$ T cell clones, 5×10^4 cells were preincubated with anti-CD8 Ab as indicated for 25 min on ice and then stained with cognate PE-conjugated tetramer (25 μg/ml) at 37°C for 15 min (reviewed in Ref. 39) prior to staining with 5 μl 7-aminoactinomycin D (Viaprobe; BD Biosciences) at 4°C for 30 min. For human CD8$^+$ T cell lines, 5×10^4 cells were preincubated with anti-CD8 Ab as indicated for 25 min on ice and then stained with cognate PE-conjugated HLA A*0201 tetramer (25 μg/ml) at 37°C for 15 min prior to staining with the amine-reactive fluorescent dye LIVE/DEAD Fixable Aqua (Life Technologies), Pacific Blue-conjugated anti-human CD14 (clone Tuk4; Caltag-Medsystems), Pacific Blue-conjugated anti-human CD19 (clone SJ25-C1; Caltag-Medsystems), PE-Cy5.5–conjugated anti-human CD4 (clone S3.5; Caltag-Medsystems), and FITC-conjugated anti-human CD8 (clone SK1; BD Biosciences) at 4°C for 20 min. For human PBMCs directly ex vivo, 1×10^5 cells were preincubated with anti-CD8 Ab as indicated for 25 min on ice and then stained with allophycocyanin-conjugated HLA A*0201 tetramer (25 μg/ml) at 37°C for 15 min prior to staining with LIVE/DEAD Fixable Aqua (Life Technologies), Pacific Blue-conjugated anti-human CD14 (clone Tuk4; Caltag-Medsystems), Pacific Blue-conjugated anti-human CD19 (clone SJ25-C1; Caltag-Medsystems), FITC-conjugated anti-human CD3 (clone HIT3a; BD Biosciences), PE-Cy5.5–conjugated anti-human CD4 (clone S3.5; Caltag-Medsystems), and PE-Cy7–conjugated anti-human CD8 (clone RPA-T8; BD Biosciences) at 4°C for 20 min. For mouse experiments, 5×10^4 cells were preincubated with 100 μg/ml CT-CD8a (Caltag-Medsystems), 53.6.7 (BioLegend), KT112 (in-house), or CT-CD8b (Caltag-Medsystems) for 25 min on ice and then stained with cognate PE-conjugated H-2D^b tetramer (25 μg/ml) at 37°C for 15 min prior to staining with LIVE/DEAD Fixable Aqua (Life Technologies), Pacific Blue-conjugated anti-mouse CD4 (clone RM4-5; BD Biosciences), FITC-conjugated anti-mouse CD45R/B220 (clone RA3-6B2; BD Biosciences), and PerCP-Cy5.5–conjugated anti-mouse CD3 (clone 17A2; BD Biosciences) at 4°C for 20 min. Data were acquired using either a FACSCantoII or a modified FACSAriaII flow cytometer (both BD Biosciences) and analyzed with FlowJo software (Tree Star, Ashland, OR).

Intracellular cytokine staining

PBMCs were harvested from a healthy donor and cultured with or without 1 μg/ml PHA (Alere, Cheshire, U.K.) and 25 ng/ml IL-15 (Promega, Hampshire, U.K.) for 7 d and then washed and cultured overnight in R2

medium. A total of 5×10^4 PBMCs (unstimulated or stimulated with PHA/IL-15) were resuspended in the presence of 1 μl/ml brefeldin A (GolgiPlug; Sigma-Aldrich), 0.7 μl/ml monensin (GolgiStop; BD Biosciences), and 5 μl/ml anti-CD107a-FITC (clone H4A3; BD Biosciences) and then incubated with anti-human CD8 Abs at the indicated concentrations for 18 h at 37°C in a 5% CO_2 atmosphere. After washing with PBS, cells were stained with LIVE/DEAD Fixable Violet (ViViD; Life Technologies), Pacific Blue-conjugated anti-human CD14 (clone Tuk4; Caltag-Medsystems), and Pacific Blue-conjugated anti-human CD19 (clone SJ25-C1; Caltag-Medsystems) at room temperature for 15 min. Subsequently, cells were washed and stained with H7-allophycocyanin–conjugated anti-human CD3 (clone SK7; BD Biosciences) and PE-Cy5.5–conjugated anti-human CD4 (clone S3.5; Caltag-Medsystems) at 4°C for 20 min, then washed an additional three times, resuspended in 200 μl BD Cytofix/Cytoperm, and incubated at 4°C for 20 min. After three additional washes in Perm/Wash (BD Biosciences), cells were stained with PE-Cy7–conjugated anti-human IFN-γ (clone B27; BD Biosciences), allophycocyanin-conjugated anti-human TNF-α (clone MAb11; BD Biosciences), and PE-conjugated anti-human MIP1β (clone D21-1351; BD Biosciences) at 4°C for 20 min, washed again three more times, and resuspended in 200 μl Perm/Wash. Data were acquired using a modified FACSAriaII flow cytometer (BD Biosciences) and analyzed with FlowJo software (Tree Star).

Tetramer kinetics experiments

For tetramer association assays, 5×10^5 $CD8^+$ T cells were washed twice and resuspended in 200 μl PBS with or without anti-human CD8 Ab and then incubated with cognate tetramer (5 μg/ml). At indicated time points, 12 μl of the cell suspension was removed and acquired using a FACSCalibur flow cytometer (BD Biosciences). Data were analyzed using FlowJo software (Tree Star). Tetramer decay analysis was performed as described previously (3).

Surface plasmon resonance analysis

Soluble TCRs derived from the MEL5 and MEL187.c5 $CD8^+$ T cell clones were manufactured as described previously (40–42). Binding analysis was performed using a BIAcore 3000 equipped with a CM5 sensor chip (43). Between 200 and 400 response units of biotinylated pMHCI was immobilized to streptavidin, which was chemically linked to the chip surface. The pMHCI was injected at a slow flow rate (10 μl/min) to ensure uniform distribution on the chip surface. Combined with the small amount of pMHCI bound to the chip surface, this reduced the likelihood of off-rate limiting mass transfer effects. The MEL5 TCR and MEL187.c5 TCRs were purified and concentrated to ~100 μM on the day of surface plasmon resonance analysis to reduce the likelihood of TCR aggregation affecting the results. For equilibrium analysis, eight serial dilutions were carefully prepared in triplicate for each sample and injected over the relevant sensor chips at 25°C. The TCRs were injected over the chip surface at a flow rate of 45 μl/min. Results were analyzed using BIAevaluation 3.1, Microsoft Excel, and Origin 6.1. The equilibrium binding constant (K_D) values were calculated using a nonlinear curve fit ($y = [P_1x]/[P_2 + x]$).

Results

Anti-CD8 Abs can trigger T cell effector function in the absence of TCR engagement

Several studies suggest that Ab-mediated ligation of CD8 in the absence of TCR engagement can elicit downstream effector function (25–27); however, others have reported the delivery of negative signals with this manipulation (28, 29). To reconcile these apparently disparate findings, we conducted a systematic study of the effects of multiple different anti-human CD8 Abs on $CD8^+$ T cells with several different specificities. For this purpose, we used a panel of anti-human CD8 Abs that comprised six anti-CD8α Abs (OKT8, SK1, MCD8, 32/M4, C8/144B, and DK25) and one anti-CD8β Ab (2ST8.5H7). Six of seven anti-human CD8 Abs from the panel (SK1, MCD8, 32/M4, C8/144B, DK25, and 2ST8.5H7) did not elicit any chemokine production when incubated with four different HLA A*0201-restricted $CD8^+$ T cell clones (ILA1, ALF3, MEL5, and MEL187.c5) with a total of three different specificities in the absence of specific pMHCI Ag (Fig. 1). However, the anti-CD8α Ab OKT8 induced MIP1α, MIP1β, and RANTES release from all four HLA A*0201-restricted $CD8^+$ T cell clones (Fig. 1). Chemokine secretion was apparent over a range of OKT8 concentrations (Supplemental Fig. 1).

In addition, we measured chemokine release by two non-HLA A*0201-restricted $CD8^+$ T cell clones following incubation with each anti-human CD8 Ab from the panel. Both of these non-HLA A*0201-restricted $CD8^+$ T cell clones produced MIP1α, MIP1β, and RANTES in response to OKT8 but did not activate in the presence of the other Abs tested (Fig. 2). Remarkably, the highly Ag-sensitive HLA B*3508-restricted EBV BZLF1-specific $CD8^+$ T cell clone SB10 released >2000 pg/ml of each chemokine in response to OKT8 (Fig. 2*B*). OKT8 was incapable of staining the HLA DR*0101-restricted $CD4^+$ T cell clone C6 (Supplemental Fig. 2*A*) and failed to induce chemokine release from this clone (Supplemental Fig. 2*B–D*). Thus, the stimulatory effects of OKT8 appear to be $CD8^+$ T cell specific.

The panel of seven anti-human CD8 Abs was further tested in cytotoxicity assays with four different $CD8^+$ T cell clones (MEL187.c5, ALF3, LC13, and SB10). Anti-human CD8 Abs that were incapable of inducing chemokine release failed to elicit cytotoxic activity in any of these four $CD8^+$ T cell clones (Fig. 3). In contrast, SB10 $CD8^+$ T cells exhibited substantial cytotoxicity in response to stimulation with OKT8; lower levels of specific lysis

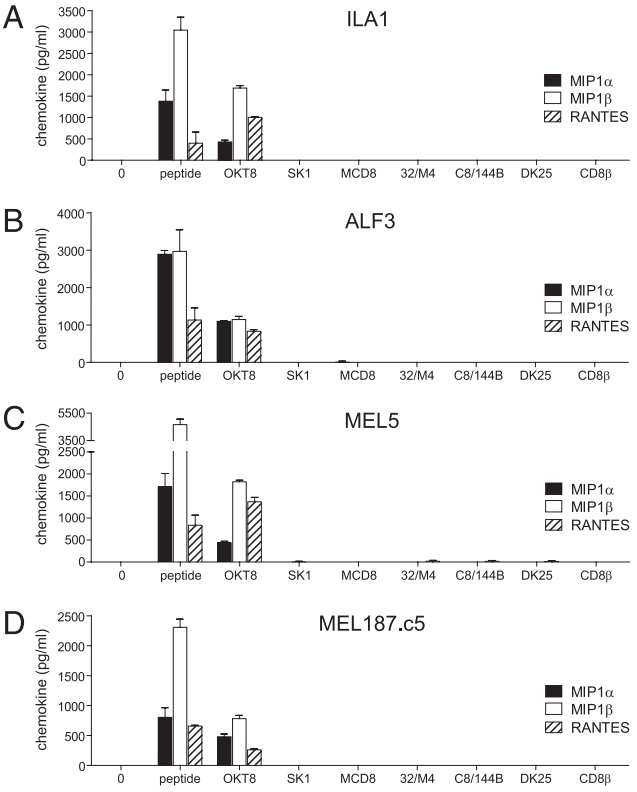

FIGURE 1. Ab-mediated CD8 ligation can trigger chemokine release from HLA A*0201-restricted $CD8^+$ T cells. A total of 3×10^4 ILA1 $CD8^+$ T cells (*A*), ALF3 $CD8^+$ T cells (*B*), MEL5 $CD8^+$ T cells (*C*), or MEL187.c5 $CD8^+$ T cells (*D*) were incubated for 18 h with each of the following individual anti-human CD8 Abs in parallel: 100 μg/ml OKT8, 6.25 μg/ml SK1, 50 μg/ml MCD8, 100 μg/ml 32/M4, 100 μg/ml C8/144B, 25 μg/ml DK25, and 100 μg/ml 2ST8.5H7 (CD8β). The maximum possible Ab concentrations were used, determined by the concentration of the commercially available preparation in each case. For each $CD8^+$ T cell clone, 3×10^4 C1R-A*0201 B cells pulsed with cognate peptide at 10^{-7} M were used as positive controls. 0 represents T cells only. Supernatant was harvested and assayed for MIP1α, MIP1β, and RANTES by ELISA. Error bars represent SDs.

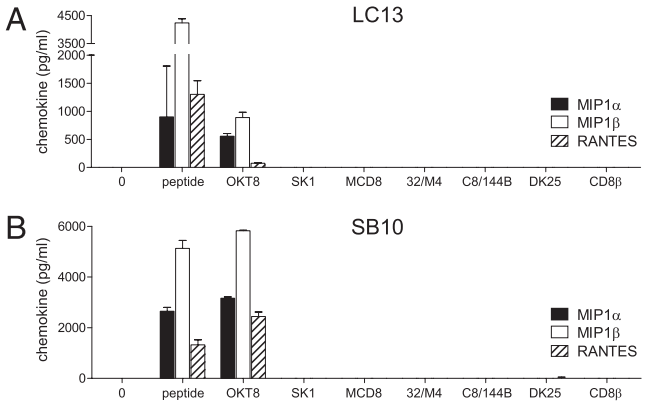

FIGURE 2. Ab-mediated CD8 ligation can trigger chemokine release from non-HLA A*0201-restricted CD8+ T cells. A total of 3×10^4 LC13 CD8+ T cells (*A*) or SB10 CD8+ T cells (*B*) were incubated for 18 h with each of the following individual anti-human CD8 Abs in parallel: 100 μg/ml OKT8, 6.25 μg/ml SK1, 50 μg/ml MCD8, 100 μg/ml 32/M4, 100 μg/ml C8/144B, 25 μg/ml DK25, and 100 μg/ml 2ST8.5H7 (CD8β). For each CD8+ T cell clone, 3×10^4 HLA-matched B cells pulsed with cognate peptide at 10^{-7} M were used as positive controls. Supernatant was harvested and assayed for MIP1α, MIP1β, and RANTES by ELISA. Error bars represent SDs.

were also induced in the CD8+ T cell clones LC13 (3.18%), ALF3 (5.1%), and MEL187.c5 (3.8%) (Fig. 3; data not shown). These results are consistent with a previous study that described a mouse anti-CD8 Ab, KT112, capable of inducing cytotoxicity (27). Collectively, these data indicate that considerable heterogeneity exists in the ability of anti-CD8 Abs to activate CD8+ T cells.

OKT8 induces chemokine secretion in the absence of cytokine secretion

Next, we examined the ability of Ab-mediated CD8 ligation to elicit cytokine release by CD8+ T cells in the absence of TCR engagement. As expected, the anti-human CD8 Abs that did not elicit chemokine release or cytotoxic activity (SK1, MCD8, 32/M4, C8/144B, DK25, and 2ST8.5H7) also failed to induce IFN-γ, TNF-α, or IL-2 release (Fig. 4). Interestingly, OKT8 similarly failed to elicit cytokine production from the majority of CD8+ T cell clones

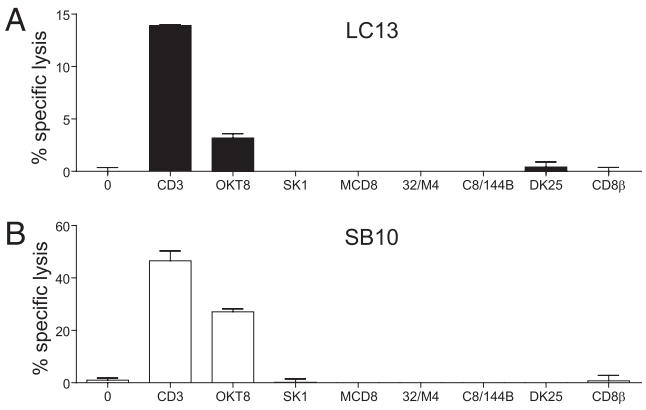

FIGURE 3. The anti-human CD8 Ab OKT8 can trigger cytotoxic activity. A total of 2×10^3 LC13 CD8+ T cells (*A*) or SB10 CD8+ T cells (*B*) were incubated with each of the following individual anti-human CD8 Abs in parallel: 100 μg/ml OKT8, 6.25 μg/ml SK1, 50 μg/ml MCD8, 100 μg/ml 32/M4, 100 μg/ml C8/144B, 25 μg/ml DK25, and 100 μg/ml 2ST8.5H7 (CD8β). The anti-human CD3 Ab UCHT1 (10 μg/ml) served as a positive control. Cytotoxicity assays were then performed over a period of 18 h as described in *Materials and Methods* using ^{51}Cr-labeled C1R-A*0201 B cells as targets. Error bars represent SDs.

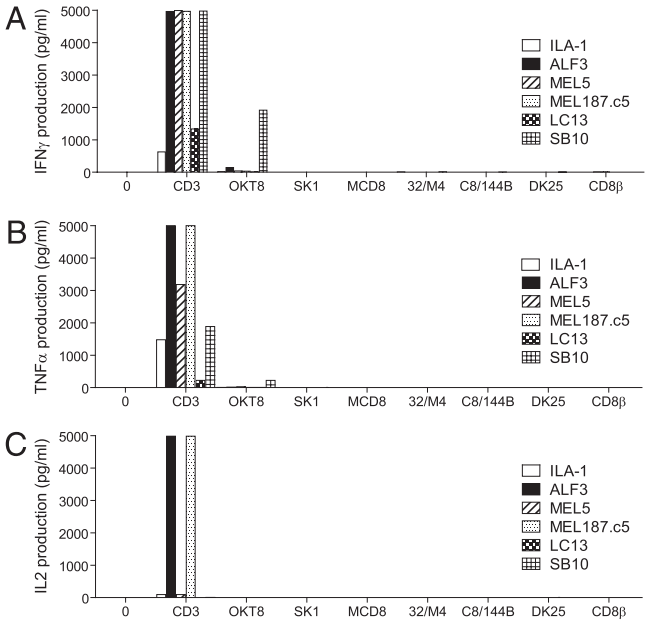

FIGURE 4. Anti-CD8 Ab-mediated chemokine release occurs in the absence of cytokine release. A total of 3×10^4 ILA1, ALF3, MEL5, MEL187.c5, LC13, or SB10 CD8+ T cells were incubated for 18 h with each of the following individual anti-human CD8 Abs in parallel: 100 μg/ml OKT8, 6.25 μg/ml SK1, 50 μg/ml MCD8, 100 μg/ml 32/M4, 100 μg/ml C8/144B, 25 μg/ml DK25, and 100 μg/ml 2ST8.5H7 (CD8β). The anti-human CD3 Ab UCHT1 (10 μg/ml) served as a positive control. Supernatant was harvested and assayed for IFN-γ (*A*), TNF-α (*B*), and IL-2 (*C*) by CBA.

tested (Fig. 4). Importantly, chemokine and cytokine assays were performed using the same supernatant, thereby confirming that OKT8 stimulated CD8+ T cells to secrete chemokines in the absence of cytokine production; one exception to this dichotomy occurred with the CD8+ T cell clone SB10, which released IFN-γ in response to treatment with OKT8. These data suggest that OKT8-mediated CD8 ligation delivers a signal that falls below the threshold required for cytokine production in most CD8+ T cells.

Neither secondary Ab cross-linking nor PHA/IL-15 treatment alter the functional phenotype of anti-human CD8 Abs

To probe the possibility that the degree of cross-linking mediated by each of the anti-human CD8 Abs tested could explain the functional heterogeneity observed between these reagents, we performed activation experiments with the addition of secondary Abs. Secondary cross-linking of OKT8 increased the level of MIP1α, MIP1β, and RANTES release by ILA1, ALF3, MEL5, MEL187.c5, LC13, and SB10 CD8+ T cells above that observed with OKT8 alone (Fig. 5; data not shown). However, secondary Ab-mediated cross-linking did not reverse the phenotype of the nonactivating anti-human CD8 Abs (Fig. 5).

We also examined the effect of PHA/IL-15 treatment on the ability of anti-human CD8 Abs to elicit effector function from CD8+ T cells in healthy donor PBMCs. PHA is capable of cross-linking glycosylated proteins at the T cell surface. The seven anti-human CD8 Abs tested did not substantially activate CD8+ T cells in untreated PBMCs (Fig. 6*A*). The six nonactivating anti-human CD8 Abs also failed to induce substantial levels of CD8+ T cell activation in PBMCs cultured for 7 d in PHA/IL-15 (Fig. 6*B*). In contrast, OKT8 activated CD8+ T cells in PHA/IL-15–stimulated PBMCs to release MIP1β and degranulate as measured by surface mobilization of CD107a. Interestingly, OKT8 also induced IFN-γ

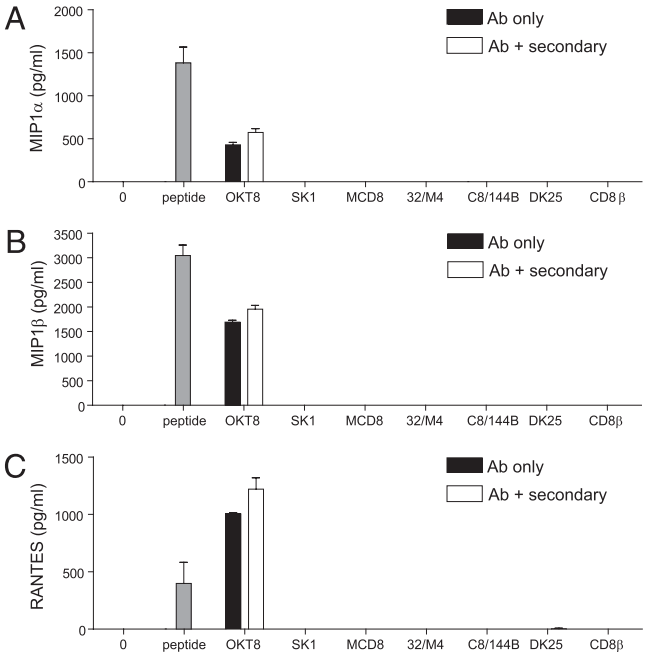

FIGURE 5. Secondary crosslinking does not alter the functional phenotype of anti-human CD8 Abs. A total of 3×10^4 ILA1 $CD8^+$ T cells were incubated with each of the following individual anti-human CD8 Abs in parallel: 100 μg/ml OKT8, 6.25 μg/ml SK1, 50 μg/ml MCD8, 100 μg/ml 32/M4, 100 μg/ml C8/144B, 25 μg/ml DK25, and 100 μg/ml 2ST8.5H7 (CD8β). The positive control comprised 3×10^4 C1R-A*0201 B cells pulsed with cognate peptide at 10^{-7} M. Abs were then cross-linked with the addition of 5 μl anti-mouse IgG Ab (serum IgG) and incubated for 18 h at 37°C in a 5% CO_2 atmosphere. Supernatant was harvested and assayed for MIP1α (*A*), MIP1β (*B*), and RANTES (*C*) by ELISA. Secondary cross-linking of OKT8 increased the levels of all analytes measured; this also applied to anti-CD3 Ab-induced chemokine release (data not shown). Similar results were obtained with all other $CD8^+$ T cell clones tested: ALF3, MEL5, MEL187.c5, LC13, and SB10 (data not shown). Error bars represent SDs.

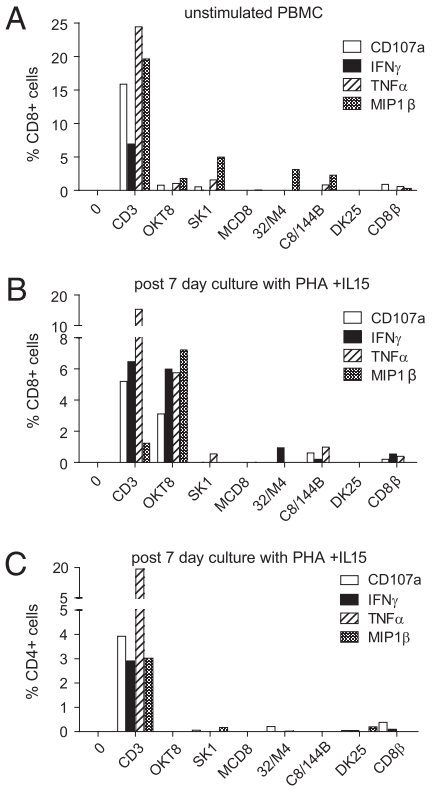

FIGURE 6. PHA/IL-15 treatment does not alter the functional phenotype of anti-human CD8 Abs. PBMCs were harvested from healthy donors and cultured either without (*A*) or with (*B*, *C*) 1 μg/ml PHA and 25 ng/ml IL-15 for 7 d and then washed and cultured overnight in R2 medium. A total of 5×10^4 PBMCs were then incubated for 18 h with each of the following individual anti-human CD8 Abs in parallel: 100 μg/ml OKT8, 6.25 μg/ml SK1, 50 μg/ml MCD8, 100 μg/ml 32/M4, 100 μg/ml C8/144B, 25 μg/ml DK25, and 100 μg/ml 2ST8.5H7 (CD8β). The anti-human CD3 Ab UCHT1 (10 μg/ml) served as a positive control. $CD8^+$ T cell effector functions were measured by intracellular cytokine staining and surface CD107a mobilization as described in *Materials and Methods*. Data were acquired using a modified FACSAriaII flow cytometer and analyzed with FlowJo software. Results obtained by gating on either the $CD3^+CD4^-$ (*A*, *B*) or $CD4^+$ (*C*) population are shown for a representative experiment ($n = 2$). Minor differences in background levels of $CD8^+$ T cell activation were observed with the non-OKT8 anti-human CD8 Abs (*A*, *B*); this may reflect heterogeneity within the $CD8^+$ PBMC population.

and TNF-α production by $CD8^+$ T cells in PHA/IL-15–stimulated PBMCs, thereby suggesting that this treatment regimen synergistically lowered the activation threshold of the responding cells. OKT8 failed to activate $CD4^+$ T cells in PHA/IL-15–stimulated

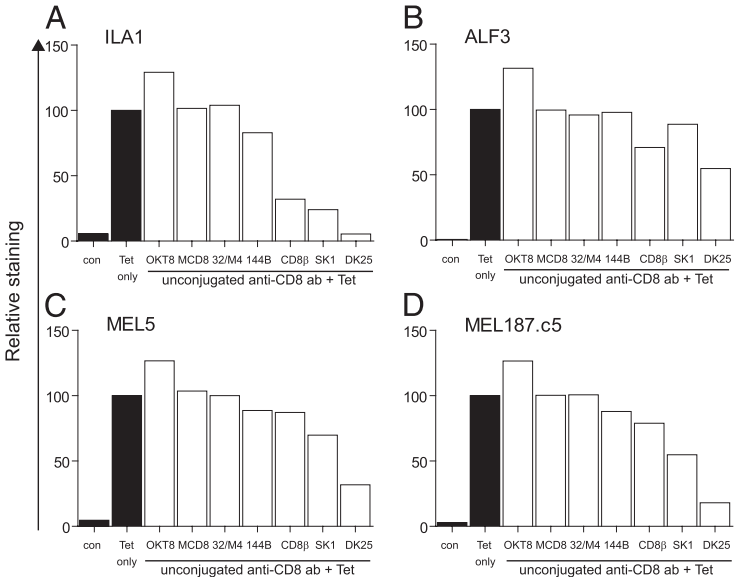

FIGURE 7. Anti-human CD8 Abs can either enhance or inhibit the binding of pMHCI tetramers. A total of 5×10^4 ILA1 (*A*), ALF3 (*B*), MEL5 (*C*), or MEL187.c5 (*D*) $CD8^+$ T cells were preincubated at 4°C for 25 min with each of the following individual anti-human CD8 Abs in parallel: 100 μg/ml OKT8, 6.25 μg/ml SK1, 50 μg/ml MCD8, 100 μg/ml 32/M4, 100 μg/ml C8/144B (144B), 25 μg/ml DK25, and 100 μg/ml 2ST8.5H7 (CD8β). $CD8^+$ T cells were subsequently stained with cognate PE-conjugated HLA A*0201 tetramers (25 μg/ml) and 7-aminoactinomycin D as described in *Materials and Methods*. Data were acquired using a FACSCalibur flow cytometer and analyzed with FlowJo software. Relative median fluorescence intensity (MFI) values with respect to pMHCI tetramer staining in the absence of preincubation with anti-CD8 Ab are shown. Fluorescence in the absence of added cognate tetramer (con) is shown in each case. Data are representative of four separate experiments using ILA1 and ALF3 $CD8^+$ T cells, and six separate experiments using MEL5 and MEL187.c5 $CD8^+$ T cells.

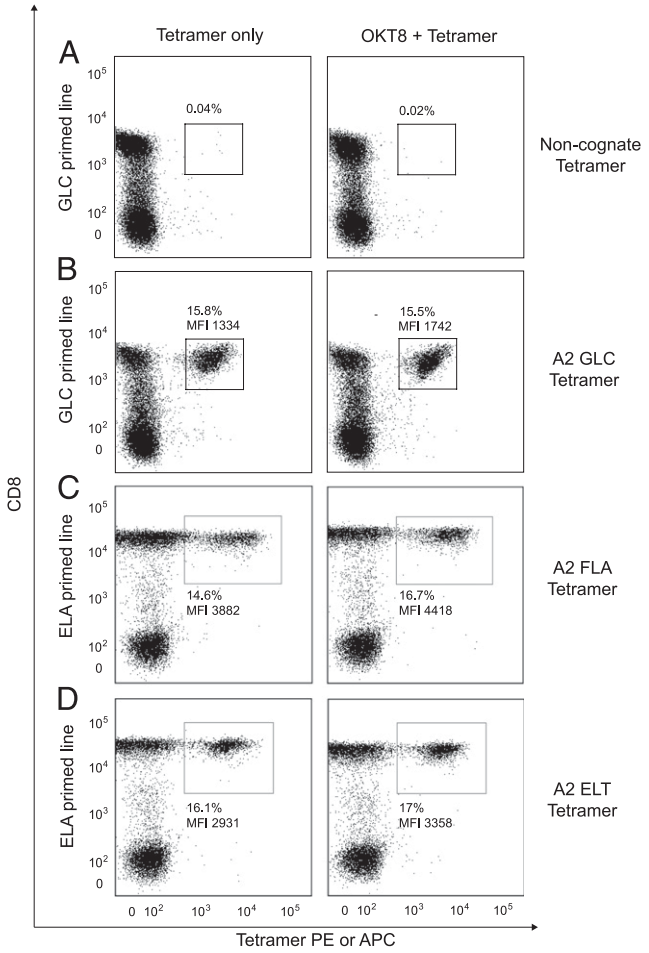

FIGURE 8. OKT8 enhances pMHCI tetramer staining in mixed cell populations. *A* and *B*, A total of 5×10^4 cells from a CD8$^+$ T cell line primed with the EBV BMLF1-derived epitope GLCTLVAML (residues 280–288) were either mock treated or incubated with 100 μg/ml OKT8 at 4°C for 25 min and then stained with either noncognate HLA A*0201-ELAGIGILTV (*A*) or cognate HLA A*0201-GLCTLVAML (*B*) APC-conjugated tetramer (25 μg/ml each) at 37°C for 15 min. *C* and *D*, A total of 5×10^4 cells from a CD8$^+$ T cell line primed with the Melan-A–derived epitope ELAGIGILTV (residues 26–35) were either mock treated or incubated with 100 μg/ml OKT8 at 4°C for 25 min and then stained with either HLA A*0201-**F**LAGIGILTV (*C*) or HLA A*0201-EL**T**GIGILTV (*D*) PE-conjugated tetramer (25μg/ml each) at 37°C for 15 min. Additional stains were performed as detailed in *Materials and Methods*. Data were acquired using a FACSCantoII flow cytometer and analyzed with FlowJo software.

PBMCs (Fig. 6*C*), consistent with previously discussed data (Supplemental Fig. 2).

OKT8 enhances pMHCI tetramer staining

Next, we tested the effects of anti-human CD8 Abs on the staining of ILA1, ALF3, MEL5, and MEL187.c5 CD8$^+$ T cells with cognate pMHCI tetramers. Three anti-human CD8 Ab clones (SK1, DK25, and 2ST8.5H7) inhibited tetramer staining; clones MCD8, 32/M4, and C8/144B had little or no effect on staining. However, preincubation with OKT8 enhanced cognate pMHCI tetramer staining of all four CD8$^+$ T cell clones (Fig. 7). Thus, OKT8 can enhance the binding of pMHCI tetramers in a range of systems. These findings suggested that OKT8 might facilitate the identification of Ag-specific CD8$^+$ T cells within mixed cell populations. To test this idea, we examined pMHCI tetramer staining of CD8$^+$ T cell lines raised against the HLA A*0201-restricted EBV BMLF1-derived epitope GLCTLVAML (residues 280–288). OKT8 enhanced the staining intensity of cognate CD8$^+$ T cells with the relevant pMHCI tetramer without concomitant increases in noncognate HLA A*0201 tetramer binding (Fig. 8*A*, 8*B*). No increase in the percentage of tetramer$^+$CD8$^+$ cells was observed in the presence of OKT8 (Fig. 8*A*, 8*B*), which likely reflects the high-affinity TCR/pMHCI interactions that characterize antiviral CD8$^+$ T cell populations (41).

We hypothesized that OKT8-mediated enhancement of TCR/pMHCI binding at the cell surface might have beneficial effects on pMHCI tetramer staining with low-affinity ligands, an effect that could prove very useful for the detection of CD8$^+$ T cells with TCRs that bind weakly to cognate Ag, such as those that appear to predominate in anticancer and autoimmune responses (32, 41). To test this hypothesis, we used two monoclonal CD8$^+$ T cell systems and a series of altered peptide ligands that vary in their affinity for cognate TCR by >5-fold (Table I, Supplemental Fig. 3). Preincubation with OKT8 enhanced staining efficiency with all variant pMHCI tetramers, including low-affinity variants (Table I, Supplemental Fig. 4). Consistent with this finding, OKT8 increased both the staining intensity and the percentage of Ag-specific events detected when CD8$^+$ T cell lines raised against the HLA A*0201-restricted Melan-A–derived epitope ELAGIGILTV (residues 26–35) were stained with HLA A*0201 tetramers folded around the low-affinity peptide variants **F**LAGIGILTV or EL**T**GIGILTV (Fig. 8*C*, 8*D*).

OKT8 enhances TCR/pMHCI on-rates at the cell surface

To examine how OKT8 enhances Ag binding at the CD8$^+$ T cell surface in more detail, we examined the effects of this Ab on TCR/pMHCI kinetics using pMHCI tetramers. Differences in tetramer off-rates were minimal (data not shown). However, pretreatment of CD8$^+$ T cells with OKT8 resulted in a significant increase in the TCR/pMHCI on-rate at the cell surface in each CD8$^+$ T cell clone tested (Fig. 9). In contrast, DK25 inhibited pMHCI tetramer binding at the cell surface (Fig. 9*B*). OKT8 Ab-

Table I. OKT8 increases tetramer staining of MEL5 and MEL187.c5 CD8$^+$ T-cells with low-affinity pMHCI ligands

Peptide[a]	MEL5 K_D (μM)	MEL5 Tetramer Only (MFI)	MEL5 OKT8 + Tetramer (MFI)	MEL187 K_D (μM)	MEL187 Tetramer Only (MFI)	MEL187 OKT8 + Tetramer (MFI)
ELAGIGILTV	17 ± 1	855	917	18 ± 1	353	418
FLAGIGILTV	92 ± 1	194	227	30 ± 2	300	373
EL**T**GIGILTV	82 ± 4	36	87	37 ± 1	128	181
ELAGIGI**I**TV	77 ± 3	123	236	36 ± 3	195	257
FLAGIGI**I**TV	75 ± 3	367	426	47 ± 2	246	311

Summary of equilibrium binding analysis of MEL5 and MEL187.c5 TCRs with pMHCI variants and the effect of OKT8 on HLA A*0201 tetramer staining. Raw surface plasmon resonance data are shown in Supplemental Fig. 3; flow cytometry data are shown in Supplemental Fig. 4.

[a]Amino acid residues marked in bold and underlined indicate substitutions made in the ELAGIGILTV peptide backbone.

MFI, median fluorescence intensity.

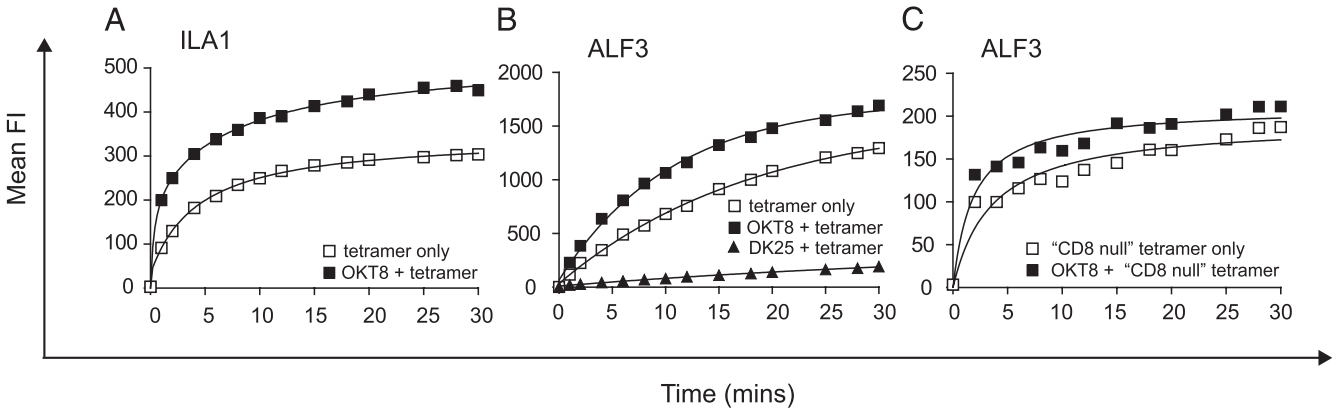

FIGURE 9. OKT8 increases TCR/pMHCI on-rates at the cell surface. A total of 5×10^5 ILA1 (*A*) or ALF3 (*B*, *C*) $CD8^+$ T cells were removed from culture, washed twice, and resuspended in 100 μl PBS with or without 100 μg/ml OKT8 or 25 μg/ml DK25 and then incubated at 4°C for 25 min. Cognate PE-conjugated HLA A*0201 tetramer was added in each case at 5 μg/ml. At various time points as indicated, 12 μl cell suspension was removed and acquired using a FACSCalibur flow cytometer and analyzed with FlowJo software. In *C*, the CD8-null (D227K/T228A) cognate HLA A*0201 tetramer was used (10).

induced enhancement of pMHCI tetramer on-rates was also apparent with CD8-null tetramers (Fig. 9*C*). Collectively, these data indicate that OKT8 enhances pMHCI tetramer staining by increasing the on-rate. Furthermore, OKT8 Ab-mediated augmentation of Ag binding at the cell surface occurs independently of the pMHCI/CD8 interaction.

OKT8 F(ab′)$_2$ fragments can enhance tetramer staining and elicit CD8$^+$ T cell effector function

Abs can be digested by papain or pepsin to produce Fab or F(ab′)$_2$ fragments, respectively. These enzymatically generated fragments have been used extensively in the past to study the structure and function of Abs. We examined the ability of OKT8 Fab and F(ab′)$_2$ fragments to enhance pMHCI tetramer staining and to induce chemokine release in the absence of TCR engagement. Not surprisingly, Fab fragments of OKT8 failed to activate $CD8^+$ T cells or enhance pMHCI tetramer staining (Fig. 10*A*, 10*B*). Interestingly, however, OKT8 F(ab′)$_2$ fragments retained some ability to enhance pMHCI tetramer staining and elicit chemokine release (Fig. 10*A*, 10*B*). OKT8-mediated effects were diminished by pepsin digestion, but anti-human CD3 Abs were similarly impaired functionally after digestion with this enzyme (Fig. 10*C*); this latter effect has been described previously (44–46). Thus, it appears that intact OKT8 exerts effects on pMHCI tetramer binding and $CD8^+$ T cell activation more efficiently than derived F(ab′)$_2$ fragments. However, cellular activation by OKT8 F(ab′)$_2$ fragments confirms that this effect is not entirely Fc′ dependent.

Anti-mouse CD8 Abs can trigger CD8$^+$ T cell effector function in the absence of TCR engagement

To extend these findings beyond human systems (summarized in Table II), we examined the effects of the anti-mouse CD8α Ab CT-CD8a and the anti-mouse CD8β Ab CT-CD8b on pMHCI tetramer staining and $CD8^+$ T cell activation in the absence of TCR engagement. We observed that CT-CD8a inhibited tetramer staining of mouse transgenic F5 $CD8^+$ T cells, whereas CT-CD8b enhanced tetramer staining of the same Ag-specific population (Fig. 11*A*). These results are consistent with our previous findings (26). Interestingly, despite opposing effects on pMHCI tetramer staining, both of these anti-mouse CD8 Abs induced MIP1β production in the absence of TCR engagement from both naive and Ag-exposed F5 $CD8^+$ T cells (Fig. 11*B*; data not shown). These effects were shown to be CD8-specific and occurred in the absence of any concomitant IL-2 release (data not shown). The anti-mouse CD8 Abs 53.6.7 and KT112 both enhanced pMHCI tetramer staining and induced small amounts of MIP1β production

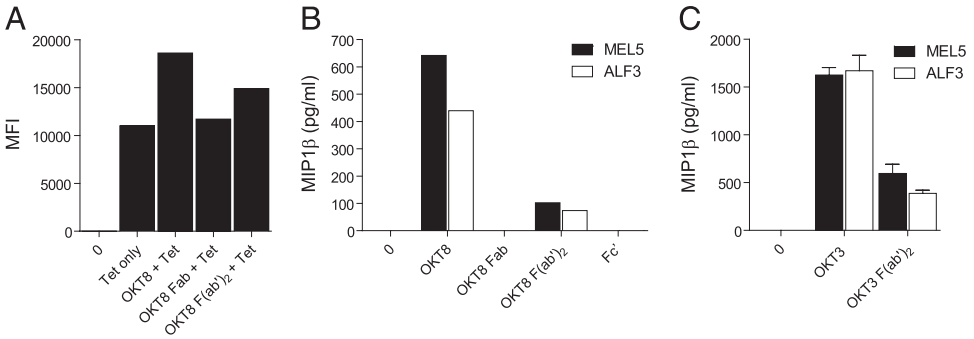

FIGURE 10. OKT8 F(ab′)$_2$ fragments can enhance pMHCI tetramer staining and elicit $CD8^+$ T cell effector function. *A*, A total of 5×10^4 MEL5 $CD8^+$ T cells were either mock treated or incubated with 100 μg/ml OKT8, 100 μg/ml OKT8 Fab, or 100 μg/ml OKT8 F(ab′)$_2$ and then stained with PE-conjugated HLA A*0201-ELAGIGILTV tetramer (25 μg/ml) as described in *Materials and Methods*. Data were acquired using a FACSCantoII flow cytometer and analyzed with FlowJo software. *B*, A total of 3×10^4 MEL5 or ALF3 $CD8^+$ T cells were incubated with 100 μg/ml OKT8, 100 μg/ml OKT8 Fab, 100 μg/ml OKT8 F(ab′)$_2$, or 100 μg/ml OKT8 Fc′ for 18 h. Supernatant was harvested and assayed for MIP1α, MIP1β, and RANTES by ELISA. *C*, A total of 3×10^4 MEL5 or ALF3 $CD8^+$ T cells were incubated with either 10 μg/ml OKT3 or 10 μg/ml OKT3 F(ab′)$_2$ for 18 h. Supernatant was harvested and assayed for MIP1α, MIP1β, and RANTES by ELISA (only MIP1β is shown). Data in *A–C* are representative of three separate experiments. Error bars represent SDs.

Table II. The heterogeneity of anti-human CD8 Abs

Ab Clone	α or β	Tetramer Binding	MIP1β	MIP1α	RANTES	IFN-γ	TNF-α	IL-2	Cytoxicity
OKT8	α	Enhance	Yes	Yes	Yes	No[a]	No[a]	No	Yes
SK1	α	Inhibit	No	No	No	No	No	No	No
MCD8	α	Neutral	No	No	No	No	No	No	No
32/M4	α	Neutral	No	No	No	No	No	No	No
C8/144B	α	Neutral	No	No	No	No	No	No	No
DK25	α	Inhibit	No	No	No	No	No	No	No
2ST8.5H7	β	Inhibit	No	No	No	No	No	No	No

Summary of the effects exerted by anti-human CD8 Abs on pMHCI tetramer binding and CD8+ T cell activation in the absence of TCR engagement.

[a]OKT8 was shown to elicit IFN-γ and TNF-α release by SB10 and PHA/IL-15–stimulated PBMC.

(Fig. 11*A*, 11*B*). Thus, three different phenotypes were identified within a panel of four different anti-mouse CD8 Abs (Table III), which further underscores the considerable heterogeneity that exists within this group of reagents.

Discussion

Anti-CD8 Abs are integral to the flow cytometric detection of pMHCI-restricted T cells and have been used extensively in the past to identify an important role for CD8 in CD8+ T cell activation (16–18, 20). Most studies have concluded that anti-CD8 Abs inhibit the recognition of cognate Ag (19, 21, 22). Furthermore, a recent study provided evidence that a single anti-CD8 Ab could deliver a negative signal to a CD8+ T cell clone in the absence of cognate Ag (29). In contrast, however, earlier studies concluded that anti-CD8 Abs could activate CD8+ T cells (25, 27). Thus, contradictory effects of Ab-mediated CD8 ligation have been reported and the overall picture remains unclear. To clarify this issue, we examined the ability of seven different monoclonal anti-human CD8 Abs to activate six different human CD8+ T cell clones specific for a total of five different pMHCI Ags.

In the absence of cognate Ag, the anti-human CD8 Ab OKT8 induced chemokine release from all six human CD8+ T cell clones tested and cytotoxic activity in all four human CD8+ T cell clones tested (Figs. 1–3). Interestingly, this activation appeared to occur in the absence of any detectable cytokine release, with the exception of CD8+ T cell clone SB10, which released IFN-γ (Fig. 4). It is well established that a hierarchy of CD8+ T cell effector functions exists with respect to Ag sensitivity (47, 48); thus, each function exhibits a distinct activation threshold that must be exceeded for triggering to occur. Our findings suggest that OKT8 delivers a positive signal to CD8+ T cells that is generally sufficient to exceed the activation threshold required for chemokine release and cytotoxic activity but is not sufficient to trigger cytokine release in the majority of CD8+ T cells. In contrast to OKT8, the anti-human CD8α Ab clones SK1, MCD8, C8/144B, 32/M4, and DK25 as well as the anti-human CD8β Ab clone 2ST8.5H7 did not induce any measurable T cell effector functions in the absence of cognate Ag. It was not possible to reverse the phenotype of the nonactivating anti-human CD8 Abs by secondary Ab-mediated cross-linking or PHA/IL-15 treatment (Figs. 5, 6). Thus, we conclude that anti-CD8 Abs can exert differential effects on CD8+ T cells. These findings help to reconcile disparate observations and suggest that previous reports in the literature may not be intrinsically contradictory but rather reflective of the considerable heterogeneity that characterizes the ability of anti-CD8 Abs to induce CD8+ T cell effector function.

Anti-CD8 Ab-mediated activation of CD8+ T cells is consistent with a recent report, in which we demonstrated that MHCI molecules with superenhanced CD8 binding properties can also activate CD8+ T cells in the absence of a specific TCR/pMHCI interaction (49). Furthermore, thymus leukemia Ag interacts strongly (K_D = 12 μM) with cell surface CD8αα expressed by intraepithelial lymphocytes and can modulate T cell responses independently of the TCR (50–52). These studies all demonstrate that the engagement of CD8 in the absence of cognate Ag binding to the TCR can activate CD8+ T cells and, collectively, underscore the importance of CD8 in T cell signaling.

To examine the effects of OKT8 on Ag binding at the CD8+ T cell surface, we used soluble pMHCI tetramer technology, which has transformed the study of Ag-specific CD8+ T cells by

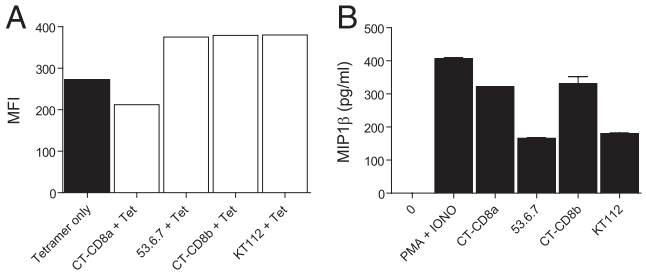

FIGURE 11. Anti-mouse CD8 Abs can exhibit the same phenotype as OKT8. *A*, A total of 5×10^4 naive mouse transgenic F5 T cells were either mock treated or incubated with 100 μg/ml CT-CD8a, 100 μg/ml 53.6.7, 100 μg/ml CT-CD8b, or 100 μg/ml KT112 at 4°C for 25 min and then stained with cognate PE-conjugated H-2D^b tetramer (25μg/ml) as described in *Materials and Methods*. No staining was observed under any of the conditions shown with a control H-2D^b tetramer folded around the lymphocytic choriomeningitis virus GP1-derived epitope KAVYNFATC (residues 33–41). Data were acquired using a modified FACSAriaII flow cytometer and analyzed with FlowJo software. Results were obtained by gating on the CD3$^+$CD4$^-$ population. *B*, A total of 3×10^4 naive mouse transgenic F5 T cells were incubated at 37°C for 18 h with 100 μg/ml CT-CD8a, 100 μg/ml 53.6.7, 100 μg/ml CT-CD8b, 100 μg/ml KT112, or 50 ng/ml PMA and 1 μg/ml ionomycin. Supernatants were harvested and assayed for MIP1β by ELISA. Error bars represent SDs.

Table III. The heterogeneity of anti-mouse CD8 Abs

Ab Clone	α or β	Tetramer Binding	MIP1β	IFN-γ	IL-2
CT-CD8a	α	Inhibit	Yes	No	No
53.6.7	α	Enhance	Weak[a]	No	No
CT-CD8b	β	Enhance	Yes	No	No
KT112	β	Enhance	Weak	NT	NT

Summary of the effects exerted by anti-mouse CD8 Abs on pMHCI tetramer binding and CD8+ T cell activation in the absence of TCR engagement.

[a]53.6.7 elicited low levels of MIP1β production from naive F5 CD8+ T cells, F5 CD8+ T cell lines, and blasted BALB/c CD8+ cells but not from naive BALB/c CD8+ cells (data not shown).

NT, not tested.

enabling their visualization, enumeration, phenotypic characterization, and isolation from ex vivo samples. Preincubation with OKT8 enhanced the capture of cognate pMHCI tetramers from solution and produced higher intensity staining (Figs. 7–9). Accordingly, OKT8 enhanced the identification of $CD8^+$ T cells with low-affinity TCR/pMHCI interactions (Fig. 8, Table I), such as those that typically predominate in tumor-specific and autoimmune responses (41). The other anti-CD8 Abs examined in this study either exerted inhibitory effects on pMHCI tetramer binding (SK1, DK25, and 2ST8.5H7) or displayed no biologically significant activity in this regard (MCD8, 32/M4, and C8/144B). Thus, OKT8 can be used as a tool to improve pMHCI tetramer staining; this property may be especially useful in the context of low-avidity Ag-specific $CD8^+$ T cell populations.

The findings described above suggest that OKT8 has properties that are distinct from other anti-human CD8 Abs. Furthermore, these properties are not entirely Fc′ dependent (Fig. 10). To extend these results, we conducted additional experiments with the anti-mouse CD8α Ab CT-CD8a and the anti-mouse CD8β Ab CT-CD8b. CT-CD8a was shown to inhibit pMHCI tetramer staining, whereas CT-CD8b enhanced pMHCI tetramer binding, consistent with a previous report (26). Despite their differential effects on pMHCI tetramer binding, both of these anti-mouse CD8 Abs activated $CD8^+$ T cells efficiently (Fig. 11). These results demonstrate that the ability of anti-CD8 Abs to elicit $CD8^+$ T cell effector function does not always correlate with their effect on pMHCI tetramer staining. This lack of correspondence was further supported by the identification of a third phenotype in the mouse system. The anti-mouse CD8α Ab 53.6.7 and the anti-mouse CD8β Ab KT112 both enhanced pMHCI tetramer staining but only activated $CD8^+$ T cells weakly (Table III). Taken together, these data further underline the heterogeneity that exists within this group of reagents.

The mechanism by which anti-CD8 Abs exert either inhibitory or stimulatory effects on pMHCI recognition remains elusive. Previous studies have shown that anti-CD8 Abs retain their effects in the absence of a pMHCI/CD8 interaction (26, 53–55). In this study, we confirm that the enhancing effects of OKT8 on HLA A*0201 tetramer on-rate at the cell surface are still apparent in the context of CD8-null MHCI molecules (Fig. 9); thus, these effects are independent of any interaction between pMHCI and CD8. Subtle local rearrangements of the TCR relative to CD8 on pMHCI engagement are required for optimal $CD8^+$ T cell activation (56, 57). By extension, it seems likely that anti-CD8 Abs exert their effects by interfering with, or enhancing, this surface receptor topology. The observation that anti-CD4 Abs can block cell surface intermolecular interactions essential for calcium flux and inhibit subsequent synapse formation is consistent with this hypothesis (58). Furthermore, we have previously demonstrated that anti-CD4 Abs can interfere with pMHCII tetramer binding even though the pMHCII/CD4 interaction does not stabilize TCR/pMHCII interactions (59).

In summary, we have shown the following: 1) heterogeneity exists in the ability of anti-CD8 Abs to activate $CD8^+$ T cells; 2) Ab-mediated ligation of CD8 in the absence of TCR engagement can induce chemokine release and cytotoxic activity, largely in the absence of cytokine release; 3) the anti-human CD8 Ab OKT8 can enhance pMHCI tetramer staining; and 4) anti-mouse CD8 Abs (CT-CD8a and CT-CD8b) can activate $CD8^+$ T cells in the absence of TCR engagement despite differential effects on pMHCI tetramer staining. Thus, anti-CD8 Abs can have potent effects on TCR/pMHCI binding kinetics and activation. These effects vary according to the Ab clone under investigation and should be taken into account when interpreting studies using these reagents. Furthermore, the ability of Ab-mediated CD8 engagement to activate $CD8^+$ T cells underscores the importance of coreceptor function in $CD8^+$ T cell signaling.

Acknowledgments

We thank Rose Zamoyska for helpful discussions and provision of the KT112 hybridoma. We also thank Katherine Adams for the MEL187.c5 $CD8^+$ T cell clone.

Disclosures

The authors have no financial conflicts of interest.

References

1. Gao, G. F., J. Tormo, U. C. Gerth, J. R. Wyer, A. J. McMichael, D. I. Stuart, J. I. Bell, E. Y. Jones, and B. K. Jakobsen. 1997. Crystal structure of the complex between human CD8α(α) and HLA-A2. *Nature* 387: 630–634.
2. Gao, G. F., Z. Rao, and J. I. Bell. 2002. Molecular coordination of αβ T-cell receptors and coreceptors CD8 and CD4 in their recognition of peptide-MHC ligands. *Trends Immunol.* 23: 408–413.
3. Wooldridge, L., H. A. van den Berg, M. Glick, E. Gostick, B. Laugel, S. L. Hutchinson, A. Milicic, J. M. Brenchley, D. C. Douek, D. A. Price, and A. K. Sewell. 2005. Interaction between the CD8 coreceptor and major histocompatibility complex class I stabilizes T cell receptor-antigen complexes at the cell surface. *J. Biol. Chem.* 280: 27491–27501.
4. Gakamsky, D. M., I. F. Luescher, A. Pramanik, R. B. Kopito, F. Lemonnier, H. Vogel, R. Rigler, and I. Pecht. 2005. CD8 kinetically promotes ligand binding to the T-cell antigen receptor. *Biophys. J.* 89: 2121–2133.
5. van den Berg, H. A., L. Wooldridge, B. Laugel, and A. K. Sewell. 2007. Coreceptor CD8-driven modulation of T cell antigen receptor specificity. *J. Theor. Biol.* 249: 395–408.
6. Veillette, A., M. A. Bookman, E. M. Horak, and J. B. Bolen. 1988. The CD4 and CD8 T cell surface antigens are associated with the internal membrane tyrosine-protein kinase p56lck. *Cell* 55: 301–308.
7. Barber, E. K., J. D. Dasgupta, S. F. Schlossman, J. M. Trevillyan, and C. E. Rudd. 1989. The CD4 and CD8 antigens are coupled to a protein-tyrosine kinase (p56lck) that phosphorylates the CD3 complex. *Proc. Natl. Acad. Sci. USA* 86: 3277–3281.
8. Zamoyska, R., P. Derham, S. D. Gorman, P. von Hoegen, J. B. Bolen, A. Veillette, and J. R. Parnes. 1989. Inability of CD8 α′ polypeptides to associate with p56lck correlates with impaired function in vitro and lack of expression in vivo. *Nature* 342: 278–281.
9. Chalupny, N. J., J. A. Ledbetter, and P. Kavathas. 1991. Association of CD8 with p56lck is required for early T cell signalling events. *EMBO J.* 10: 1201–1207.
10. Purbhoo, M. A., J. M. Boulter, D. A. Price, A. L. Vuidepot, C. S. Hourigan, P. R. Dunbar, K. Olson, S. J. Dawson, R. E. Phillips, B. K. Jakobsen, et al. 2001. The human CD8 coreceptor effects cytotoxic T cell activation and antigen sensitivity primarily by mediating complete phosphorylation of the T cell receptor ζ chain. *J. Biol. Chem.* 276: 32786–32792.
11. Hutchinson, S. L., L. Wooldridge, S. Tafuro, B. Laugel, M. Glick, J. M. Boulter, B. K. Jakobsen, D. A. Price, and A. K. Sewell. 2003. The CD8 T cell coreceptor exhibits disproportionate biological activity at extremely low binding affinities. *J. Biol. Chem.* 278: 24285–24293.
12. Arcaro, A., C. Grégoire, N. Boucheron, S. Stotz, E. Palmer, B. Malissen, and I. F. Luescher. 2000. Essential role of CD8 palmitoylation in CD8 coreceptor function. *J. Immunol.* 165: 2068–2076.
13. Arcaro, A., C. Grégoire, T. R. Bakker, L. Baldi, M. Jordan, L. Goffin, N. Boucheron, F. Wurm, P. A. van der Merwe, B. Malissen, and I. F. Luescher. 2001. CD8β endows CD8 with efficient coreceptor function by coupling T cell receptor/CD3 to raft-associated CD8/$p56^{lck}$ complexes. *J. Exp. Med.* 194: 1485–1495.
14. Wooldridge, L., B. Laugel, J. Ekeruche, M. Clement, H. A. van den Berg, D. A. Price, and A. K. Sewell. 2010. CD8 controls T cell cross-reactivity. *J. Immunol.* 185: 4625–4632.
15. Laugel, B., D. A. Price, A. Milicic, and A. K. Sewell. 2007. CD8 exerts differential effects on the deployment of cytotoxic T lymphocyte effector functions. *Eur. J. Immunol.* 37: 905–913.
16. Norment, A. M., R. D. Salter, P. Parham, V. H. Engelhard, and D. R. Littman. 1988. Cell-cell adhesion mediated by CD8 and MHC class I molecules. *Nature* 336: 79–81.
17. Shinohara, N., and D. H. Sachs. 1979. Mouse alloantibodies capable of blocking cytotoxic T-cell function. I. Relationship between the antigen reactive with blocking antibodies and the Lyt-2 locus. *J. Exp. Med.* 150: 432–444.
18. Nakayama, E., H. Shiku, E. Stockert, H. F. Oettgen, and L. J. Old. 1979. Cytotoxic T cells: Lyt phenotype and blocking of killing activity by Lyt antisera. *Proc. Natl. Acad. Sci. USA* 76: 1977–1981.
19. Janeway, C. A. Jr. 1992. The T cell receptor as a multicomponent signalling machine: CD4/CD8 coreceptors and CD45 in T cell activation. *Annu. Rev. Immunol.* 10: 645–674.
20. Miceli, M. C., and J. R. Parnes. 1993. Role of CD4 and CD8 in T cell activation and differentiation. *Adv. Immunol.* 53: 59–122.
21. MacDonald, H. R., A. L. Glasebrook, C. Bron, A. Kelso, and J. C. Cerottini. 1982. Clonal heterogeneity in the functional requirement for Lyt-2/3 molecules

on cytolytic T lymphocytes (CTL): possible implications for the affinity of CTL antigen receptors. *Immunol. Rev.* 68: 89–115.
22. MacDonald, H. R., A. L. Glasebrook, and J. C. Cerottini. 1982. Clonal heterogeneity in the functional requirement for Lyt-2/3 molecules on cytolytic T lymphocytes: analysis by antibody blocking and selective trypsinization. *J. Exp. Med.* 156: 1711–1722.
23. Clark, S. J., D. A. Law, D. J. Paterson, M. Puklavec, and A. F. Williams. 1988. Activation of rat T lymphocytes by anti-CD2 monoclonal antibodies. *J. Exp. Med.* 167: 1861–1872.
24. Lühder, F., Y. Huang, K. M. Dennehy, C. Guntermann, I. Müller, E. Winkler, T. Kerkau, S. Ikemizu, S. J. Davis, T. Hanke, and T. Hünig. 2003. Topological requirements and signaling properties of T cell-activating, anti-CD28 antibody superagonists. *J. Exp. Med.* 197: 955–966.
25. Veillette, A., J. C. Zúñiga-Pflücker, J. B. Bolen, and A. M. Kruisbeek. 1989. Engagement of CD4 and CD8 expressed on immature thymocytes induces activation of intracellular tyrosine phosphorylation pathways. *J. Exp. Med.* 170: 1671–1680.
26. Wooldridge, L., S. L. Hutchinson, E. M. Choi, A. Lissina, E. Jones, F. Mirza, P. R. Dunbar, D. A. Price, V. Cerundolo, and A. K. Sewell. 2003. Anti-CD8 antibodies can inhibit or enhance peptide-MHC class I (pMHCI) multimer binding: this is paralleled by their effects on CTL activation and occurs in the absence of an interaction between pMHCI and CD8 on the cell surface. *J. Immunol.* 171: 6650–6660.
27. Tomonari, K., and S. Spencer. 1990. Epitope-specific binding of CD8 regulates activation of T cells and induction of cytotoxicity. *Int. Immunol.* 2: 1189–1194.
28. Grebe, K. M., R. L. Clarke, and T. A. Potter. 2004. Ligation of CD8 leads to apoptosis of thymocytes that have not undergone positive selection. *Proc. Natl. Acad. Sci. USA* 101: 10410–10415.
29. Abidi, S. H., T. Dong, M. T. Vuong, V. B. Sreenu, S. L. Rowland-Jones, E. J. Evans, and S. J. Davis. 2008. Differential remodeling of a T-cell transcriptome following CD8- versus CD3-induced signaling. *Cell Res.* 18: 641–648.
30. Laugel, B., H. A. van den Berg, E. Gostick, D. K. Cole, L. Wooldridge, J. Boulter, A. Milicic, D. A. Price, and A. K. Sewell. 2007. Different T cell receptor affinity thresholds and CD8 coreceptor dependence govern cytotoxic T lymphocyte activation and tetramer binding properties. *J. Biol. Chem.* 282: 23799–23810.
31. Purbhoo, M. A., Y. Li, D. H. Sutton, J. E. Brewer, E. Gostick, G. Bossi, B. Laugel, R. Moysey, E. Baston, N. Liddy, et al. 2007. The HLA A*0201-restricted hTERT(540–548) peptide is not detected on tumor cells by a CTL clone or a high-affinity T-cell receptor. *Mol. Cancer Ther.* 6: 2081–2091.
32. Cole, D. K., E. S. Edwards, K. K. Wynn, M. Clement, J. J. Miles, K. Ladell, J. Ekeruche, E. Gostick, K. J. Adams, A. Skowera, et al. 2010. Modification of MHC anchor residues generates heteroclitic peptides that alter TCR binding and T cell recognition. *J. Immunol.* 185: 2600–2610.
33. Argaet, V. P., C. W. Schmidt, S. R. Burrows, S. L. Silins, M. G. Kurilla, D. L. Doolan, A. Suhrbier, D. J. Moss, E. Kieff, T. B. Sculley, and I. S. Misko. 1994. Dominant selection of an invariant T cell antigen receptor in response to persistent infection by Epstein–Barr virus. *J. Exp. Med.* 180: 2335–2340.
34. Green, K. J., J. J. Miles, J. Tellam, W. J. van Zuylen, G. Connolly, and S. R. Burrows. 2004. Potent T cell response to a class I-binding 13-mer viral epitope and the influence of HLA micropolymorphism in controlling epitope length. *Eur. J. Immunol.* 34: 2510–2519.
35. Lissina, A., K. Ladell, A. Skowera, M. Clement, E. Edwards, R. Seggewiss, H. A. van den Berg, E. Gostick, K. Gallagher, E. Jones, et al. 2009. Protein kinase inhibitors substantially improve the physical detection of T-cells with peptide-MHC tetramers. *J. Immunol. Methods* 340: 11–24.
36. Mamalaki, C., J. Elliott, T. Norton, N. Yannoutsos, A. R. Townsend, P. Chandler, E. Simpson, and D. Kioussis. 1993. Positive and negative selection in transgenic mice expressing a T-cell receptor specific for influenza nucleoprotein and endogenous superantigen. *Dev. Immunol.* 3: 159–174.
37. Wooldridge, L., A. Lissina, J. Vernazza, E. Gostick, B. Laugel, S. L. Hutchinson, F. Mirza, P. R. Dunbar, J. M. Boulter, M. Glick, et al. 2007. Enhanced immunogenicity of CTL antigens through mutation of the CD8 binding MHC class I invariant region. *Eur. J. Immunol.* 37: 1323–1333.
38. Betts, M. R., J. M. Brenchley, D. A. Price, S. C. De Rosa, D. C. Douek, M. Roederer, and R. A. Koup. 2003. Sensitive and viable identification of antigen-specific CD8$^+$ T cells by a flow cytometric assay for degranulation. *J. Immunol. Methods* 281: 65–78.
39. Wooldridge, L., A. Lissina, D. K. Cole, H. A. van den Berg, D. A. Price, and A. K. Sewell. 2009. Tricks with tetramers: how to get the most from multimeric peptide-MHC. *Immunology* 126: 147–164.
40. Li, Y., R. Moysey, P. E. Molloy, A. L. Vuidepot, T. Mahon, E. Baston, S. Dunn, N. Liddy, J. Jacob, B. K. Jakobsen, and J. M. Boulter. 2005. Directed evolution of human T-cell receptors with picomolar affinities by phage display. *Nat. Biotechnol.* 23: 349–354.
41. Cole, D. K., N. J. Pumphrey, J. M. Boulter, M. Sami, J. I. Bell, E. Gostick, D. A. Price, G. F. Gao, A. K. Sewell, and B. K. Jakobsen. 2007. Human TCR-binding affinity is governed by MHC class restriction. *J. Immunol.* 178: 5727–5734.
42. Cole, D. K., F. Yuan, P. J. Rizkallah, J. J. Miles, E. Gostick, D. A. Price, G. F. Gao, B. K. Jakobsen, and A. K. Sewell. 2009. Germ line-governed recognition of a cancer epitope by an immunodominant human T-cell receptor. *J. Biol. Chem.* 284: 27281–27289.
43. Wyer, J. R., B. E. Willcox, G. F. Gao, U. C. Gerth, S. J. Davis, J. I. Bell, P. A. van der Merwe, and B. K. Jakobsen. 1999. T cell receptor and coreceptor CD8αα bind peptide-MHC independently and with distinct kinetics. *Immunity* 10: 219–225.
44. Woodle, E. S., J. R. Thistlethwaite, I. A. Ghobrial, L. K. Jolliffe, F. P. Stuart, and J. A. Bluestone. 1991. OKT3 F(ab′)$_2$ fragments—retention of the immunosuppressive properties of whole antibody with marked reduction in T cell activation and lymphokine release. *Transplantation* 52: 354–360.
45. Herold, K. C., J. B. Burton, F. Francois, E. Poumian-Ruiz, M. Glandt, and J. A. Bluestone. 2003. Activation of human T cells by FcR nonbinding anti-CD3 mAb, hOKT3γ1(Ala-Ala). *J. Clin. Invest.* 111: 409–418.
46. Chatenoud, L., and J. A. Bluestone. 2007. CD3-specific antibodies: a portal to the treatment of autoimmunity. *Nat. Rev. Immunol.* 7: 622–632.
47. Valitutti, S., S. Müller, M. Dessing, and A. Lanzavecchia. 1996. Different responses are elicited in cytotoxic T lymphocytes by different levels of T cell receptor occupancy. *J. Exp. Med.* 183: 1917–1921.
48. Price, D. A., A. K. Sewell, T. Dong, R. Tan, P. J. Goulder, S. L. Rowland-Jones, and R. E. Phillips. 1998. Antigen-specific release of β-chemokines by anti–HIV-1 cytotoxic T lymphocytes. *Curr. Biol.* 8: 355–358.
49. Wooldridge, L., M. Clement, A. Lissina, E. S. Edwards, K. Ladell, J. Ekeruche, R. E. Hewitt, B. Laugel, E. Gostick, D. K. Cole, et al. 2010. MHC class I molecules with superenhanced CD8 binding properties bypass the requirement for cognate TCR recognition and nonspecifically activate CTLs. *J. Immunol.* 184: 3357–3366.
50. Leishman, A. J., O. V. Naidenko, A. Attinger, F. Koning, C. J. Lena, Y. Xiong, H. C. Chang, E. Reinherz, M. Kronenberg, and H. Cheroutre. 2001. T cell responses modulated through interaction between CD8αα and the nonclassical MHC class I molecule, TL. *Science* 294: 1936–1939.
51. Tsujimura, K., Y. Obata, E. Kondo, K. Nishida, Y. Matsudaira, Y. Akatsuka, K. Kuzushima, and T. Takahashi. 2003. Thymus leukemia antigen (TL)-specific cytotoxic T lymphocytes recognize the α1/α2 domain of TL free from antigenic peptides. *Int. Immunol.* 15: 1319–1326.
52. Cole, D. K., and G. F. Gao. 2004. CD8: adhesion molecule, co-receptor and immuno-modulator. *Cell. Mol. Immunol.* 1: 81–88.
53. Van Seventer, G. A., R. A. Van Lier, H. Spits, P. Ivanyi, and C. J. Melief. 1986. Evidence for a regulatory role of the T8 (CD8) antigen in antigen-specific and anti–T3-(CD3)–induced lytic activity of allospecific cytotoxic T lymphocyte clones. *Eur. J. Immunol.* 16: 1363–1371.
54. Hoo, W. S., and D. M. Kranz. 1993. Role of CD8 in staphylococcal enterotoxin B-mediated lysis by cytotoxic T lymphocytes. *J. Immunol.* 150: 4331–4337.
55. Campanelli, R., B. Palermo, S. Garbelli, S. Mantovani, P. Lucchi, A. Necker, E. Lantelme, and C. Giachino. 2002. Human CD8 co-receptor is strictly involved in MHC-peptide tetramer-TCR binding and T cell activation. *Int. Immunol.* 14: 39–44.
56. Lee, P. U., and D. M. Kranz. 2003. Allogeneic and syngeneic class I MHC complexes drive the association of CD8 and TCR on 2C T cells. *Mol. Immunol.* 39: 687–695.
57. Block, M. S., A. J. Johnson, Y. Mendez-Fernandez, and L. R. Pease. 2001. Monomeric class I molecules mediate TCR/CD3ε/CD8 interaction on the surface of T cells. *J. Immunol.* 167: 821–826.
58. Krummel, M. F., M. D. Sjaastad, C. Wülfing, and M. M. Davis. 2000. Differential clustering of CD4 and CD3ζ during T cell recognition. *Science* 289: 1349–1352.
59. Wooldridge, L., T. J. Scriba, A. Milicic, B. Laugel, E. Gostick, D. A. Price, R. E. Phillips, and A. K. Sewell. 2006. Anti-coreceptor antibodies profoundly affect staining with peptide–MHC class I and class II tetramers. *Eur. J. Immunol.* 36: 1847–1855.

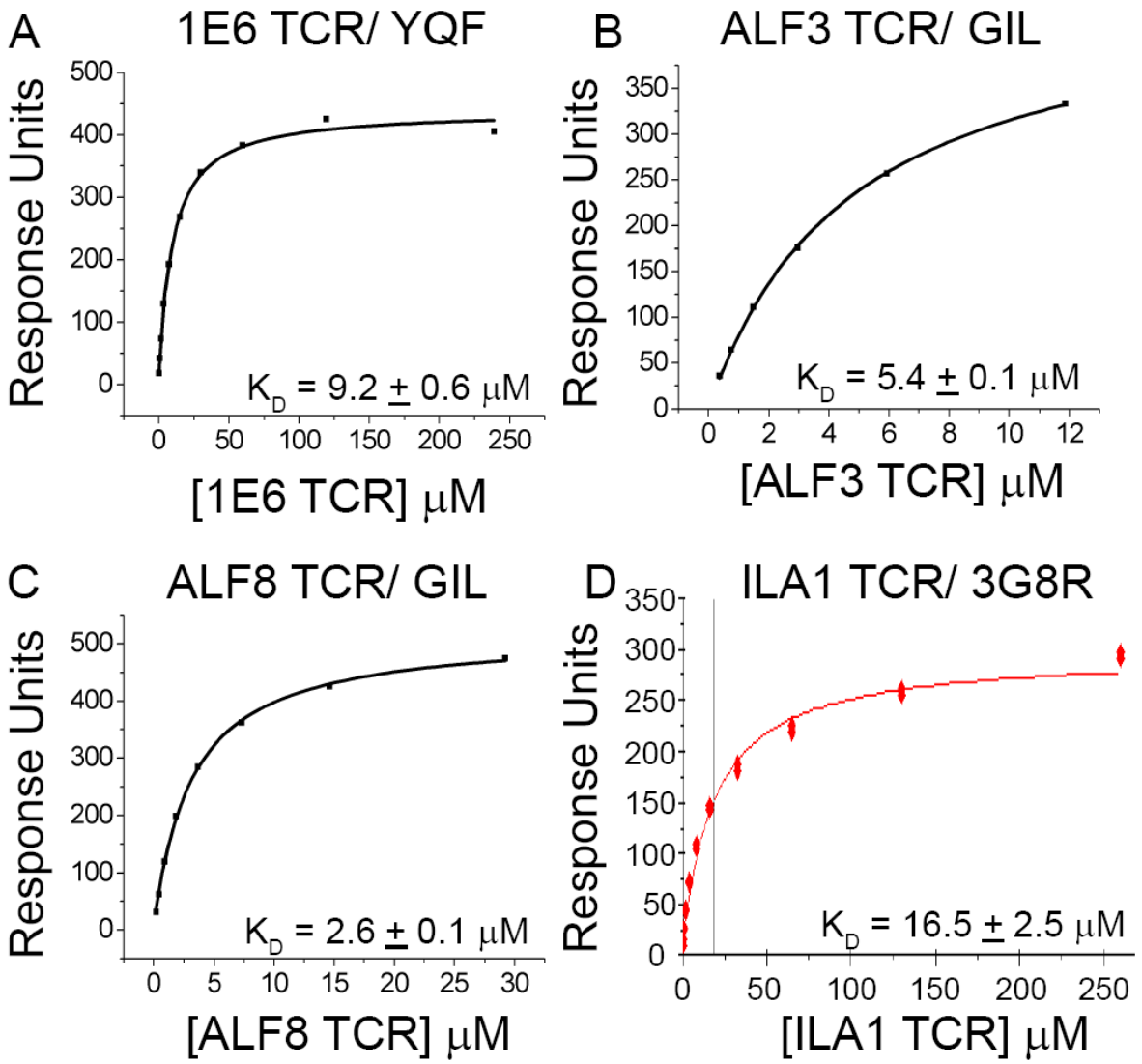

Appendix 3. Surface plasmon resonance measurements of 1E6, ALF8, and 1LA TCR binding to peptide variants complexed with HLA A*0201. SPR equilibrium binding of soluble of (**A**) 1E6 TCR to HLA A*0201-**YQF**GPD**FPI**A, (**B**) ALF3 TCR to HLA A*0201-GILGFVFTL, (**C**) ALF8 TCR to HLA A*0201-GILGFVFTL and (**D**) ILA1 TCR to HLA A*0201-IL**G**KFLH**R**L. The mean response for each concentration is plotted (n = 3). The equilibrium dissociation constant (KD) values were calculated assuming 1:1 Langmuir binding and plotted using a nonlinear curve fit (y = (P1x)/(P2 + x)).